

CAPITAL UNIVERSITY OF SCIENCE AND
TECHNOLOGY, ISLAMABAD



**Potential Utilization of Wheat
Straw in Concrete for Pavement
Applications from Engineering
Perspectives**

by

Muhammad Usman Farooqi

A thesis submitted in partial fulfillment for the
degree of Doctor of Philosophy

in the

Faculty of Engineering

Department of Civil Engineering

2020

Potential Utilization of Wheat Straw in Concrete for Pavement Applications from Engineering Perspectives

By

Muhammad Usman Farooqi
(DCE153004)

Dr. Ana Armada Bras, Associate Professor
Liverpool John Moores University, Liverpool, UK
(Foreign Evaluator 1)

Dr. Zhang Pu, Associate Professor
Zhengzhou University, Zhengzhou, China
(Foreign Evaluator 2)

Engr. Prof. Dr. Majid Ali
(Thesis Supervisor)

Engr. Dr. Ishtiaq Hassan
(Head, Department of Civil Engineering)

Engr. Prof. Dr. Imtiaz Ahmad Taj
(Dean, Faculty of Engineering)

DEPARTMENT OF CIVIL ENGINEERING
CAPITAL UNIVERSITY OF SCIENCE AND TECHNOLOGY
ISLAMABAD

2020

Copyright © 2020 by Muhammad Usman Farooqi

All rights reserved. No part of this thesis may be reproduced, distributed, or transmitted in any form or by any means, including photocopying, recording, or other electronic or mechanical methods, by any information storage and retrieval system without the prior written permission of the author.

This humble effort is dedicated to

My Father

*For his visionary sacrifices to bring best out of
me, as this Ph.D. is his dream came true*

My Mother

For her soulful prayers and her faith in me

My Supervisor

For his presistent concern to make it possible.



**CAPITAL UNIVERSITY OF SCIENCE & TECHNOLOGY
ISLAMABAD**

Expressway, Kahuta Road, Zone-V, Islamabad
Phone: +92-51-111-555-666 Fax: +92-51-4486705
Email: info@cust.edu.pk Website: <https://www.cust.edu.pk>

CERTIFICATE OF APPROVAL

This is to certify that the research work presented in the thesis, entitled “**Potential Utilization of Wheat Straw in Concrete for Pavement Applications from Engineering Perspectives**” was conducted under the supervision of **Dr. Majid Ali**. No part of this thesis has been submitted anywhere else for any other degree. This thesis is submitted to the **Department of Civil Engineering, Capital University of Science and Technology** in partial fulfillment of the requirements for the degree of Doctor in Philosophy in the field of **Civil Engineering**. The open defence of the thesis was conducted on **November 17, 2020**.

Student Name : Muhammad Usman Farooqi
(DCE-153004)

The Examination Committee unanimously agrees to award PhD degree in the mentioned field.

Examination Committee :

- (a) External Examiner 1: Dr. Ayub Elahi
Professor
UET Taxila
- (b) External Examiner 2: Dr. Naveed Ahmad
Associate Professor
UET Taxila
- (c) Internal Examiner : Dr. Ishtiaq Hassan
Associate Professor
CUST, Islamabad

Supervisor Name : Dr. Majid Ali
Professor
CUST, Islamabad

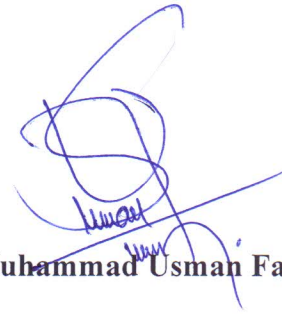
Name of HoD : Dr. Ishtiaq Hassan
Associate Professor
CUST, Islamabad

Name of Dean : Dr. Imtiaz Ahmed Taj
Professor
CUST, Islamabad

AUTHOR'S DECLARATION

I, **Muhammad Usman Farooqi (Registration No. DCE-153004)**, hereby state that my PhD thesis titled, '**Potential Utilization of Wheat Straw in Concrete for Pavement Applications from Engineering Perspectives**' is my own work and has not been submitted previously by me for taking any degree from Capital University of Science and Technology, Islamabad or anywhere else in the country/ world.

At any time, if my statement is found to be incorrect even after my graduation, the University has the right to withdraw my PhD Degree.



(**Muhammad Usman Farooqi**)

Dated: 17- November, 2020

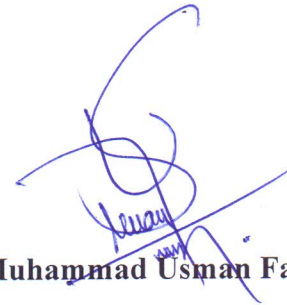
Registration No : DCE153004

PLAGIARISM UNDERTAKING

I solemnly declare that research work presented in the thesis titled “**Potential Utilization of Wheat Straw in Concrete for Pavement Applications from Engineering Perspectives**” is solely my research work with no significant contribution from any other person. Small contribution/ help wherever taken has been duly acknowledged and that complete thesis has been written by me.

I understand the zero tolerance policy of the HEC and Capital University of Science and Technology towards plagiarism. Therefore, I as an author of the above titled thesis declare that no portion of my thesis has been plagiarized and any material used as reference is properly referred/ cited.

I undertake that if I am found guilty of any formal plagiarism in the above titled thesis even after award of PhD Degree, the University reserves the right to withdraw/ revoke my PhD degree and that HEC and the University have the right to publish my name on the HEC/ University Website on which names of students are placed who submitted plagiarized thesis.



(Muhammad Usman Farooqi)

Dated: 17, November, 2020

Registration No : DCE153004

List of Publications

It is certified that following publication(s) have been made out of the research work that has been carried out for this thesis:-

Journal Publications:

1. **M. U. Farooqi** and M. Ali, "Effect of pre-treatment and content of wheat straw on energy absorption capability of concrete," *Construction and Building Materials*, vol. 224, pp. 572-583, 2019.
2. **M. U. Farooqi** and M. Ali, "Contribution of plant fibers in improving the behavior and capacity of reinforced concrete for structural applications," *Construction and Building Materials*, vol. 182, pp. 94-107, 2018.
3. **M. U. Farooqi** and M. Ali, "Effect of Fibre Content on Splitting-Tensile Strength of Wheat Straw Reinforced Concrete for Pavement Applications," *In Key Engineering Materials*, vol. 765, pp. 349-354, 2018.

Conference Proceedings:

1. **M. U. Farooqi** and M. Ali, "Construction practices for first ever wheat straw reinforced concrete pavement for light traffic," *In proceedings of 5th International Conference on Sustainable Construction Materials and Technologies (SCMT5), London, UK, 2019.*
2. **M. U. Farooqi** and M. Ali, "Effect of Fibre Content on Compressive Strength of Wheat Straw Reinforced Concrete for Pavement Applications," *IOP Conference Series: Materials Science and Engineering*, vol. 422, no. 1, p. 012014, IOP Publishing, 2018.
3. **M. U. Farooqi** and M. Ali, "Short-term durability of wheat straw reinforced concrete for pavement applications," *In proceedings of 5th International Conference on Infrastructure Engineering in Developing Countries (IEDC), Karachi, Pakistan, 2017.*

4. **M. U. Farooqi** and M. Ali, “Compressive behavior of wheat straw reinforced concrete for pavement applications,” *In proceedings of 4th International Conference on Sustainable Construction Materials and Technologies (SCMT4), Las Vegas, USA, 2016.*
5. **M. U. Farooqi** and M. Ali, “Flexural behavior of wheat straw reinforced concrete for pavement applications,” *In Proceedings of 36th Cement And Concrete Science Conference, Cardiff, UK, 2016.*

(Muhammad Usman Farooqi)

Registration No: DCE153004

Acknowledgements

In the name of Allah, the Most Gracious and the Most Merciful! All praises are for **Almighty Allah**, the Creator of everything, with Whose grace I am here, as one can't even wish without His will. And all the respect for the **Holy Prophet Muhammad (Peace be upon Him)**.

Foremost, the most special indebtedness goes to my research supervisor, **Prof. Dr. Majid Ali**, for his valuable guidance, hidden directions (to let me explore these), pearls of wisdom, motivation (of his own kind) during hard times, his amazingly timely feedback, his patience, persistence and untiring efforts (via mails, text messages and one-to-one interactions) to push me up for bringing this piece of work out of me. Simply, without his smart training technique(s), it would have been nearly impossible to realize that so much could be done with little.

Additionally, the research work reported in this dissertation has been carried out in the laboratories of Capital University of Science and Technology, by the help of the staff. I really appreciate all the staff members, particularly **Mr. Talha Ahmed**, **Mr. Ghulam Mustafa**, **Mr. Sohail Afzal**, **Mr. Muhammad Nadeem**, **Mr. Muhammad Junaid**, **Mr. Muhammad Saqib**, **Mr. Muhammad Khalid** and **Mr. Muhammad Asif Jalal** for their kind help during lab work. **Mr. Mehran Khan**, my class fellow, is also acknowledged for his kind guidance during this research journey.

I would also like to express my gratitude to the honorable **Prof. Dr. Muhammad Mansoor Ahmed** (my motivation) for all his encouraging steps towards this achievement, whether to buck me up (off and on) with his motivational remarks or to financially support me, in terms of scholarships and research grants, and permissions for innovative development in the campus premises.

My acknowledgments can't be completed without appreciating the selfless sacrificial life and most sincere efforts along with unceasing and dedicated soulful prayers of my beloved parents (**Father, Ijaz Ali Chishti** and **Mother, Khadija Tul Kubra**), due to which I am able to be at this position in my life today. I won't

be able to pay back the love and affection of my parents. Furthermore, I would also like to acknowledge my wife and son for abiding my ignorance with patience during critical stages of my Ph.D. Words would never say how much I am grateful to them. Collectively, I am really blessed to have such a lovely and caring siblings, standing beside me with all their unconditional love and support. Also, I would like to acknowledge my all the time key motivator, **Mr. Suleman Liaquat**, my best friend.

Finally, I thank all those, including my friends and relatives, who encouraged me and helped me, directly or indirectly, in the completion of this most interesting and tedious job of my Ph.D. thesis, in anyway.

(Muhammad Usman Farooqi)

Registration No: DCE153004

Abstract

The abundant availability of plant fibres, around the globe, seeks researcher's attention on their potential use as construction materials. There is a need to explore the structural integrity of concrete reinforced with such plant fibres. To start with, among all plant fibres, wheat straw is selected to be studied for its possible use as a construction material. As, out of 731 million tonnes global annual wheat production, Pakistan produces 26 million tonnes. Accordingly, 22 million tonnes wheat straw i.e. agricultural waste/by-product of wheat crop, is produced annually in Pakistan, depicting its abundant availability. On the other hand, the usage of rigid pavements has become more frequent over the past decades in developing countries. As per AASHTO pavement design guide, the serviceability of concrete pavements is almost 15% more than that of asphalt pavements for an averaged design life of 20 years. However, its more extensive use is still prevented due to its higher initial cost, mainly due to the cost of cement and reinforcement. Moreover, plain concrete is an inherently brittle material with low tensile strength and strain capacity. Accordingly, the pavement distresses, like early-age micro cracking and punch-outs etc., usually occur in rigid pavements, particularly in developing countries. These premature distresses can be minimized by using dispersed fibres in concrete. Therefore, the overall aim of this research program is to have the development of economic and durable design and/or construction techniques for new rigid pavements by using locally available natural fibres in concrete. However, natural fibres reinforced concrete pavements are slightly explored yet. Furthermore, to the best of author's knowledge, wheat straw is not studied yet for rigid pavement applications. Accordingly, the specific aim of this doctoral study is to explore, in detail, the potential of wheat straw reinforced concrete for structural applications i.e. rigid pavements.

In this research program, in-depth investigation is made to evaluate the structural capacity of wheat straw reinforced concrete (WSRC) in terms of optimization, durability, and structural performance. The effect of pre-treatment and content of wheat straw on the energy absorption capability of concrete has been studied

by evaluating its static properties. Almost 25 mm long soaked, boiled, and chemically treated straw having content of 1%, 2%, and 3%, by mass of wet concrete, are considered. The durability of concrete having straw is determined, in terms of residual behaviors, after its exposure to room, climatic, and alternate wetting and drying conditions for 4-years. The contribution of wheat straw in improving the behavior and capacity of reinforced concrete for structural applications is also studied. WSRC beam-lets with varying flexure and shear rebars are experimentally investigated. The structural performance of jointed WSRC pavement is also evaluated by constructing its test section. The laboratory and field investigations are made to determine the compressive properties, deflection measurements and cracks progression, after the exposure of test section to vehicular movement for 18-months. The properties of plain concrete (PC) specimens and test section are taken as reference. Micro-structural analysis is also done to verdict the straw behavior at all the stages.

Concrete, having soaked straw with 1% content, is optimized in terms of enhanced and durable properties. Splitting-tensile toughness index of concrete with 1% soaked straw is increased significantly by 105%. Optimized WSRC shows 79% residual flexural strength under natural weathering. Structural and/or load carrying capacity of WSRC having flexural and shear re-bars is enhanced up to 7.5%, along with the delayed crack initiation due to crack arresting mechanism provided by the presence of dispersed straw. WSRC pavement test section shows 34% higher energy absorption capacity, as compared to that of plain concrete section. Micro-structural analysis reveals that proper bonding between durable straw and concrete matrix is resulted is come out with enhanced properties. The structural performance of WSRC pavement (with 7% less design thickness as compared to PC pavement), in terms of load transfer efficiency, is also enhanced up to 16%. Accordingly, the construction cost and carbon emissions of WSRC pavements can be reduced up to 14% and 28%, respectively. Hence, WSRC is recommended for economical and sustainable rigid pavements.

Keywords: Natural fibres; Wheat straw; Wheat straw reinforced concrete; Durability; Residual strength; Structural performance; Rigid pavements.

Contents

Author’s Declaration	v
Plagiarism Undertaking	vi
List of Publications	vii
Acknowledgements	ix
Abstract	xi
List of Figures	xix
List of Tables	xxiii
Abbreviations	xxvi
Symbols	xxix
1 Introduction	1
1.1 Theoretical Background	1
1.2 Research Motivation and Problem Statement	5
1.3 Overall Aim of the Research Program and Specific Goal of this Doctoral Study	7
1.4 Research Significance, Perceived Innovation and Utilization as a Product	8
1.4.1 Significance of this Study	8
1.4.2 Perceived Innovation from this Study	9
1.4.3 Utilization of Current Study as a Product	11
1.5 Scope of Work and Study Limitation	12
1.5.1 Scope of this Doctoral Study	12
1.5.1.1 Rationale Behind the Selected Variables	14
1.5.2 Limitations of this Doctoral Study	14
1.6 Brief Methodology	15

1.6.1	Flaws in Rigid Pavements	15
1.6.2	Optimization of Wheat Straw Reinforced Concrete	16
1.6.3	Durability of Wheat Straw Reinforced Concrete	16
1.6.4	Structural Capacity of Wheat Straw Reinforced Concrete	17
1.6.5	Performance Evaluation of Wheat Straw Reinforced Con- crete Pavement	17
1.7	Thesis Layout	19
2	Literature Review	22
2.1	Background	22
2.2	Flaws in Concrete Pavements	23
2.2.1	Rigid Pavement Distresses	24
2.2.2	Flaws in Rigid Pavements of Developing Countries	25
2.2.3	Identified Research Gap on Rigid Pavement Flaws	27
2.3	Behavior and Capacity of Fibre Reinforced Concrete	28
2.3.1	Concrete Reinforced with Short-discrete Artificial, Steel and Natural Fibres	28
2.3.2	Typical Role of Steel Fibres on Design Capacity	29
2.3.3	Behavior of Steel and Artificial Fibre Reinforced Concrete	31
2.3.3.1	Steel Fibre Reinforced Concrete	31
2.3.3.2	Artificial Fibre Reinforced Concrete	31
2.3.4	Behavior of Natural Fibre Reinforced Concrete	34
2.3.5	Wheat Straw Reinforced Concrete	38
2.3.6	Identified Research Gap on Fibre Reinforced Concrete	38
2.4	Durability of Natural Fibre Reinforced Concrete	40
2.4.1	Durability Evaluation Techniques for Natural Fibres in Ce- ment Composites	40
2.4.2	Treatment Techniques to Improve Durability of Natural Fibres in Cement Composites	41
2.4.3	Identified Research Gap on Durability of Natural Fibre Reinforced Concrete	42
2.5	Structural Capacity of Fibre Reinforced Concrete for Pavement Applications	44
2.5.1	Incorporation of Fibres in Concrete Pavements	44
2.5.1.1	Addition of Steel Fibres in Concrete for Pavement Applications	44
2.5.1.2	Addition of Artificial Fibres in Concrete for Pave- ments	45
2.5.2	Natural Fibres in Concrete for Pavements	47

2.5.3	Identified Research Gap on Structural Capacity of Fibre Reinforced Concrete for Pavements	47
2.6	Structural Performance of Rigid Pavements	48
2.6.1	Rigid Pavements	48
2.6.2	Performance Evaluation Techniques for Pavement Test Sections	49
2.6.3	Identified Research Gap on Structural Performance of Wheat Straw Reinforced Concrete	51
2.7	Summary	51
3	Optimization of Wheat Straw Reinforced Concrete Mix	53
3.1	Background	54
3.2	Materials and Methods	55
3.2.1	Materials	55
3.2.1.1	Wheat Straw Treatment	56
3.2.2	Mix Proportions and Casting Procedure	58
3.2.3	Specimens	59
3.2.4	Testing Methods	60
3.2.4.1	Density	60
3.2.4.2	Compression Test	60
3.2.4.3	Splitting-tensile Test	61
3.2.4.4	Flexural Test	61
3.2.4.5	Scanning Electron Microscope (SEM) Test	61
3.3	Results Analysis and Discussions	62
3.3.1	Density	62
3.3.2	Properties under Compressive Loading	62
3.3.2.1	Compressive Behavior	62
3.3.2.2	Compressive Strengths, Compressive Energy Absorption and Compressive Toughness Index	65
3.3.3	Properties under Splitting-tensile Loading	71
3.3.3.1	Splitting-tensile Behavior	71
3.3.3.2	Splitting-tensile Strength, Splitting-tensile Energy Absorption and Splitting-tensile Toughness Index	72
3.3.4	Properties under Flexural Loading	76
3.3.4.1	Flexural Behavior	76
3.3.4.2	Modulus of Rupture (MoR), Flexural Energy Absorption and Flexural Toughness Index	78
3.3.5	Micro-structural Analysis of Straw and WSRC	81
3.4	Summary	86
4	Durability of Wheat Straw Reinforced Concrete	88
4.1	Background	88
4.2	Experimental Investigation	90
4.2.1	Materials Used	90

4.2.1.1	Preparation of Wheat Straw	91
4.2.2	Mix Proportion and Mixing Technique	92
4.2.3	Specimens and Labelling/Testing Scheme	93
4.2.4	Ageing Conditions	94
4.2.4.1	Room Conditions	94
4.2.4.2	Climatic/Environmental Conditions	96
4.2.4.3	Alternate Wetting and Drying Conditions	97
4.2.5	Testing	98
4.2.5.1	Residual Compressive Strength Test	98
4.2.5.2	Residual Splitting-tensile Strength Test	98
4.2.5.3	Residual Flexural Strength Test	98
4.2.5.4	Micro-structural Analysis of 4-years Aged Straw and it's Bond with Composite	99
4.3	Experimental Results and Discussions	99
4.3.1	Residual Properties under Compressive Loading	99
4.3.1.1	Residual Compressive Behavior	99
4.3.1.2	Residual Compressive Strength (σ_r), Energy Ab- sorption (Ce_r) and Toughness Index (CTI_r)	101
4.3.2	Residual Properties under Splitting-tensile Loading	106
4.3.2.1	Residual Splitting-tensile Behavior	106
4.3.2.2	Residual Splitting-tensile Strength (SS_r), Energy Absorption (Se_r) and Toughness Index (STI_r)	108
4.3.3	Residual Properties under Flexural Loading	112
4.3.3.1	Residual Flexural Behavior	112
4.3.3.2	Residual Modulus of Rupture (MoR_r), Energy Ab- sorption (Fe_r) and Toughness Index (FTI_r)	114
4.3.4	Micro-structural Findings	118
4.3.4.1	X-Ray Diffraction (XRD) Analysis of Straw	118
4.3.4.2	Thermogravimetric Analysis (TGA) of Straw	119
4.3.4.3	SEM Analysis of Straw and Straw-concrete Matrix at 4 Years	120
4.4	Empirical Modelling	123
4.4.1	Background of WSRC Properties at 4 Years	123
4.4.2	Empirical Relation Between Flexural Properties and Struc- tural Long-term Performance	124
4.4.3	Design Life Anticipation of WSRC Structure	126
4.5	Summary	129
5	Structural Capacity of Wheat Straw Reinforced Concrete for Pave- ments	132
5.1	Background	132
5.2	Materials and Experimental Procedures	134
5.2.1	Raw Ingredients	134
5.2.2	Mix Design and Procedure for Casting	135
5.2.3	Specimens	136

5.2.4	Testing Methodology	139
5.2.4.1	Flexural Strength Test	139
5.3	Test Results and Analyses	140
5.3.1	Properties under Flexural Loading	140
5.3.1.1	Specimens with Varying Flexural and Constant Shear Reinforcement (i.e. $\varnothing 6$ -76 mm)	140
5.3.1.2	Specimens with Varying Shear and Constant Flex- ural Rebars (i.e. 3 – $\varnothing 6$)	149
5.4	Discussion	156
5.5	Summary	166
6	Structural Performance of Wheat Straw Reinforced Concrete Pavement	168
6.1	Background	168
6.2	Materials and Testing Mechanism	170
6.2.1	Raw Materials	170
6.2.1.1	Wheat Straw Processing	170
6.2.1.2	Micro-structural Testing of Wheat Straw	171
6.2.2	Mix Design, Mixing Procedure, Laying Technique and Ma- terial Testing	172
6.2.2.1	Compressive Strength Test of Cylinder Specimens	175
6.2.3	Test Sections	178
6.2.4	Test Sections Evaluation	181
6.2.4.1	Compressive Strength Test of Cores	181
6.2.4.2	Micro-structural (i.e. SEM) Analysis of WSRC	183
6.2.4.3	Pavement Deflection Measurement	183
6.2.4.4	Visual Inspection to Observe Crack Initiation and Propagation	184
6.3	Result Findings	185
6.3.1	Compressive Properties of Test Sections Cores	185
6.3.1.1	Compressive Behavior	185
6.3.1.2	Compressive Strengths, Corresponding Strains, Com- pressive Energies Absorption and Compressive Tough- ness Indices of Drilled Cores	186
6.3.2	Micro-structural Analysis	188
6.3.2.1	SEM Analysis of Straw-concrete Matrix	188
6.3.3	Deflection Measurements of Test Sections	189
6.3.3.1	Vehicular Movement on Test Sections in terms of ESAL's	189
6.3.3.2	Load Carrying Capacities of PC and WSRC Pavement Test Sections	191
6.3.3.3	Load Transfer Efficiency (LTE) of PC and WSRC Pavement Test Sections	194
6.3.4	Crack Progression in PC and WSRC Pavement Test Sections	198
6.3.4.1	Crack Formation, Propagation and Patterns	198

6.4	Modelling	199
6.4.1	Reduced Thickness Validation of WSRC Pavement	199
6.4.2	Empirical Relationship Between Laboratory and Field Testing for WSRC Pavements	202
6.5	Summary	203
7	Conclusions and Recommendations	206
7.1	Conclusions	206
7.2	Recommendations for Future Research	209
	Bibliography	211
	Annexure A	244
	Annexure B	246
	Annexure C	256

List of Figures

1.1	Research motivation (a) Improved road network and (b) Economical and durable design and construction of rigid pavements	6
1.2	Flow diagram of research methodology.	18
2.1	Existing flexible and rigid pavement lanes in road network of Islamabad, Pakistan.	24
2.2	Stress distribution in reinforced concrete beam (a) Whitney stress distribution concept for plain concrete reported by Nilson <i>et al.</i> [119], and (b) FRC by Beshara <i>et al.</i> [118].	30
3.1	Wheat Straw (a) Soaked (b) Boiled and (c) Chemically treated.	58
3.2	Testing setup (a) Compressive strength test, (b) Splitting-tensile strength test, and (c) Flexural strength test.	61
3.3	Compressive stress \sim strain curves of (a) SWSRC, (b) BWSRC, (c) CWSRC with 1%, 2% and 3% content and (d) schematic diagram for energy absorption calculations.	64
3.4	Tested cylinder specimens of PC and WSRC with varied treatment and fibre content under compressive loading.	66
3.5	Comparison of σ_c , C_{em} , C_{ce} , and CTI of PC and WSRC with 1%, 2% and 3% content for (a) Soaked, (b) Boiled, and (c) Chemically treated straw.	70
3.6	Typical splitting-tensile load \sim deflection curves of (a) PC, (b) SWSRC, (c) BWSRC and (d) CWSRC with 1%, 2% and 3% content.	73
3.7	Tested cylinder specimens of PC and WSRC with varied treatment and fibre content under splitting-tensile loading.	74
3.8	Comparison of SS, S_{em} , S_{ce} , and STI of PC and WSRC with 1%, 2% and 3% content for (a) Soaked, (b) Boiled, and (c) Chemically treated straw.	77
3.9	Flexural load-displacement curves of (b) SWSRC, (c) BWSRC, (d) CWSRC with 1%, 2% and 3% content.	79
3.10	Tested beam specimens of PC and WSRC with varied treatment and fibre content under flexural loading	80
3.11	Comparison of MoR, F_{em} , F_{ce} , and FTI of PC and WSRC with 1%, 2% and 3% content for (a) Soaked, (b) Boiled, and (c) Chemically treated straw.	83
3.12	Micro-structural analysis of Soaked, Boiled and Chemically treated straw and their bond with concrete	85

4.1	EDX analysis of wheat straw (a) spectrum and (b) chemical composition.	92
4.2	Climatic conditions i.e. (a) Temperature, (b) Humidity and (c) Rain, of Islamabad, Pakistan from January 2016 to December 2019.	96
4.3	Compressive stress – strain curves of PC, SWSRC, BWSRC and CWSRC at (a) 0-day age [267], (b) 4-years aged under room conditions, (c) 4-years aged under climatic conditions and (d) 4-years aged under alternate wetting and drying conditions.	101
4.4	Tested cylinder specimens of PC and SWSRC-1% under compressive loading (a) at 0-day age [267] and (b) after 4-years ageing.	102
4.5	Effect of 4-years ageing conditions on residual (a) Compressive strength and (b) Compressive behavior of PC and SWSRC-1%.	105
4.6	Splitting-tensile load - deformation curves at (a) 0-day age [267], (b) 4-years aged under room conditions, (c) 4-years aged under climatic conditions and (d) 4-years aged under alternate wetting and drying conditions.	107
4.7	Tested cylinder specimens of PC and SWSRC-1% under splitting-tensile loading (a) at 0-day age [267] and (b) after 4-years ageing.	108
4.8	Effect of 4-years ageing conditions on residual (a) Splitting-tensile strength and (b) Splitting-tensile behavior of PC and SWSRC-1%.	111
4.9	Flexural load - displacement curves at (a) 0-day age [267], (b) 4-years aged under room conditions, (c) 4-years aged under climatic conditions and (d) 4-years aged under alternate wetting and drying conditions.	113
4.10	Tested specimens of PC and SWSRC-1% under flexural loading (a) at 0-day age [267] and (b) after 4-years ageing.	114
4.11	Effect of 4-years ageing conditions on residual (a) Modulus of Rupture and (b) Flexural behavior of PC and SWSRC-1%.	117
4.12	XRD analysis of Soaked Wheat Straw with and without ageing.	119
4.13	TGA analysis of Soaked Wheat Straw with and without ageing.	120
4.14	Micro-structural analysis of Soaked Straw and SWSRC-1% at (a) 0-day age (taken from Farooqi and Ali [267]), (b) 4-years aged under room conditions, (c) 4-years aged under climatic conditions and (d) 4-years aged under alternate wetting and drying.	122
4.15	Empirical relationship between flexural properties (i.e. <i>MoR</i> and <i>FTI</i>) of PC and SWSRC-1% with time.	127
5.1	Prepared wheat straw.	135
5.2	Beam-lets cross-sections of PC and WSRC with flexural and shear reinforcement detailing (a) PC, and (b) WSRC.	138
5.3	Testing setup (a) Schematic diagram, and (b) Experimental setup.	139
5.4	Load – deflection curves of PC and WSRC with flexural reinforcement (a) 2 – $\emptyset 6$, (b) 3 – $\emptyset 6$, and (c) 2 + 2 – $\emptyset 6$ and constant shear reinforcement (i.e. $\emptyset 6 - 76mm$).	142

5.5	Crack behavior of PC and WSRC specimens during flexural loading with varying flexural reinforcement and constant shear reinforcement (i.e. $\varnothing 6 - 76mm$).	143
5.6	Straw – concrete interaction with naked eye.	146
5.7	Comparison of FS, FEP, FE, FTI, and Δ of PC and WSRC with varying flexural reinforcement (i.e. $2 - \varnothing 6$, $3 - \varnothing 6$, and $2 + 2 - \varnothing 6$) with constant shear reinforcement (i.e. $\varnothing 6 - 76 mm$).	148
5.8	Load – deflection curves of PC and WSRC with shear reinforcement (a) $\varnothing 6 - 64 mm$, (b) $\varnothing 6 - 76 mm$, and (c) $\varnothing 6 - 89 mm$ and constant flexural reinforcement (i.e. $3 - \varnothing 6$).	151
5.9	Crack behavior of PC and WSRC specimens during flexural loading with varying shear reinforcement and constant flexural reinforcement (i.e. $3 - \varnothing 6$).	152
5.10	Comparison of FS, FEP, FE, FTI, and Δ of PC and WSRC with varying shear reinforcement (i.e. $\varnothing 6 - 64 mm$, $\varnothing 6 - 76 mm$, and $\varnothing 6 - 89 mm$) and with constant flexural reinforcement (i.e. $3 - \varnothing 6$).	155
6.1	Wheat straw (a) with naked eye and (b) SEM image from 2mm.	171
6.2	Wheat Straw analysis (a) EDX, (b) XRD and (c) TGA.	173
6.3	Workability tests (a) Slump value and (b) Compaction factor test of PC and WSRC mix	174
6.4	Stages in construction (a) Earthwork Preparation, (b) Levelling, (c) Lean layer & Levels, (d) Batching & Mixing, (e) Pouring, Laying & Finishing, (f) PC & WSRC Test Sections, (g) Curing and (h) Vehicular Movement.	176
6.5	Compressive behavior (a) Stress – strain curves and (b) tested specimens of PC and WSRC cylinders	178
6.6	PC and WSRC pavement test sections drawings (a) Plan, (b) Longitudinal section, and (c) Cross sections.	182
6.7	Core drilling test assembly.	184
6.8	Benkelman beam apparatus (a) Schematic diagram and (b) In-placed test assembly.	185
6.9	Compressive behavior (a) Stress – strain curves and (b) tested specimens of PC and WSRC cores.	187
6.10	SEM images of (a) Pulling-out and (b) Rupture of straw in concrete.	189
6.11	Per pass damaging vehicles with \geq ESAL on PC and WSRC pavement test sections.	192
6.12	Benkelman beam deflection measurements for PC and WSRC pavement test sections	194
6.13	Behavior of (a) JPCP and (b) JWSRCP test sections in terms of LTE.	197
6.14	Cracks progression on JPCP and JWSRCP test sections.	199
A1	Specimens at different stages; (a) fresh state tests and moulding, (b) ageing conditions, (c) hardened state tests and (d) just before testing.	245

B1	Tested cylinder specimens of SWSRC-2-3%, BWSRC-1-3% and CWSRC-1-3% under compressive loading after 4-years ageing under (a) room conditions, (b) climatic conditions, and (c) alternate wetting and drying conditions.	253
B2	Tested cylinder specimens of SWSRC-2-3%, BWSRC-1-3% and CWSRC-1-3% under splitting-tensile loading after 4-years ageing under (a) room conditions, (b) climatic conditions, and (c) alternate wetting and drying conditions.	254
B3	Tested specimens of SWSRC-1-3%, BWSRC-1-3% and CWSRC-1-3% under flexural loading after 4-years ageing under (a) room conditions, (b) climatic conditions, and (c) alternate wetting and drying conditions.	255
C1	Trip cycles of heavy commercial vehicles to and from construction site through PC and JWSRCP test sections.	257

List of Tables

2.1	Distresses in rigid pavements.	25
2.2	Distresses in rigid pavements of developing countries.	27
2.3	Typical proportions for normal weight fibre reinforced concrete.	29
2.4	Properties and applications of steel fibre reinforced concrete.	32
2.5	Properties and applications of artificial fibre reinforced concrete.	33
2.6	Studies on natural fibres and natural fibre reinforced concrete.	36
2.7	Studies on wheat straw reinforced composites.	39
2.8	Evaluation techniques for durability of natural fibres.	42
2.9	Proposed treatment techniques for natural fibres in cement composites.	43
2.10	Use of steel fibre reinforced concrete for pavement applications.	45
2.11	Use of artificial fibre reinforced concrete for pavement applications.	46
2.12	Use of natural fibre reinforced concrete for pavement applications.	48
3.1	Chemical composition of BESTWAY cement.	56
3.2	Chemical composition of wheat straw.	57
3.3	Water absorption of wheat straw and fresh and hardened state properties of PC, SWSRC, BWSRC and CWSRC.	63
3.4	Compressive Strength (σ), Energies absorption under compressive load (Cem, Cep, Ce) and Compressive Toughness Index (CTI) of PC, SWSRC, BWSRC and CWSRC.	69
3.5	Splitting-tensile Strength (SS), Energies absorption under splitting-tensile load (Sem, Sep, Se) and Splitting-tensile Toughness Index (STI) of PC, SWSRC, BWSRC and CWSRC.	75
3.6	Modulus of Rupture (MoR), Energies absorption under flexural load (Fem, Fep, Fe) and Flexural Toughness Index (FTI) of PC, SWSRC, BWSRC and CWSRC.	82
4.1	Physical properties of wheat straw.	91
4.2	Specimen labelling and testing scheme of wheat straw reinforced concrete for 4-years ageing under different conditions.	95
4.3	Residual properties under compressive loading (i.e. σ_r , Ce_r and CTI_r) of PC and SWSRC-1% at 0 and 4-years age.	104
4.4	Residual properties under splitting-tensile loading (i.e. SS_r , Se_r and STI_r) of PC and SWSRC-1% at 0 and 4-years age.	110
4.5	Residual properties under flexural loading (i.e. MoR_r , Fe_r and FTI_r) of PC and SWSRC-1% at 0 and 4-years age.	116

4.6	Optimization of straw content and treatment for wheat straw reinforced concrete after 4-years age.	125
4.7	Performance index of PC and WSRC at 5, 10, 15 and 20 years.	128
5.1	Labelling scheme of PC and WSRC beam-lets with steel rebars.	137
5.2	Loads and Deflections for tested PC and WSRC beam-lets with varying flexural reinforcement and constant shear reinforcement (i.e. $\varnothing 6 - 76 \text{ mm}$).	145
5.3	Flexural strengths, Flexural energies absorbed (FE1, FEM, FEP, FE), and Flexural Toughness Index (FTI) for PC and WSRC beam-lets with varying flexural reinforcement and constant shear reinforcement (i.e. $\varnothing 6 - 76 \text{ mm}$).	148
5.4	Loads and deflections for tested PC and WSRC beam-lets with varying shear reinforcement and constant flexural reinforcement (i.e. $3 - \varnothing 6$).	153
5.5	Flexural strengths, Flexural energies absorbed (FE1, FEM, FEP, FE), and Flexural Toughness Index (FTI) for PC and WSRC beam-lets with varying shear reinforcement and constant flexural reinforcement (i.e. $3 - \varnothing 6$).	155
5.6	Comparison of theoretical and experimental moment capacities for PC and WSRC with flexural and shear rebars.	157
5.7	Comparison of theoretical and experimental shear capacities for PC and WSRC with flexural and shear rebars.	159
5.8	Increased flexural strengths of WSRC specimens w.r.t PC specimens.	164
5.9	Design parameters for 1998 AASHTO rigid pavement design model.	164
5.10	Comparison of PC and WSRC pavement in terms of thicknesses, cost and CO_2e emissions.	165
6.1	Percentage (%) contents of elements in Wheat Straw.	172
6.2	Compressive properties of PC and WSRC cylinders.	179
6.3	Design considerations for concrete layer thickness in plain concrete pavement test section.	180
6.4	Compressive properties of PC and WSRC cores.	188
6.5	Quantification of ESAL's on PC and WSRC test sections over 18-months period.	191
6.6	Benkelman beam deflection measurements for PC and WSRC pavement test sections for both loaded and unloaded cases.	195
6.7	Load Transfer Efficiency (LTE) of PC and WSRC pavement test sections.	197
6.8	Cracks progression and punch-out(s) in JPCP and JWSRCP test sections over 18-months period.	200
6.9	Performance index of JPCP and JWSRCP test sections.	202
B1	Monthly-average climatic data of Islamabad, Pakistan (January 2016 - December 2019).	247

B2	Residual compressive properties (i.e. σ_r , Ce_r and CTI_r) of SWSRC at 4-years age.	248
B3	Residual compressive properties (i.e. σ_r , Ce_r and CTI_r) of BWSRC at 4-years age.	248
B4	Residual compressive properties (i.e. σ_r , Ce_r and CTI_r) of CWSRC at 4-years age.	249
B5	Residual splitting-tensile properties (i.e. SS_r , Se_r and STI_r) of SWSRC - at 4-years age.	249
B6	Residual splitting-tensile properties (i.e. SS_r , Se_r and STI_r) of BWSRC at 4-years age.	250
B7	Residual splitting-tensile properties (i.e. SS_r , Se_r and STI_r) of CWSRC at 4-years age.	250
B8	Residual flexural properties (i.e. MoR_r , Fe_r and FTI_r) of SWSRC at 4-years age.	251
B9	Residual flexural properties (i.e. MoR_r , Fe_r and FTI_r) of BWSRC at 4-years age.	251
B10	Residual flexural properties (i.e. MoR_r , Fe_r and FTI_r) of CWSRC at 4-years age.	252

Abbreviations

ACI	American Concrete Institute
AASHTO	American Association of State Highway and Transportation Officials
ASTM	American Society for Testing and Materials
BB	Benkelman Beam
BWSRC	Boiled Wheat Straw Reinforced Concrete
C_e	Absorbed Compressive Energy (kJ/m^3)
C_{e,c}	Compressive Energy Absorbed by Cylinder Specimen (kJ/m^3)
C_{e,f}	Compressive Energy Absorbed by Drilled Core (kJ/m^3)
C_{e,r}	Residual Compressive Energy Absorbed (kJ/m^3)
C_{em}	Energy Absorption up to Maximum Stress (kJ/m^3)
C_{em,c}	Compressive Energy Absorbed up to the Maximum Stress by Cylinder (kJ/m^3)
C_{em,f}	Compressive Energy Absorbed up to the Maximum Stress by Core (kJ/m^3)
C_{ep}	Energy Absorption after the Maximum Stress (kJ/m^3)
C_{ep,c}	Compressive Energy Absorbed Post the Maximum Stress by Cylinder (kJ/m^3)
C_{ep,f}	Compressive Energy Absorbed Post the Maximum Stress by Core (kJ/m^3)
CTI	Compressive Toughness Index
CTI_c	Compressive Toughness Index of Cylinder Specimens
CTI_f	Compressive Toughness Index of Drilled Cores
CTI_r	Residual Compressive Toughness Index

CWSRC	Chemically (NaOH) Treated Wheat Straw Reinforced Concrete
D_f	Final Deflection (mm)
D_i	Intermediate Deflection (mm)
D_o	Initial Deflection (mm)
EDX	Energy Dispersive X-ray
ESAL	Equivalent Standard Axle Load
Fe	Flexural Energy Absorbed (J)
Fe_r	Residual Energy Absorption under Flexural Loading (J)
Fem	Energy Absorption up to Maximum Flexural Load (J)
Fep	Energy Absorption after the Maximum Flexural Load (J)
FE1	Flexural Energy Absorbed up to the First Crack (kN.mm)
FE	Total Flexural Energy Absorbed (kN.mm)
FEM	Flexural Energy Absorbed from First Crack to the Maximum Load (kN.mm)
FEP	Flexural Energy Absorbed Post the Maximum Load (kN.mm)
FRC	Fibre Reinforced Concrete
FS	Flexural Strength (MPa)
FTI	Flexural Toughness Index
FTI_r	Residual Toughness Index under Flexural Loading
FWD	Falling Weight Deflectometer
ITZ	Interfacial Transition Zone
JPCP	Jointed Plain Concrete Pavement
JWSRCP	Jointed Wheat Straw Reinforced Concrete Pavement
LEF	Load Equivalency Factor
LTE	Load Transfer Efficiency
l_f	Length of Fibres
L₁	Load at the First crack (kN)
L_m	Maximum Load (kN)
L_u	Ultimate Load (kN)
MoR	Modulus of Rupture
MoR_r	Residual Modulus of Rupture (MPa)

NA	Neutral Axis
NDT	Non-Destructive Testing
NFRC	Natural Fibre Reinforced Concrete
OPC	Ordinary Portland Cement
PC	Plain Concrete
PFRC	Polyester Fiber Reinforced Concrete
PI	Performance Index
Se	Splitting-tensile Energy Absorbed (J)
Se_r	Residual Energy Absorption under Splitting-tensile Loading (J)
Sem	Energy Absorption up to Maximum Splitting-tensile Load (J)
SEM	Scanning Electron Microscope
Sep	Energy Absorption after the Maximum Splitting-tensile Load (J)
SS	Splitting-tensile Strength (MPa)
SS_r	Residual Splitting-tensile Strength (MPa)
STI	Splitting-tensile Toughness Index
STI_r	Residual Toughness Index under Splitting-tensile Loading
SWSRC	Soaked Wheat Straw Reinforced Concrete
TGA	Thermogravimetric Analysis
T_f	Tensile Strength of Fibres in Tension Region (N)
T_s	Tensile Strength of Steel in Tension Region (N)
T_{WSRC}	Tensile Strength of Straw in Tension Region (N)
UNDP	United Nations Development Programme
USDA	United States Department of Agriculture
V_f	Volume of Fibres in Concrete
WSRC	Wheat Straw Reinforced Concrete
XRD	X-Ray Diffraction

Symbols

f_y	Tensile Strength of Steel (MPa)
f_s	Compressive Strength of Concrete (MPa)
M_r	Theoretical Moment Capacity of PC (kN.mm)
M_{PCExp}	Experimental Moment Capacity of PC (kN.mm)
M_{WSRC}	Theoretical Moment Capacity of WSRC (kN.mm)
$M_{WSRCExp}$	Experimental Moment Capacity of WSRC (kN.mm)
V	Shear Capacity (kN)
V_{PCExp}	Experimental Shear Capacity of PC (kN)
V_{PCTheo}	Theoretical Shear Capacity of PC (kN)
$V_{WSRCExp}$	Experimental Shear Capacity of WSRC (kN)
$V_{WSRCTheo}$	Theoretical Shear Capacity of WSRC (kN)
X_i	Temperature Correction
Δ	Deflection
ϕ	Diameter
ϕ_f	Diameter of Fibres
σ	Compressive Strength (MPa)
σ_r	Residual Compressive Strength (MPa)
σ_c	Compressive Strength of Cylinder Specimens (MPa)
σ_f	Compressive Strength of Drilled Cores (MPa)
ϵ_c	Corresponding Strain of Cylinder Specimens
ϵ_f	Corresponding Strain of Drilled Cores
μ	Mean Deflection

Chapter 1

Introduction

1.1 Theoretical Background

Road networks are key consideration in any country as its socio-economic progress is based on it. Accordingly, the design, construction, maintenance and/or rehabilitation, of pavements demand more attention. Pavements aim to sustain the vehicular and pedestrian movements and are broadly classified as flexible and rigid pavements, based on load distribution mechanism. In flexible pavements, the magnitude of vehicular load diminishes over a larger area while its transmission towards sub-grade through wearing, base and sub-base course. However, in rigid pavements, the high strength cement concrete slab, due to its rigidity and high elastic modulus, resists and distributes the traffic load over a wider area of subgrade. Increased traffic volume (i.e. Heavy Traffic) and less stable natural soil strata demands pavements with long structural life and more durability. Conventional concrete pavements have longer structural life and superior durability as compared to the asphaltic concrete pavements. Therefore, the rigid pavements, due to lower maintenance and reduction in lifetime energy consumption, can provide more sustainable solution [1]. However, the combination of drying shrinkage, temperature gradients, built-in temperature curls, and moisture gradients increase the

number of locations which can be prone to many distresses (i.e. early age micro-shrinkage-cracking, fatigue failure, bottom-up and top-down transverse cracking, and punch-outs etc.) in concrete pavements. The use of concrete pavements has increased over the past decades in developing countries like Pakistan. But, due to poor construction practices and measures to control the quality, many types of early age distresses and premature failures have been observed in the newly constructed rigid pavements. The commonly observed flaws in the rigid pavements of developing countries are in the form of micro-shrinkage cracking, full depth longitudinal and transverse cracking, durability cracking, punchouts, and settlement cracking etc. Lack of understanding some fundamental concepts regarding behavior of concrete in pavements is one of the reasons behind rigid pavement failures. Concrete is the most widely used civil engineering construction material by far, and its usage in various civil engineering applications is raising all over the globe. The only issue of concrete is that it is basically a brittle material i.e. poor resistance to crack opening and propagation and relatively low tensile strength. Due to this, a number of distresses (as mentioned earlier) occur in the rigid pavements, and steel reinforcement is usually required in concrete for providing resistance to various types of cracks. Hence, the initial cost of concrete pavements is very much higher than that of asphalt pavements, therefore, its extensive use is still prevented.

Fibres play an important role in reducing the brittleness of conventional concrete, when used as dispersed reinforcement. For strengthening the brittle matrices, straw and horsehair have been used since Biblical times. Romualdi, for the very first time in his two papers [2, 3], introduced the steel fibres as the dispersed reinforcement in concrete. The addition of dispersed fibres in concrete enhances the energy absorption capability and crack resistance in the conventional brittle natured plain concrete [4, 5]. Erdogmus [6] summarized his findings of 10 years of research on usage of fibre reinforced concrete in structural rehabilitation and masonry construction. A technique, named “FRC retrofit technique”, was also proposed in this study to rehabilitate two-way slabs of reinforced concrete.

Sustainable development is a key consideration in current era. Each and every step to achieve sustainable development goals has its own significance. In this global effort to get the sustainable solutions, the focus is on reduction of biodegradable materials and to minimize the waste, which ultimately contributes in global warming. Saving, re-using, and re-cycling are paramount concerns now a days, which are gaining the attention of researchers to cater the environmental issues [7–10]. In recent years, considerable interest has been developed in using the natural fibres in the cement composites for having the alternate sustainable, economical, and eco-friendly building materials. Natural fibres have the potential to be used as reinforcement for overcoming the conventional deficiencies in the concrete. Researchers have used natural fibres in concrete for various applications as an alternative economical replacement of artificial or steel fibres. The benefit of natural fibres over artificial fibres may also include their flexibility in form of easy handling. Natural/vegetable fibres are cheap and available in surplus in tropical and sub-tropical regions. Hence, for improving the properties of composites, the use of plant based natural fibres as a low-cost flexible and renewable construction material can contribute towards sustainable development. Ramakrishna and Sundrajaan [11] reported that the use of natural fibres can lead to sustainable development. The natural fibres, figured out as reinforcement in cement composites for civil engineering applications are; coir, sisal, sugarcane, banana, bamboo, malva, date, vakka, kenaf bast, jute, palm, hemp, pineapple leaf, flax, ramie bast, abbaca leaf, hibiscus cannabinus, elephant grass, wheat straw and sansevieria leaf [12–19].

The effect of artificial fibres in concrete composites, for rigid pavements, has also been investigated by many researchers [20–36]. Generally improved behavior of fibre reinforced concrete, for rigid pavement applications, has been observed compared to that of plain concrete. The incorporation of steel fibres in concrete pavement improves the mechanical properties of concrete, resulting in significant increase in its load carrying capacity even after cracking [37]. The presence of fibres resists the formation of first crack. In addition to the formation of first crack, the crack propagation phenomenon is also delayed due to the arresting of cracks by fibres. Accordingly, the capacity of fibre reinforced concrete, in terms of load

carrying, is enhanced. The addition of fibres in concrete can also lead towards high tensile strength and strain capacity allowing reduction of pavement layer thickness [38]. Sinha *et al.* [26] reported that the use of fibres can lead towards reduction in pavement depth also by reducing the reinforcement and thus reducing the overall costs. As far as use of natural fibres for concrete pavement applications is concerned; as discussed earlier, natural fibre reinforced concrete is comparable with artificial fibre reinforced concrete and steel fibre reinforced concrete. But, to the best of author's knowledge, natural fibres have been investigated for concrete pavements, but with limited scope so far.

However, the durability of natural fibres is a matter of concerns; as some deficiencies/degradation of agricultural/plant fibre reinforced cement composites in terms of durability have been observed along with the enhanced behavior. This might be due to the mineralization of fibres and alkali attacks under the exposure of climatic/environmental conditions [39]. Natural fibres are prone to deterioration under the exposure of moisture depicting their moisture sensitivity. The chemical and mechanical properties of natural fibres are highly affected considering their exposure to moisture/alkaline environments. Therefore, when natural fibres bring in contact with alkaline matrix of cement, the phenomenon of alkaline hydrolysis occurs, which results in deterioration of natural fibre thereby affecting their durability [11, 40–42]. Hence, in construction industry, application of natural fibres is still quite limited. The limited use of natural fibres for civil engineering applications is due to the lack in understanding the techniques for improving the durability while making ductile materials [43–45]. Accordingly, the durability evaluation studies on natural fibre reinforced concrete are made after exposing it in different environmental and ageing conditions [11, 15, 16, 46–50]. A number of solutions (i.e. immersion in fresh water, slurried silica fume, NaOH, Ca (OH)₂, and H₂SO₄ solutions; carbonation of studied matrix; cement replacement with calcined clay and metakaoline etc.) were proposed and studied by various researchers to increase the durability of natural fibres [11, 15, 48, 51, 52]. Thus, the durability of natural fibres does not provide much hindrance for civil engineering applications. But the durability should be given proper consideration due to organic nature of

fibres. Concrete pavements are mostly used for airfield runways, bridge decks, road surfaces, and parking lots. These pavements are exposed to dynamic loading and are also subjected to rigorous environmental conditions. It has been a technical and significant issue to enhance the durability and to prolong the design service life of concrete pavements in the world [53]. Therefore, the long-term durability of WSRC pavements should be investigated in detail as pavements are directly exposed to climatic conditions.

1.2 Research Motivation and Problem Statement

Conventional concrete pavements have longer structural life and superior durability as compared to the asphalt pavements. However, its more extensive use is still not common due to its higher initial cost, mainly due to the cost of cement and reinforcement. Moreover, concrete is basically a material having brittle nature with minimum strain-capacity and ultimately low toughness. Therefore, the fatigue failure and cracking can potentially be exhibited at more locations in concrete pavements due to the combination of temperature gradients, moisture gradients, drying shrinkage, and built-in temperature curl, as pavements are directly exposed to environmental conditions. Accordingly, the motivation for conducting this research is to have improved and better road network in Pakistan for the prosperity (Figure 1.1(a)). And the development of economical, durable design and/or construction techniques for new cement concrete pavements by using locally and abundantly available natural fibres (Figure 1.1(b)).

Whereas, the problem statement is as follows:

The frequent movement of overloaded heavy traffic vehicles causes the generation of continuous distresses in flexible pavements which demands high maintenance activities. To cater this issue, dedicated lanes of rigid pavement are high in demand for accommodation of heavy commercial traffic and weak soil strata. However, the high initial cost of rigid pavements is still the point of concern in developing countries like Pakistan. In addition, the poor construction practices and brittle nature



FIGURE 1.1: Research motivation (a) Improved road network and (b) Economical and durable design and construction of rigid pavements

of cement concrete leads towards early age deterioration of newly constructed rigid pavements. The use of dispersed steel/artificial fibres reinforcement in concrete for improving the load carrying capacities, crack resistance, and post cracking behavior is reported by many researchers. The results of natural fibre reinforced concrete are comparable with artificial fibre reinforced concrete. However, the in-depth knowledge on wheat straw as dispersed fibre in cement concrete composites is missing. Therefore, there is a need to investigate wheat straw reinforced concrete in detail. Natural fibre reinforced concrete can be used for construction economical and durable rigid pavements. But, it has not been explored yet in that way for pavement applications. Hence, the wheat straw reinforced concrete needs to be evaluated for pavement applications. However, wheat straw is an organic material and pavements are directly exposed to climatic conditions (i.e. variation in temperature, rainfall, snow-fall etc.). Accordingly, for such applications, the durability of wheat straw reinforced concrete needs to be examined. Pavements are live in nature due to their exposure to vehicular loading and real environmental conditions all the time. Therefore, the true behavior of pavements, in terms of performance, needs to be evaluated.

Accordingly, the research questions of this doctoral study are:

- What are the major flaws or distresses in rigid pavements?
- What are the main distresses observed in rigid pavements of developing countries?

- How can these issues in concrete pavements be resolved?
- How the brittleness of concrete can be reduced?
- Do the capacities and behavior of concrete improve with the addition of fibres?
- Can the behavior of wheat straw reinforced concrete be improved?
- How can the durability of wheat straw reinforced concrete be examined?
- What can be the possible ageing conditions to study the durability of wheat straw reinforced concrete?
- Can wheat straw reinforced concrete have better residual strength after accelerated ageing?
- Can crack initiation in pavements be delayed by using wheat straw in concrete?
- Can post cracking behavior of concrete pavement be improved by using straw?
- Can capacity of wheat straw reinforced concrete be enhanced?
- Can performance of wheat straw reinforced concrete test sections be better?
- Can incorporation of wheat straw result in reduction of pavement thickness?
- What can be the effect on cost and sustainability of wheat straw reinforced concrete pavement?

1.3 Overall Aim of the Research Program and Specific Goal of this Doctoral Study

The overall aim of the research program is to develop durable and economic design and/or construction techniques for new rigid pavements by using locally and

abundantly available natural fibres in concrete. The main focus of this doctoral research is to explore the suitability of wheat straw for the said aim.

Accordingly, the specific goals of this doctoral study are:

- To identify the current flaws in rigid pavements and future recommendations for betterment of rigid pavements in developing countries.
- Optimization of wheat straw reinforced concrete mix.
- Long-term durability of wheat straw reinforced concrete to be used in concrete pavements.
- Structural capacity of wheat reinforced concrete to be considered for pavement design.
- Performance evaluation of wheat straw reinforced concrete pavement.

1.4 Research Significance, Perceived Innovation and Utilization as a Product

1.4.1 Significance of this Study

Road network is the backbone of the economy of any country. So, the better road network to accommodate the wide variety of traffic, including heavy freight vehicles, is always high in demand. To meet the said needs, efforts are made to increase the serviceability of pavements. Rigid pavements depict more service life as compared to that of flexible one, however, their high construction cost poses much hindrance in their use. Moreover, the construction of pavements demands huge amount of materials due to which bulk quantity of fossil fuels and natural resources are consumed to get the materials from cradle to site and then transformation into a product. Which is ultimately contributing to environmental degradation at a larger scale. Heading towards the sustainable development, in

pursuance of United Nation Development Programme (UNDP) sustainable goals, the increasing environmental pollution (which is depleting the ozone layer), needs to be addressed. The said major portion of environmental/air pollution has been the result of burning agricultural wastes in tropical and sub-tropical regions. Similarly, as mentioned earlier, the consumption of natural resources and fossil fuels, which is increasing day by day to meet the requirements of construction industry, is also contributing towards environmental degradation. In order to achieve these sustainable goals, the current study can significantly play its role by using agricultural waste/plant fibres (i.e. wheat straw) as a dispersed reinforcing material in concrete, for concrete pavements. This will contribute not only in reducing the high initial cost of concrete pavements by consuming low-cost, which is negligible with respect to other construction materials, natural fibres to address the economic crisis, but it will also reduce the consumption of conventional materials, ultimately reducing the consumption of natural resources. Furthermore, the environmental pollution in terms of CO₂ emissions, caused by burning of that particular agricultural wastes/plant fibres can also be reduced up to a large extent. Hence, the usage of wheat straw as a construction material in concrete roads can significantly lead towards green, sustainable and economical development.

1.4.2 Perceived Innovation from this Study

Wheat is globally the most widely cultivated crop. The annual world wheat production (i.e. for 2018-2019) is 731.46 million tons as reported by United States Department of Agriculture (USDA). The grain to straw yield ratio for wheat crop is 0.94, which is shown as a result of regression analysis reported by [54-56]. However, the actual grain yield ratio is usually less than that of theoretical estimates. The less extraction of straw in field may be due to the economic and environmental factors (rain etc.), along with straw collection machinery, and other field specific factors. Therefore, the actual wheat grain yield ratio is approximately 0.85 based on the statistics reported by Bakker et al. [56]. These statistics provide an idea of average lump sum 55 – 45% (grain-straw%) per wheat crop cultivation,

which is ultimately concluded with surplus availability of wheat straw in most of the tropical and sub-tropical regions of the world. Out of 731.46 million tons global annual wheat production, Pakistan produced 25.6 million tons (2018-2019) as reported by United States Department of Agriculture (USDA). Accordingly, 22 million tonnes wheat straw, i.e. agricultural waste/by-product of wheat crop, is produced annually in Pakistan, depicting its abundant availability. This agricultural waste, i.e. wheat straw, is usually generated during harvesting process [57]. These crop residues (i.e. wheat straw) are usually considered as waste but actually these are valuable natural resources which are somewhat used for livestock feed and some other non-technical applications. Therefore, the commercial cost of wheat straw is PKR 10/- per kg which is minimal, when compared to that of artificial/steel fibres, i.e. ranges from PKR 285/- to 335/- per kg. The portion of wheat straw production, which is surplus to said applications (including livestock feed), is considered as waste material and is usually burnt for disposal, that adversely effects the environment. Henceforth, the incorporation of low-cost wheat straw in concrete pavement, as dispersed reinforcement, can significantly play its role in reduction of construction cost and environmental degradation (in terms of natural resources consumption and less CO₂ emissions). This will ultimately be contributing towards 12,131 km length of major highways, motorways and expressways etc. out of 263,775 kms of Pakistan total road network, as reported by National Highway Authority (NHA). These highways carry 65% of total commercial freight that demands dedicated rigid pavement lane on both ends throughout the length, to accommodate the heavy traffic loading. Therefore, wheat straw are considered for their potential utilization in cement concrete composites, for possible civil engineering structural application i.e. rigid pavement. Thus, the perceived innovation from this study is as follows:

- Use of wheat straw in cement concrete composite in civil engineering domain.
- Wheat straw reinforced concrete as an alternative civil engineering construction material, for structural and non-structural applications, in Pakistan.

- Wheat straw reinforced concrete for rigid pavement applications for better road network system in Pakistan.

1.4.3 Utilization of Current Study as a Product

Sustainable development is a key concern now a days. In pursuit of this, the rapid depletion of ozone layer due to global warming and environmental degradation is also a major issue. Degradation in environment is mainly due to the excessive consumption of fossil fuels and natural resources. Considerable amount of this consumption is related to construction industry. The development of a civil engineering construction project, from cradle to grave, is all about utilization of natural resources in terms of naturally occurred raw materials and excessive burning of fossil fuels for production of manufactured materials. Cement is the most widely used construction material but its manufacturing consumes 1.6 MWh against one-ton production of cement and exhales almost one-ton of CO₂ emissions that contributes towards environment degradation. Currently, 7% of worldwide CO₂ emissions are contributed only by the cement industry [58–62]. Furthermore, transportation of materials and all the construction processes also contribute towards fossil fuel burning. Road networks are the backbone of any country's economy. Therefore, it demands extra attention whether in terms of brainstorming or fiscal budgetary allocations. So, the bulk portion of fiscal budget in any country is usually reserved for development, including design, construction, maintenance and/or rehabilitation, of pavements. The violation of overloading rule is usually observed in different countries particularly developing ones, i.e. Pakistan, which ultimately results in frequent maintenance and rehabilitation cycles of asphaltic pavements. Accordingly, the trend is shifting from usage of asphalt pavements to rigid pavements, in order to bear more load and to strengthen the poor subgrades. However, the development/construction of rigid pavements in developing countries is still restricted due to higher initial cost and early age distresses in concrete pavements as well. The higher initial cost is due to the usage of materials in bulk quantities up to the large extent of lengths in kilometers. Therefore, the need is to

economize the construction of rigid pavements, whether in terms of construction cost or reduction in occurrence and rapid propagation of distresses.

Hence, the usage of natural fibres can lead towards sustainable and economic development. Use of natural fibres enables saving of approximately 20-50% of energy and CO₂ emissions as per Life Cycle Assessment done by [63–65]. Wheat straw is an agricultural waste/by-product of wheat crop, the major portion of which is burnt to waste otherwise. The annual production of wheat is up to 731.6 million tons which yields almost 695 million tons production of wheat straw as per 0.85 grain to straw ratio. The cost of wheat straw is almost nothing when compared to that of high cost cement concrete ingredients. Moreover, 7% reduction in thickness of concrete layer in rigid pavements with comparable improved performance will accumulate with significantly less requirement of material(s) when considered in kilometers of length. Accordingly, the construction cost and maintenance activities can be economized by using low-cost, flexible and abundantly available wheat straw. Secondly, the productive utilization of wheat straw instead of wastage, will ultimately result in sustainable development. Therefore, the possible application of wheat straw reinforced concrete is the construction of sustainable rigid pavements.

1.5 Scope of Work and Study Limitation

1.5.1 Scope of this Doctoral Study

The scope of this work is set in line with the specific aims of the current doctoral study. Firstly, the types and functions of rigid pavements, their behavior under the application of vehicular movement and the distresses, major or minor, occurring in cement concrete pavements have been explored through detailed literature. In addition to that, the governing parameters for these distresses and their possible remedial measures have also been explored through literature. Out of these, the

literature review regarding usage of fibre reinforced concrete for pavement applications, with the focus on usage of natural fibres, has also been conducted. The data regarding pavements of Pakistan are also collected from NHA.

Secondly, wheat straw reinforced concrete is considered to be explored for structural applications. Accordingly, the optimization for mix design of wheat straw reinforced concrete i.e. contents and pre-treatment techniques of straw to be incorporated in cement concrete composite, is done. Three straw contents, i.e. 1%, 2% and 3%, by mass of wet concrete, and three pre-treatment techniques i.e. soaking, boiling and chemical treatment of straw, are considered for the optimization of wheat straw reinforced concrete mix.

However, due to bio-degradable organic nature of wheat straw, its durability is of major concern for its incorporation in cement composites, which are to be used in structural applications. Henceforth, in parallel, the detailed investigation on long-term laboratory durability of wheat straw reinforced concrete has also been made by keeping the specimens in different natural and accelerated ageing conditions i.e. at room conditions, in alternate wetting and drying conditions, and under real environmental conditions of Islamabad, Pakistan, for a period of 4 years (48-months).

Accordingly, to get an indication regarding the potential of wheat straw reinforced concrete for rigid pavements, the flexural strength, i.e. governing parameter for rigid pavement design, is determined experimentally in laboratory through monotonic testing.

Afterwards, detailed comparative evaluation of jointed wheat straw reinforced concrete pavement and jointed plain concrete pavement test sections has also been made. This evaluation is made after the application of heavy vehicular traffic on the constructed test sections. The construction of plain concrete test section is done by using AASHTO rigid pavement design equation. However, for wheat straw reinforced concrete pavement test section, the modified design equation is considered. The construction practices and structural performance of wheat straw reinforced concrete pavement is explored.

1.5.1.1 Rationale Behind the Selected Variables

The bulk annual production of wheat straw, i.e. 22 Million Tons, in Pakistan and its commercial availability in the ready form are the reasons for its selection to start with. The commercially available wheat straw length, i.e. approximately 25 mm, is selected to avoid any additional processing cost. As reported in literature, the ranges of fibre contents for cement composites are; 1-6%, by mass of wet concrete [11, 18, 44, 66–68]. However, to avoid improper compaction issue (due to higher contents of low-density straw) in order to achieve maximum possible strength, only 1%, 2% and 3% straw contents, by mass of wet concrete, are considered. For removal of extraneous material and dust/dry particles from straw surface, three simple pre-treatment techniques, out of many [14, 15, 48, 52, 69, 70], i.e. soaking in tap water, boiling water processing and NaOH treatment, are selected. Aiming towards intended application, i.e. rigid pavement, three ageing conditions are selected to get an idea regarding long-term durability of wheat straw reinforced concrete (WSRC), when implemented in the respective application. As pavements are exposed to natural weathering/climatic/environmental conditions throughout the design life, therefore open-air weathering ageing condition is selected. In addition, to predict the performance of WSRC pavement under worst circumstances as in case of urban flooding or effect of vehicular movement on the pavement under stranded water, the accelerated ageing condition, i.e. alternate wetting and drying, is selected. Whereas, room ageing condition is selected to get the reference values.

1.5.2 Limitations of this Doctoral Study

Only the commercially available wheat straw length is considered. The equally important monotonic testing is performed in the laboratory to explore the material properties as the cyclic testing is not in the scope of this particular PhD study. However, the fatigue behavior of wheat straw reinforced concrete (WSRC) pavement is explored by the application of heavy vehicular loading cycles on field test

sections, as it is difficult to generate the combined effect of environmental/climatic (i.e. temperature and alternate wetting and drying due to precipitation cycles) and traffic stresses in laboratory to depict the behavior of WSRC pavement. But, the application of mixed traffic on regular basis is also unable to achieve on constructed test sections. In addition, due to limitations of equipment, only Benkelman beam apparatus is considered for deflection measurements of plain concrete and wheat straw reinforced concrete pavement test sections.

1.6 Brief Methodology

Rigid pavement distresses, governing parameters and their possible remedial measures are identified. Material properties of WSRC are explored for its optimization. In parallel, specimens are placed under three ageing conditions for 4 years to investigate its durability. The optimized WSRC with steel rebars is studied experimentally for flexural strength, i.e. governing parameter for rigid pavement design. Based on the structural capacity of WSRC in terms of flexural strength, the performance evaluation of optimized WSRC pavement test section is made.

1.6.1 Flaws in Rigid Pavements

In this task, the flaws or distresses in the concrete pavements of developed and developing countries are identified through detailed literature review. The governing parameters are studied and possible remedial measures are also extracted from the findings of various researchers. The existing rigid pavements of Islamabad, Pakistan are also identified with the help of site visits and are associated with the data acquired from the local highway authority (i.e. NHA). The deteriorations and distresses in pavements are explored for existing concrete pavements in the surrounding areas. The possible governing reasons for these flaws are rationally analysed. Accordingly, the crunch remedial measures are extracted through this exercise and literature, keeping in mind economical and fast repairs, long service durable life and sustainable solutions.

1.6.2 Optimization of Wheat Straw Reinforced Concrete

In this task, the mix proportions along with the contents of straw and the treatment techniques, required for straw before using it in concrete, are optimized for wheat straw reinforced concrete. The effect of pre-treatment and content of wheat straw on the behavior of concrete is explored by evaluating its static properties (i.e. compressive, splitting-tensile and flexural behaviours) after curing period. The properties of plain concrete are taken as reference. Almost 25 mm long straw having content of 1%, 2%, and 3%, by mass of wet concrete, are considered. Cylinder and beam specimens are cast. Soaked, boiled and chemically treated wheat straw are used to make soaked wheat straw reinforced concrete, boiled wheat straw reinforced concrete, and chemically treated wheat straw reinforced concrete, respectively. The specimens of above-mentioned combinations are tested to determine the mechanical properties for optimization of contents and pre-treatment techniques for wheat straw reinforced concrete. The tests standards and references used for this task are; ASTM C138/C138M-17a (Standard Test Method for Density (Unit Weight), Yield, and Air Content (Gravimetric) of Concrete), ASTM C39/C39M-20 (Standard Test Method for Compressive Strength of Cylindrical Concrete Specimens), ASTM C496/C496M-17 (Standard Test Method for Splitting Tensile Strength of Cylindrical Concrete Specimens), ASTM C293/C293M-16 (Standard Test Method for Flexural Strength of Concrete - Using Simple Beam with Centre-Point Loading), [66, 71–73].

1.6.3 Durability of Wheat Straw Reinforced Concrete

Durability of cement concrete having wheat straw, over a certain period for different real, accelerated and ideal environmental conditions has been studied. To study the effect of different conditions on the durability of wheat straw reinforced concrete specimens, the specimens are bifurcated in three categories and are kept under following ageing conditions:

- Ideal room conditions of Islamabad, Pakistan

- Real environmental conditions (i.e. open-air weathering) of Islamabad region
- Accelerated ageing (i.e. alternate wetting and drying with an interval of one week).

Same testing, as done for optimization task, is performed after the specified period of approximately 48 months and the residual behaviors are evaluated using the same testing techniques as adopted for optimization.

1.6.4 Structural Capacity of Wheat Straw Reinforced Concrete

In this section, the contribution of wheat straw in improving the behavior and capacity of concrete for rigid pavement applications is determined experimentally. Reinforced concrete beam-slabs with varying flexure and shear re-bars, with and without wheat straw, are experimentally investigated for studying the altered behavior due to straw. The test standard used for this task is; ASTM C78/C78-M18 (Standard Test Method for Flexural Strength of Concrete - Using Simple Beam with Third-Point Loading). This experimental investigation is intended to get an indication of potential use of wheat straw reinforced concrete as rigid pavement. Accordingly, a modification has also been proposed in AASHTO rigid pavement design guide equation for wheat straw reinforced concrete pavements.

1.6.5 Performance Evaluation of Wheat Straw Reinforced Concrete Pavement

Structural performance evaluation of wheat straw reinforced concrete pavement test section is made after exposure to 18-months of vehicular movement. Pavement testing (i.e. performance evaluation) is performed to have a correlation between mechanical properties and pavement performance. For this purpose, jointed plain concrete and wheat straw reinforced concrete road test sections are constructed and

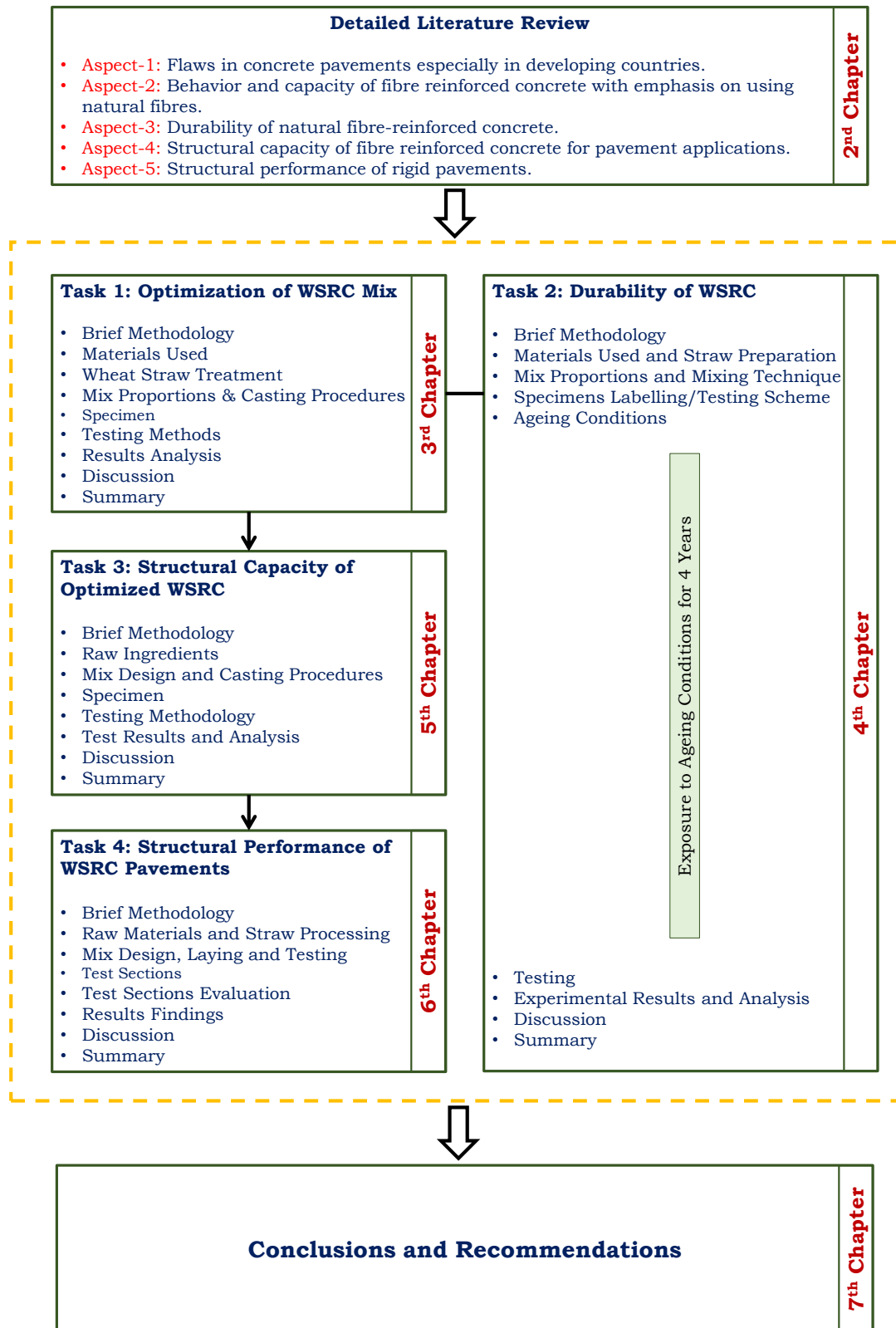


FIGURE 1.2: Flow diagram of research methodology.

evaluated. The tested sections are evaluated for the load bearing capacity, in terms of deflection measurements, and crack progression. The laboratory testing is also performed for the development of lab-field co-relation. The tests standards and references used for this task are; ASTM C39/C39M-20 (Standard Test Method for Compressive Strength of Cylindrical Concrete Specimens), AASHTO T256/ASTM D4695 (Standard Test Methods for General Pavement Deflection Measurements), Mahler and Kharoufa [74], Bisshop and Mier [75], Feiteira *et al.* [76], Choi *et al.* [77], AASHTO 1993: II-45 (Pavement Design Guide) and ASTM C174/C174M-17 (Standard Test Method for Measuring Thickness of Concrete Elements Using Drilled Concrete Cores).

A flow diagram of research methodology is shown in Figure 1.2.

1.7 Thesis Layout

The thesis consists of seven chapters, out of which Chapter 3 to 6 are aimed for independent journal articles. However, slight modifications (in original paper format) are made to keep the write-up in line with thesis layout. The experimental research presented in this thesis is broadly classified into two main aspects; i. material characterization i.e. optimization of wheat straw reinforced concrete mix and durability of wheat straw in cement concrete; and ii. structural aspects of wheat straw reinforced concrete. Accordingly, the thesis is organized in the following way:

Chapter 2 presents the literature review regarding the flaws in concrete pavements of developed and developing countries. The governing parameters associated with these distresses/flaws and possible remedial measures are studied. Out of which, the incorporation of discrete fibres in concrete, for enhancing the capacities, is also presented in light of various researches. Narrowing down the fibres list, the usage of natural plant fibres, for economic purpose, is also exhibited in detail. Among all the natural plant fibres, studies on wheat straw reinforced cementitious composites are also summarized in this Chapter 2. In light of considering wheat

straw in concrete pavements, the studies on natural fibre reinforced concrete for pavement applications and their durability aspect are also highlighted. Conclusively, the studies on performance evaluation of rigid pavements are also explored and presented.

In **Chapter 3**, the effect of pre-treatment techniques and contents of straw in concrete for enhancing its energy absorption capability is presented. The influences of soaked, boiled and chemically treated straw having contents of 1%, 2% and 3%, by mass of wet concrete, are presented in this chapter. In addition to static properties and behaviors, the micro-analysis of straw and its bond with surrounded matrix is also determined and explained with logical reasoning.

Chapter 4 focuses on the durability evaluation of cement concrete having wheat straw. The influences of controlled room conditions, natural weathering and accelerated ageing (alternate wetting and drying) conditions for a long period of 4-years, i.e. 48 months, on the residual strengths and behaviors of wheat straw concrete, are explored and presented in this chapter. In addition to that, the straw and its bonding conditions under the mentioned ageing for specific period are also extracted through micro-structural analysis. Moreover, the empirical modelling for anticipating the design life of wheat straw reinforced concrete structure is provided in this chapter.

Chapter 5 portrays the structural integrity of wheat straw reinforced concrete to be intended for rigid pavement applications. Experimental investigation on plain and wheat straw reinforced concrete having flexural and shear steel re-bars is made in detail. Accordingly, the structural performance indication for wheat straw reinforced concrete is provided along with the modified rigid pavement design equation for WSRC.

Chapter 6 presents the structural performance evaluation of wheat straw reinforced concrete pavement test section. The construction practices for first ever constructed jointed wheat straw reinforced concrete pavement test section are described in detail. Furthermore, the laboratory and field investigations are made. The structural capacity of wheat straw reinforced concrete pavement, in terms

of deflection measurements, is also explored and presented in this chapter. The development of cracks and their progression under the application of heavy vehicular loading for the period of 18-months is also monitored and explained in this chapter. Conclusively, the validation of modified design equation for wheat straw reinforced pavement as proposed in Chapter 5 is made, by studying its influence on load transfer efficiency, along with the development of empirical relationship between laboratory and field testing.

The study is concluded along with future recommendations in **Chapter 7**, followed by a list of references.

Chapter 2

Literature Review

2.1 Background

Rigid pavements have longer structural life and superior durability as compared to the flexible pavements and are used to accommodate heavy traffic loading. Even though it demands less maintenance, however the initial cost of concrete pavement restricts its excessive construction. In addition to high cost, concrete is basically a brittle material with minimum strain-capacity and ultimately low toughness. Due to which, distresses occur in rigid pavements which deteriorate rapidly due to application of moving loads. Hence, the efforts have been made to increase its ductility by increasing the tensile strength of conventional concrete. Addition of fibres in the cement concrete composites comes up with an effective solution to increase the energy-absorption capability of concrete by resisting cracks progression. The depletion of ozone layer due to environmental pollution is caused by consumption of fossil fuels/natural resources for construction materials and large-scale burning of agricultural waste. Heading towards UNDP sustainable goals, the use of agricultural waste/by-product instead of artificial/steel fibres for reinforcing concrete may prove to be a sustainable solution. However, long-term performance of structure having agricultural fibre reinforced concrete is questionable due to the organic nature of agricultural fibres.

Accordingly, in this Chapter 2, the extensive literature has been reviewed to explore all the factors to be considered for conduct of the intended study. Starting with the identification of rigid pavement distresses which usually occur particularly in pavements of developing countries like Pakistan and the governing parameters responsible for these distresses. Narrowing down the distresses, among many, which can be avoided and/or reduced with the usage of dispersed fibres in concrete. The studies regarding incorporation of fibres in cement concrete and its positive outcomes are also explored to get an idea about toughness enhancing mechanism of fibre reinforced concrete. As already mentioned, that the sustainable development is primary goal, therefore the behavior of concrete reinforced with agricultural fibres is also scrutinized from literature. But, the natural fibres are organic in nature and suspect to degradation under weathering conditions, therefore studies regarding durability evaluation of natural fibres and cement composites reinforced with natural fibres are also reviewed in detail to sort out the durability evaluation processes and durability enhancing techniques. Keeping in mind that pavement applications are intended, the literature regarding structural performance of concrete roads is also studied. Hence, the whole literature review is broadly classified in five categories and presented in the rest of Chapter as follows; Section 2.2 shows the literature findings regarding concrete pavement distresses particularly in developing countries. The literature regarding use of artificial/steel fibres particularly natural fibres in cement composites are summarized in Section 2.3. Section 2.4 is comprised of durability studies; and the studies regarding structural capacity of fibre reinforced concrete for rigid pavements are presented in Section 2.5. Lastly, the literature on performance of concrete roads is explained in Section 2.6, followed by the summarized identified research gaps in Section 2.7.

2.2 Flaws in Concrete Pavements

Pavement is the surface which aims to sustain the vehicular movements. There are mainly two types of pavement; flexible and rigid pavement. A typical image of a road, having both flexible and rigid pavement lanes, in a developing country,

i.e. Pakistan, is shown in Figure 2.1. The common difference between these, is in the material used in top layer. Asphaltic concrete, i.e. ductile in nature, is used in flexible pavements whereas, Portland cement concrete, i.e. brittle in nature, is used in rigid pavements.



FIGURE 2.1: Existing flexible and rigid pavement lanes in road network of Islamabad, Pakistan.

2.2.1 Rigid Pavement Distresses

The use of concrete pavements has increased over the past decades. The serviceability of concrete pavements is more than that of asphalt pavements [1]. However, its more extensive use is still not common due to its higher initial cost. Moreover, concrete is basically a brittle material with minimum strain-capacity. Therefore, the pavement distresses usually occur in the rigid pavements as well. D'Ambrosia *et al.* [78] highlighted the issue of early age micro cracking as the primary issue in rigid pavements. Shrinkage reducing admixtures were used to reduce shrinkage and creep in concrete pavements. Uni-axial test under restrained conditions and constant compressive/tensile loading was performed on the sampled specimen. A decrease up to 30% in the early-age micro-shrinkage of concrete was observed with

TABLE 2.1: Distresses in rigid pavements.

S. No.	Distresses	References
(1)	(2)	(3)
i.	Fatigue cracking	Treybig <i>et al.</i> [80];
ii.	Reflective cracking	D'Ambrosia <i>et al.</i> [78];
iii.	Durability Cracking	Hiller <i>et al.</i> [1]; Olivares <i>et al.</i> [81];
iv.	Micro-shrinkage cracking	Gupta <i>et al.</i> [22]; Graeff <i>et al.</i> [23];
v.	Longitudinal cracking	Mubaraki <i>et al.</i> [82];
vi.	Transverse cracking	Li <i>et al.</i> [83];
vii.	Punchouts	Daniel <i>et al.</i> [84];
viii.	Settlement Cracking	Subramani <i>et al.</i> [85];
ix.	Creep	Sujaet <i>et al.</i> [79];
x.	Abrasion	Guanet <i>et al.</i> [86];
xi.	Polished Aggregates	Kim <i>et al.</i> [87];
xii.	Scaling	Zollinger [88]; Shi <i>et al.</i> [89]

an admixture dosage of 0.75 gal/yd³. Suja *et al.* [79] reported that the primary failures usually observed in concrete pavements are: polished aggregates, scaling, transverse cracking, corner breaks, and punch-outs. Few major reasons behind these distresses were erosion of sub-base, usage of poor-quality materials, deviation from design standards, and absence of drainage line. The remedial measures proposed in the study were asphaltic overlay, full depth repair, and dowels and tie bars. The concrete pavement distresses in developed countries, as reported in different studies, are summarized in Table 2.1.

2.2.2 Flaws in Rigid Pavements of Developing Countries

However, in developing countries, the cement concrete pavements are usually prone to early-age distresses due to the poor construction practices, low quality materials usage, and improper implementation/execution of design procedures. In addition

to that, over loading of the heavy vehicular traffic is also a major factor in premature failures of rigid pavements in developing countries due to lack of awareness among truck drivers regarding adverse effects of this practice and thinking of overloading as an effective way to make more profit. The deviation of heavy axle loading from the designed load is the key factor behind premature distresses in rigid pavements of developing countries. Due to this variation in axle loads, high tensile stresses are generated in top surface of pavements that cause premature failures including various types of cracking, ultimately resulting in early maintenance and/or rehabilitation.

Highway agencies are seeking the cost-effective practices to minimize the capital cost. Khurshid *et al.* [90] reported the annual maintenance/rehabilitation cost, against Portland Cement Concrete Pavement (PCCP) patching, Portland Cement Concrete Pavement overlays and Portland Cement Concrete Pavement repair along with Hot Mix Asphalt overlay, for rigid pavements under Federal Highway Authority (FHWA) construction price index. The equivalent uniform annual cost per mile of Portland Cement Concrete Pavement repair with HMA overlay, plain cement concrete pavement patching and plain cement concrete pavement overlays came out to be 17389.72\$, 204225.1\$ and 79214.2\$, respectively.

Accordingly, to minimize the occurrence of distresses and capital construction cost of rigid pavements, fibre reinforced concrete was proposed by Gupta *et al.* [22]. The mechanical (i.e. compressive, splitting-tensile, and flexural strengths) properties of concrete reinforced with polyester fibre, were determined experimentally along with the abrasion resistance test. Compressive and flexural strengths of polyester fibre reinforced concrete were increased by 21% and 6%, respectively, as compared to that of plain concrete. The durability of fibre reinforced concrete was also studied under accelerated ageing conditions (i.e. heating and cooling). It was reported that the performance of fibre reinforced concrete under wetting and drying and sulphate attack is comparable with controlled concrete. In addition to that, it was also reported that, the incorporation of fibres in concrete can also be helpful in saving the cost of overall composite up to 10%.

TABLE 2.2: Distresses in rigid pavements of developing countries.

S. No.	Distresses	References
(1)	(2)	(3)
i.	Durability Cracking	Gupta <i>et al.</i> [22];
ii.	Micro-shrinkage cracking	Suja <i>et al.</i> [79], Chaudry <i>et al.</i> [93];
iii.	Longitudinal cracking	Kanalli <i>et al.</i> [27];
iv.	Transverse cracking	Kumar <i>et al.</i> [29], Singh <i>et al.</i> [94];
v.	Punchouts	Subramani <i>et al.</i> [85]; Mehta <i>et al.</i> [95]; Sarsam [96]; Silva <i>et al.</i> [97]; Al-Rubaei <i>et al.</i> [98]; Niken <i>et al.</i> [99]

The most frequent distress in rigid pavements is the early-age cracking (i.e. micro-shrinkage cracking, transverse/longitudinal cracking). When these cracks are clustered due to less spacing between them, the punchouts take place that are categorized under the severe pavement distresses [91, 92]. The summary of distresses/flaws in rigid pavements of developing countries is given in Table 2.2.

2.2.3 Identified Research Gap on Rigid Pavement Flaws

Therefore, it can be concluded that overloading of heavy traffic vehicles increases the demand of rigid pavements in comparison to that of flexible pavements for accommodation of heavy vehicular traffic. However, the use of rigid pavements is still prevented developing countries due to higher construction cost. In addition, the probability of premature distresses and failures in rigid pavements, due to brittleness of conventional concrete, is still a notable issue in developing countries. The major distresses are micro-shrinkage, durability, longitudinal and transverse cracking, and punch-outs. The early age/premature distresses which are usually observed in rigid pavements of developing countries can be minimized by using dispersed fibres in concrete composites [22, 27, 29, 100].

2.3 Behavior and Capacity of Fibre Reinforced Concrete

2.3.1 Concrete Reinforced with Short-discrete Artificial, Steel and Natural Fibres

Concrete, due to its comparatively simple production, abundantly available components, and a number of various types of applications, has been used widely all over the world. However, concrete is basically a brittle in nature material with minimum strain-capacity, low energy absorption capacity and ultimately low toughness. Hence, the efforts have been made to increase its ductility by increasing the tensile strength of conventional concrete. Addition of short-discrete dispersed fibres in the cement concrete composites has become the effective way to increase the energy-absorption capability of concrete [4, 5, 18, 101–107]. The development/initiation of cracks in cement concrete can also be resisted due to the incorporation of dispersed fibres [108, 109]. Unlike the continuous reinforcement, the coefficient of thermal expansion is not of much importance for addition of short-discrete dispersed fibres in concrete. Liu *et al.* [110] reported reduced thermal expansion of fibre reinforced concrete with respect to plain concrete. The cement concrete toughness can be increased considerably by enhancing the cracking resistance due to bridging mechanism of dispersed fibres across the cracks in it Merta and Tschegg [18].

This technique had been used since biblical times for strengthening the brittle matrices. This concept of reinforcing concrete with dispersed fibres was developed with the invention of Hatschek technology for the production of roofing, pipes etc. in 1900. The incorporation of artificial/steel/natural fibres in concrete composites are investigated by various researchers for concrete pavements [18, 20, 22, 24–27, 29–36, 105, 106]. The incorporation of uniformly dispersed/distributed fibres in cement concrete as construction material for various applications, has ultimately

TABLE 2.3: Typical proportions for normal weight fibre reinforced concrete.

Material (1)	Proportions (2)
Cement: Sand: Aggregates	1: 1: 2 to 1: 4: 8 1: 4: 2 (to cater the balling affect)
Water-cement ratio	0.4 – 0.7
Maximum aggregate size	19.5 mm
Fibre content	0.5 – 5%, by volume of mix / 1 – 6%, by mass of cement / 0.25 – 4%, by mass of wet concrete
Fibre length	20 – 80 mm
Diameter	0.0015 – 1 mm
Tensile strength	108 – 3600 MPa
Specific gravity	680 – 7840 kg/m ³
Maximum elongation	0.5 – 25 %
References	Majumdar [112]; Zollo [113]; Corinaldesi and Moriconi [114] ; Brandt [111]; ACI [108]; Hollaway [115]; Bagherzadeh <i>et al.</i> [116]; Ali <i>et al.</i> [66]; Ardeshana and Desai [117]; Erdogmus [6].

resulted in improved behavior surprisingly [111]. The typical proportions for the normal weight fibre reinforced concrete are given in Table 2.3.

2.3.2 Typical Role of Steel Fibres on Design Capacity

Beshara *et al.* [118] studied the high strength fibre reinforced concrete beams with steel rebars. The steel ratios used were 0.0017, 0.0064, 0.0075, 0.012, 0.015, and 0.022 for tensile reinforcement. And for compression reinforcement, 0.0045 and 0.0047 steel ratios were used. The percentages content for the steel fibres used were 0.5%, 1%, and 2%, by volume, of wet concrete. The study resulted in significant increase of flexural strength. A modification in the equation developed by Whitney stress distribution concept as reported by Nilson *et al.* [119] was also proposed in this study to incorporate the effect of fibre's tensile strength in the

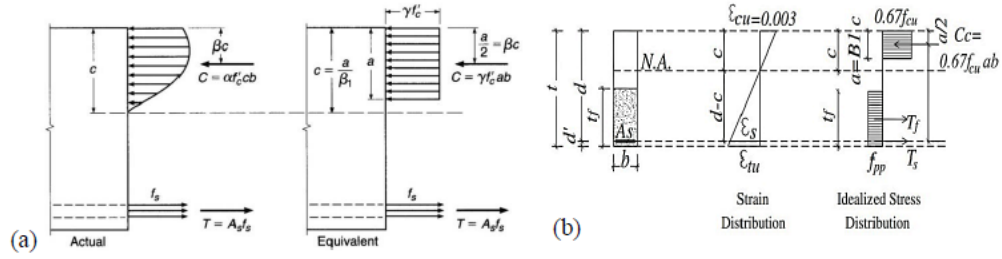


FIGURE 2.2: Stress distribution in reinforced concrete beam (a) Whitney stress distribution concept for plain concrete reported by Nilson *et al.* [119], and (b) FRC by Beshara *et al.* [118].

effective height of equivalent stress in tensile region. Nilson's equation is as follows:

$$Mr = Ts \left(d - \frac{a}{2} \right) \quad \text{'N-mm'}$$

Where Ts = tensile strength = $As \times fy$ in 'N'

and

$$a = \frac{As \times fy}{0.85 \times f_c'} \quad \text{'mm'}$$

Whereas, the modified equation by Beshara *et al.* is as follows:

$$M_{F1} = Ts \left(d - \frac{a}{2} \right) + T_{f1} \left\{ Ts \left(t - \frac{tf}{2} \right) - \frac{a}{2} \right\}$$

Here, in this modified equation, the first part is same as in Whitney stress distribution equation and the fibre's tensile strength in the effective height of equivalent stress in tensile region is added. The tensile strength of fibres in modified equation can be calculated as follows:

$$T_{f1} = \left[1.64 V_f \left(\frac{l_f}{\phi_f} \right) \right] b tf$$

Where: V_f = Volume of fibres in concrete, l_f = Fibres length and ϕ_f = Fibres diameter. The basic concept of modifying the equation developed by Nilson *et al.* for fibre reinforced concrete to effectively utilize tension region of concrete with the help of dispersed fibres by crack arresting mechanism is also illustrated in Figure 2.2.

2.3.3 Behavior of Steel and Artificial Fibre Reinforced Concrete

2.3.3.1 Steel Fibre Reinforced Concrete

Steel fibre reinforced concrete was also evaluated to study the structural performance of high strength concrete beams by Yoo and Yoon [120]. The steel ratio used in the beams were $\rho = 0.94\%$ and 1.50% . And the optimum fibre content was 2% , by volume of concrete. Load carry capacity was increased by $27 - 54\%$ in case of concrete reinforced with steel fibres, in comparison to that of plain concrete beams. The steel fibre reinforced concrete is also studied by many other researchers for structural applications. Some of these studies are summarized in Table 2.4.

2.3.3.2 Artificial Fibre Reinforced Concrete

Shear behavior of fibre reinforced concrete (FRC) beams was studied by Furlan and Hanai [103]. Polypropylene fibres with 0.5% and steel fibres with 0.5% , 1% , and 2% , by volume of wet concrete, were used. The splitting-tensile and compressive strengths were enhanced by 4.3 MPa and 54.8 MPa, respectively. Bagherzadeh *et al.* [116] reported the improvement in mechanical and physical properties of concrete by using polypropylene fibres. The polypropylene FRC showed an increase in compressive strength by 6% , splitting-tensile strength by 3% , flexural strength by 5% , and bending toughness by 67% , as compared to the respective specimens of PC. The early age micro cracking in glass and nylon fibre reinforced concrete was also studied by Khan and Ali [126] for bridge deck applications. The optimum content of glass and nylon fibres used were 5% , by mass of cement. Splitting-tensile strength of studied fibre reinforced concrete was increased up to 11% , whereas flexural strength was increased up to 5.6% when compared to the controlled concrete. Some more studies on artificial fibre reinforced concrete are summarized in Table 2.5.

TABLE 2.4: Properties and applications of steel fibre reinforced concrete.

Reference	Fibre	Fibre Reinforced Concrete Properties	Obtained Values	Applications
(1)	(2)	(3)	(4)	(5)
Purkiss [121]		a. Residual Compressive Strength b. Residual Flexural Strength	i. 16-22% loss@300 °C ii. 57-74% loss@800 °C i. 5-41% loss@300 °C ii. 78-91% loss@800 °C	Refractory material
Boulekbache <i>et al.</i> [122]		a. Compressive Strength b. Flexural Strength	27-28.5 MPa 3.5-5.5 MPa	Structural Beams
Gholamhoseini <i>et al.</i> [123]	STEEL	a. Compressive Strength b. Flexural Strength	33.8-36.2 MPa 3.9-4.3 MPa	Slabs
Patil and Sangale [124]		a. Compressive Strength b. Split-tensile Strength c. Load Carrying Capacity	45.7 MPa 5.3 MPa 9.9 - 10.3 kN (at 2.9-3.1 kN.m Torsional Load)	Beams
Noaman <i>et al.</i> [125]		a. Compressive Strength b. Fracture Toughness	47 MPa 3.0-3.9 MPa.m ^{0.5}	-

TABLE 2.5: Properties and applications of artificial fibre reinforced concrete.

Reference	Fibre	Fibre Reinforced Concrete Properties	Obtained Values	Applications
(1)	(2)	(3)	(4)	(5)
Wang <i>et al.</i> [127]	Nylon	a. Toughness b. Flexural Strength c. Tensile Strength	37.6-57.7 2.7-3.9 MPa 2.2 MPa	-
	Arcylic	a. Toughness b. Flexural Strength c. Tensile Strength	19-181.3 4.2-6.3 MPa 2.5-3.3 MPa	-
Mufti <i>et al.</i> [128]	Polypropylene	a. Compressive Strength b. Splitting-tensile Strength	29.9-46.1 MPa 2.1-4.1 MPa	Bridge deck slabs
Aidoo <i>et al.</i> [129]	Carbon	a. Compressive Strength b. Tensile Strength c. Fatigue Resistance	22.7-26.6 MPa 5.3 MPa 20.3 mm deflection (at 1.28 million cycles)	Bridge girders
Rai and Joshi [25]	Polymer and glass	Flexural strengths, Shock	-	-
Khan and Ali [126]	Nylon	a. Compressive Strength b. Splitting-tensile Strength c. Flexural Strength	14.5 MPa 1.78 MPa 3.39 MPa	Bridge deck
	Glass	a. Compressive Strength b. Splitting-tensile Strength c. Flexural Strength	14.1 MPa 1.73 MPa 3.31 MPa	-
Khan and Ali [130]	Wave Polypropylene	a. Compressive Strength b. Splitting-tensile Strength c. Flexural Strength d. Thickness Reduction e. Cost Reduction	13.7-14.0 MPa 1.83-1.87 MPa 3.5-3.7 MPa 6% 1.7%	Pavement

2.3.4 Behavior of Natural Fibre Reinforced Concrete

Sustainable development is a key consideration in current era. Each and every step to achieve sustainable development goals has its own significance. In this global effort to get the sustainable solutions, the focus is on reduction of biodegradable materials and to minimize the waste, which ultimately contributes in global warming. Saving, re-using, and re-cycling are the most widely used concerns now a days, which grab the attention of people to cater environmental issues [7–10, 131–137]. However, the results of natural fibre reinforced concrete (NFRC) are comparable with those of artificial fibre reinforced concrete (AFRC) and steel fibre reinforced concrete (SFRC) for many civil engineering applications [11, 25, 68]. In the recent few years, considerable interest has been developed on using the natural fibres in the cement composites for having the alternate sustainable, economical, and eco-friendly building materials. Natural fibres have the potential to be used as reinforcement for overcoming the conventional deficiencies in the concrete. The appearance (images) and properties of some of the natural fibres as well as natural fibre reinforced concrete are summarized in Table 2.6.


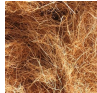
Natural fibres are used in the brittle cementitious composites to increase and maintain the energy absorption capability and toughness [11, 25, 68, 138, 139]. Researchers have used natural fibres in concrete for various applications as an alternative replacement of steel or artificial fibres. The natural fibres figured out as reinforcement in cement composites for civil engineering applications include sugarcane, sisal, coir, bamboo, banana, date, malva, kenaf bast, vakka, palm, jute, pineapple leaf, hemp, ramie bast, flax, hibiscus cannabinus, abbaca leaf, wheat straw, sansevieria leaf, and elephant grass [12–14, 16–19, 140–148]. Natural fibres are cheap and locally available in abundance in many countries. Hence, for improving the properties of composites, the use of plant based natural fibres as a low-cost renewable construction material can contribute towards the sustainable development. Also, the natural fibres are more flexible and easier to handle as compared to artificial/steel fibres [12, 40, 149, 150]. Moreover, for improving the properties of composites, the use of plant based natural fibres as a low-cost




renewable construction material can contribute towards the sustainable development [11, 145].

Therefore, the use of natural fibres in concrete composites can result in the alternative eco-friendly, sustainable, and economical civil engineering construction materials. Mechanical and dynamic properties of coir reinforced concrete were determined by Ali *et al.* [66]. The studied properties were intended for earthquake resistant housing materials applications. The optimum length and content of coir came out to be 5 cm and 5%, respectively. An increase of 4%, 21%, 2%, and 910% was observed in the compressive strength and toughness, and modulus of rupture of optimized coir fibre reinforced concrete. Flexural and shear cracking strength of Bamboo fibre reinforced concrete members were examined by [141]. The improved properties for bamboo fibre reinforced concrete were reported when compared to that of reinforced concrete. Similar type of results were observed in case of chemically treated bamboo fibre reinforced concrete [144].

Among all natural fibres, the incorporation of different straw (i.e. rice, rape, barely, wheat etc.), due to the abundant production of these crops in various sub-tropical regions, in different matrices (i.e. soil, straw boards, bales, brick earth, brick block, mud mortar, cement-sand mortar, lightweight cement wall etc.) for a number of structural and non-structural applications have been studied by many researchers [18, 67, 131, 151–165]. Wheat straw is the end product of wheat crop and usually available in surplus in many countries. Therefore, due to its cheap availability and easy access, the use of wheat straw in civil engineering applications will be effective, as reported by Bainbridge [166]. Wheat straw have been used by different researchers in the form of straw bales and dispersed reinforcement for the structural members and cement concrete composites, respectively. Straw bales were evaluated as structural member by Ashour *et al.* [154]. These bales were determined in compression and resulted in increased compressive strength. The other researchers also reported the improved properties of cement concrete composites with the incorporation of natural fibres. The findings of such some studies are summarized in Table 2.6.

TABLE 2.6: Studies on natural fibres and natural fibre reinforced concrete.

Natural Fibres		Natural Fibre Reinforced Concrete Properties										Reference
Type	Image	Fibre Properties						Matrix	Properties	Obtained Values	Applications	
(1)	(2)	Tensile Strength (MPa)	Elongation (%)	Elastic Modulus (GPa)	Water Absorption (%)	Specific Gravity (kg/m ³)	Density (g/cm ³)	(9)	(10)	(11)	(12)	(13)
Sisal		227-1002	2.08-14.8	10.9-26.7	110-240	1117-1165	0.75-10.70	x	x	x	x	Joseph <i>et al.</i> [167]; Toledo Filho <i>et al.</i> [140]; Gupta & Srivastava [168]
		x	x	x	x	x	x	Concrete	a. Compressive Strength b. Split-tensile Strength	21-26 MPa 1.95-2.81 MPa	-	Sumithra & Dadapheer [169]
		31-221	14.8	-	-	-	-	Concrete Composite	a. Compressive Strength b. Shear Strength a. Four Point Bending b. Direct Tension c. Bending Toughness	25.5 MPa 1.55 MPa 18.5 MPa 8.03 MPa 20.3 kJ/m ²	Construction Material	Oriola <i>et al.</i> [170] Silva <i>et al.</i> [171]
Coir		126-148	30.0	1.7-2.3	85-180	1104-1370	0.87	x	x	x	x	Agopyan <i>et al.</i> [14]; Li <i>et al.</i> [16]; Munawar <i>et al.</i> [17]; Rao & Rao [172]; Danso <i>et al.</i> [173]
		x	x	x	x	x	x	Mortar	a. Compressive Strength b. Flexural Strength	2.95 MPa 1.07 MPa	Plastering	Sathiparan <i>et al.</i> [174]
		15-327	75	-	-	-	-	Concrete	a. Split-tensile Strength	2.96 MPa	-	Lumingkewas <i>et al.</i> [175]
								Mortar	a. Compressive Strength b. Flexural Strength	17.3 MPa 4.7 MPa	-	Ramakrishna & Sundrajan [11]

Natural Fibres		Natural Fibre Reinforced Concrete Properties										Reference
Type	Image	Fibre Properties						Matrix	Properties	Obtained Values	Applications	
(1)	(2)	Tensile Strength (MPa) (3)	Elongation (%) (4)	Elastic Modulus (GPa) (5)	Water Absorption (%) (6)	Specific Gravity (kg/m ³) (7)	Density (g/cm ³) (8)	(9)	(10)	(11)	(12)	(13)
Jute		320-800	1.5-1.8	-	281	1400	1.3	x	x	x	x	Fernandez <i>et al.</i> [68]; Jayamani <i>et al.</i> [176]; Gopinath <i>et al.</i> [177]
		x	x	x	x	x	x	Concrete	a. Compressive Strength b. Flexural Strength	27.5 MPa 4.9 MPa	Paver Blocks	Kundu <i>et al.</i> [178]
		50	-	9.59	-	-	-		a. Compressive Strength b. Tensile Strength	31.4 MPa 1.20 MPa	-	Mansur & Aziz [179]
		29-312	19	-	-	-	-	Mortar	a. Compressive Strength b. Flexural Strength	11.3 MPa 4.3 MPa	-	Ramakrishna & Sundrajan [11]
Hemp		550-900	1.60-4.0	34	-	-	1.47	x	x	x	x	Fernandez <i>et al.</i> [68]; Wambua <i>et al.</i> [180]; Li <i>et al.</i> [47]
		x	x	x	x	x	x	Mortar	a. Compressive Strength b. Flexural Strength	23.9 MPa 5.7 MPa	-	Poletanovic <i>et al.</i> [181]
		600-700	-	-	-	-	-	Concrete	a. Compressive Strength b. Notch Tensile Strength c. Fracture Energy	34.6 MPa 3.59 MPa 204.4 MPa	-	Merta & Tschegg [18]
Wheat Straw		21.2-40.0	5.4	-	-	-	0.024-0.111	x	x	x	x	Lam <i>et al.</i> [182]; Dogherty <i>et al.</i> [183]
		x	x	x	x	x	x	Colemanite Concrete	a. Compressive Strength b. Abrasion Resistance	31-32.1 MPa 7.9 cm ³ /50 cm ²	Radiation Shielding	Aksogan <i>et al.</i> [159]
		40	-	-	-	-	-	Concrete	a. Compressive Strength b. Notch Tensile Strength c. Fracture Energy	31.7 MPa 3.5 MPa 122.5 MPa	-	Merta & Tschegg [18]

2.3.5 Wheat Straw Reinforced Concrete

Wheat straw is slightly explored yet in cement composites for civil engineering structural and non-structural applications [18, 155, 184]. The effect of hemp, elephant grass and wheat straw fibres on the fracture energy of concrete has been studied by Merta and Tschegg [18]. The fibre content and length of these fibres used were 0.19% (by concrete mass) and 40 mm, respectively. The fracture-energy of hemp, elephant grass and wheat straw reinforced concrete were determined experimentally in comparison to that of controlled plain concrete. The fracture energy is significantly enhanced by 70%, 5%, and 2% for hemp, elephant grass and wheat straw, respectively, in comparison with that of plain concrete. The incorporation of wheat straw, as a dispersed reinforcement, in cementitious mortar was also studied by Albhattiti *et al.* [155]. Long and short wheat straw and polypropylene fibres were used with the contents ranged 0.5%–5%, by volume of concrete. Mechanical properties (i.e. strengths under flexural and compressive loadings) were determined experimentally. An increase of 23% in the stiffness of optimized fibre content (i.e. 0.75% by volume) was observed in comparison with that of plain mortar.

The studies on wheat straw reinforced cementitious composites are summarized in Table 2.7.

2.3.6 Identified Research Gap on Fibre Reinforced Concrete

Hence, it can be concluded that natural fibre reinforced concrete is comparable with steel and artificial fibre reinforced concrete in terms of enhanced load carrying capacities and better post-cracking behavior. However, among all natural fibres, wheat straw has been explored slightly for cement concrete composites. The role of wheat straw in altering the behavior and capacity of concrete is important.

TABLE 2.7: Studies on wheat straw reinforced composites.

Reference	Fibre	Matrix	Fibre Reinforced Concrete Properties	Obtained Values	Applications
(1)	(2)	(3)	(4)	(5)	(6)
Merta and Tschegg [18]		Cement Concrete	a. Compressive Strength b. Notch Tensile Strength	31.7 MPa 3.3-3.7 MPa	Building Material
Albhattiti <i>et al.</i> [155]	Wheat Straw	Cement Mortar	c. Fracture Energy a. Maximum Bending Loading	111-133 MPa 2.4-2.9 kN	-
Nepal [184]		Concrete	a. Residual Tensile Strength	i. 1.88 MPa (0.47 m deflection) ii. 1.33 MPa (3.02 mm deflection)	Ground Floor Slab

Therefore, wheat straw reinforced concrete needs to be investigated in detail for its application in civil engineering structures.

2.4 Durability of Natural Fibre Reinforced Concrete

2.4.1 Durability Evaluation Techniques for Natural Fibres in Cement Composites

In addition to improve toughness and energy absorption capacity of cement concrete composites by incorporating natural fibres, the durability must also be given proper consideration. Deficiencies/degradation of natural fibre reinforced cement composites, in terms of durability, is usually observed due to organic nature of natural fibres. This might be due to the mineralization of fibres and alkali attacks under the exposure of climatic conditions. The degradation mechanism of natural fibres in the cement matrix occurred due to mineralization is also reported by [185, 186]. Furthermore, the interaction of natural fibres with cementitious composites is influenced by their complex micro-structural heterogeneity.

Therefore, the bonding mechanism of natural fibres should also be explored in detail. Natural fibres in concrete have been determined experimentally for durability, after exposing it in different environmental and ageing conditions [11, 15, 41, 46–48, 187–189]. The environmental and ageing conditions include (i) alternate wetting and drying, (ii) immersion in water, saturated lime and sodium hydroxide solutions for specific period, (iii) immersion in water at specified temperature and for a specified period, and (iv) alternate freeze and thaw cycles. A considerable amount (i.e. 58.7%) of residual strength of natural fibres in composites was observed by [46]. Salemi and Behfarnia [24] compared the frost resistance and mechanical properties of plain concrete, concrete with nano-particles and concrete with polypropylene fibers for pavement application. In this study, the specimens

were subjected to freezing and thawing cycles according to ASTM C666A. The percentages of polypropylene (PP) used were 0.1% and 0.2% (by volume of concrete). The percentages of nano-silica (NS) used were 3%, 5%, and 7% (by weight of cementitious material). The percentages of nano-alumina used were 1%, 2%, and 3% (by weight of cementitious material). Optimum content of NS in concrete came out to be 5% in order to improve its compressive strength as high as 30%. This resulted in 84% reduction in deterioration of concrete after freezing and thawing cycles. The study concluded that concrete containing 5% NS incorporating 0.2% PP fibers improved durability by 87% and showed most frost resistance up to 82%.

Some, out of many, ageing conditions for durability evaluation of concrete reinforced with various natural fibres, as reported in literature, are provided in Table 2.8.

2.4.2 Treatment Techniques to Improve Durability of Natural Fibres in Cement Composites

The durability of natural fibres does not provide much hindrance for their use in civil engineering applications. But the durability should be given proper consideration due to organic nature of fibres. However, the shelf life of natural fibres is quite long (limited information is available on this in literature). John *et al.* [190] studied physical and chemical condition of 12 years aged coconut fibres extracted from in-built walls and reported good retained strength. Accordingly, a number of solutions were also proposed by various researchers to increase the durability of natural fibres [15, 48, 52, 69, 70, 190]. Acetylation and alkaline treatment of sisal fibres in cement concrete composite to cater the effect of alkaline attack was done by [189]. The durability evaluation technique opted was the immersion of specimens in water at 24°C and 70°C and alternate wetting and drying for the period of 90 days. An improvement in sisal fibre reinforced concrete durability was reported as a result of chemical treatment. In addition, the fibres impregnation with fly-ash and water repellent agents incorporation in cement matrix for fibre mineralization

TABLE 2.8: Evaluation techniques for durability of natural fibres.

Reference	Fibre	Ageing Conditions	Time Period
(1)	(2)	(3)	(4)
Filho <i>et al.</i> [46]	Sisal and Coconut	Immersion in water, saturated lime and NaOH solutions Immersion in water at specified temperature Alternate freeze and thaw cycles Alternate wetting and drying Open air weathering in the city of study	60-730 days
Ramakrishna and Subdrajan [11]	Jute, hibiscus cannabinus, coconut fibres, and sisal fibres	Immersion in saturated lime Immersion in sodium hydroxide solution Immersion in water	60 days 60 days
Sivaraja <i>et al.</i> [48]	Coconut	Alternate wetting and drying	2 years

reduction was also done. This technique was implemented on Hemp and Agave Lechuguilla fibres by [191]. Some of the solutions for treating the fibres to evaluate or to improve the durability of natural fibres or cement composites reinforced with natural fibres, from different researches are summarized in Table 2.9.

2.4.3 Identified Research Gap on Durability of Natural Fibre Reinforced Concrete

The durability of natural fibres does not provide much hindrance for the civil engineering structural applications. The bio-degradable nature of natural fibres needs special consideration. As pavements are directly exposed to vigorous environmental/climatic conditions. Therefore, for pavement applications, wheat straw

TABLE 2.9: Proposed treatment techniques for natural fibres in cement composites.

Reference	Fibre	Proposed Treatment	Specimen(s)
(1)	(2)	(3)	(4)
Ramakrishna and Subdrajan [11]	Sisal	Immersion in:	Fibres
	Coir	1. Clean and fresh water (pH=7.5)	
	Jute	2. Saturated lime solution ($Ca(OH)_2$)	
	Hibiscus Cannabinus	3. Sodium hydroxide solution ($NaOH$)	
Toledo <i>et al.</i> [15]	Vegetable Fibres	1. Carbonation of the matrix in a CO_2 -rich environment	Fibres Cement Matrix
		2. Immersion in slurred silica fume	
		3. Partial replacement of cement with blast furnace slag	
		4. Ageing in water	
		5. Open air-weathering	
		6. Exposure in alternate wetting and drying	
Sivaraja <i>et al.</i> [48]	Coir, and Sugarcane Bagasse	1. Immersion in sulphate solution H_2SO_4 (5% sulphuric acid) for 2 years, and	Fibre Cement Matrix
		2. Freezing and thawing as per ASTM C666 (0-40° F-0 for 4 hours) for 2 years.	
Silva <i>et al.</i> [192]	Sisal	Replacement of ordinary Portland cement with calcined clay (metakaolin and calcined waste crushed clay brick)	Fibre Cement Matrix
D'Almeida and Toledo [193]	Curaua	Replacement of ordinary Portland cement with 50% metakaolin, by weight.	

reinforced concrete needs to be explored, in terms of durability, due to organic nature of straw.

2.5 Structural Capacity of Fibre Reinforced Concrete for Pavement Applications

2.5.1 Incorporation of Fibres in Concrete Pavements

The incorporation of dispersed fibres in the plain concrete pavements can lead towards enhanced load carrying capacity and more crack resistance under vehicular loading. The propagation of cracks in fibre reinforced concrete can also be delayed by the help of dispersed fibres. The effect of artificial fibres in concrete composites, for rigid pavements, has also been investigated by many researchers [20–34, 36]. The major reason of crack initiation in concrete pavements is its poor resistance against tension and bending. Reinforcement of concrete with dispersed fibres can enhance the tensile bending performance of rigid pavements.

2.5.1.1 Addition of Steel Fibres in Concrete for Pavement Applications

The plastic shrinkage cracking can also be minimized with the addition of hybrid and steel fibres [194, 195]. Ramakrishnan *et al.* [11] determined the fresh concrete properties, static flexural strength, hardened concrete properties and pulse velocity. All these properties are studied for fibre reinforced concrete to evaluate its flexural behavior and toughness for concrete pavements. Four different fiber types (i.e., straight steel, polypropylene, corrugated steel and hooked-end steel) and four contents (0.5, 1.0, 1.5, and 2.0% by volume) were considered. Results showed an increase in static flexural strength (15% to 129%) and first-crack strength (15% to 90%). Kumar *et al.* [29] determined the splitting-tensile, flexural, and compressive strengths of steel and polypropylene fibre reinforced concrete. The percentages of steel and polypropylene fibres used were 0.5%, 1.0%, and 1.5%. Polypropylene fibre

TABLE 2.10: Use of steel fibre reinforced concrete for pavement applications.

Reference	Fibre	Fibre Reinforced Concrete Properties	Obtained Values	Application
(1)	(2)	(3)	(4)	(5)
Lankard and Newell [196]	STEEL	a. Compressive Strength	140 MPa	PAVEMENTS
		b. Flexural Strength	80 MPa	
Singh and Kaushik [197]		a. Fatigue Stress Ratio	0.1-0.3	
Kamada and Li [198]		a. Compressive Strength	47.2 MPa	
		b. Elastic Modulus	27.5 GPa	
Elsaigh <i>et al.</i> [199]		a. Flexural Strength	4.3 MPa	
		b. Slab Thickness Reduction	25%	
Kumar <i>et al.</i> [29]		a. Compressive Strength	54-57 MPa	
		b. Split-tensile Strength	5-6.2 MPa	
		c. Flexural Strength	8.3 MPa	
Hu <i>et al.</i> [200]		a. Compressive Strength	41.8-50.3 MPa	
		b. Residual Flexural Strength	0.42-0.72 MPa	
Alsaif <i>et al.</i> [33]		a. Fatigue Stress Ratio	0.7-0.9	
Elizondo-Martínez <i>et al.</i> [36]		a. Indirect Tensile-strength	2.5 MPa	
	b. Infiltration Capacity	0.40 cm/s		

reinforced concrete with 1.5% fibre content showed better results. The compressive strength of concrete with 1.5% of polypropylene fibre was higher as compared to that of control plain concrete by 14.78%. Some more studies regarding use of steel fibres in concrete for pavement applications are summarized in Table 2.10.

2.5.1.2 Addition of Artificial Fibres in Concrete for Pavements

Gupta *et al.* [22] used Polyester Fiber Reinforced Concrete (PFRC), with and without fly ash, for pavement applications. Compressive and flexural strength, reduced drying shrinkage, abrasion resistance and deflection test were determined to evaluate the durability and mechanical properties of PFRC. The range of fibre contents used was 0 – 1% at increments of 0.25%. The optimum fiber content was 0.25%, which was selected for its better flexural strength and abrasion resistance. Results showed that the abrasion resistance of optimum PFRC was higher by about 25% than that of reinforced concrete. Choi *et al.* [201] also evaluated the

TABLE 2.11: Use of artificial fibre reinforced concrete for pavement applications.

Reference	Fibre	Fibre Reinforced Concrete Properties	Obtained Values	Application
(1)	(2)	(3)	(4)	(5)
Glavind [202]	Polypropylene	a. Shrinkage Crack Resistance b. Tensile Strain	-	PAVEMENTS
Gupta [22]	Polyester	a. Compressive Strength b. Flexural Strength c. Abrasion Loss	48-60 MPa 4.4-5.0 MPa 0.15-0.21%	
Salemi and Behfarnia [24]	Polypropylene	a. Compressive Strength b. Frost Resistance	43-54.9 MPa 12.8-28% Strength Loss (at 300 cycles)	
Kanalli <i>et al.</i> [27]	Polymer	a. Compressive Strength b. Flexural Strength	33.3-39 MPa 18.9-20.2 MPa	
Kumar <i>et al.</i> [29]	Polypropylene	a. Compressive Strength b. Split-tensile Strength c. Flexural Strength	56.3-59 MPa 4.2-5.1 MPa 8.9 MPa	
Yang <i>et al.</i> [203]	Amorphous Metallic	a. Compressive Strength b. Flexural Strength	23.7 MPa 4.2 MPa	

artificial fibre reinforced concrete for controlling the shrinkage cracking in concrete pavements. The study concluded that the drying shrinkage strain was remarkably reduced by using 0.2% of fibre, by volume of concrete. Kanalli *et al.* [27] studied the effect of polypropylene fiber (varying ratio of dosage of 0.25% by volume from 0.25% to 1.25%) in concrete pavement by testing its tensile strength, flexural strength and compressive strength. Fiber reinforced concrete exhibited an increase in 28 days flexural and compressive strength by about 6.4% and 21%, respectively, when compared to that of controlled specimen. There was also a reduction in drying shrinkage from 0.062% to 0.03%. Furthermore, they also concluded that higher initial cost is reduced by 15-20% by the reduction in maintenance and rehabilitation operations, making polypropylene fibre reinforced concrete cheaper than flexible pavement by 30-35%.

The findings of some studies on artificial fibre reinforced concrete for pavement applications are summarized in Table 2.11.

2.5.2 Natural Fibres in Concrete for Pavements

As discussed earlier, natural fibre reinforced concrete is comparable with steel fibre reinforced concrete and artificial fibre reinforced concrete for various civil engineering applications. Hence, the natural fibre reinforced concrete has also been studied for rigid pavement applications, but with limited scope [204–209]. Sugarcane bagasse fibre reinforced concrete was investigated by Patel D and Patel V [208] for pavement applications. Three fibre contents i.e. 0.5%, 1%, and 1.5% (by weight of concrete) were used with the aspect ratios of 30, 60 and 90. The optimum content and aspect ratio came out to be 1% and 90%, respectively. An increase of 6% in flexural strength and 9% in compressive strength of concrete was observed at this optimized material.

Khan and Ali [130] have also studied hair fibre reinforced concrete for concrete pavements. The compressive, splitting-tensile, and flexural strengths of concrete reinforced with hair fibres were increased by 12.4%, 16.2%, and 19.1%, respectively. The study also reported that the pavement thickness of hair fibre reinforced concrete was reduced by 0.5 inches when compared to that of reference concrete for particular loading conditions. The summary of these two studies is given in Table 2.12.

2.5.3 Identified Research Gap on Structural Capacity of Fibre Reinforced Concrete for Pavements

Hence, the crack arresting mechanism due to addition of fibres in concrete, delays the propagation of cracks under traffic loading, resulting in improved post cracking behavior of fibre reinforced concrete pavements. However, to economize the cost of pavements, locally available natural fibres can be used. Only limited studies have been reported on the natural fibre reinforced concrete for structural applications. However, knowledge on structural capacity of natural fibre reinforced concrete for pavement applications, especially by using wheat straw, is missing.

TABLE 2.12: Use of natural fibre reinforced concrete for pavement applications.

Reference	Fibre	Fibre Reinforced Concrete Properties	Obtained Values	Application
(1)	(2)	(3)	(4)	(5)
Patel D and Patel V [208]	Sugarcane Bagasse	a. Compressive Strength	27.9-30.8 MPa	PAVEMENTS
		b. Flexural Strength	3.2-4.8 MPa	
Khan and Ali [130]	Hair	a. Compressive Strength	13.9-14.1 MPa	
		b. Splitting-tensile Strength	1.7-1.8 MPa	
		c. Flexural Strength	3.5-3.6 MPa	
		d. Thickness Reduction	6%	
		e. Cost Reduction	3%	

2.6 Structural Performance of Rigid Pavements

2.6.1 Rigid Pavements

In the rigid pavements, the vehicular load is resisted by the flexural strength of concrete, whereas steel reinforcement is provided to control cracks formation or to resist the cracks propagation [210]. Conventional concrete pavements are generally classified as jointed plain concrete pavement (JPCP), jointed reinforced concrete pavement (JRCP), and continuous reinforced concrete pavement (CRCP). Huang [211] reported that the basic rigid pavement design equation as per American Association of State Highway and Transportation Officials (AASHTO) 1993: II-45 is used for the design of rigid pavements. The equation is as follows:

$$\log_{10} W_{10} = Z_R S_o + 7.35 \log_{10} (D + 1) - 0.06 + \frac{\log_{10} \left[\frac{\Delta PSI}{4.5-1.5} \right]}{1 + \frac{1.624 \times 10^7}{(D+1)^{8.46}}} + (4.22 - 0.32Pt) \left[\frac{S'_c C_d [D^{0.75} - 1.132]}{215.63j \left[D^{0.75} - \frac{18.42}{\left(\frac{E_c}{k}\right)^{0.25}} \right]} \right] \quad (2.1)$$

Where:

W_{18} = Traffic load in equivalent standard axle loads

Z_R = Standard normal deviation for desired reliability

S_O = Overall standard deviation

D = Slab thickness (in)

ΔPSI = Serviceability index

S'_c = Flexural strength of concrete (psi)

C_d = Drainage coefficient

J = Load transfer coefficient

E_c = Elastic modulus of concrete (psi)

k = subgrade reaction modulus (psi/in)

The structural evaluation of rigid pavements can be performed by using the standard AASHTO T256 / ASTM D4695, in which load carrying capacity of rigid pavements can be determined.

2.6.2 Performance Evaluation Techniques for Pavement Test Sections

With the increase of heavy traffic and violation against maximum load conditions, highways/pavements become aged and deteriorated rapidly at very early stage. Regular maintenance and rehabilitation are required on frequent basis to keep the pavements serviceable for regular traffic, which is indeed a hectic, time consuming and cost consuming task. Usually, destructive, i.e. laboratory, testing and Non-Destructive Testing (NDT) methods are used for the evaluation of structural performance of pavements [132]. An expensive and time-consuming process in terms of laboratory/destructive testing is coring of existing pavements/test-sections [212]. As far as non-destructive testing techniques are concerned, the most

widely used techniques are Impulse device, i.e. Dynatest Falling Weight Deflectometer (FWD), Steady state dynamic device, i.e. Dynaflect / Road Ratar, Semi-continuous static device, i.e. Lecroix deflectograph and Non-continuous static device, i.e. Benkelman Beam Apparatus [213, 214]. Among all these mentioned NDT tests, Benkelman beam is most widely used for the establishment of in-situ pavement/test-section structural performance as it is simple and easy to understand [132].

Furthermore, the performance of continuously reinforced concrete pavements can also be evaluated by observing crack patterns, mainly the shapes of cracks and spacing between them. The occurrence of minimum but straight cracks with uniform spacings are recommended for better performance [215–219]. Early cracking is classified into four different types, i.e. i) cracking due to plastic settlement which usually occurs in 10 minutes of casting to 3 hours, ii) plastic shrinkage cracking which occurs after 30 minutes of casting to 6 hours, iii) cracking occurs due to thermal expansion and contraction of concrete which occurs from a day after curing up to 2 to 3 weeks, and iv) drying shrinkage cracks which occur after weeks of concreting to months. Early-age micro cracking in concrete is usually monitored with visual inspections, digital imaging, radiography, optical microscopy, scanning electron microscopy, ultra-sonic pulse velocity, acoustic emission, laser displacement sensors and three-dimensional X-rays [76, 220–224]. The ASTM standards i.e. ASTM C157 and ASTM C341 can also be used for the drying shrinkage cracks measurement in laboratory or on drilled cores as reported in state-of-the-art report on control of cracking in concrete, as reported in Transportation Research Board (2006). Furthermore, it is also reported that cracks can be classified into discrete cracks and distributed fine cracks which can be located individually and by area calculations, respectively. The cracks characterization (i.e. location, length, width, and direction) can be made after detection as also reported by Mahler and Kharoufa [74].

Therefore, the structural performance evaluation of cement concrete roads by using destructive and non-destructive testing techniques is reported in various researches.

2.6.3 Identified Research Gap on Structural Performance of Wheat Straw Reinforced Concrete

Hence, destructive and non-destructive testing mechanism are implemented to evaluate the performance of rigid pavements. Load carrying/structural capacity and cracks progression mechanism are the key performance indicators in cement concrete pavements. Field investigation on existing road and/or newly constructed test sections is performed instead of laboratory testing to study the response of respective pavement under real loading and climatic conditions. However, to the best of author's knowledge, wheat straw reinforced concrete pavement test sections are not constructed and evaluated yet.

2.7 Summary

An extensive literature has been reviewed to dig-out the rigid pavement background and distresses that usually occur in it, with the focus on rigid pavements of developing countries. The governing parameters for these distresses and possible remedial measures are also explored. Based on the conducted literature review, it can be concluded that overloading of heavy traffic and weak soil strata demand the development of rigid pavements. The conventional brittle nature of cement concrete is more prone to early-age distresses. Steel reinforcement is usually used to cater this issue. Due to which, the cost of rigid pavement construction is remarkably high. Hence, its excessive use in developing countries is prevented. The primary distresses are early-age micro-shrinkage cracking, which leads towards development of punch-outs, when occur in clusters. However, the incorporation of discrete fibres in cement concrete can result in reduction of said premature distresses in concrete pavements of developing countries [22, 27, 29, 100].

As per literature, for heading towards sustainable development, focus of researchers is the reduction of biodegradable materials, in terms of eliminating waste [7–10]. Therefore, the usage of natural fibres (i.e. plant/agricultural wastes), instead of

artificial/steel fibres, is gaining the attention of researchers around the globe. As per past studies, it can be said that the load carrying capacities and post cracking behaviors of natural fibre reinforced concrete is comparable with that of concrete reinforced with artificial fibres. Among all natural fibres, wheat straw is slightly explored yet for cement concrete composites. Accordingly, to evaluate the behavior of wheat straw in concrete, there is a need to explore it in detail for its possible use in civil engineering structural applications.

However, due to the bio-degradable organic nature, the durability of plant fibres in cement concrete does not provide much hindrance for the civil engineering structural applications. Therefore, it needs special consideration, when intended to be used for such purpose. Accordingly, the long-term durability of wheat straw reinforced concrete for rigid pavement applications needs to be determined in depth, due to the organic nature of straw, as pavements are directly exposed to natural weathering/environmental/climatic conditions throughout their design life.

The crack arresting mechanism, due to addition of fibres in concrete, delays the crack initiation and propagation under traffic loading which ultimately results in better post cracking behavior of fibre reinforced concrete pavements as reported by various researchers. However, keeping in mind the economy, the local and abundantly available natural/plant/agricultural fibres can be used. But for pavement applications, the natural fibre reinforced concrete has been studied thrice only with limited scope, so far. Whereas, wheat straw reinforced concrete has not been explored for rigid pavements yet.

The performance evaluation of rigid pavements is usually made with the help of destructive and non-destructive testing as reported in literature. The performance of rigid pavements is associated with their structural capacity and crack progression mechanism. The pavement test sections are also constructed to study the pavement response under the realistic traffic loading and climatic conditions. However, to the best of author's knowledge, wheat straw reinforced concrete pavement test section has not been constructed and evaluated yet.

Chapter 3

Optimization of Wheat Straw Reinforced Concrete Mix

Related Articles:

M. U. Farooqi and M. Ali, "Effect of pre-treatment and content of wheat straw on energy absorption capability of concrete," *Construction and Building Materials*, vol. 224, pp. 572-583, 2019. (ISI I.F. 4.064, HEC W-Platinum Category)

M. U. Farooqi and M. Ali, "Effect of Fibre Content on Splitting-Tensile Strength of Wheat Straw Reinforced Concrete for Pavement Applications," *In Key Engineering Materials*, vol. 765, pp. 349-354, 2018. (SCIMAGO I.F. 0.35, Q-3)

M. U. Farooqi and M. Ali, "Effect of Fibre Content on Compressive Strength of Wheat Straw Reinforced Concrete for Pavement Applications," *IOP Conference Series: Materials Science and Engineering*, Vol. 422, No.1, p. 012014, IOP Publishing, 2018.

M. U. Farooqi and M. Ali, "Compressive behavior of wheat straw reinforced concrete for pavement applications," *In proceedings of 4th International Conference on Sustainable Construction Materials and Technologies (SCMT4)*, Las Vegas, USA., 2016.

3.1 Background

Concrete, due to its comparatively simple production, abundantly available components, and a number of various types of applications, is used widely all over the world. However, concrete is a brittle material with minimum strain-capacity and ultimately low toughness. Hence, in making efforts to increase its ductility by increasing the tensile strength of conventional concrete, addition of dispersed fibres in the cement concrete composites has come out to be an effective way to increase the energy-absorption capability of concrete. Also, the crack development and propagation in conventional cement concrete can also be counteracted by incorporation of discrete fibres.

In the recent years, considerable interest has been developed on using natural fibres, instead of artificial/steel fibres, in cement composites for having alternate sustainable, economical, and eco-friendly building materials. For improving the properties of composites, the use of plant based natural fibres as a low-cost renewable construction material can contribute towards sustainable development. The results of natural fibres reinforcement are comparable with that of artificial/steel fibres in terms of enhanced toughness. The natural fibres that are used as dispersed reinforcement in cement composites for civil engineering applications include sugarcane, sisal, coir, bamboo, banana, date, malva, kenaf bast, vakka, palm, jute, pineapple leaf, hemp, ramie bast, flax, hibiscus cannabinus, abbaca leaf, wheat straw, sansevieria leaf, and elephant grass.

Among all natural fibers, wheat straw, the agricultural waste/by-product of one of the most widely cultivated crop in Pakistan, is selected in this study due to its abundant local availability. Furthermore, to the best of author's knowledge, wheat straw is considered only for the limited non-structural applications yet. Therefore, to get in-depth knowledge on behavior of Wheat Straw Reinforced Concrete (WSRC) for wide civil engineering applications, a detailed investigation is made. Accordingly, the effect of pre-treatment technique (i.e. soaking, boiling and chemical treatment) and content (i.e. 1%, 2%, and 3%, by mass of wet concrete) of an

additive, i.e. wheat straw, on the energy absorption capability of concrete under compressive, splitting-tensile, and flexural loadings is determined experimentally. Pre-test micro-structural analysis of soaked, boiled and chemically treated straw is done with scanning electron microscope. The scanning electron microscopic study on straw-cement bond mechanism is also conducted on tested specimens to get in-depth behavior. Comparative study of Plain Concrete (PC), Soaked Wheat Straw Reinforced Concrete (SWSRC), Boiled Wheat Straw Reinforced Concrete (BWSRC), and Chemically (NaOH) treated Wheat Straw Reinforced Concrete (CWSRC) is made. It is intended for the optimization of pre-treatment technique and straw content for WSRC matrix. Accordingly, in a sequence, materials collection, preparation, mix proportions, casting, specimens details and testing methodologies are given in Section 3.2. Section 3.3 comprises of experimental investigation, results analysis and discussions on obtained results. The findings are summarized in Section 3.4.

3.2 Materials and Methods

3.2.1 Materials

The basic constituents used in preparation of PC, SWSRC, BWSRC, and CWSRC are Ordinary Portland Cement (OPC) of local company (i.e. Bestway Cements), locally available sand of lawrence-pur source, aggregates from the crushes of Margallah, potable/tap water and commercially available wheat straw. The production of OPC from Bestway cements is as per EN 1971: 2011-CEM I 425N i.e. having 28 days strength of 52 ± 3 MPa. However, chemical composition of this product of BESTWAY is given in Table 3.1. The maximum size of aggregates used is 19.5 mm that retained 36% of the total aggregate weight. Whereas, the percentages retained on 12.5 mm and 9.5 mm sieve sizes are 44% and 15%, respectively. However, for fine aggregates, i.e. sand, the percentages of coarse sand, i.e. 4.75 - 2.36 mm, medium sand, i.e. 2.36 - 0.425 mm, and fine sand, i.e. 0.425 - 0.075 mm, are 8%, 44% and 37%, respectively. Agricultural residues of wheat

TABLE 3.1: Chemical composition of BESTWAY cement.

Oxide (1)	Symbol (2)	Percentage% (3)
Calcium Oxide	(CaO)	61.7%
Silicon Dioxide	(SiO_2)	21%
Aluminum Oxide	(Al_2O_3)	5.04%
Iron (III) Oxide	(FE_2O_3)	3.24%
Magnesium Oxide	(MgO)	2.56%
Sulphur Trioxide	(SO_3)	1.51%

crop (i.e. wheat straw), which are commercially available in a near-by source, are used. The length of wheat straw, which was available commercially, is 25 mm. Commercially (local) available wheat straw is taken by a random selection. The approximate linear dimensions of wheat straw (randomly obtained) are $25mm \times 5mm \times 1.2mm$. Whereas, the tensile strength, shear strength, and the density of wheat straw ranges between 21.2 to 40.0 MPa, 4.91 to 7.26 MPa, and 55 to 119 kg/m^3 , respectively, as reported by [18, 156, 159, 225]. Chemical analysis of wheat straw is done by Energy Dispersive X-ray (EDX). The chemical composition of wheat straw is given in Table 3.2. It is noted from chemical analysis of wheat straw that there are abundant carbohydrates (i.e. lignin, hemicellulose, and cellulose) as also reported by [183, 226, 227]. Minerals (i.e. phosphorus and calcium), silica, proteins, ash and acid detergent fibres were found in straw in addition to 84 – 91 % dry matter.

3.2.1.1 Wheat Straw Treatment

Soaked Wheat Straw: Local commercially available wheat straw are dipped in water for 15 to 20 minutes. This dipping is purposed to remove the wax/impurities/dust particles from the straw surface. After that, straw are removed from the water and then air-dried. These straw are named as soaked wheat straw.

TABLE 3.2: Chemical composition of wheat straw.

Element	Current Study		Previous Studies		References
	Soaked Straw	Un-Treated	Treated		
	Weight	Weight	Weight		
	(%)	(%)	(%)		
(1)	(2)	(3)	(4)	(5)	
Carbon	C	58.98	43.51-63.6	41.52-64.50	Nielsen <i>et al.</i> [228]; Caslin and Finnan [229];
Oxygen	O	39.90	28.65-42.4	33.05-33.45	Mac <i>et al.</i> [230]; Wanga <i>et al.</i> [231];
Silicon	Si	0.48	0.04-7.01	0.40-2.70	Petrella <i>et al.</i> [232]; Cai <i>et al.</i> [233];
Potassium	K	0.19	0.00-1.79	1.14-23.10	Medyńska-Juraszek <i>et al.</i> [234];
Calcium	Ca	0.45	0.42-20.57	0.43-8.60	Deng <i>et al.</i> [235]

Soaked wheat straw are shown in Figure 3.1(a). A dull but a clean texture of natural wheat straw is observed with the naked eye and also by scanning electronic microscope.

Boiled Wheat Straw: For having improved interfacial bond strength between cement composites and raw natural fibres, pre-treatment is required in most of the practical situations. For this purpose, different techniques are adopted by various researchers for increasing its bond strength by having the improved fibre surface. Physical and chemical modifications of fibre surface are made with the help of such pre-treatment techniques [72, 236–243]. In the current work, among two, one simple pre-treatment is used as also done by [72, 73]. Water is boiled for half an hour and dry straw are then dipped in that boiling water. Water having that straw is then kept on boiling for almost 20 minutes. Water is cooled then and straw are removed from water. These straw are then air-dried. Hereafter, these straw are referred to “boiled wheat straw” and are shown in Figure 3.1(b). The improved shiny texture of boiled wheat straw are observed with the naked eye. However, the microscopic image revealed that cracks occurred on the surface of straw. Asasutjarit *et al.* [72] reported that the increase in cellulose contents and washout of extractives from the surface of straw improves stiffness and toughness of these boiled straw. Furthermore, the resistive extraneous fibre from the straw surface can also be removed with the help of this boiling treatment which also resulted in the reduced density of flax fibre [244]. Therefore, the straw-matrix

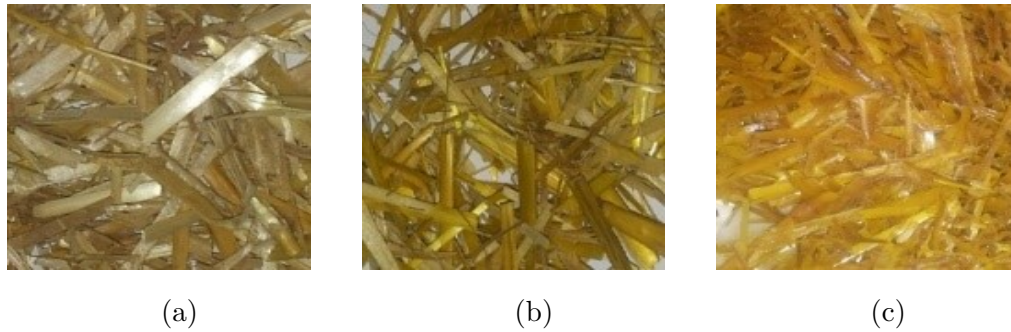


FIGURE 3.1: Wheat Straw (a) Soaked (b) Boiled and (c) Chemically treated.

adhesiveness can be enhanced. Similar type of behavior by using the boiling technique for coconut fibres is also reported by [72, 73].

Chemically Treated Wheat Straw Another technique is also used for the pre-treatment of straw for having improved bonding of straw with concrete. Wheat straw are dipped in 3% sodium hydroxide (NaOH) solution for half an hour. Straw are then removed from the solution and air surface dried. A more shiny and washed texture is observed with the naked eye. But through microscopic view, an increase in surface cracking of straw is observed. These straw are named as chemically treated straw and are shown in Figure 3.1(c). Similar type of pre-treatment technique was also adopted by Ali and Chow [245].

3.2.2 Mix Proportions and Casting Procedure

The mix proportions for plain concrete are 1 : 2 : 4 (cement: sand: aggregate) having w/c ratio of 0.55. For preparing 1 m³ of PC, 331 kg, 704 kg, 1550 kg and 182 kg of cement, sand, aggregates and water, respectively, are taken. However, for making WSRC, the wheat straw, having approximate length of 25 mm and contents of 1%, 2% and 3%, by mass of wet concrete, are incorporated (as an additive) with 0.60 w/c ratio. Accordingly, the weights of cement, sand, aggregates, water and straw are 254 kg, 542 kg, 1194 kg, 152 kg and 27 kg, respectively, for the preparation of 1 m³ of WSRC. The water absorption of soaked, boiled and NaOH treated straw are given in Table 3.3. The w/c ratio is kept higher in case of WSRC mix for achieving its proper compaction along with workability in order to

optimize strength. The free w/c ratio of WSRC may be taken as same as that of PC, because additional water is just for straw in concrete. For the preparation of PC mix: cement, sand and aggregates are simultaneously put in the drum mixer and water is then added. The mixer is started to rotate for a period of five minutes. Whereas, for WSRC: $1/3^{rd}$ of cement, sand, aggregates and straw are put in the drum mixer in four layers. The remaining cement, sand, aggregates, and straw are then added in the drum mixer using the same layering technique. $2/3^{rd}$ of water is then added and mixer is rotated for three-minutes. The $1/3^{rd}$ water is then added and the drum mixer is started again to rotate for two minutes. Still the mix is not homogenous and workable at this point. The mixer is then rotated again for three minutes to get better homogenous mix. Mixing time is increased because addition of water at that stage could have resulted in bleeding of WSRC. Therefore, the increased mixing time came out to be a successful approach for a workable WSRC. The slump and compaction factor tests are performed for fresh PC and WSRC (Table 3.3).

For preparation of WSRC specimens, prepared homogenous mixture is then poured in the moulds. Each layer is then compacted by 25 blows of tamping rod. In addition to that, for removing air voids, the mould having WSRC is lifted up to approximately 100 - 150 mm followed by free drop. The specimens are then demoulded after 24 hours and are kept for curing for 28-days. The water absorption test for hardened PC and WSRC specimens are conducted thereafter (Table 3.3). Afterwards, the specimens are equally bifurcated in four equal sets. One set is tested after 28 days of curing whereas, remaining three sets of specimens are kept under three different ageing conditions, i.e. room, climatic and alternate wetting and drying conditions for the period of 4-years. The PC and WSRC specimens, at different stages, are shown in Figure A1 in Annexure A.

3.2.3 Specimens

Cylinders with dimensions of 200 mm height and 100 mm diameter, for compressive and splitting-tensile strength tests, are prepared for PC, SWSRC, BWSRC,

and CWSRC. However, 100 mm wide, 100 mm deep and 450 mm long beam-lets are cast for performing flexural strength test. Labels OO, A, T, and N are used for PC, SWSRC, BWSRC and CWSRC, respectively. Numeric figures along with labels show the content of straw for each specimen. Two specimens for each combination are cast. For numbering of specimens; alphabets (i.e. A and B) are used. The average of two readings, with robust results, is used for hardened concrete properties. The average of two readings is also considered by other researchers as well [246, 247].

3.2.4 Testing Methods

3.2.4.1 Density

Standard test method (i.e. ASTM C138/C138M–16) is adopted for determining the density of PC. To the best of author’s knowledge, there is no test standard available for the measurement of density of WSRC. Therefore, the same test standard is also used for determining the density of SWSRC, BWSRC, and CWSRC as well.

3.2.4.2 Compression Test

Servo-hydraulic Testing Machine (STM), with high precision displacement transducer having measurement range from 0 – 1500 mm and resolution of 0.001 mm, is used for the determination of compressive strength, absorbed compressive energy (Ce), energy absorption till the maximum stress (Cem), energy absorption after the maximum stress (Cep) and compressive toughness index (CTI) of the cylinder specimens.

Cylinders are capped with sulphur before testing for the uniform distribution of load. ASTM C39/C39M-20 (Standard Test Method for Compressive Strength of Cylindrical Concrete Specimens) is used for testing the cylinders in compression. The test setup is shown in Figure 3.2(a).

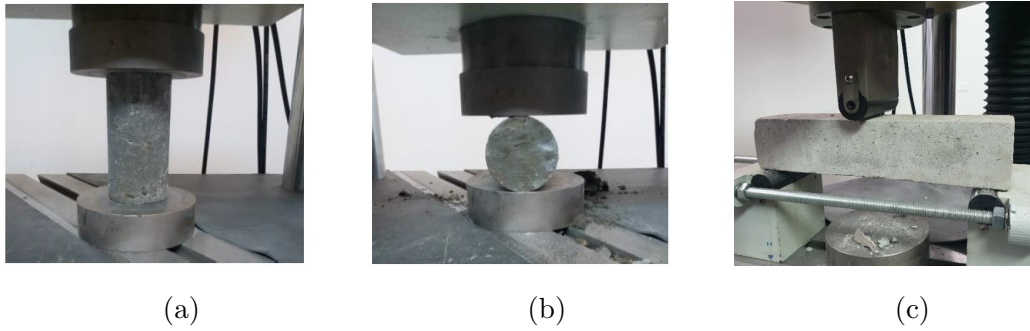


FIGURE 3.2: Testing setup (a) Compressive strength test, (b) Splitting-tensile strength test, and (c) Flexural strength test.

3.2.4.3 Splitting-tensile Test

The test standard adopted for performing splitting-tensile strength test on PC, SWSRC, BWSRC, and CWSRC specimens is ASTM C496/C496M-17 (Standard Test Method for Splitting Tensile Strength of Cylindrical Concrete Specimens). Cylinders are tested for the determination of splitting-tensile strength (SS), splitting-tensile energy absorbed (Se), splitting-tensile energy absorbed up to the maximum load (Sem), splitting-tensile energy absorbed post the maximum load (Sep) and splitting-tensile toughness index (STI). The test setup is shown in Figure 3.2(b).

3.2.4.4 Flexural Test

ASTM C293/C293M-16 (Standard Test Method for Flexural Strength of Concrete - Using Simple Beam with Centre-Point Loading) is adopted for performing the flexural strength test on PC, SWSRC, BWSRC, and CWSRC beam-lets. Flexural testing machine is used. Flexural behavior, modulus of rupture (MoR), flexural energies absorption (Fe, Fem and Fep) and flexural toughness index (FTI) are determined. The test setup is shown in Figure 3.2(c).

3.2.4.5 Scanning Electron Microscope (SEM) Test

The micro-structural analysis of soaked, boiled, and chemically treated straw and for their bonding with concrete is done by performing scanning electron microscope

imaging. This test is intended to reveal the micro-structure of straw with and without treatment, mixing of straw in concrete, in-depth mechanism of straw-concrete bonding, and nature of failure/cracking. The VEGA3 TESCAN having voltage of 10 kV is utilized for scanning electron microscopic imaging. Plasma coating is done on samples before testing.

3.3 Results Analysis and Discussions

3.3.1 Density

Densities for PC, SWSRC, BWSRC, and CWSRC are given in Table 3.3. Although the w/c ratio is increased for WSRC but the densities of WSRC specimens (with soaked, boiled, and chemically treated) are decreased in comparison to that of PC. It might be due to the presence of low-density straw in WSRC specimens. The same behavior was observed by the other researchers [66, 72, 248, 249]. As far as the straw contents are concerned, a decrease in density is observed with the increase in content of straw. Presence of low-density straw will have an effect on overall weight of the specimens which might be the reason of decrement in density with the increment in straw content. Among soaked, boiled and chemically treated straw reinforced concrete, the CWSRC has the highest value of density.

3.3.2 Properties under Compressive Loading

3.3.2.1 Compressive Behavior

Typical stress \sim strain curves of PC, SWSRC, BWSRC, and CWSRC are shown in Figure 3.3. It may be noted here that for all WSRC specimens; the ascending side of stress strain curves is less steep as compared to that of PC. For all three types of straw (i.e. soaked, boiled and chemically treated), only cracking is observed even after maximum loading, depicting the tough behavior of WSRC specimens due to

TABLE 3.3: Water absorption of wheat straw and fresh and hardened state properties of PC, SWSRC, BWSRC and CWSRC.

Specimen	Wheat Straw		W/C Ratio	Fresh State Tests		Hardened State Tests	
	Straw Type	Water Absorption (%)		Slump Values (mm)	Compaction Factor	Density (kg/m ³)	Water Absorption (%)
(1)	(2)	(3)	(4)	(5)	(6)	(7)	(8)
PC	x	x	0.55	25	0.99	2270	3.6
SWSRC-1%	Soaked	55%	0.60	20	0.98	2167	4.9
SWSRC-2%	x	x	0.60	13	0.96	2077	5.5
SWSRC-3%	x	x	0.60	0	0.92	1763	5.8
BWSRC-1%	Boiled	66%	0.60	17	0.98	2131	6.1
BWSRC-2%	x	x	0.60	15	0.97	2065	6.7
BWSRC-3%	x	x	0.60	10	0.90	1801	7.4
CWSRC-1%	NaOH	61%	0.60	19	0.97	2185	5.4
CWSRC-2%	x	x	0.60	15	0.96	2059	6.1
CWSRC-3%	x	x	0.60	5	0.93	1921	7.0

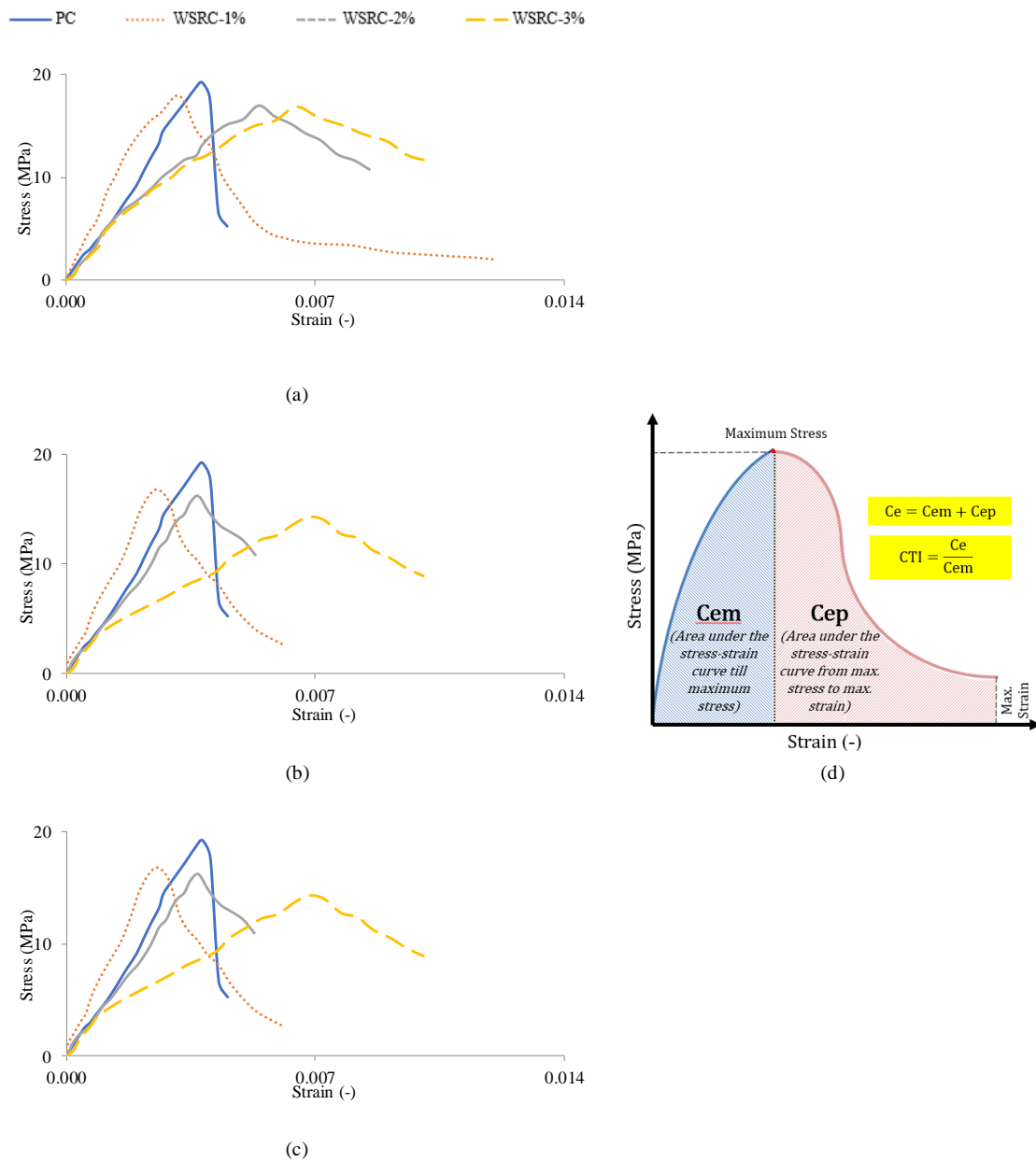


FIGURE 3.3: Compressive stress ~ strain curves of (a) SWSRC, (b) BWSRC, (c) CWSRC with 1%, 2% and 3% content and (d) schematic diagram for energy absorption calculations.

the addition of discrete straw in the composite. However, in case of PC, a sudden drop in compressive load is observed as soon as the maximum load is applied, showing the brittle behavior of conventional concrete, as expected. Reduction in concrete brittleness due to the addition of dispersed fibres (i.e. coconut fibres) in concrete is also reported by Salain et al. [250]. The cylinder specimens which are crushed under the compressive loading are shown in Figure 3.4. During testing, due to brittle nature of PC, the fragments from PC specimens are separated as can be seen at the base plate in Figure 3.4 (0% straw content). While in wheat straw reinforced concrete cylinders, a bridged behavior is observed due to incorporation of wheat straw.

3.3.2.2 Compressive Strengths, Compressive Energy Absorption and Compressive Toughness Index

In compressive stress \sim strain curves, the highest stress value is taken as compressive strength (Table 3.4). Compressive strengths (σ) of WSRC (i.e. SWSRC, BWSRC, and CWSRC) are decreased w.r.t PC. The decrease in compressive strengths of natural fibre reinforced concrete is also reported by many other researchers [40, 66, 251]. The noticeable behavior is that, with increase in straw content, the compressive strength is decreased. A decrease of 5% and 9% in compressive strengths of SWSRC-2% and SWSRC-3%, respectively, is observed in comparison to that of SWSRC-1%. Similarly, the compressive strengths of BWSRC-2% and BWSRC-3%, and CWSRC-2% and CWSRC-3% are decreased by 2% and 15%, and 7% and 19%, respectively, in comparison to that of BWSRC-1% and CWSRC-1%. This behavior might be due to improper compaction or bonding between straw and concrete due to increased amount of straw. However, among three types of straw used, the SWSRC showed better results when compared to BWSRC and CWSRC. If the WSRC with 1% straw content are compared, a decrease of 6% and 18% in the compressive strengths of BWSRC and CWSRC, respectively, is recorded as compared to the compressive strength of SWSRC. It might be because of changed chemical composition of wheat straw due to boiling and chemical treatment. The modulus of elasticity for PC and WSRC specimens



FIGURE 3.4: Tested cylinder specimens of PC and WSRC with varied treatment and fibre content under compressive loading.

is also calculated and given in Table 3.4. For PC, the elastic modulus is calculated by using formula; $E_c = 4700\sqrt{f'_c}$ (MPa), as per ACI 318-08 [252]. However, for WSRC specimens, the elastic modulus is calculated by using equation proposed by Suksawang *et al.* [253]; $E_c = \lambda_{v_f}4700\sqrt{f'_c}$ (MPa), where λ_{v_f} is 1 when $C/S > 1$ and the $\lambda_{v_f} = \frac{1 + 0.7^{v_f}}{2}$ when $C/S < 1$. The fibre effect factor, i.e. λ_{v_f} , is taken as 1 here in current study as coarse aggregate weight to sand aggregate weight ratio is greater than 1 ($C/S > 1$). The value of λ_{v_f} is recommended 1 because in

this scenario, as concluded by [253], the elastic properties are not influenced by the fibres except some fluctuations that are within 10%. Total area beneath the stress strain curve is taken as energy absorption under compressive stress (C_e). Some researchers have also taken it as compressive toughness [66, 71]. This energy absorption capacity per unit volume of concrete material was defined in MJ/m^3 by [254, 255]. If the area beneath compressive stress strain curve is calculated till the maximum stress only, it is then taken as energy absorption till the maximum compressive stress (C_{em}). Whereas, the area beneath stress \sim strain curve from the point of maximum stress to the maximum strain is taken as the energy absorption after the maximum compressive stress (C_{ep}). The ratio of energy absorption under compressive stress to the energy absorption up to the maximum compressive stress (i.e. C_e/C_{em}) is taken as compressive toughness index (CTI). The schematic diagram for energies absorption (i.e. C_{em} , C_{ep} and C_e) and toughness index calculations are shown in Figure 3.3(d). Whereas, C_{em} , C_{ep} , C_e and CTI values of PC, SWSRC, BWSRC, and CWSRC are also shown in Table 3.4.

The absorbed compressive energy by WSRC is much higher (i.e. up to 163% for SWSRC, 107% for BWSRC, and 142% for CWSRC) than that of PC. The reason might be the elongated deformation in case of WSRC specimens. As more energy is absorbed due to the addition of straw which resist the crack to apart. However, only 2% increase is observed in the fracture energy of WSRC, in comparison to the fracture energy of plain concrete, by [18]. It may be noted here that almost 40% to 50% of the compressive energy is absorbed post the maximum stress in case of SWSRC, BWSRC, and CWSRC. The incorporation of straw in concrete helps in resisting the occurrence of crack by absorbing more energy. However, once the cracks start to occur and the specimens bear the maximum load, even then straw continue to play their role by resisting the crack propagation by binding the both ends of cracks. This phenomenon results in enhanced energy absorption and improved post cracking behavior of wheat straw reinforced concrete. Due to this behavior, with the addition of fibres in concrete, the brittleness of conventional concrete (PC) is also reduced and resulted in improved toughness. The compressive toughness index is increased up to maximum of 91% in case of SWSRC-1%

when compared to that of PC. All the other straw reinforced matrices show the increase in compressive toughness index ranges from 15% to 86% in comparison with PC. Generally, a decrease in compressive properties is noted with the increase in straw content for the compressive strength and compressive toughness indices of WSRC specimens. This decrease might be due to the improper mixing of concrete ingredients along with the high content (i.e. 2 to 3%, by mass of cement). In addition to that the increased content of low-density straw might also result in less compaction of the wheat straw reinforced concrete specimen. Although the compressive strengths of WSRC specimens are decreased up to some extent however, SWSRC with 1% content shows overall better compressive properties in comparison to all other straw reinforced matrices and PC as well.

A comparison of strengths, energy absorption and toughness indices, under compressive loading, for PC, SWSRC, BWSRC, and CWSRC is shown in Figure 3.5. It can be observed that, for all three composites (i.e. SWSRC, BWSRC, and CWSRC), the WSRC with 1% content shows better results in comparison to the respective WSRC specimens with 2% and 3% contents. Although the compressive strengths of SWSRC, BWSRC and CWSRC specimens are decreased when compared to that of PC, but the compressive energies absorbed, and compressive toughness indices are increased. This might be due to the increase in toughness of WSRC because of the addition of dispersed straw in concrete. However, in case of boiled wheat straw reinforced concrete, the compressive energy absorbed by the specimens with 1% content is less than that of PC.

The increase in compressive toughness of composites incorporating natural fibres is also reported by [16, 73, 249]. Xiangwong reported decrease in compressive strength of fibre reinforced concrete with the increase in compressive toughness index [256]. The strength along with the toughness are attributed towards concrete structural performance, as reported by [256, 257]. Accordingly, significantly enhanced toughness with minimally compensated strength can be headed towards the improved performance of structure. In addition, the modulus of elasticity is also one of the main parameters for the design of rigid pavements along with its flexural strength. As, the addition of discrete fibres used to significantly change

TABLE 3.4: Compressive Strength (σ), Energies absorption under compressive load (Cem, Cep, Ce) and Compressive Toughness Index (CTI) of PC, SWSRC, BWSRC and CWSRC.

Specimen	σ	Compressive Energies Absorbed												
		COV (%)	E (GPa)	COV (%)	Cem (kJ/m ³)	COV (%)	Cep (kJ/m ³)	COV (%)	Ce (kJ/m ³)	COV (%)	CTI	COV (%)		
(1)	(2)	(3)	(4)	(5)	(6)	(7)	(8)	(9)	(10)	(11)	(12)	(13)		
PC	19.2±0.2	1.47	20.7±0.1	0.74	36.2±1.2	4.69	8.4±1.0	16.84	44.6±1.1	3.49	1.23±0.00	0.00		
SWSRC-1%	17.9±0.3	2.37	20.0±0.2	1.19	33.5±1.1	4.64	45.1±1.3	4.08	78.7±1.2	1.81	2.35±0.05	3.01		
SWSRC-2%	17.0±0.2	1.66	19.5±0.1	0.83	51.3±1.3	3.58	42.7±1.4	4.64	94.0±1.4	2.11	1.83±0.08	6.18		
SWSRC-3%	16.3±0.1	0.87	19.1±0.1	0.43	64.1±2.0	4.41	53.0±3.0	8.00	117.1±3.0	3.62	1.83±0.07	5.41		
BWSRC-1%	16.8±0.1	0.84	19.4±0.1	0.42	22.9±1.3	8.03	29.2±1.1	5.33	52.1±1.1	2.99	2.28±0.03	1.86		
BWSRC-2%	16.5±0.3	2.57	19.2±0.2	1.29	29.7±1.5	7.14	21.1±2.1	14.08	50.9±1.8	5.00	1.71±0.01	0.83		
BWSRC-3%	14.3±0.3	2.97	17.9±0.2	1.48	54.7±3.0	7.76	37.8±2.6	9.73	92.5±2.8	4.28	1.69±0.01	0.84		
CWSRC-1%	14.6±0.2	1.94	18.1±0.1	0.97	18.5±2.1	16.05	17.1±1.9	15.71	35.6±2.0	7.95	1.93±0.01	0.73		
CWSRC-2%	13.6±0.1	1.04	17.5±0.1	0.52	60.7±1.3	3.03	47.5±1.5	4.47	108.2±1.4	1.83	1.78±0.01	0.79		
CWSRC-3%	11.8±0.2	2.40	16.3±0.1	1.20	85.8±1.3	2.14	2.7±0.3	15.71	88.5±1.0	1.60	1.03±0.01	1.37		

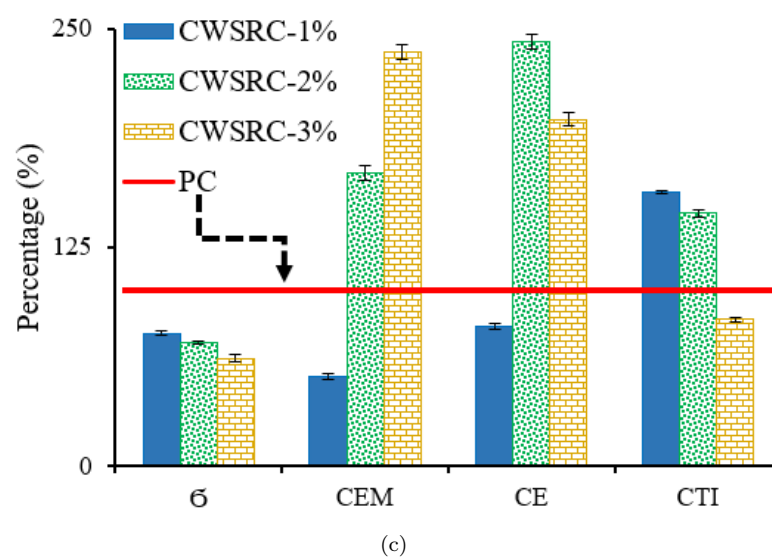
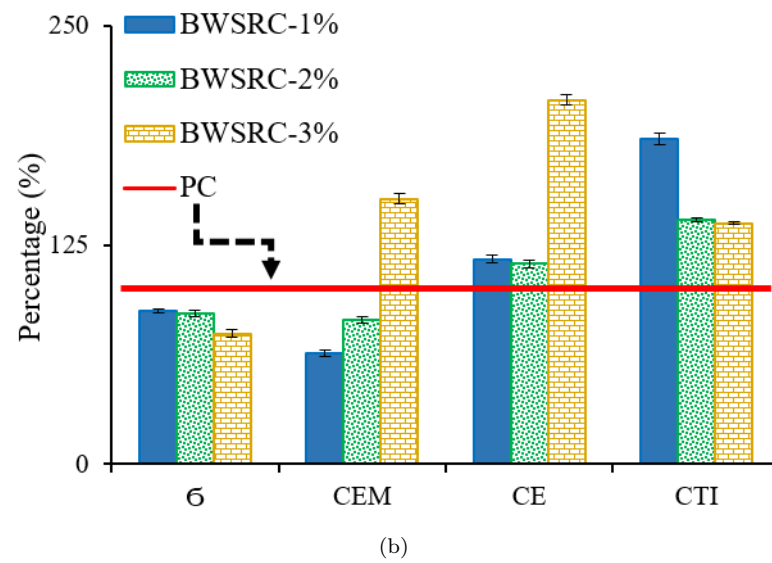
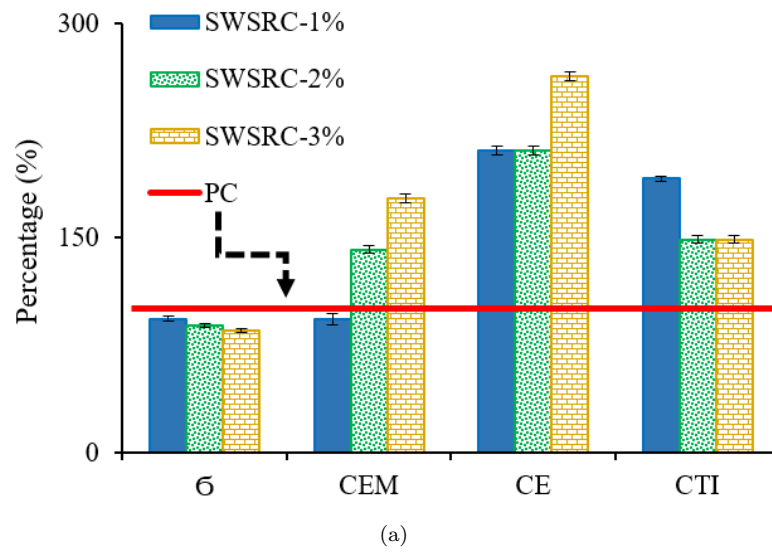


FIGURE 3.5: Comparison of σ , Cem, Ce, and CTI of PC and WSRC with 1%, 2% and 3% content for (a) Soaked, (b) Boiled, and (c) Chemically treated straw.

the compressive failure mode from brittle to ductile, thus enhancing the elastic modulus somehow [253, 258]. The rigid pavements are purposely designed with reinforcement for controlling the cracks that occurs as a result of vehicular loading and varied environmental conditions [259]. The provision of discrete fibres (i.e. wheat straw in current study) in concrete pavements generates the bridging forces across the cracks. This bridging of cracks tends to restrict the crack widths and thereby delays their propagation which ultimately results in enhanced toughness and capacity of rigid pavements [260]. Hence, the improved compressive toughness in case of SWSRC-1% is favorable.

3.3.3 Properties under Splitting-tensile Loading

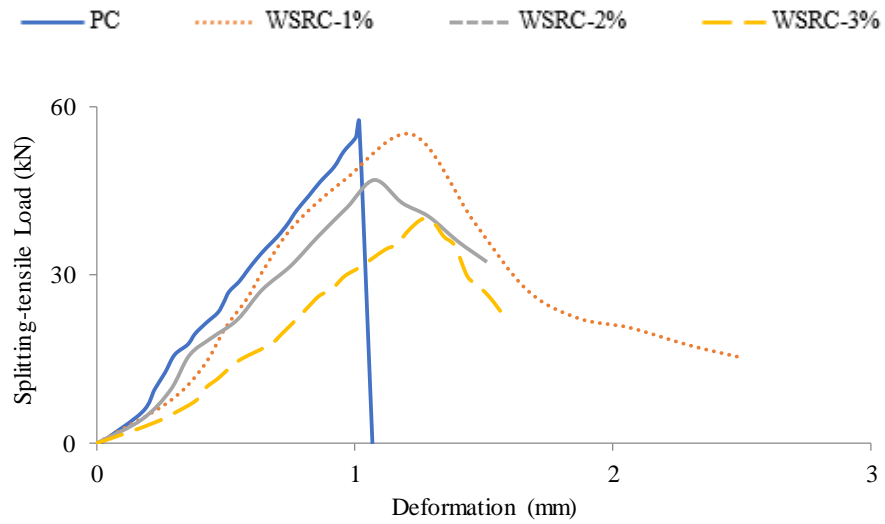
3.3.3.1 Splitting-tensile Behavior

The load ~ deformation graphs, under splitting-tensile loading, of PC, SWSRC-1%, SWSRC-2%, SWSRC-3%, BWSRC-1%, BWSRC-2%, BWSRC-3%, CWSRC-1%, CWSRC-2%, and CWSRC-3% are shown in Figure 3.6. Here, the noticeable behavior is that as soon as the maximum load is applied, the PC cylinder is collapsed but on the other hand resistance against loading is observed for SWSRC, BWSRC and CWSRC even after the maximum load. Although WSRC specimens bear less load, but even then, showing the improved post cracking behavior in result of toughness because of the incorporated straw in cement composites. The tested samples of PC, SWSRC, BWSRC, and CWSRC with 1%, 2%, and 3% straw content are presented in Figure 3.7. The PC cylinder specimens are broken into two pieces upon application of maximum loading, whereas in case of SWSRC, BWSRC, and CWSRC specimens, only cracks are observed even at the maximum loading. This shows the improved behavior of WSRC specimens due to the presence of dispersed wheat straw in concrete in comparison to that of PC. Later on, all the WSRC specimens are broken intentionally into two halves for observing the failure of straw. It is observed with the naked eye that, as an approximation, 60 – 70 % of the straw are pulled out, while the range of broken straw is almost 30-40%. The

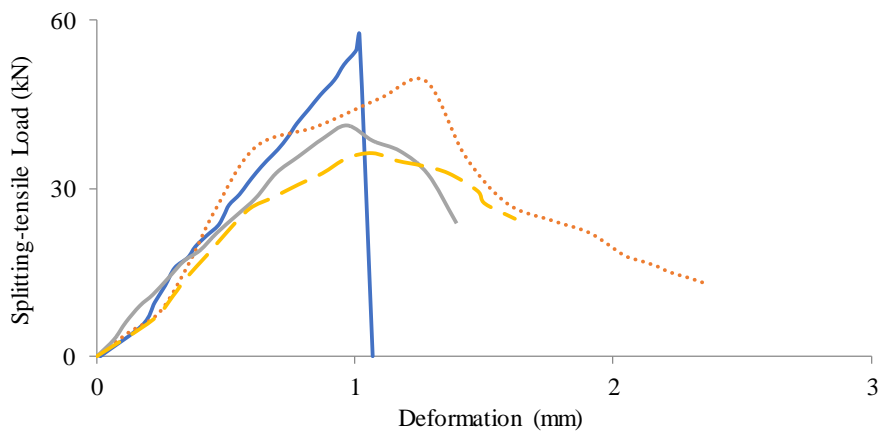
percentage of broken straw is higher in case of boiled and chemically treated straw reinforced concrete as compared to that in soaked straw reinforced concrete. This might be due to changed chemical properties of straw in result of the application of pre-treatment. The breakage of fibres might be due to equal development length of straw in both ends and proper dispersion of straw in surrounding matrix.

3.3.3.2 Splitting-tensile Strength, Splitting-tensile Energy Absorption and Splitting-tensile Toughness Index

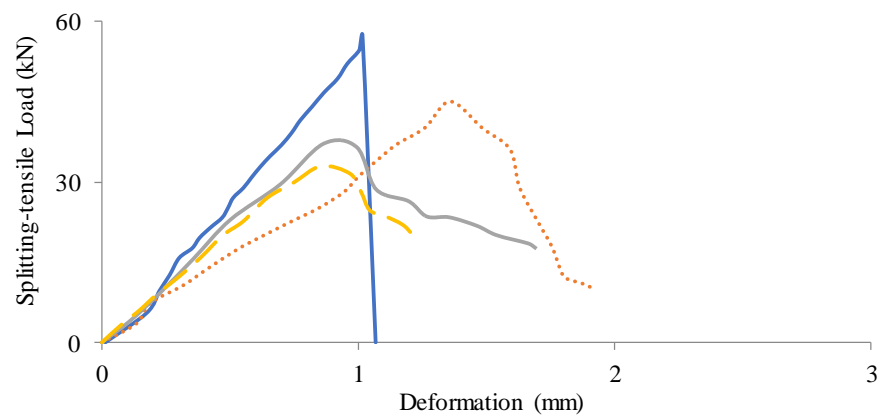
The highest load value from the splitting-tensile load deformation graph is used for calculating the splitting-tensile strength (SS) as shown in Figure 3.6. The splitting-tensile strengths of SWSRC-1%, SWSRC-2%, SWSRC-3%, BWSRC-1%, BWSRC-2%, BWSRC-3%, CWSRC-1%, CWSRC-2%, and CWSRC-3% are decreased by 4%, 18%, 30%, 14%, 28%, 37%, 21%, 35%, and 42%, respectively, in comparison with PC. The values of splitting-tensile strengths are given in Table 3.5. It may be noted that just a slight difference or decrease (i.e. 4%) in SS of SWSRC-1 is observed in comparison to PC. Energy absorption up to the maximum splitting-tensile load (S_{em}) is the area beneath splitting-tensile load deformation curve up to the point of highest load. The area beneath splitting-tensile load deformation curve from the point of highest load up to the failure of specimen is taken as the splitting-tensile energy absorbed post the maximum load (S_{ep}). The total area beneath splitting-tensile load deformation curve or the summation of S_{em} and S_{ep} is taken for the calculation of absorbed splitting-tensile energy (S_e). The ratio of splitting-tensile energy absorbed (S_e) to splitting-tensile energy absorbed up to maximum load (i.e. S_e/S_{em}) is taken as the splitting-tensile toughness index (STI). S_{em} , S_{ep} , S_e , and STI of PC, SWSRC, BWSRC, and CWSRC with 1%, 2%, and 3% content are shown in Table 3.5. Although the splitting-tensile strengths of WSRC specimens are decreased in comparison to PC, but the WSRC cylinder specimens show the bridging effect due to the presence of dispersed straw after the maximum loading. Due to this bridging effect, a significant increase of 144% is observed in the splitting-tensile energy absorption of SWSRC-1% when compared to the energy absorption by PC. This bridging effect indicates the better toughness



(a)



(b)



(c)

FIGURE 3.6: Typical splitting-tensile load ~ deflection curves of (a) PC, (b) SWSRC, (c) BWSRC and (d) CWSRC with 1%, 2% and 3% content.

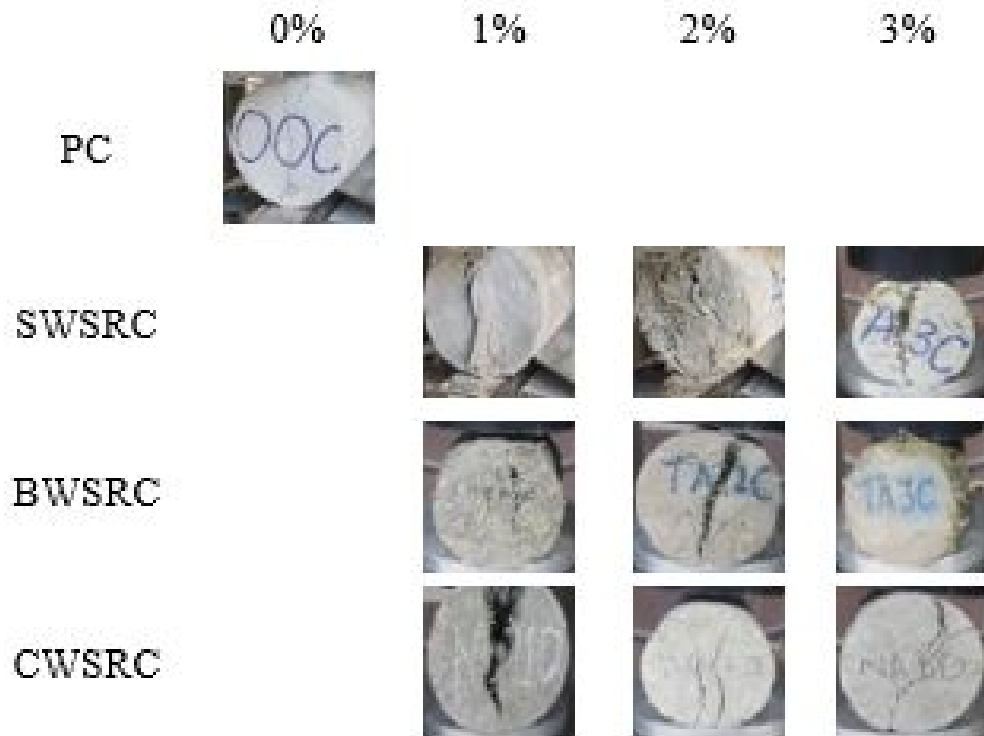


FIGURE 3.7: Tested cylinder specimens of PC and WSRC with varied treatment and fibre content under splitting-tensile loading.

of WSRC specimens. As already discussed that the phenomenon of slippage of fibres due to their more tensile strength adds up in high energy absorption. Hence the splitting-tensile toughness indices of SWSRC-1%, BWSRC-1%, CWSRC-1%, SWSRC-2%, BWSRC-2%, CWSRC-2%, SWSRC-3%, BWSRC-3, and CWSRC-3% are increased by 105%, 71%, 53%, 72%, 68%, 40%, 47%, 62%, and 67%, respectively, when compared to the STI of PC. The similar trend is observed in case of compressive behavior. Improved toughness is observed with the slight decrease in strengths.

SS, Sem, Se, and STI of PC, SWSRC, BWSRC, and CWSRC with straw content of 1%, 2%, and 3% are compared and the comparison is shown in Figure 3.8. The splitting-tensile strengths of WSRC specimens are again decreased in comparison to PC, as in case of compressive strength. But the noticeable point here is that a very minute decrease (i.e. 4%) is observed in case of SWSRC-1% when compared to the splitting-tensile strength of PC. As far as splitting-tensile energies are concerned, SWSRC-1% absorbed highest energy than that by PC and all other

TABLE 3.5: Splitting-tensile Strength (SS), Energies absorption under splitting-tensile load (Sem, Sep, Se) and Splitting-tensile Toughness Index (STI) of PC, SWSRC, BWSRC and CWSRC.

Specimen	SS (MPa)	Splitting-tensile Energies Absorbed												
		COV (%)	Sem (J)	COV (%)	Sep (J)	COV (%)	Se (J)	COV (%)	STI	COV (%)	STI	COV (%)		
(1)	(2)	(3)	(4)	(5)	(6)	(7)	(8)	(9)	(10)	(11)	(12)	(13)	(14)	(15)
PC	1.82±0.05	3.89	28.2±1.0	5.01	0.0±0.0	0.00	28.2±1.0	5.01	1.00±0.00	0.00	1.00±0.00	0.00	1.00±0.00	0.00
SWSRC-1%	1.75±0.11	8.89	33.6±2.1	8.84	35.1±1.9	7.66	68.8±2.0	4.11	2.05±0.02	1.38	2.05±0.02	1.38	2.05±0.02	1.38
SWSRC-2%	1.50±0.15	14.14	24.0±2.0	11.79	17.3±1.5	12.26	41.3±1.8	6.16	1.72±0.01	0.82	1.72±0.01	0.82	1.72±0.01	0.82
SWSRC-3%	1.27±0.08	8.91	22.5±1.1	6.91	10.5±1.4	18.86	33.0±1.3	5.57	1.47±0.01	0.96	1.47±0.01	0.96	1.47±0.01	0.96
BWSRC-1%	1.56±0.06	5.44	37.8±1.8	6.73	27.0±1.9	9.95	64.8±1.9	4.15	1.71±0.02	1.65	1.71±0.02	1.65	1.71±0.02	1.65
BWSRC-2%	1.31±0.05	5.40	21.7±1.6	10.43	14.7±1.2	11.54	36.4±1.4	5.44	1.68±0.01	0.84	1.68±0.01	0.84	1.68±0.01	0.84
BWSRC-3%	1.15±0.07	8.61	22.1±1.7	10.88	13.6±1.4	14.56	35.7±1.5	5.94	1.62±0.03	2.62	1.62±0.03	2.62	1.62±0.03	2.62
CWSRC-1%	1.43±0.16	15.82	29.2±1.1	5.33	15.6±1.3	11.79	44.8±1.2	3.79	1.53±0.01	0.92	1.53±0.01	0.92	1.53±0.01	0.92
CWSRC-2%	1.18±0.15	17.98	16.1±1.5	13.18	6.5±1.7	36.99	22.6±1.6	10.01	1.40±0.02	2.02	1.40±0.02	2.02	1.40±0.02	2.02
CWSRC-3%	1.05±0.09	12.12	14.9±1.6	15.19	10.0±1.2	16.97	24.9±1.4	7.95	1.67±0.02	1.69	1.67±0.02	1.69	1.67±0.02	1.69

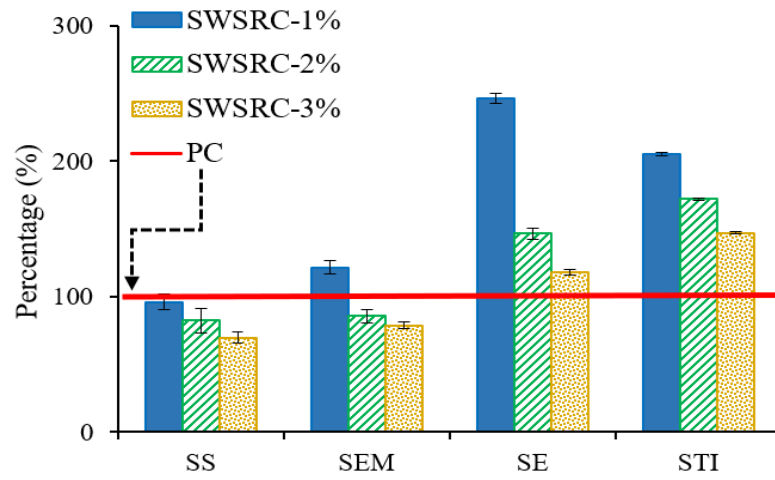
specimens. As a whole, the behavior under splitting-tensile loading is depicting the improved properties with decrease in percentage content of straw. An increase in splitting-tensile toughness indices of all WSRC specimens is observed in comparison to that of PC. This might be due to the presence of dispersed straw in concrete. It is observed that the post-cracking behavior of WSRC specimens is improved due to sewing effect of straw.

Splitting– tensile behavior of concrete is a governing parameter for a number of civil applications. Transverse cracking occurs in rigid pavements when thermally induced tensile stresses exceeds the tensile strength of concrete slab [211]. Conventionally, transverse reinforcement is usually provided to cater this issue. A significant increment of 105% in splitting-tensile toughness index of SWSRC-1%, with little compromised strength, can enhance the performance of rigid pavements. Furthermore, the discrete wheat straw would hold the initiated transverse cracks towards minimum width and would delay the cracks propagation mechanism. This type of material behavior is also favorable for bridge deck applications as reported by Khan and Ali [126].

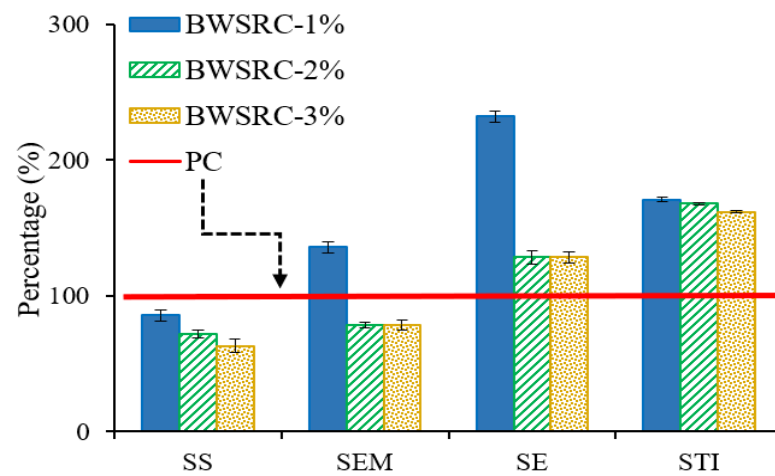
3.3.4 Properties under Flexural Loading

3.3.4.1 Flexural Behavior

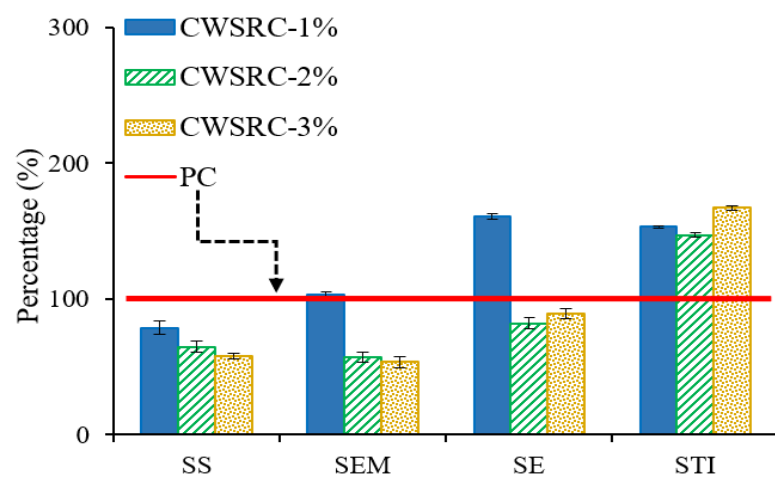
The history recorded under the flexural loading during the flexural testing is given in Figure 3.9. The SWSRC, BWSRC, and CWSRC specimens bear the application of load even after cracking. However, the PC specimen is broken into two pieces as soon as the application of load is reached up to the maximum level, depicting the brittle nature of PC. Dispersed straw show proper sewing of both ends of specimen after cracking. The tested beam-lets under the application of flexural loading for PC, SWSRC, BWSRC, and CWSRC with 1%, 2%, and 3% content are shown in Figure 3.10. The WSRC specimens (i.e. soaked, boiled, and treated) beam-lets remained in contact even under the application of the maximum load and after cracking. The crack propagation rate in case of straw reinforced concrete



(a)



(b)



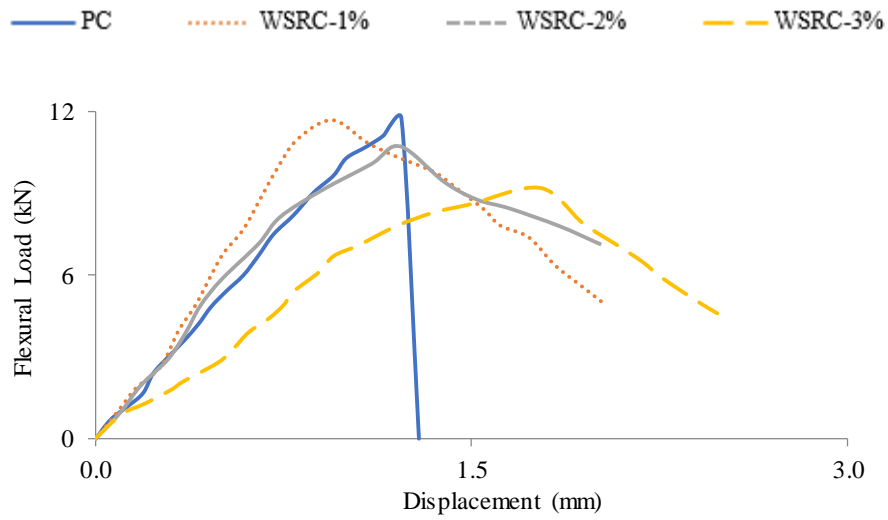
(c)

FIGURE 3.8: Comparison of SS, Sem, Se, and STI of PC and WSRC with 1%, 2% and 3% content for (a) Soaked, (b) Boiled, and (c) Chemically treated straw.

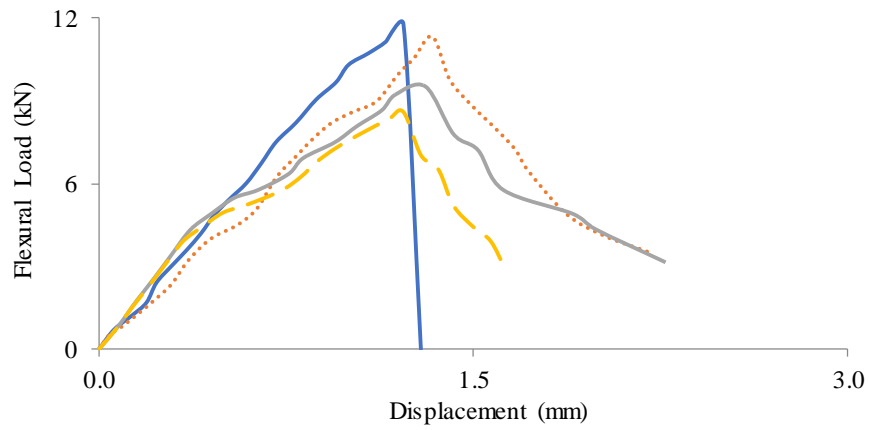
specimens is very slow due to dispersed straw in it. The beam-lets of SWSRC, BWSRC, and CWSRC are intentionally broken into two pieces for its examination with the help of naked eye and SEM to observe the mechanism of straw failure. It is observed that, there is an approximate ratio of 70 : 30 in the straw-failure between pulling-out and straw fracture. It is observed that straw fracture is occurred in case of straw's equal development length at both halves of fractured surfaces. This behavior depicts that the bonding strength of straw is higher within matrix as compared to its tensile strength. However, the pull-out of straw is observed in case of less embedded straw's length at any one half of fractured side. This may be due to less bonding strength of straw within matrix than the straw's tensile strength. The similar behavior was also reported by [19, 126]. However, in case of BWSRC and CWSRC, the shiny texture of straw and the changed chemical composition of straw might be the reason for relatively high percentage of fractured straw in comparison to that of SWSRC. In addition to that, the changed surface conditions of straw might be the cause of weaker bond between straw and the surrounding composite. However, it may also be noted that, for enhancing the capacity of energy absorption of concrete/composite, the fibre pulling out phenomenon is more favourable in comparison to rupture of fibres.

3.3.4.2 Modulus of Rupture (MoR), Flexural Energy Absorption and Flexural Toughness Index

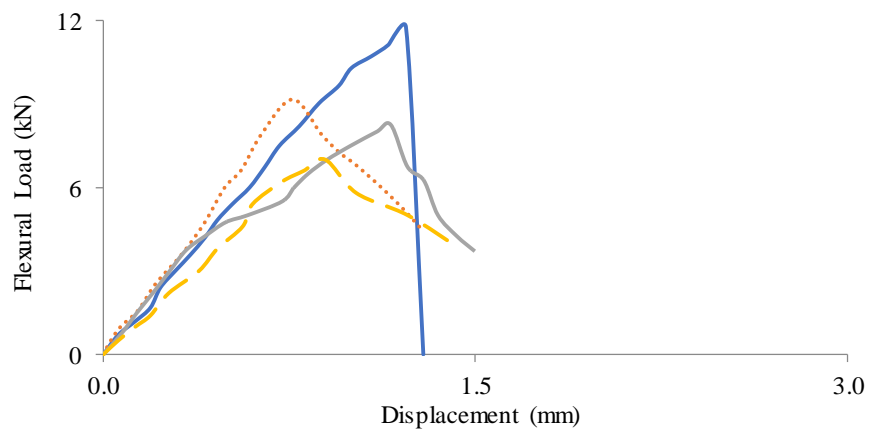
The highest load from the load displacement history recorded under flexural loading is taken for calculating the Modulus of Rupture (MoR). The MoR of PC and WSRC is calculated by using equation; $MoR = 3Pl/2bd^2$, as per ASTM C293/C293 M-16 (Standard Test Method for Flexural Strength of Concrete - Using Simple Beam with Centre-Point Loading). Where P is the maximum load and l, b and d are the dimensions, i.e. length, width and depth, of tested PC and WSRC beam specimens. The energy absorbed by the specimen under the flexural loading up to the point of maximum load (F_{em}) is taken as the area underneath flexural load displacement history up to the point of highest load. Energy absorbed by the specimen after the maximum flexural load (F_{ep}) is the area underneath flexural



(a)



(b)



(c)

FIGURE 3.9: Flexural load-displacement curves of (b) SWSRC, (c) BWSRC, (d) CWSRC with 1%, 2% and 3% content.

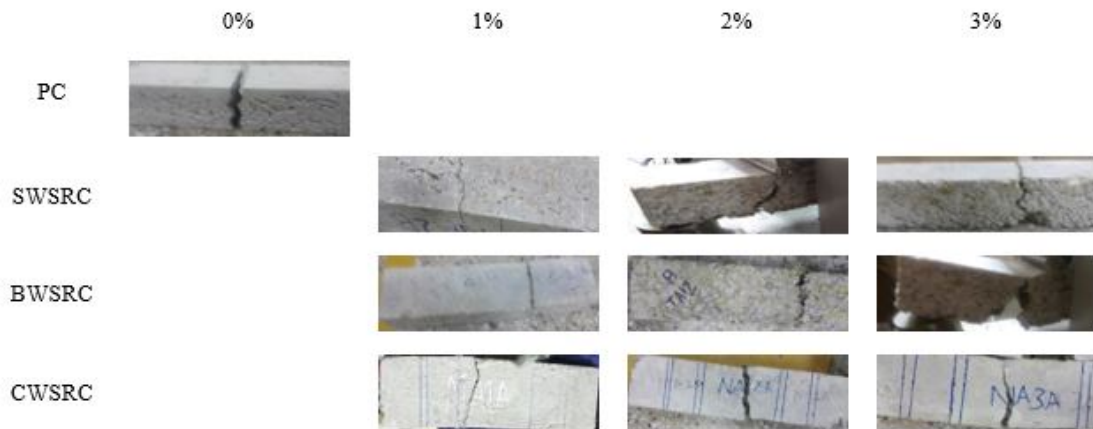


FIGURE 3.10: Tested beam specimens of PC and WSRC with varied treatment and fibre content under flexural loading

load displacement history after the highest load up to the termination of test. The summation of F_{em} and F_{ep} or the whole area underneath flexural load displacement history is taken as the flexural energy absorbed (F_e). The ratio of the energy absorption under flexural loading to the energy absorption up to the maximum flexural load (i.e. F_e / F_{em}) is taken as the flexural toughness index (FTI). The MoR, F_{em} , F_{ep} , F_e and FTI of PC, SWSRC, BWSRC, and CWSRC with 1%, 2%, and 3% content are shown in Table 3.6. The Modulus of Rupture (MoR) of WSRC specimens are decreased up to some extent when compared to that of PC. Among all straw reinforced concrete specimens, the maximum MoR is of SWSRC-1% (i.e. 7.64 MPa), which is only 2% less than that of PC. However, with an increase in straw content, the MoR is decreasing further. Ali et al. also reported the reduction in MoR of fibre reinforced concrete in comparison to that of plain concrete [245]. The noticeable thing here is that the better post cracking behavior occurs in case of WSRC as the maximum of approximately 62% energy absorption by the SWSRC-1% post the maximum load. Whereas, in case of PC, no energy is absorbed after maximum loading as the specimen get collapsed. Toughness of WSRC beamlets is also improved in case of WSRC due to this post cracking behavior. A maximum of 92% increase in flexural toughness index of SWSRC-1% is observed when compared to that of PC. Hence, for pavements, a slight decrease (i.e. 1–2%) in MoR can be balanced against significantly improved flexural toughness to resist the crack prorogation under the application of dynamic loading and

for enhancing the duration from first crack to permanent failure of pavement.

A comprehensive comparison of MoR, Fem, Fe and FTI of PC, SWSRC, BWSRC, and CWSRC is shown in Figure 3.11. Although the MoR of SWSRC, BWSRC, and CWSRC is decreased in comparison to MoR of PC, but flexural energy absorbed and flexural toughness index of SWSRC-1% are increased significantly when compared to that of PC. The composites with 1% content show relatively better results. The similar trend is observed here as in case of compressive and splitting-tensile strengths. Improved behavior (i.e. post cracking) of concrete is noted with the addition of dispersed straw in cement concrete.

It may be noted that critical properties for road and airport pavement applications are the flexural properties of concrete [261]. Accordingly, the key parameter for design of rigid pavements is the modulus of rupture as per AASHTO pavement design guide. The contribution of remarkable enhanced flexural toughness of SWSRC-1%, along with almost same MoR as of PC, can leads towards better performance with even reduced pavement thickness [209, 262]. In addition, the crack propagation rate is very much high in pavements due to application of vehicular loading and varied environmental conditions. So, the improved post cracking behavior in case of SWSRC-1% seems highly favorable for rigid pavement applications.

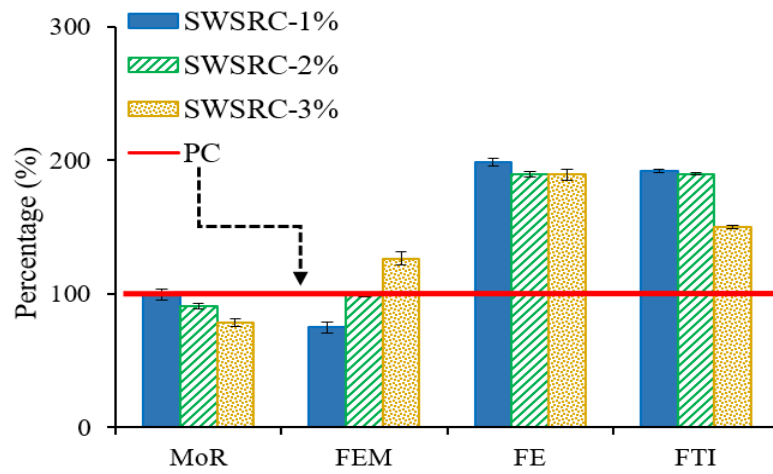
3.3.5 Micro-structural Analysis of Straw and WSRC

The scanning electronic microscopic images of soaked straw and soaked straw concrete bond, boiled straw and boiled straw concrete bond, and chemically treated straw and chemically treated straw concrete bond are shown in Figure 3.12, which shows that the surface of soaked straw is comparatively very much better than the surface of boiled and chemically treated straw. It may be noted that the surface of chemically treated fiber is more affected by the treatment through NaOH solution followed by boiling. This behavior depicts that the air-dried soaked straw are more favorable for proper bonding with cement concrete composites. It may

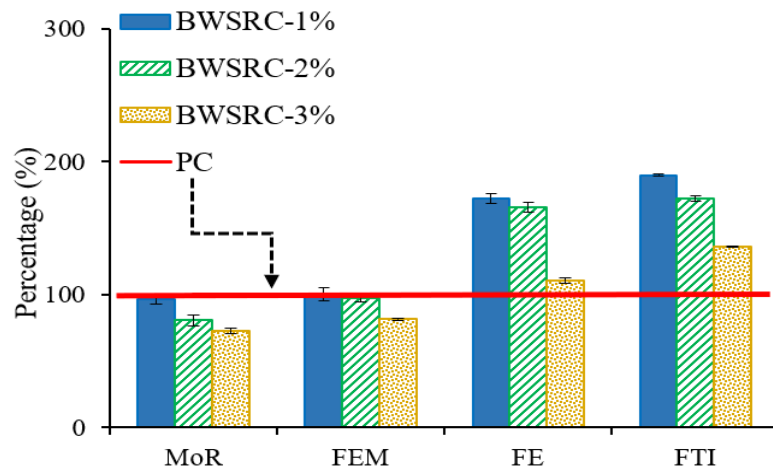
TABLE 3.6: Modulus of Rupture (MoR), Energies absorption under flexural load (Fem, Fep, Fe) and Flexural Toughness Index (FTI) of PC, SWSRC, BWSRC and CWSRC.

Specimen	MoR (MPa)	COV (%)	Fem (J)	COV (%)	Fep (J)	COV (%)	Fe (J)	COV (%)	FTI	CoV (%)
PC	7.69±0.3	5.52	7.6±0.2	3.72	0.0±0.0	0	7.6±0.2	3.72	1.00±0.00	0.00
SWSRC-1%	7.64±0.4	7.40	5.7±0.4	9.92	9.4±0.2	3.01	15.1±0.3	2.81	1.92±0.01	0.74
SWSRC-2%	7.01±0.2	4.03	7.5±0.1	1.89	6.9±0.3	6.15	14.4±0.2	1.96	1.90±0.01	0.74
SWSRC-3%	6.02±0.3	7.05	9.6±0.5	7.37	4.8±0.3	8.84	14.4±0.4	3.93	1.50±0.01	0.94
BWSRC-1%	7.40±0.4	7.64	7.6±0.3	5.58	5.5±0.5	12.86	13.1±0.4	4.32	1.90±0.02	1.49
BWSRC-2%	6.21±0.2	4.55	7.4±0.1	1.91	5.3±0.3	8.00	12.6±0.2	2.24	1.72±0.05	4.11
BWSRC-3%	5.61±0.4	10.08	6.2±0.3	6.84	2.2±0.2	12.86	8.4±0.3	5.05	1.36±0.02	2.08
CWSRC-1%	5.99±0.3	7.08	3.5±0.4	16.16	3.5±0.5	20.20	7.1±0.5	9.96	1.85±0.02	1.53
CWSRC-2%	5.39±0.4	10.50	5.6±0.3	7.58	1.9±0.3	22.33	7.4±0.3	5.73	1.34±0.01	1.06
CWSRC-3%	4.58±0.3	9.26	3.3±0.2	8.57	2.8±0.3	15.15	6.1±0.3	6.96	1.87±0.01	0.76

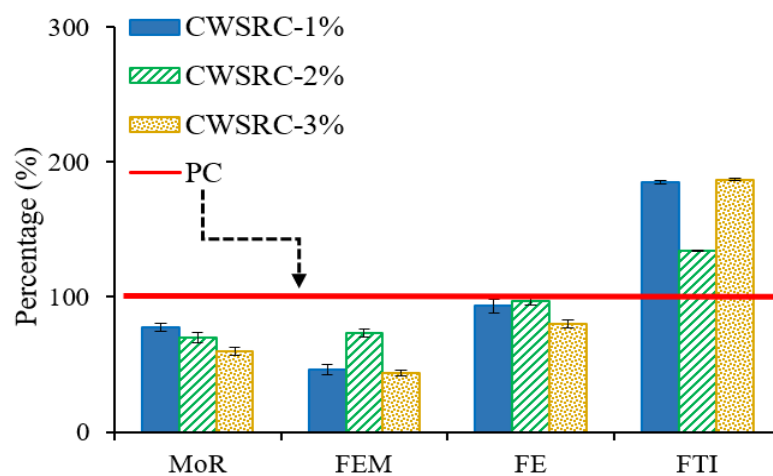
Note: Modulus of Rupture is calculated by using formula $MoR = 3PI/2bd^2$, as per ASTM C293/C293 M-16.



(a)



(b)



(c)

FIGURE 3.11: Comparison of MoR, Fem, Fe, and FTI of PC and WSRC with 1%, 2% and 3% content for (a) Soaked, (b) Boiled, and (c) Chemically treated straw.

be noted that the dust particles are removed from the straw surface by soaking them in water for a specified period. As for as the bond between matrix and straw is concerned, it can be seen in soaked straw-concrete bond figure that the proper bonding between the straw and the matrix became the reason for improved mechanical properties. Also, the straw is properly surrounded by the matrix which presents the capability of natural fiber proper bonding with concrete. The proper bonding with addition of natural fiber in concrete improves the mechanical properties [209].

The dense interfacial transition zone (ITZ) and proper bonding between the straw and the matrix, as can be observed from the image, may also be the cause of enhanced mechanical properties. In another study, Khan et al. reported that the dense interface between ITZ and fiber also results in improved mechanical properties [263]. However, in case of chemical treatment, the straw is affected so badly due to the NaOH solution treatment and this can be observed from the cracks in fiber shown in Figure 3.12. Whereas, the proper development length of fiber on both sides of the matrix resulted in the straw fracture, instead of straw pull-out, as can be observed in image showing the bond between chemically treated straw with concrete.

Similar type of mechanism is observed in case of boiled straw and the bonding between boiled straw and concrete matrix as shown in Figure 3.12. The cracked surface of straw due to boiling treatment is the reason behind poor ITZ between boiled straw and surrounding concrete matrix. The addition of fiber delays the crack propagation by bridging mechanism as also shown in Figure 3.12 having soaked straw-concrete interaction, which ultimately enhanced its mechanical properties. Also, the fiber-cement matrix is responsible for transfer of applied load, as reported by Ferrara *et al.* and Khan and Ali [264, 265]. The high energy absorption and toughness may be due to fiber slippage.

Therefore, this phenomenon is favorable to be used in civil engineering applications especially pavements, where crack propagation is the major issue due to application of vehicular loading.

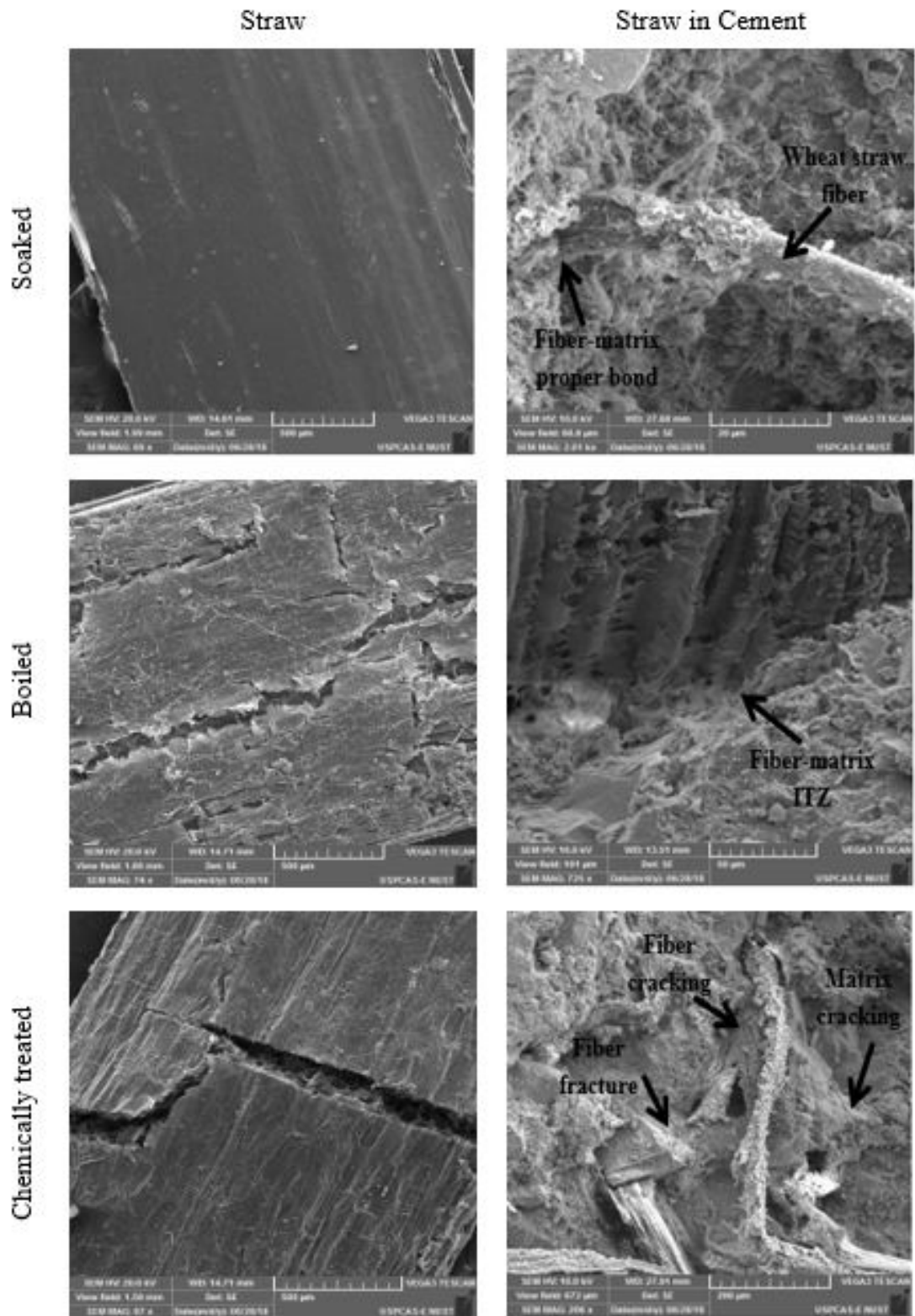


FIGURE 3.12: Micro-structural analysis of Soaked, Boiled and Chemically treated straw and their bond with concrete

3.4 Summary

The effect of pre-treatment technique and content of wheat straw on energy absorption capability of concrete and in-depth mechanism of straw-concrete bond is studied. An experimental investigation is made to study the mechanical behavior of Plain Concrete (PC) and Wheat Straw Reinforced Concrete (WSRC) having 1%, 2%, and 3% content of soaked, boiled, and chemically (NaOH) treated straw. The conclusions are as follows:

- Compressive energy absorbed and compressive toughness index of SWSRC are increased by 162% and 91%, respectively when compared to that of PC. However, in case of CWSRC, the total energy absorbed is decreased by 20%. The bridging effect due to presence of straw is the reason for this increased energy absorption.
- A significant increase of 105%, 71% and 67% in splitting-tensile toughness index of SWSRC, BWSRC and CWSRC respectively is observed when compared to that of PC. The straw's strength with the capability of holding both the ends is the reason for improved toughness.
- When the flexural toughness index of SWSRC, BWSRC and CWSRC is compared with that of PC, an increase of 92%, 90% and 87% is observed. The specimens absorbed energy even after maximum loading in comparison to that of PC specimen which collapsed right after maximum loading.
- SWSRC performed better under the compressive, splitting-tensile, and flexural loading, when compared to that of BWSRC and CWSRC. The changed surface conditions of straw due to boiling and chemical treatment are the reason for relative reduction in properties.
- Specimens with 1% straw, by mass of wet concrete, show better mechanical properties in comparison to that with 2% and 3% straw content. The improper compaction due to the presence of more low-density straw content contribute towards less strengths, energy absorption and toughness indices.

- The improved properties of SWSRC are resulted due to better bonding of uncracked surfaced soaked straw with the surrounding matrix as revealed by SEM analysis. Whereas, boiling and chemical treatment on straw have adverse effects, which ultimately resulted in weakened straw-concrete bonding in case of BWSRC and CWSRC.

Based on conducted analysis, soaked wheat straw reinforced concrete (SWSRC) with 1% straw content can be claimed as a potential construction material for civil engineering applications including rigid pavements. However, the long-term durability of wheat straw reinforced concrete should be explored in detail.

Chapter 4

Durability of Wheat Straw Reinforced Concrete

Related Article:

M. U. Farooqi and M. Ali, “Short-term durability of wheat straw reinforced concrete for pavement applications,” *In proceedings of 5th International Conference on Infrastructure Engineering in Developing Countries (IEDC)*, Karachi, Pakistan, 2017.

4.1 Background

The results of concrete reinforced with natural fibres are comparable with that of artificial/steel fibre reinforced concrete. Accordingly, a detailed study has been conducted to evaluate the use of agricultural waste/by-product (i.e. wheat straw) in cement concrete composite, as in-depth knowledge on behavior of WSRC is missing. The effect of pre-treatment and content of wheat straw on the energy absorption capability of concrete under compressive, splitting-tensile, and flexural loadings is determined in previous Chapter 3. The experimental investigation is also supported with micro-structural analysis to analyze the straw-cement bond mechanism. Comparative study of Plain Concrete (PC), Soaked Wheat Straw

Reinforced Concrete (SWSRC 1-3%), Boiled Wheat Straw Reinforced Concrete (BWSRC 1-3%), and Chemically (NaOH) treated Wheat Straw Reinforced Concrete (CWSRC 1-3%) is made. In result of detailed analysis, the concrete matrix reinforced with 1% content of soaked straw i.e. SWSRC – 1% has come out to be an optimized matrix among all the WSRC matrices.

However, the durability of agricultural fibres is a matter of concern. As some deficiencies/degradation of agricultural/plant fibre reinforced cement composites in terms of durability are usually observed along with the enhanced behavior due to the mineralization of fibres and alkali attacks under the exposure of climatic/environmental conditions as agricultural wastes/by-products are organic in nature. Therefore, the application of agricultural fibres in construction industry is still quite limited due to the lack of understanding in how to improve the durability while making ductile materials. Accordingly, in spite of the fact that WSRC comes with the enhanced behavior, the durability factor in case of cement concrete reinforced with agricultural waste particularly wheat straw, should be given proper consideration. A number of solutions (immersion in fresh water, slurried silica fume, NaOH, Ca (OH)₂, and H₂SO₄ solutions; carbonation of studied matrix; cement replacement with calcined clay and metakaoline etc.) are proposed in various studies for enhancing the durability of agricultural fibres for their potential use in civil structures [15, 48, 52, 69, 70, 190]. Furthermore, the durability of agricultural fibres in concrete has already been determined experimentally in various studies by adopting multiple durability evaluation techniques. The agricultural/plant fibres and agricultural fibre reinforced cementitious composites are used to evaluate, in terms of durability, by having exposure to different environmental and ageing conditions like: immersion in water, slurried silica fume, saturated lime and NaOH solutions; immersion in water at specified/elevated temperatures; ageing in water; open-air weathering; alternate wetting and drying; alternate freeze and thaw cycles etc. for the specified time periods.

Hence, in light of above discussion, the durability factor, in terms of structural performance, is addressed for WSRC matrix in this Chapter 4. As, to the best of author's knowledge, no long-term durability evaluation study has been conducted for

Wheat Straw Reinforced Concrete (WSRC) to be used for civil engineering structural applications. Therefore, to get an idea about the behavior of WSRC structure throughout its design life, the long-term laboratory durability of Plain Concrete (PC), Soaked Wheat Straw Reinforced Concrete (SWSRC), Boiled Wheat Straw Reinforced Concrete (BWSRC) and Chemically-treated Wheat Straw Concrete (CWSRC) is studied in detail in this Chapter 4. The specimens are exposed to three different ageing conditions for a period of 4-years. The ageing conditions are; i) exposure to controlled room conditions, ii) exposure to natural climatic conditions, and iii) exposure to alternate wetting and drying. The residual properties (i.e. residual compressive, splitting-tensile and flexural strengths, residual energies absorption and residual toughness indices) are determined experimentally. The micro-structural analysis (i.e. X-Ray Diffraction (XRD), Thermogravimetric analysis (TGA) and Scanning Electron Microscope (SEM)) is also performed on straw. Furthermore, straw-concrete matrix has also been studied, in terms of micro-structural analysis, to assess the condition of wheat straw in concrete after undergoing 4 years ageing. The comparative analysis of WSRC specimens with that of controlled specimen (i.e. PC) is made after 4-years ageing. The findings are also compared with that of respective specimens at 0-day age, as reported in Chapter 3. Accordingly, the rest of the chapter is presented in a manner that Section 4.2 portrays the materials used and preparation, considered ageing conditions and testing methodologies whereas, all the results, analyses and discussions are presented in Section 4.3. Section 4.4 shows the development of empirical relations for anticipation of WSRC structure's design life and all the findings of this laboratory durability evaluation are summarized in Section 4.5.

4.2 Experimental Investigation

4.2.1 Materials Used

BESTWAY cement (locally manufactured with 28 days strength of 52 ± 3 MPa), sand extracted from local quarries, i.e. lawrence-pur, Margallah crush, i.e. locally

TABLE 4.1: Physical properties of wheat straw.

Wheat Straw Property (1)	Value Range (2)
Linear Dimensions (mm×mm×mm)	25×5×1.2
Tensile Strength (MPa)	40.0*
Shear Strength (MPa)	9.47 – 9.60*
Density (kg/m ³)	55 – 119*

*These values are reported by [18, 225, 266]

available aggregates of 19.5 mm maximum size, tap/potable water, 25 mm long wheat straw (that are commercially available) are the basic ingredients which are used for preparing PC and WSRC matrices. The approximate ranges for physical characterization of wheat straw from local region, i.e. Asia, are presented in Table 4.1 as reported by [18, 225, 266]. Moreover, Energy Dispersive X-ray (EDX) analysis is also done to evaluate chemical characterization of wheat straw as shown in Figure 4.1. Carbohydrates (i.e. cellulose, hemicellulose, and lignin) are found abundantly in wheat straw as observed from its chemical analysis. The weight and atomic percentage of Carbon (C), Oxygen (O), Silicon (Si), Potassium (K), and calcium (Ca) present in straw are 58.98%, 39.90%, 0.48%, 0.19%, and 0.45%, respectively and 66.02%, 33.53%, 0.23%, 0.07%, and 0.15%, respectively. Similar type of findings are also reported by [226, 227]. In addition to 84 – 91 % dry matter, proteins, acid detergent fibres, silica and ash are also found in straw. All these material properties are also reported in reference study [267].

4.2.1.1 Preparation of Wheat Straw

Soaking of Straw: Soaking of wheat straw is done by dipping it in potable/-tap water for approximately 20 minutes. The presence of impurities/wax/dust particles, as a dry matter on the surface of straw, is removed by this soaking, which is then followed by air-drying. The straw which are processed through this mechanism are labelled as soaked wheat straw. A clean texture of wheat straw is observed after this soaking mechanism as reported in reference study [267].

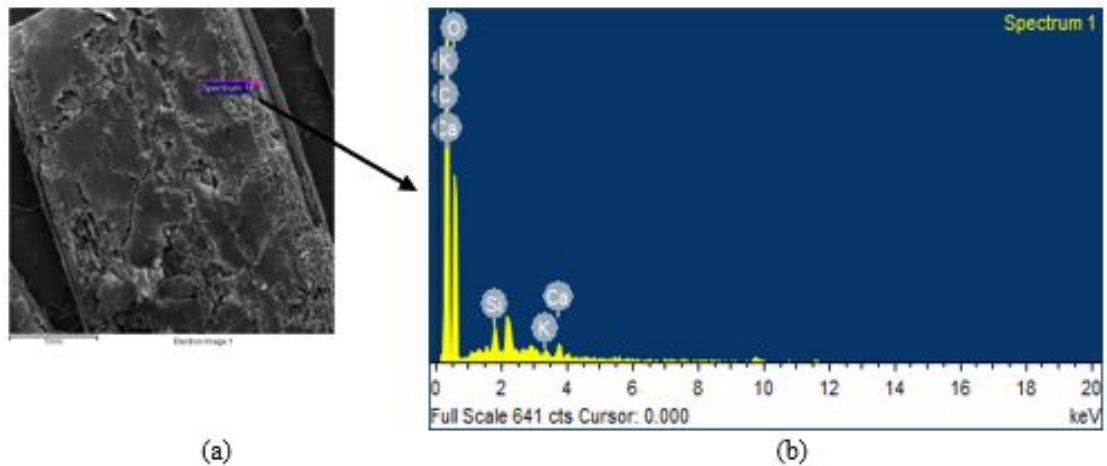


FIGURE 4.1: EDX analysis of wheat straw (a) spectrum and (b) chemical composition.

Boiling of Straw: In light of studies reported by [72, 73], a simple boiling pre-treatment technique is opted to get an enhanced interfacial bond between straw and concrete. For this purpose, straw are dipped in half an hour boiled water. Water with straw is kept on boiling for approximately 15 – 20 minutes. Straw removal from water is done after cooling of water, followed by the air-drying. These straw are then labelled as boiled wheat straw. Naked eye observation has shown the shiny and washed texture of straw after boiling mechanism, as reported in reference study [267].

Chemical Treatment of Straw: Chemical treatment of straw is also done to have an enhanced straw concrete bond. For this purpose, the straw are dipped in NaOH – 3% (Sodium Hydroxide) solution, for a period of approximately 30 minutes. Afterwards, straw are removed, followed by the air-drying. More smooth, shiny, and washed texture is observed through naked eye and surface disintegration is observed through microscopic view after this chemical treatment mechanism, as reported in reference study [267].

4.2.2 Mix Proportion and Mixing Technique

As reported in reference study [267], the plain concrete mix proportions and materials weight per m^3 are 1: 2: 4: 0.55, i.e. 331 kg: 704 kg: 1550 kg: 182 kg (C: S:

A: W). However, in WSRC, 1%, 2% and 3% (by wet concrete mass) straw content (of an approximate 25 mm length) are also added. The w/c ratio in WSRC mix proportion is 0.60. In this way, the cement, sand, aggregates, water and straw weights per m³ of WSRC become 254 kg, 542 kg, 1194 kg, 152 kg and 27 kg, respectively. The conventional procedure of mixing PC is adopted by putting all the materials (i.e. cement, sand and aggregates) at a time, followed by the addition of water with the mixing of 5 minutes afterwards. Whereas, a layering technique is adopted for preparing WSRC mix to get a homogeneous mixture and to avoid balling effect. Cement, sand, aggregates, and straw are divided in three parts each and is put in mixer one by one in layers. Approximately 65% of water is then added in the mixer, followed by the rotation of 3 minutes. Afterwards, the mixer is rotated again after the addition of remaining water. As the homogeneity of WSRC mix isn't achieved at that stage, therefore an increased mixing time option is adopted to get workable WSRC and to avoid the bleeding (in case of more water addition at that stage).

The slump and compaction factor tests of fresh PC and WSRC are also conducted (Table 3.3). Furthermore, a little modification is also made at the time of filling the moulds for WSRC specimens to achieve proper consolidation. After compaction with 25 blows of tamping rod, lifting of mould to a certain height of 100 - 150 mm approximately and then a free drop is done for removing air voids. This technique is followed for all the three layers. The water curing for 28-days is done after de-moulding of specimens. All the specimens are divided in four equal sets (i.e. 40 cylinders and 20 beam-lets). Among these four, specimens of one set are tested and are reported in the reference study [267]. Rest of the three sets of specimens are kept for ageing under three different conditions for the period of 4-years.

4.2.3 Specimens and Labelling/Testing Scheme

For determination of residual compressive and residual splitting-tensile properties of PC, SWSRC, BWSRC, and CWSRC, cylindrical specimens having dimensions of 200mm × 100mm (height × diameter) are prepared. However, for flexural

strength tests, beam-let specimens having dimensions of $100\text{mm} \times 100\text{mm} \times 450\text{mm}$ (width \times depth \times length) are cast. PC, SWSRC, BWSRC and CWSRC specimens are labelled as 00, A, T, and N, respectively along with the percentages (i.e. 1%, 2%, and 3%) to represent the straw content for respective specimens. The 4-years aged specimen and labelling details are given in Table 4.2.

4.2.4 Ageing Conditions

As mentioned earlier, the standard samples (beam-lets and cylinders) are bifurcated in three sets and have been kept under three different ageing conditions for the period of 4-years (i.e. 48 months). The climatic data of the considered region (i.e. Islamabad, Pakistan) for the aged period (i.e. from January, 2016 – December, 2019) is taken from Pakistan Metrological Department. The climatic data of the considered region for the considered ageing period is shown in Figure 4.2.

4.2.4.1 Room Conditions

A set of specimens is aged under the controlled and idealized conditions, i.e. room conditions of Islamabad city, Pakistan for the specified ageing period, i.e. from the month of January 2016 to December 2019. A physical laboratory of Civil Engineering Department at Capital University of Science and Technology, Islamabad is used for the storage of specimens under room conditions (left image of Figure A1(b)).

Although, the environmental conditions for the studied area and considered period (i.e. January 2016 - December 2019) are shown in Figure 4.2, but the room conditions varied a little from the open-air conditions. The average room temperature of considered region is 23 ± 2 °C. The temperature of room is used to keep constant with the help of HVAC systems of the respective building. The humidity level inside the room at night is usually up to 35% and at morning, it falls up to 18% within the room.

TABLE 4.2: Specimen labelling and testing scheme of wheat straw reinforced concrete for 4-years ageing under different conditions.

Sr.	Straw type	% Content	Abbreviation	Room Conditions			Climatic Conditions			AWD Conditions		
				Compression test	Splitting Test	Flexural Test	Compression test	Splitting Test	Flexural Test	Compression test	Splitting Test	Flexural Test
(1)	(2)	(3)	(4)	(5)	(6)	(7)	(8)	(9)	(10)	(11)	(12)	(13)
1	-	0%	PC	$OO_{(E+F)}$	$OO_{(G+H)}$	$OO_{(E+F)}$	$OO_{(I+J)}$	$OO_{(K+L)}$	$OO_{(I+J)}$	$OO_{(M+N)}$	$OO_{(O+P)}$	$OO_{(M+N)}$
2	Soaked	1%	SWSRC	$A1_{(E+F)}$	$A1_{(G+H)}$	$A1_{(E+F)}$	$A1_{(I+J)}$	$A1_{(K+L)}$	$A1_{(I+J)}$	$A1_{(M+N)}$	$A1_{(O+P)}$	$A1_{(M+N)}$
3	Soaked	2%	SWSRC	$A2_{(E+F)}$	$A2_{(G+H)}$	$A2_{(E+F)}$	$A2_{(I+J)}$	$A2_{(K+L)}$	$A2_{(I+J)}$	$A2_{(M+N)}$	$A2_{(O+P)}$	$A2_{(M+N)}$
4	Soaked	3%	SWSRC	$A3_{(E+F)}$	$A3_{(G+H)}$	$A3_{(E+F)}$	$A3_{(I+J)}$	$A3_{(K+L)}$	$A3_{(I+J)}$	$A3_{(M+N)}$	$A3_{(O+P)}$	$A3_{(M+N)}$
5	Boiled	1%	BWSRC	$TA1_{(E+F)}$	$TA1_{(G+H)}$	$TA1_{(E+F)}$	$TA1_{(I+J)}$	$TA1_{(K+L)}$	$TA1_{(I+J)}$	$TA1_{(M+N)}$	$TA1_{(O+P)}$	$TA1_{(M+N)}$
6	Boiled	2%	BWSRC	$TA2_{(E+F)}$	$TA2_{(G+H)}$	$TA2_{(E+F)}$	$TA2_{(I+J)}$	$TA2_{(K+L)}$	$TA2_{(I+J)}$	$TA2_{(M+N)}$	$TA2_{(O+P)}$	$TA2_{(M+N)}$
7	Boiled	3%	BWSRC	$TA3_{(E+F)}$	$TA3_{(G+H)}$	$TA3_{(E+F)}$	$TA3_{(I+J)}$	$TA3_{(K+L)}$	$TA3_{(I+J)}$	$TA3_{(M+N)}$	$TA3_{(O+P)}$	$TA3_{(M+N)}$
8	NaOH Treated	1%	CWSRC	$NA1_{(E+F)}$	$NA1_{(G+H)}$	$NA1_{(E+F)}$	$NA1_{(I+J)}$	$NA1_{(K+L)}$	$NA1_{(I+J)}$	$NA1_{(M+N)}$	$NA1_{(O+P)}$	$NA1_{(M+N)}$
9	NaOH Treated	2%	CWSRC	$NA2_{(E+F)}$	$NA2_{(G+H)}$	$NA2_{(E+F)}$	$NA2_{(I+J)}$	$NA2_{(K+L)}$	$NA2_{(I+J)}$	$NA2_{(M+N)}$	$NA2_{(O+P)}$	$NA2_{(M+N)}$
10	NaOH Treated	3%	CWSRC	$NA3_{(E+F)}$	$NA3_{(G+H)}$	$NA3_{(E+F)}$	$NA3_{(I+J)}$	$NA3_{(K+L)}$	$NA3_{(I+J)}$	$NA3_{(M+N)}$	$NA3_{(O+P)}$	$NA3_{(M+N)}$

Two specimens are cast against each combination.

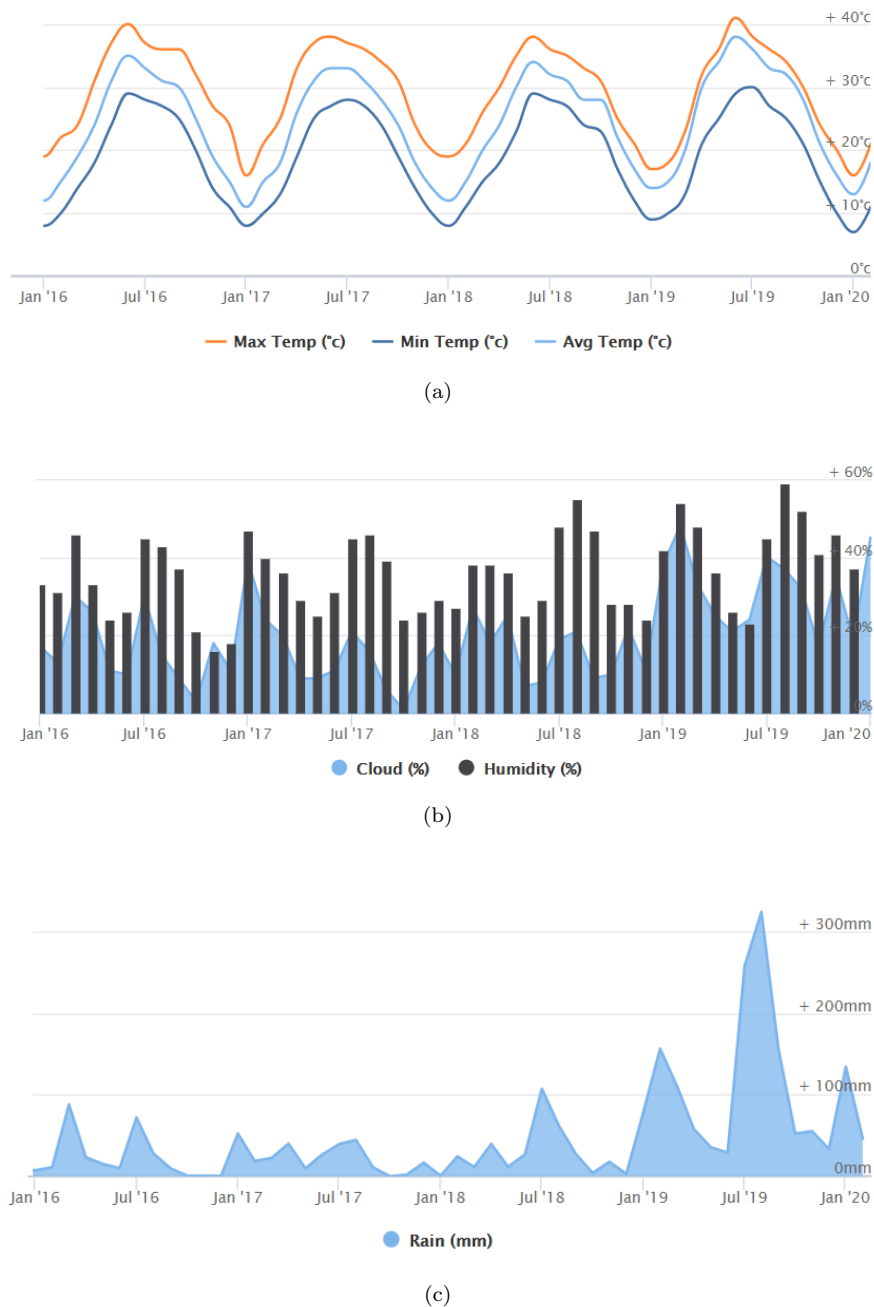


FIGURE 4.2: Climatic conditions i.e. (a) Temperature, (b) Humidity and (c) Rain, of Islamabad, Pakistan from January 2016 to December 2019.

4.2.4.2 Climatic/Environmental Conditions

Secondly, a set of specimens (40 cylinders and 20 beam-lets) is aged under the exposure of natural weathering, i.e. real environmental/climatic conditions of Islamabad, Pakistan. For this purpose, a set of specimens has been placed at the roof of a multi-storey (ground + 3 floors) building at Capital University of Science

and Technology, Islamabad, Pakistan to observe the effect of natural weathering conditions (center image of Figure A1(b)). The climatic data of the considered region for the period of 48-months (from January 2016 – December 2019) is shown through Figure 4.2, as reported by Pakistan Metrological Department. A significant variance in temperature and humidity is observed during this period. The monthly-average low and high temperature of Islamabad region during this period is varied from 8 °C to 29 °C and 18 °C to 39 °C, respectively (Figure 4.2(a)). While the humidity ranges from 23% to 52%. A whole cycle of change in temperature is observed four times during this period (from January 2016 to December 2019). It may be noted that temperature of Islamabad during this period is as low as 2 °C and as high as 48 °C, whereas, the humidity is as minimum as 4% and as maximum as 100%. The precipitation in the considered region is recorded 88 mm, 52 mm, 107 mm and 324 mm in year 2016, 2017, 2018 and 2019, respectively. Hence, the specimens have undergone the effect of an average 143 mm rain during the studied period.

4.2.4.3 Alternate Wetting and Drying Conditions

The third set of the specimens is aged under accelerated ageing conditions to anticipate the long-term behavior of WSRC specimens in terms of durability. Other researchers have also considered the accelerated ageing, i.e. alternate wetting and drying, to depict the long-term behavior of fibre reinforced composites [240, 268, 269]. The specimens are exposed to 104 cycles of alternate wetting and drying. The water bath facility of materials laboratory at Civil Engineering Department of Capital University of Science and Technology, Islamabad, Pakistan is used for the specimens to undergo alternate wetting and drying (right image of Figure A1(b)). The specimens are kept in the water bath of an averaged water temperature of 21-22 °C for 7 days and then in air of an averaged mean temperature of 26.5 °C, as already shown in Figure 4.2, for the same period (7 days). The humidity level is same as reported for climatic conditions. However, the precipitation effect is not considered in this scenario as the specimens are kept under the roof during drying period.

4.2.5 Testing

4.2.5.1 Residual Compressive Strength Test

The residual compressive strength (σ_r), residual energy absorbed under compressive loading (Ce_r), and residual toughness index under compressive loading (CTI_r) of the cylinder specimens are determined by performing compressive strength test in Servo-hydraulic Testing Machine (STM), with in-built high precision displacement transducer having measurement range from 0 – 1500 mm and resolution of 0.001 mm. All the tests, under compressive loading, are performed as per ASTM C39/C39M-20 (Standard Test Method for Compressive Strength of Cylindrical Concrete Specimens).

4.2.5.2 Residual Splitting-tensile Strength Test

The residual properties under splitting-tensile loading i.e. residual splitting-tensile strength (SS_r), residual splitting-tensile energy absorption (Se_r) and residual toughness index under splitting-tensile loading (STI_r) of PC, SWSRC, BWSRC and CWSRC specimens are determined by splitting-tensile strength test as per ASTM C496/C496M-17 (Standard Test Method for Splitting Tensile Strength of Cylindrical Concrete Specimens).

4.2.5.3 Residual Flexural Strength Test

For performing the flexural strength test to have the residual properties of PC, SWSRC, BWSRC and CWSRC beam-lets, the standard adopted is ASTM C293 / C293M-16 (Standard Test Method for Flexural Strength of Concrete - Using Simple Beam with Centre-Point Loading).

The beam-lets are tested in flexural testing machine to determine the residual Modulus of Rupture (MoR_r), residual energy absorbed under flexural loading (Fe_r) and residual toughness index under flexural loading (FTI_r).

4.2.5.4 Micro-structural Analysis of 4-years Aged Straw and it's Bond with Composite

The micro-structural analysis, comprising of X-Ray Diffraction (XRD) analysis, Thermogravimetric analysis (TGA) and Scanning Electron Microscope (SEM) analysis, is done to study the degradation of soaked straw in concrete composite after undergoing the ageing of 4-years. SEM is also performed to study the interfacial bonding of straw with concrete after 4 years. These microscopic tests are intended to reveal the decay mechanism in wheat straw and straw-concrete interfacial bond after exposure to 4-years different ageing condition for an idea of WSRC's durability. Crystallinity of straw is determined with the help of smart lab model 3KW, with the employment of $\text{CuK}\alpha$ ($\lambda = 1.54$) radiation. The graphite monochromator with diffraction intensity of 5-60 ° of 2θ having 0.02 °/s scanning speed is used. The Perkin Elmeris instrument is used for performing the TGA of straw. Straw, weighs approximately 25 mg, are heated up to 500 °C with the rate of 10 °/min. The VEGA3 TESCAN (10 kV) is used for performing scanning electron microscopic imaging. Prior to testing, samples got Plasma coating.

4.3 Experimental Results and Discussions

4.3.1 Residual Properties under Compressive Loading

4.3.1.1 Residual Compressive Behavior

The residual stress \sim strain curves for 4-years aged PC, SWSRC, BWSRC and CWSRC, tested after exposure to three different ageing conditions, i.e. room conditions, climatic conditions, and alternate wetting and drying conditions, are shown in Figure 4.3. The stiffness of PC curves in all the three conditions may be noted here in comparison with WSRC curves. Although the corresponding strain is remarkably increased for both PC and WSRC from 0.014 up to the 0.5 from 0-age to 4-years ageing. This is might be due to the effect, that the specimens

after undergoing the ageing conditions are comparatively deformed more with respect to 0-day aged specimens as shown in Figure 4.3 (b). As, it is observed that the surfaces of specimens are deteriorated after undergoing 4 years ageing. The specimens under room conditions are slightly affected. However, under the climatic conditions, the specimens after undergoing environmental variations, in terms of humidity, temperature and precipitation cycles, are substantially deteriorated. This may be attributed towards decomposition of organic straw due to chemical dissolution. In case of alternate wetting and drying conditions, the specimens are significantly deteriorated. It might be due to the straw decomposition in result of alkaline solution absorption in straw through its porous surface after 104 cycles. The difference between PC and WSRC specimens at 4 years age may be noted from Figure 4.4. As also reported in reference study, here again, cracking is observed only in all the WSRC matrices even at the maximum loading. Which depicts the tough behavior of WSRC specimens (with incorporation of dispersed wheat straw) after the passage of 4 years and under the effect of climatic and severe conditions as well. However, once again, PC specimens show a sudden drop in stress (under the compressive loading) when the applied load reaches up to the maximum level. This behavior, as observed and reported in reference study also, shows the brittleness (low strain capacity) of conventional concrete even after 4 years, as expected. The brittleness of conventional concrete can be reduced with the addition of agricultural wastes (i.e. coconut fibres) in discrete form [250].

Among all WSRC specimens (i.e. SWSRC 1-3%, BWSRC 1-3% and CWSRC 1-3%), SWSRC-1% is behaved well in comparison with PC and all other WSRC specimens as also optimized in reference study. The tested 0-day aged and 4-years aged cylinder specimens of PC and SWSRC-1% are shown in Figure 4.4. The mechanism of PC failure continues after 4 years and under all the three conditions, as broken fragments can be observed on the assembly base plates for all four PC specimens, i.e. i) 0-day aged, ii) 4-years aged under room conditions, iii) 4-years aged under climatic conditions, and iv) 4-years aged under alternate wetting and drying. On the other side, in SWSRC-1% specimens, no fragment is broken from the specimens and the bridging/sewing mechanism can easily be observed even

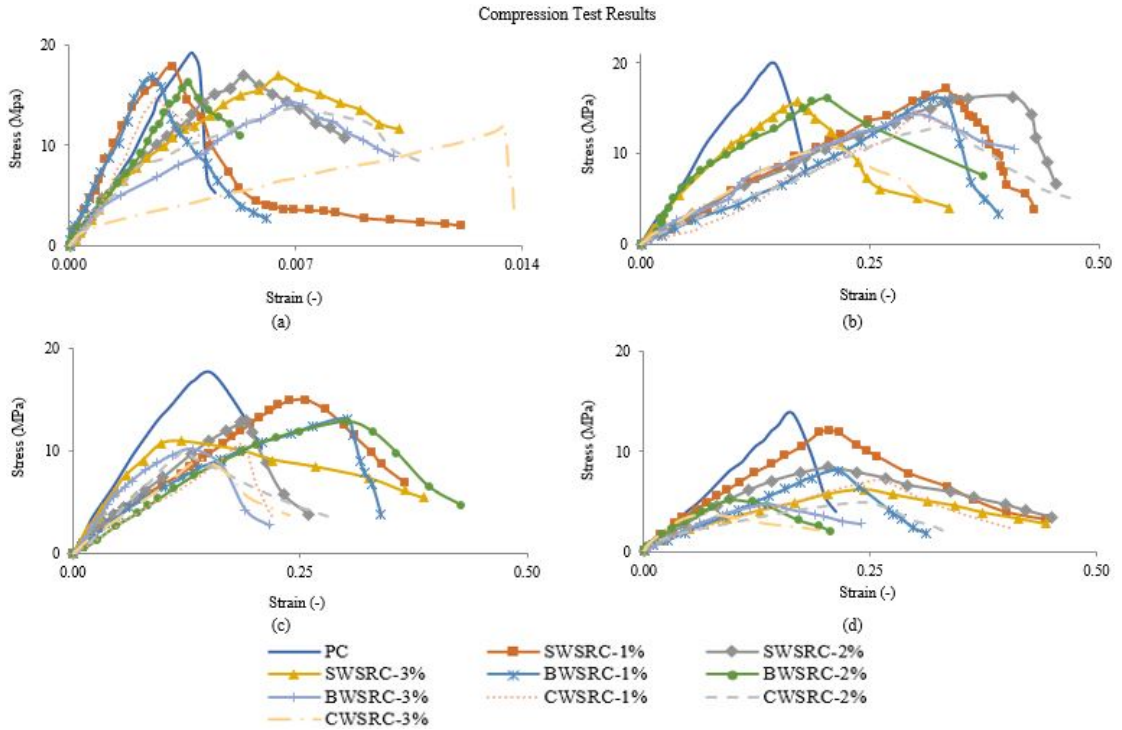


FIGURE 4.3: Compressive stress – strain curves of PC, SWSRC, BWSRC and CWSRC at (a) 0-day age [267], (b) 4-years aged under room conditions, (c) 4-years aged under climatic conditions and (d) 4-years aged under alternate wetting and drying conditions.

in the specimen under the worst condition (i.e. undergone alternate wetting and drying).

4.3.1.2 Residual Compressive Strength (σ_r), Energy Absorption (Ce_r) and Toughness Index (CTI_r)

The residual compressive strength (σ_r) is taken as the maximum stress value from residual compressive stress ~ strain curves (Table 4.3). The decrement in σ_r of 4-years aged SWSRC-1% (with the maximum σ_r among all WSRC matrices) in comparison with that of PC is observed here again as also reported in reference study. Which shows the continuation of phenomenon with the passage of time. As far as decrement in compressive strength is concerned, it is usually observed in case of agricultural waste/plant reinforced composites [40, 66, 238]. However, in case of 4 years ageing, the decomposition of wheat straw in concrete composite due to continuous contact with varied moisture conditions, particularly under

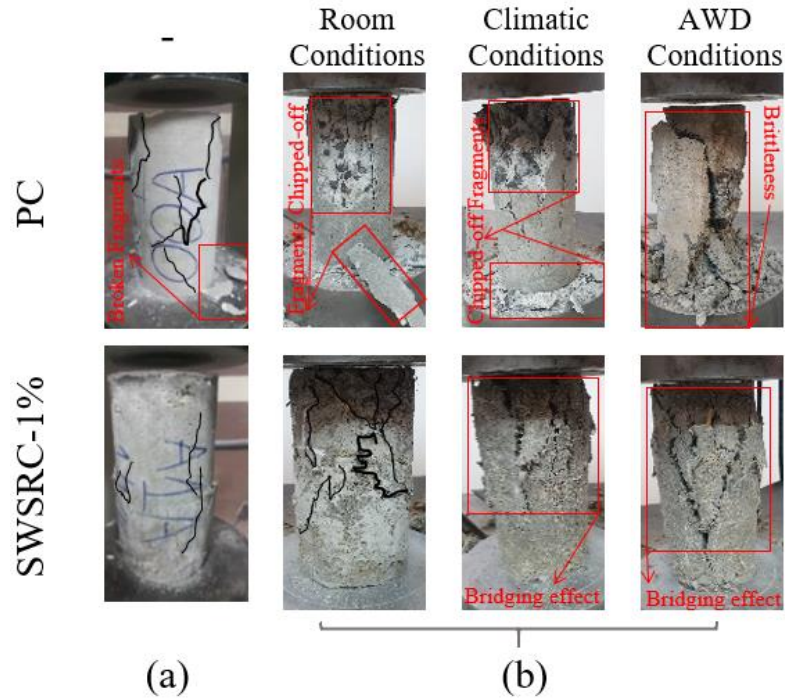


FIGURE 4.4: Tested cylinder specimens of PC and SWSRC-1% under compressive loading (a) at 0-day age [267] and (b) after 4-years ageing.

climatic and alternate wetting and drying conditions, could be the reason behind comparatively more strength decrement as for PC. The decrement in strength of natural fibre reinforced concrete under severe ageing conditions is also reported by [70]. A consistent decrement (i.e. approximately 14%) in residual compressive strengths (σ_r) of SWSRC-1% as compared to that of PC is observed after 4 years of ageing under all the three ageing conditions. Which shows the reliable behavior of SWSRC-1% under compressive loading. However, the rate of decrement in compressive strengths of PC and SWSRC-1% in comparison to that of respective 0-day aged specimens, is slightly varied.

The residual compressive energy absorption (Ce_r) is taken as the area under residual stress \sim strain curve. It can also be referred as compressive toughness [66, 71]. This is also defined as capacity of concrete to absorb energy (MJ/m^3) by [254, 255]. However, the residual toughness index (CTI_r) under compressive loading is calculated as the ratio of Ce_r to the residual energy absorbed till the highest residual stress. Ce_r and CTI_r values of 4-years aged PC and SWSRC-1% are also given in

Table 4.3. The residual energy absorption under compressive loading by SWSRC-1% is significantly high (95% under room conditions, 46% under climatic conditions and 95% under alternate wetting and drying) than that of PC. Elongated deformation and more strain capacity due to the incorporation of dispersed straw in composite might be the reason behind it. The crack occurrence and propagation is resisted due to increased energy absorption which ultimately contributes towards enhanced toughness. This phenomenon indicates that the post-cracking behavior is enhanced for concrete having wheat straw. However, the crack arresting by straw continues even after the occurrence of cracks. The CTI_r of SWSRC-1% is enhanced up to 62% in comparison to CTI_r of PC. Usually, a decrement in properties, under compression, is noted after 4-years ageing under all three conditions, except for CTI_r .

A comparison of residual compressive behavior of PC and SWSRC-1% after 4-years ageing under controlled room conditions, natural weathering/climatic conditions and alternate wetting and drying conditions are shown in Figure 4.5. It can be seen that, for all three ageing conditions, the σ_r of SWSRC-1% is decreased as compared to PC and the respective SWSRC-1% specimen at 0-day age. Contrary to it, under the controlled room conditions, the residual strength of PC is increased a bit with passage of time, as expected (Figure 4.5). But, in case of SWSRC-1%, it is decreased by 5% because of organic natured straw presence in the composite. The straw might be tended towards degradation due to the presence of moisture in air (i.e. humidity) when exposed for a long time (i.e. 48 months). As far as the exposure to climatic and alternate wetting and drying conditions are concerned, the decrements of 9% and 28%, respectively in PC and 16% and 33%, respectively in case of SWSRC-1% is observed. The more decrement in case of SWSRC-1% in comparison with PC is due to the organic degradation of straw under natural weathering and alternate wetting and drying.

The severe the ageing conditions, more will be the decrement in residual compressive strengths of fibre reinforced concrete [70]. The decrement in compressive strength with enhanced toughness of composites having agricultural waste is also

TABLE 4.3: Residual properties under compressive loading (i.e. σ_r , Ce_r and CTI_r) of PC and SWSRC-1% at 0 and 4-years age.

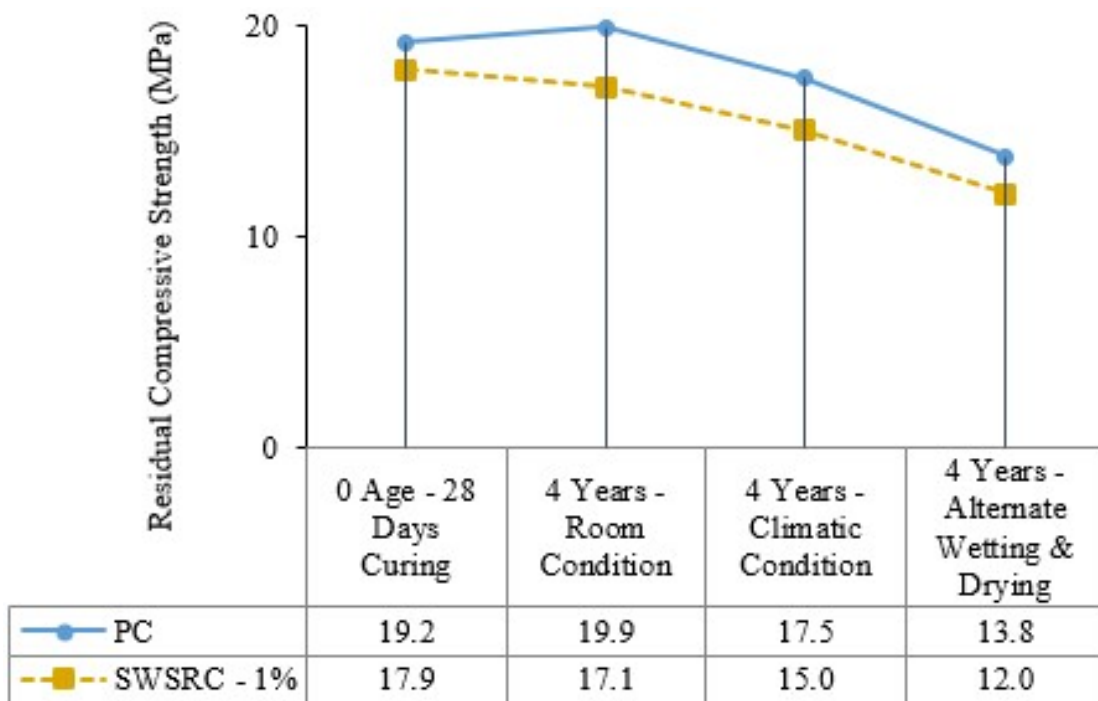
Properties	0 Age Specimens*		4-years Aged Specimens						
			Room Conditions		Climatic Conditions		AWD Conditions		
	PC	SWSRC-1%	PC	SWSRC-1%	PC	SWSRC-1%	PC	SWSRC-1%	
(1)	(2)	(3)	(4)	(5)	(6)	(7)	(8)	(9)	
σ_r (MPa)	19.2	17.9	19.9	17.1	17.5	15.0	13.8	12.0	
	± 0.2	± 0.3	$[-7\%]$	± 0.4	± 0.6	$[-14\%]$	± 0.3	± 0.9	$[-14\%]$
	-	-	(4%)	(-5%)	(-9%)	(-16%)	(-28%)	(-33%)	
Ce_r	44.6	94.0	2084	4061	2324	3387	1543	3013	
(kJ/m ³)	± 1.1	± 1.2	$[+111\%]$	± 18	± 24	$[+95\%]$	± 27	± 33	$[+46\%]$
	-	-	-	-	-	-	-	-	
CTI_r	1.23	2.35	1.32	1.35	1.49	1.57	1.38	2.24	
(-)	± 0.00	± 0.05	$[+91\%]$	± 0.02	± 0.01	$[+2\%]$	± 0.04	± 0.05	$[+5\%]$
	(+7%)	(-42%)	(+21%)	(-33%)	(+12%)	(-4%)	(+12%)	(-4%)	

1. * These values are reported by [267].

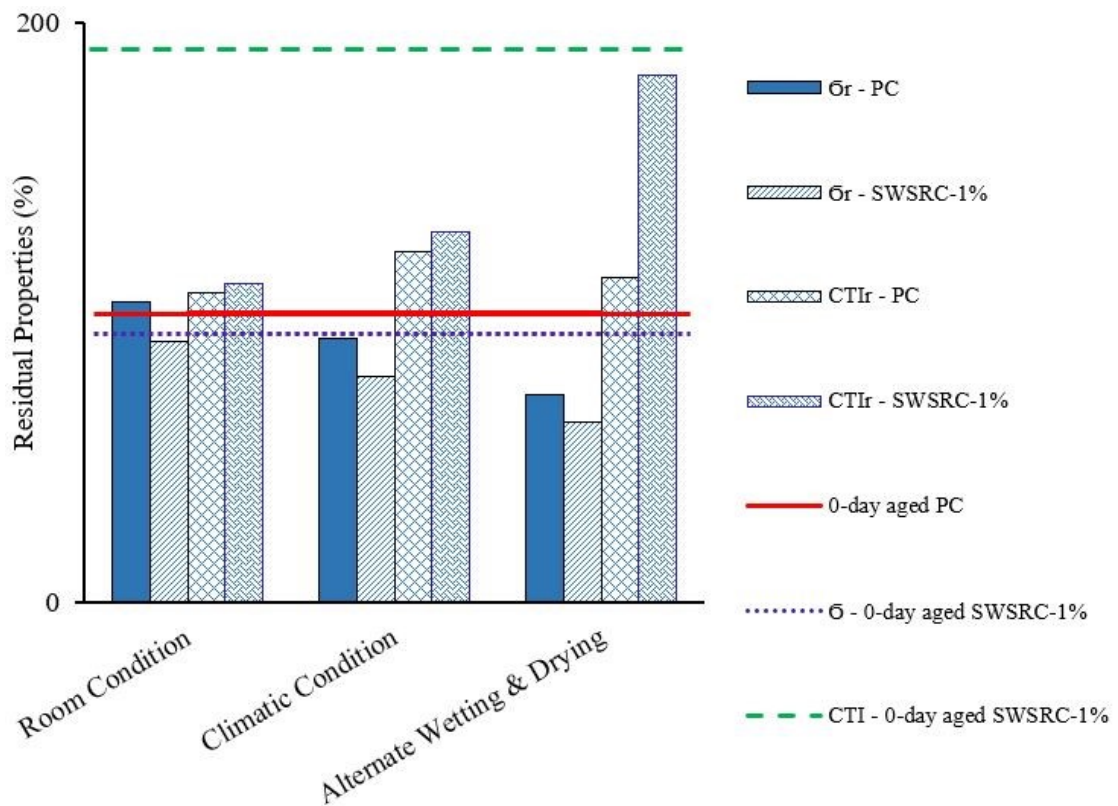
2. Percentage in bracket [] shows percentage difference w.r.t value of PC at same considered age.

3. Percentage in bracket () show percentage difference w.r.t value of respective specimen at 0-age.

4. The plus (+) shows an increase and negative (-) shows a decrease in percentage.



(a)



(b)

FIGURE 4.5: Effect of 4-years ageing conditions on residual (a) Compressive strength and (b) Compressive behavior of PC and SWSRC-1%.

observed by [16, 249]. Furthermore, it is also reported that in addition to compressive strength, toughness also contributes towards achievement of structural strength [256, 257].

4.3.2 Residual Properties under Splitting-tensile Loading

4.3.2.1 Residual Splitting-tensile Behavior

The residual splitting-tensile load ~ deformation graphs of PC and WSRC, with 1%, 2% and 3% content of soaked, boiled and chemically treated straw are presented in Figure 4.6. The similar type of behavior, as reported in reference study (i.e. Figure 4.6(a)), is observed after the 4 years of ageing under different conditions. The resistance against failure is observed after maximum load whereas in case of PC, the specimens collapsed completely at maximum load. The deformation, however, increased at 4-years age for both PC and WSRC specimens as compared to that at 0-day age. Same behavior is observed under compressive loading as well. The post peak loading performance (i.e. the inclination of curves towards right) in case of WSRC may be due to crack arresting mechanism produced in result of adding dispersed agricultural waste in cement concrete composite. Even at the worst scenario, i.e. accelerated ageing by alternate wetting and drying, the consistency in WSRC behavior is observed.

Soaked Wheat Straw Reinforced Concrete with 1% straw content, among all WSRC specimens, seems to have better behavior in terms of load and post peak load behavior as well. As, although, SWSRC-1% specimens bear slightly lesser load as compared to PC but even then, the improved post peak load behavior contributes towards better performance of structure in terms of toughness. Similarly, the improved tensile behavior of natural fibre reinforced concrete after undergoing the ageing conditions is also reported by [270].

Hence, the 0-day aged and 4-years aged PC and SWSRC-1% specimens tested after exposure to controlled room conditions, climatic conditions and alternate wetting

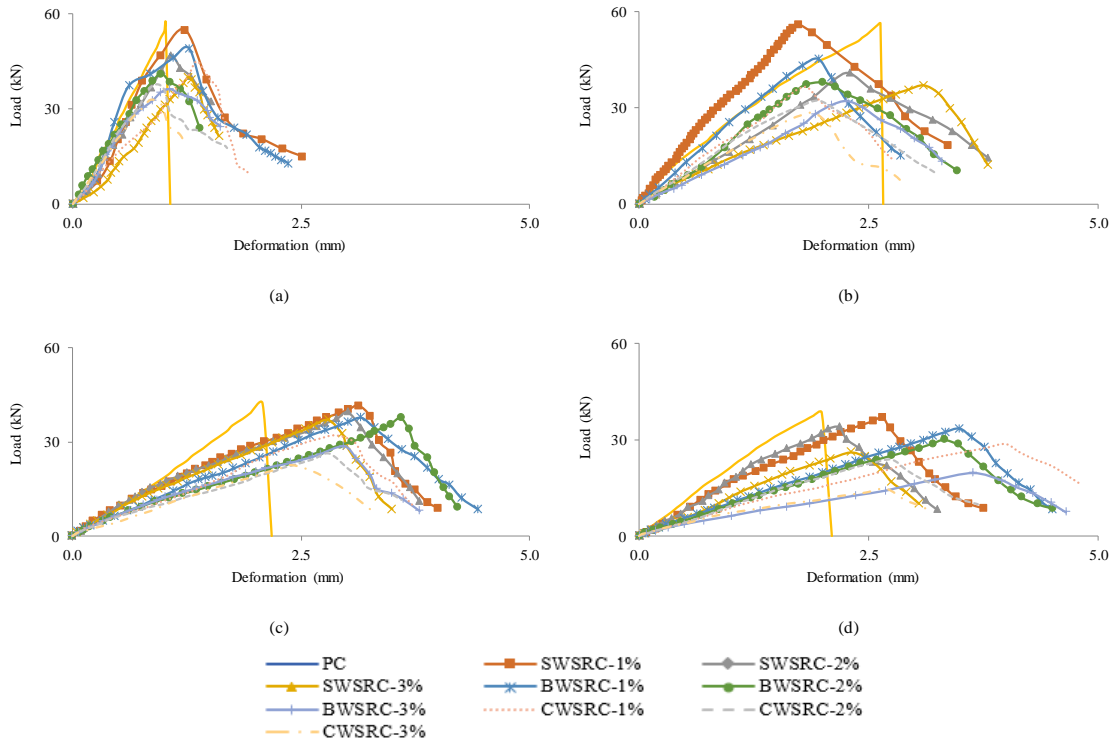


FIGURE 4.6: Splitting-tensile load - deformation curves at (a) 0-day age [267], (b) 4-years aged under room conditions, (c) 4-years aged under climatic conditions and (d) 4-years aged under alternate wetting and drying conditions.

and drying are presented in Figure 4.7. Due to brittleness of PC, at maximum load, its specimens are broken into two pieces at both the ages (i.e. 0-day and 4-years under different conditions). However, in case of WSRC, particularly SWSRC-1%, only cracking is observed even upon the application of maximum load. The same behavior is observed in the specimens exposed to climatic conditions and to alternate wetting and drying as well, which depicts the consistent behavior of WSRC even under severe conditions.

The crack arresting mechanism is achieved with the help of dispersed agricultural straw. Approximately, 65-75% pulling of straw is observed with the naked eye, in case of SWSRC-1%, when broken intentionally later on. However, the broken straw percentage is higher in specimens exposed to climatic conditions (30-40%) and alternate wetting and drying (40-50%). This might be due to the disintegration of organic straw in concrete when exposed to natural and accelerated weathering. In addition, the equal development length or uniform dispersion in concrete matrix may also be the reason behind straw fracture.

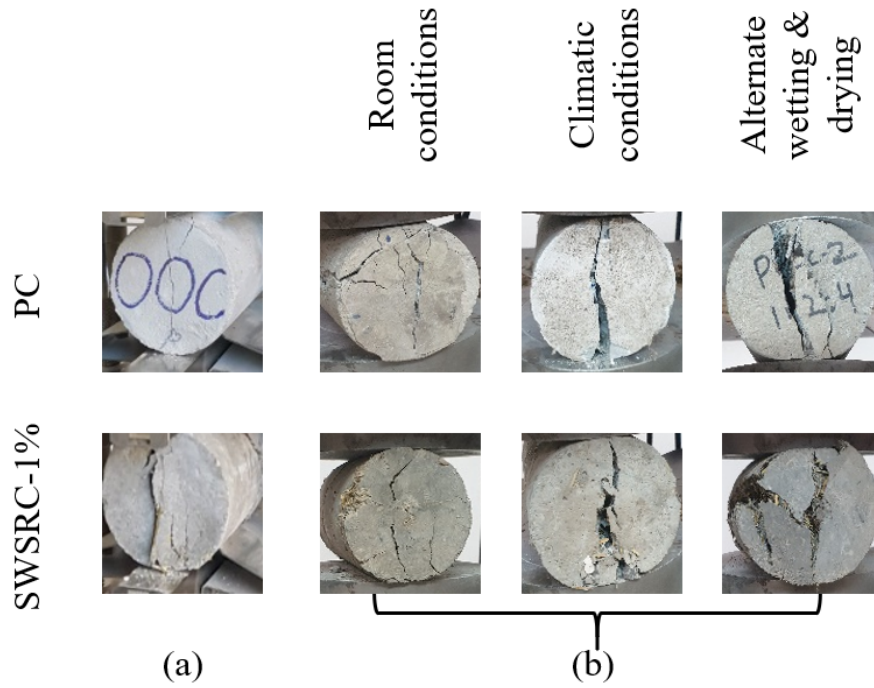


FIGURE 4.7: Tested cylinder specimens of PC and SWSRC-1% under splitting-tensile loading (a) at 0-day age [267] and (b) after 4-years ageing.

4.3.2.2 Residual Splitting-tensile Strength (SS_r), Energy Absorption (Se_r) and Toughness Index (STI_r)

The residual splitting-tensile strength (SS_r) is calculated by using the maximum value of load from residual splitting–tensile load ~ deformation curve (Figure 4.6). In pursuance of the better behavior of SWSRC-1% (as also optimized in reference study), the residual splitting-tensile strengths of PC and SWSRC-1% are given in Table 4.4. The residual strengths of SWSRC-1% aged under room conditions, climatic conditions and alternate wetting and drying are decreased by 4%, 2% and 3%, respectively, in comparison to that of 4-years aged PC under the respective ageing conditions. Here again, as in reference study, a slight decrement ($< 5\%$) in residual strength of SWSRC-1% under splitting-tensile loading is noted in comparison with PC. The highest decrement of 33%, as compared to respective 0-day aged specimen, is noted in case of accelerated ageing conditions. The bio-degradable nature of straw when come in contact with weathering and/or moisture conditions is might be the reason behind reduction in splitting-tensile strength of SWSRC-1%. The reduction of more than 50% was also observed in case of vegetable fibre

reinforced concrete, when exposed to accelerated ageing process, i.e. immersion in solution of pH 12 [14]. On the other hand, as mentioned earlier, the residual behavior post the peak load is remarkably improved in terms of energy absorption capability.

The residual splitting-tensile energy absorption (Se_r) is calculated as the measurement of area under residual splitting-tensile load \sim deformation curve. And, the ratio of Se_r to the residual splitting-tensile energy absorption till the maximum load is the residual toughness index under splitting-tensile loading (STI_r). Se_r and STI_r of PC and SWSRC-1% are also given in Table 4.4. The sewing effect of straw in concrete composite remains consistent, even after 4-years of ageing under different ageing conditions, by contributing a significant increase of 37%, 119% and 95% in residual energy absorption of SWSRC-1%, in comparison with controlled specimens. As reported by [267], the slippage phenomenon of straw is because of its tensile strength, which contributes towards more energy absorption, ultimately depicts the improved toughness of SWSRC-1%. The STI_r of SWSRC-1%, in comparison with PC, is persistently increased from 0-day age to 4 years age and from controlled conditions to accelerated ageing process. This improved post peak load behavior with slight reduction in strength is also observed in case of compressive loading.

The percentage comparison for residual properties (i.e. SS_r and STI_r) of PC and SWSRC-1% at different ageing conditions and with respective 0-day aged specimens is shown in Figure 4.8. Overall, the residual properties decreased from room conditions towards accelerated ageing conditions. The consistency in decrement upon exposure to ageing conditions, in comparison to that with respective 0-day aged specimens, is more or less same for both PC and SWSRC-1%. Therefore, it can be concluded that the residual results are comparable with that of PC as enhanced toughness is observed with minimum reduction in strength at all the stages. Overall, the residual behavior under splitting-tensile loading is depicting improvement, falling from ideal conditions towards worst conditions. This decrement in behavior might be due to straw decomposition due to induced humid environments and temperature changes.

TABLE 4.4: Residual properties under splitting-tensile loading (i.e. SS_r , Se_r and STI_r) of PC and SWSRC-1% at 0 and 4-years age.

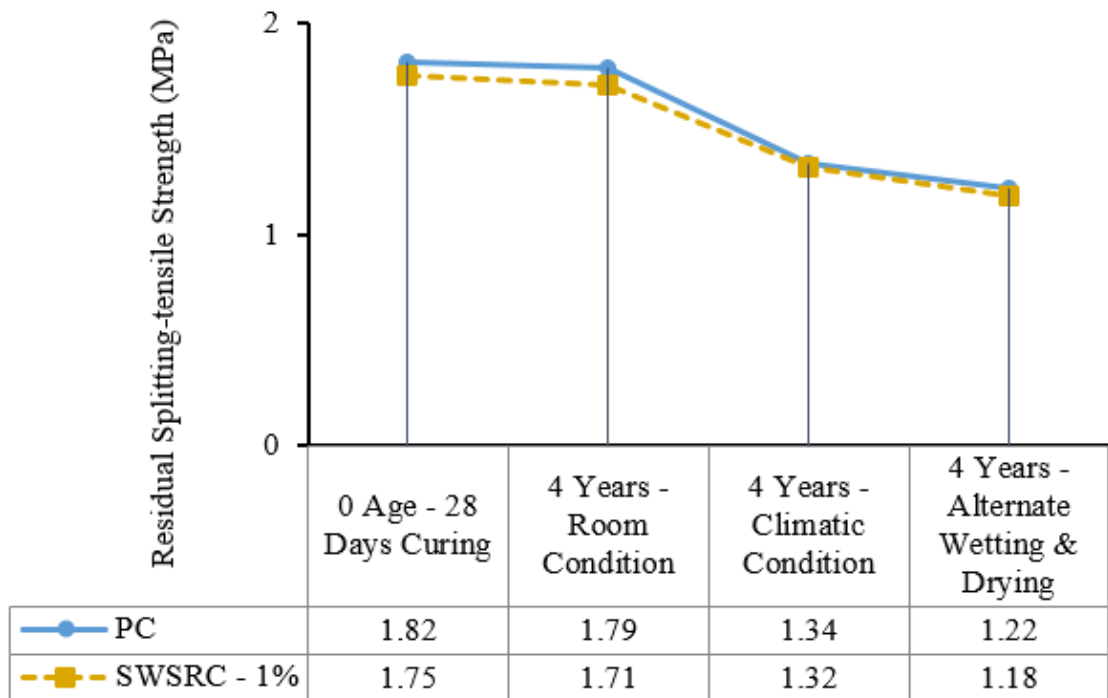
Properties	4-years Aged Specimens											
	0 Age Specimens*			Room Conditions			Climatic Conditions			AWD Conditions		
	PC	SWSRC-1%		PC	SWSRC-1%	PC	PC	SWSRC-1%	PC	PC	SWSRC-1%	PC
(1)	(2)	(3)	(4)	(5)	(6)	(7)	(8)	(9)				
SS_r	1.82	1.75	1.79	1.71	1.34	1.32	1.22	1.18				
(MPa)	± 0.05	± 0.11	± 0.06	± 0.13	± 0.05	± 0.12	± 0.08	± 0.22	$[-4\%]$	$[-2\%]$	$[-3\%]$	
	-	-	(-2%)	(-2%)	(-26%)	(-25%)	(-33%)	(-33%)				
Se_r	28.2	68.8	81.7	112.3	41.7	91.3	41.3	74.7				
(J)	± 1.0	± 2.0	± 3.8	± 4.4	± 2.7	± 3.3	± 3.7	± 3.9	$[+144\%]$	$[+37\%]$	$[+119\%]$	$[+95\%]$
	-	-	-	-	-	-	-	-				
STI_r	1.00	2.05	1.00	1.89	1.00	1.27	1.00	1.41				
-	± 0.00	± 0.02	± 0.00	± 0.03	± 0.00	± 0.03	± 0.00	± 0.09	$[+105\%]$	$[+89\%]$	$[+27\%]$	$[+41\%]$
	-	(-8%)	-	(-38%)	-	(-38%)	-	(-31%)				

1. * These values are reported by [267].

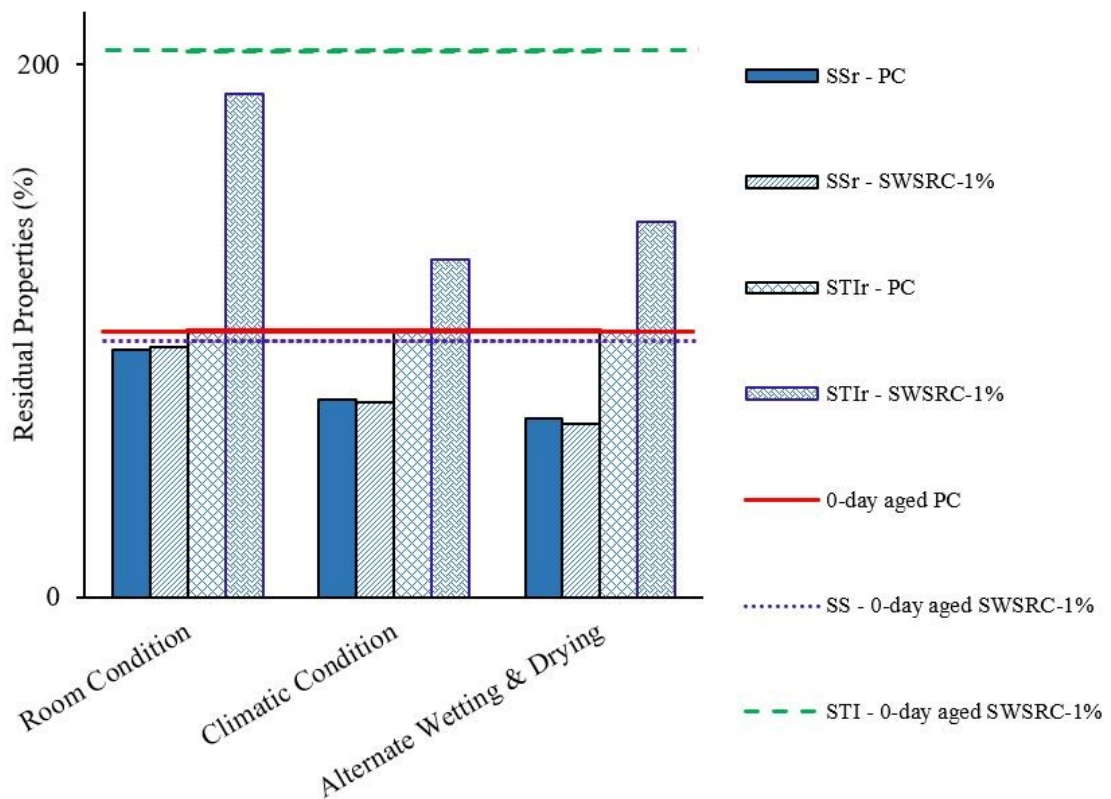
2. Percentage in bracket [] shows percentage difference w.r.t value of PC at same considered age.

3. Percentage in bracket () show percentage difference w.r.t value of respective specimen at 0-age.

4. The plus (+) shows an increase and negative (-) shows a decrease in percentage.



(a)



(b)

FIGURE 4.8: Effect of 4-years ageing conditions on residual (a) Splitting-tensile strength and (b) Splitting-tensile behavior of PC and SWSRC-1%.

It can be said that, for number of civil engineering applications, splitting-tensile behavior is usually taken as a governing parameter. Therefore, the tough behavior under splitting-tensile loading even after 4 years of ageing with a remarkable increase up to 89% in STIr and a maximum reduction of 4% in respective strength for SWSRC-1% in comparison to PC, is suitable.

4.3.3 Residual Properties under Flexural Loading

4.3.3.1 Residual Flexural Behavior

The residual flexural behavior (i.e. load– displacement curve) of PC, SWSRC 1-3%, BWSRC 1-3% and CWSRC 1-3% is shown in Figure 4.9. The noticeable behavior after 48 months of ageing is that the WSRC specimens' curves show remarkable elongation towards right indicating the tough behavior of WSRC in comparison to brittle natured conventional PC. SWSRC specimens tend to bear the flexural load even after highest load and cracking as well. Contrary to this, the PC specimen, at all the stages, broke in two pieces without any warning.

However, the displacement increased significantly (i.e. up to 5 mm) for WSRC here as well, likewise in residual compressive and splitting-tensile behavior, when compared to that at 0-day age. The presence of organic straw in SWSRC-1% matrix behaved more or less same at all the ageing conditions with the decrement in loading. Similarly, the consistency of residual flexural behavior at multiple curing stages is also reported by Sivaraja *et al.* [48].

Following the better and more persistent residual behavior of Soaked Wheat Straw Reinforced Concrete having 1% content (SWSRC-1%), the 4-years aged beam-lets of PC and SWSRC-1% tested after exposure to room, natural weathering and alternate wetting and drying conditions are presented in Figure 4.10. The SWSRC-1% beam-lets, show resistance against breaking, however, cracks occurred instead, unlikely to PC specimens which used to break in two halves as soon as the flexural load reaches up to the maximum point at all the three ageing

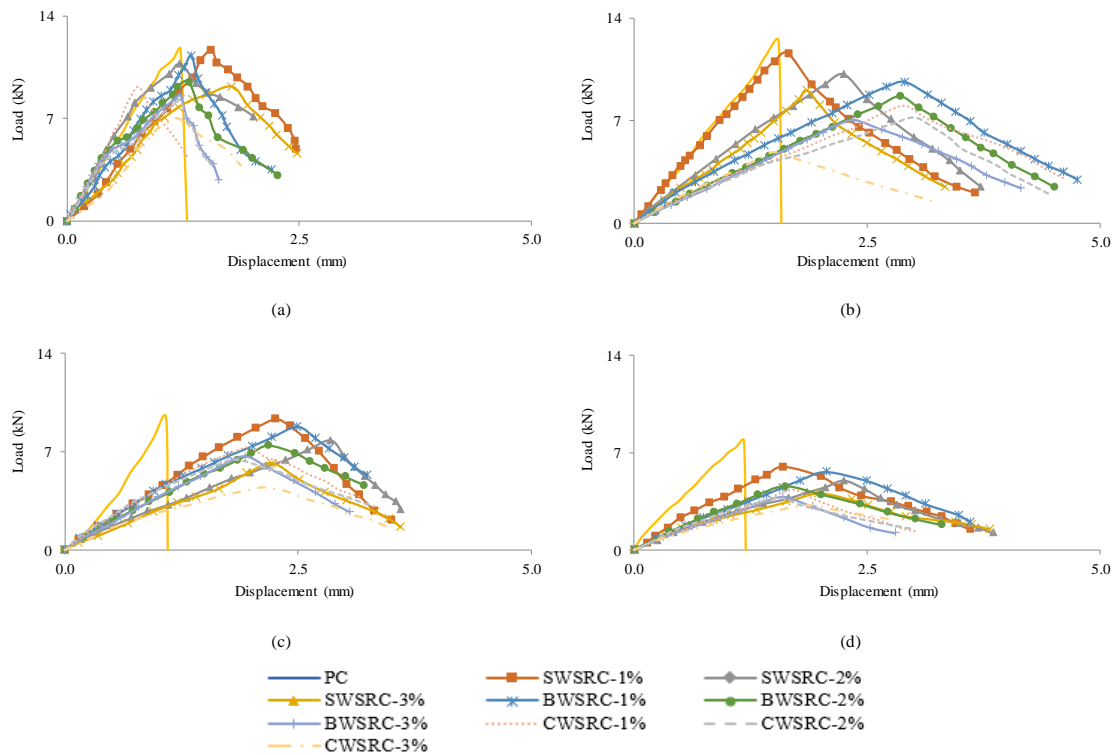


FIGURE 4.9: Flexural load - displacement curves at (a) 0-day age [267], (b) 4-years aged under room conditions, (c) 4-years aged under climatic conditions and (d) 4-years aged under alternate wetting and drying conditions.

conditions (Figure 4.10) similar to that at 0-day age as reported in reference study (Figure 4.10 (a)). The dispersed straw in the matrix also slow down the crack propagation.

Soaked Wheat Straw Reinforced Concrete, having 1% content, specimens are intentionally broken into two halves. The failure mechanism, in terms of fibre pull-out and/or fibre fracture, is observed with the help of naked eye. The straw sample is also taken from here for micro-structural analysis. It is observed that, there is a gradual change from straw pulling dominant behavior towards rupture of straw dominance while moving from room conditioned specimens towards specimens exposed under natural weathering and then the specimens which have undergone the exposure of accelerated ageing conditions. This shift of mechanism could be due to intensity of temperature variations, induced humid environment, moisture exposure due to rain and other degrading factors on organic natured straw when exposed to such conditions for a long period.

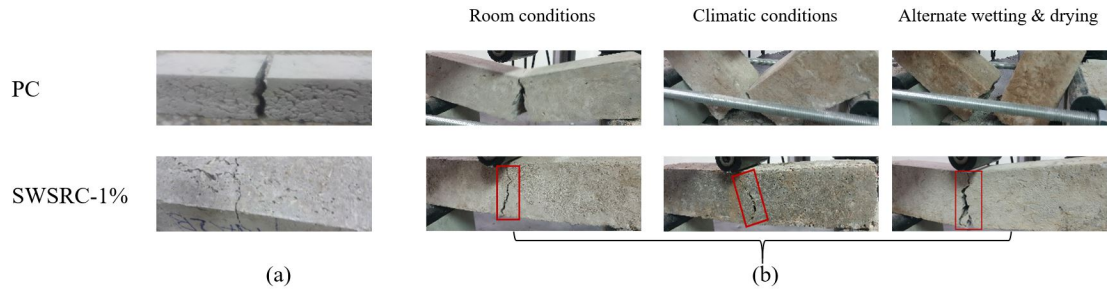


FIGURE 4.10: Tested specimens of PC and SWSRC-1% under flexural loading (a) at 0-day age [267] and (b) after 4-years ageing.

4.3.3.2 Residual Modulus of Rupture (MoR_r), Energy Absorption (Fe_r) and Toughness Index (FTI_r)

Residual Modulus of Rupture (MoR_r) is calculated by using the highest value of load from the flexural load \sim displacement curve. The residual energy absorption (Fe_r) is calculated as the total area under the flexural load \sim displacement curve of 4-years aged specimens. Furthermore, the residual flexural energy absorption (FE_r) to the residual flexural energy absorbed till the highest load ratio is calculated for residual toughness index under flexural loading (FTI_r). The MoR_r , Fe_r and FTI_r of PC and SWSRC-1% are given in Table 4.5. Likewise, in the reference study, the flexural strength (i.e. MoR_R) of SWSRC-1% specimens are slightly decreased by 7%, 2% and 24% after exposure to room conditions, climatic conditions and alternate wetting and drying conditions, respectively, in comparison with PC. Here, the noticeable thing is that the behavior in terms of MoR_r seems better when exposed to natural weathering which is favourable towards development/construction of WSRC structures where flexural strength is a governing parameter. The MoR_r of PC is increased (6%) as compared to the respective 0-day aged specimens under ideal conditions showing the typical behavior of conventional concrete. However, the residual flexural strength (i.e. MoR_r) of SWSRC-1% is 99%, 79% and 51% after exposure to idealized controlled room conditions, climatic conditions, and accelerated ageing (i.e. alternate wetting and drying) conditions, respectively; which are comparable with that of controlled specimens i.e. PC. The accelerated effect of moisture infiltration in WSRC specimens, under climatic

and alternate wetting and drying conditions, is might be the reason of straw decomposition and specimen's deterioration that ultimately contributed in strength reduction. Such type of results for natural fibre reinforced concrete after exposure to alternate wetting at elevated temperature and drying are also reported by Wei and Meyer [271].

The main contribution of dispersed agricultural fibres in cement composites is the improvement in its toughness, not the strength. As the micro cracks, which usually occur before even maximum loading, are arrested by dispersed fibres through sewing/bridging mechanism [272]. In addition to the significant residual strengths under flexural loading, there is a remarkable increase (up to 116%) in residual toughness of SWSRC-1% under flexural loading. The noticeable enhancement in residual toughness of SWSRC-1% with respect to PC (where there is a brittle response with no toughness at all) when contributes towards its strength, can balance the minor reduction of strength. This phenomenon/behavior is most suitable for rigid pavements.

A comparison of residual flexural properties (i.e. MoR_r and FTI_r) of 4-years aged PC and SWSRC-1% after exposure to room, climatic, and alternate wetting and drying conditions and with the respective 0-day aged specimens, as reported by [267], is shown in Figure 4.11. The differences of residual flexural properties between ideal/controlled, natural weathering and accelerated ageing conditions indicate the humidity effect on degradation rate of straw-reinforced cement concrete composites. It can be observed that, at natural weathering/climatic conditions, the soaked straw reinforced samples yielded lower residual flexural strength and toughness than those exposed to controlled conditions. For the specimens exposed to alternate wetting and drying cycles, the frequent change in humidity shows a remarkable effect on enhancing/accelerating the degradation rate of straw and straw-concrete composites ultimately encountered the significant drop in residual flexural strength and toughness. After 24 alternate wetting and drying cycles, the residual flexural strength of the beam-lets declined by 49%, which is 51% and 64% lower than those under room and climatic conditions, respectively.

TABLE 4.5: Residual properties under flexural loading (i.e. MoR_r , Fe_r and FTI_r) of PC and SWSRC-1% at 0 and 4-years age.

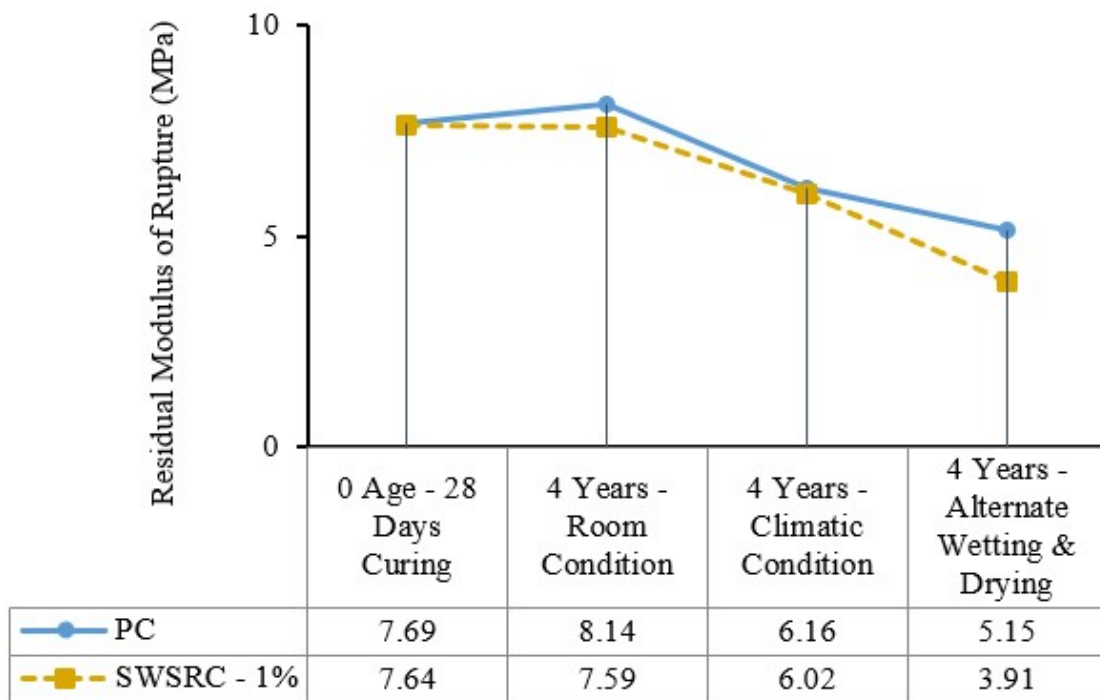
Properties	4-years Aged Specimens														
	0 Age Specimens*			Room Conditions			Climatic Conditions			AWD Conditions					
	PC	SWSRC-1%	(1)	PC	SWSRC-1%	(2)	PC	SWSRC-1%	(3)	PC	SWSRC-1%	(4)	PC	SWSRC-1%	(5)
MoR_r	7.69	7.64	7.64	8.14	7.59	7.59	6.16	6.02	5.15	3.91					
(MPa)	± 0.3	± 0.4	$[-1\%]$	± 0.6	± 0.9	$[-7\%]$	± 0.2	± 0.3	$[-2\%]$	± 0.1	± 0.2	$[-24\%]$			
Fe_r	-	-	-	$(+6\%)$	(-1%)	(-20%)	(-21%)	(-33%)	(-49%)						
(J)	± 0.2	± 0.3	$[+99\%]$	± 0.8	± 1.4	$[+133\%]$	± 0.7	± 1.3	$[+307\%]$	± 1.0	± 1.1	$[+154\%]$			
FTI_r	1.00	1.92	1.92	1.00	2.16	2.16	1.00	2.08	1.00	1.99					
-	± 0.00	± 0.01	$[+92\%]$	± 0.00	± 0.10	$[+116\%]$	± 0.00	± 0.09	$[+108\%]$	± 0.00	± 0.13	$[+99\%]$			
	-	-	$(+13\%)$	-	-	$(+8\%)$	-	-	-	-	-	$(+4\%)$			

1. * These values are reported by [267].

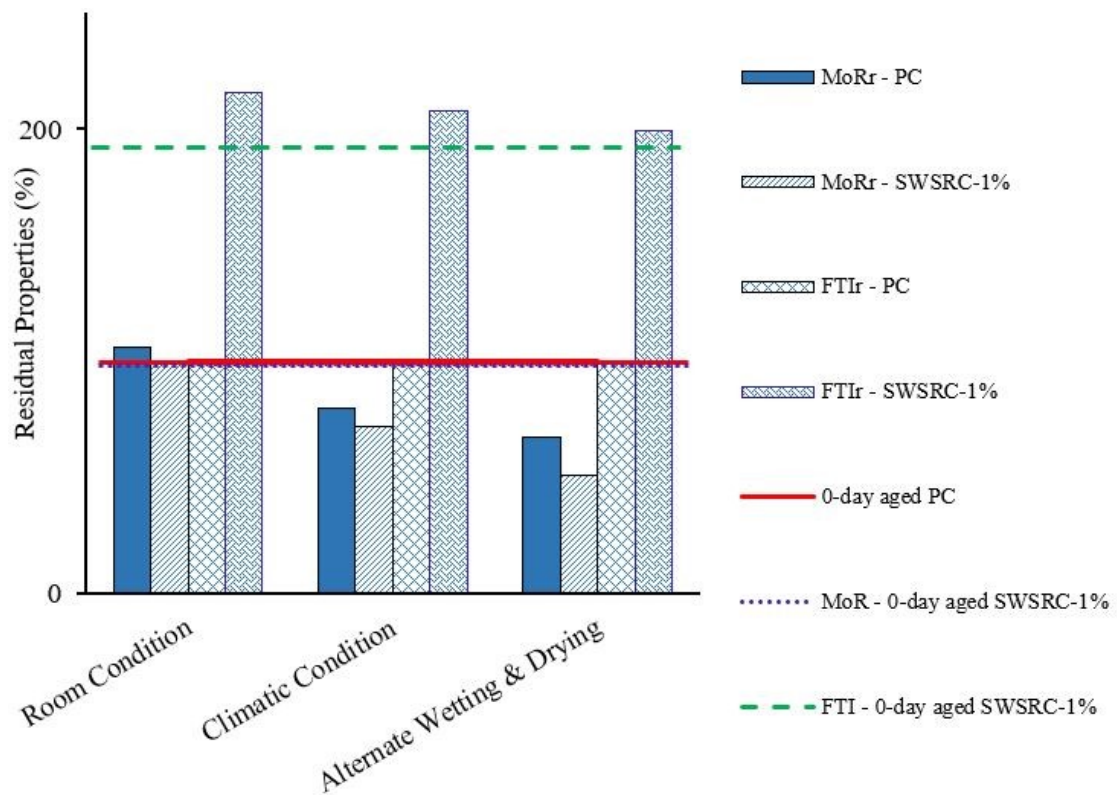
2. Percentage in bracket [] shows percentage difference w.r.t value of PC at same considered age.

3. Percentage in bracket () show percentage difference w.r.t value of respective specimen at 0-age.

4. The plus (+) shows an increase and negative (-) shows a decrease in percentage.



(a)



(b)

FIGURE 4.11: Effect of 4-years ageing conditions on residual (a) Modulus of Rupture and (b) Flexural behavior of PC and SWSRC-1%.

As mentioned earlier that flexural properties are critical for rigid pavements [261]. The rigid pavements are vulnerable to development of cracks and their propagation due to effect of vehicular loading. Furthermore, pavements are directly exposed to climatic conditions. So, the improved residual performance of SWSRC-1% in terms of post cracking behavior after exposure to 4 years of natural weathering conditions seems highly favourable for such civil engineering structures.

4.3.4 Micro-structural Findings

4.3.4.1 X-Ray Diffraction (XRD) Analysis of Straw

Crystallographic characterization of wheat straw at 0-day and at 4-years (after exposure to room, climatic and alternate wetting and drying conditions) is analysed with X-ray Diffraction (XRD) as shown in Figure 4.12. Agricultural fibres i.e. Wheat straw mainly contain lignin, hemicellulose and cellulose. Cellulose is further composed of crystalline and amorphous structures, whereas the hemicellulose and lignin are basically amorphous. XRD data show that maximum crystalline peak gained at around 2θ varies from 26.10° - 29.89° , while that of amorphous peak obtained at 2θ between 23.71° – 25.58° . The enhancement in crystalline percentage and crystallinity index of the wheat straw may be due to the development of new hydrogen bonds among cellulose enhance by variation in humidity and temperature during ageing period under controlled conditions. However, the comparatively declined crystallinity in case of straw extracted from the specimen tested after exposure to climatic conditions could be due to probability of acidic rain during ageing period (Figure 4.2 (c)). The frequent variation in temperature and humid environment, in case of alternate wetting and drying, may be the reason behind breakdown of amorphous structure in straw as shown in Figure 4.12. It can be concluded from XRD pattern that straw can be more crystalline by eliminating non-cellulosic parts. The crystallinity structure is likely to be broken in case of chemical treatment of straw for CWSRC; which might be the reason behind the

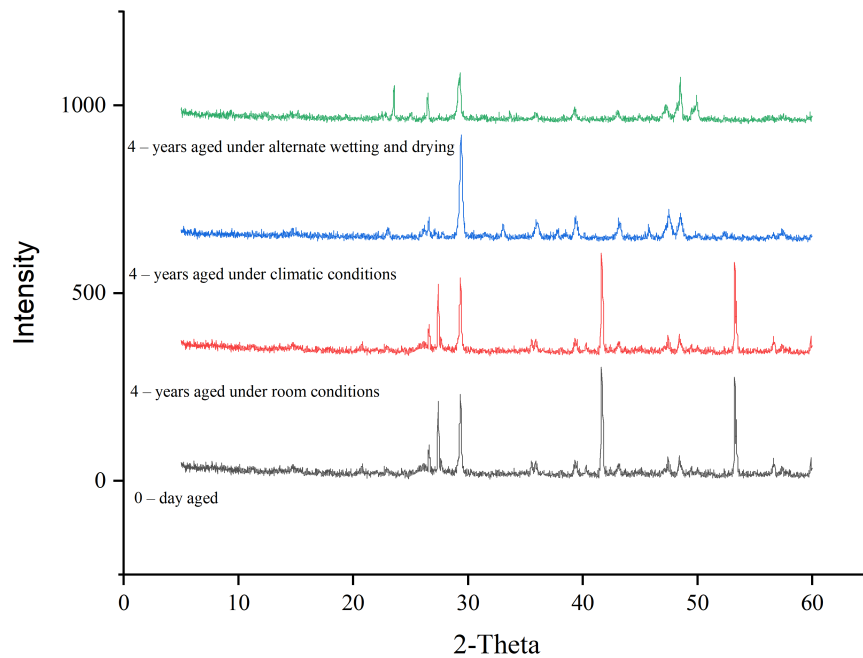


FIGURE 4.12: XRD analysis of Soaked Wheat Straw with and without ageing.

worst results of CWSRC, among all considered matrices, at 0-day and even at 4-years.

4.3.4.2 Thermogravimetric Analysis (TGA) of Straw

Thermogravimetric analysis (TGA) is done to evaluate the thermal stability of wheat straw. In this analysis, the degradability of fibres is evaluated by subjecting the sample to elevated temperature. With increase in temperature, the weight loss (%) of sample is noted till that certain temperature range, where the weight is declined sharply over a narrow range. Afterwards, the curve is converted into a straight constant line as soon as the specimen is exhausted. The decomposition of 0-day aged and 4-years aged (extracted from tested specimen) soaked wheat straw in terms of weight loss against the temperature is shown in Figure 4.13. All the four straw samples degraded in three steps in terms of temperature ranges and disintegration of its ingredients. The ranges and disintegrated ingredients are: i) $100\text{ }^{\circ}\text{C}$, ii) $200\text{ }^{\circ}\text{C} - 400\text{ }^{\circ}\text{C}$, and iii) $400\text{ }^{\circ}\text{C} - 550\text{ }^{\circ}\text{C}$ and lignin, cellulose, and hemicellulose, respectively. The moisture content present in fibres samples usually

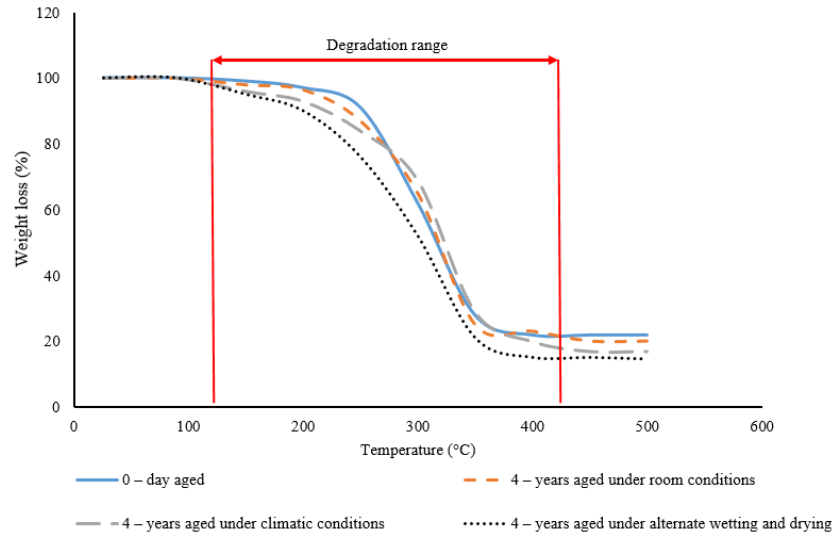


FIGURE 4.13: TGA analysis of Soaked Wheat Straw with and without ageing.

eliminates in the first temperature range i.e. $100\text{ }^{\circ}\text{C}$ [239]. Approximately 3.99-7.01% of weight is lost in terms of moisture elimination from straw. The second stage up to $200\text{ }^{\circ}\text{C}$ shows the decomposition of hemicelluloses followed by that of cellulose. And in third stage, major thermal decomposition is observed due to degradation of lignin and cellulose, as at $200\text{ }^{\circ}\text{C}$ to $500\text{ }^{\circ}\text{C}$, lignin peak is wider and appears superposed on the other peaks.

The climatic conditions of the considered region are far below in temperature variation as compared to the decomposition temperature of straw. Therefore, the incorporation of soaked straw with 1% content in cement concrete composites shows the comparable results to that of PC even after 4-years ageing under natural weathering conditions. However, the declined results in case of composites reinforced with boiled straw at 0-day and 4-years aged specimens could be due to the early decomposition of straw while boiling.

4.3.4.3 SEM Analysis of Straw and Straw-concrete Matrix at 4 Years

The variation in the soaked straw and its bond with cement concrete matrix due to 4-years ageing, under room, climatic and alternate wetting and drying conditions, at microscopic level via SEM is shown Figure 4.14. The SEM images of 0-day aged soaked straw and its bond with cement composite is also shown here for reference

(Figure 4.14 (a)). The decomposition at the straw surface can be seen easily with the surface degradation rate increasing from room to climatic conditions towards alternate wetting and drying which is depicting the most disintegrated condition of straw. This might be the reason behind more straw rupture rate in the specimens exposed under accelerated ageing conditions. It may be noted that the surface of straw, extracted from the specimens tested after exposure to natural weathering conditions, is comparatively less affected. And the straw extracted from controlled samples (i.e. under room conditions) is slightly degraded due to prolonged exposure to humid environment. This behavior depicts the degradation of soaked straw, as organic in nature, due to the variation in temperature and moisture conditions.

In straw – concrete bond, it is observed that in spite of fact that the straw is degraded, it has appropriate bonding with surrounding matrix, which ultimately resulted in comparable and durable residual mechanical properties. Also, the uniform straw distribution in cement concrete matrix depicts enhanced toughness capability of concrete reinforced with straw (Figure 4.14 (b) and 4.14 (c)). Improvement in mechanical properties due to the proper bonding is also observed by Khan and Ali [209]. Enhanced toughness may also be result of dense interfacial transition zone (ITZ) between wheat straw and cement composite which is found in all SWSRC-1% specimens both at 0-day age and even after 4-years of ageing under different conditions. However, in case of exposure to alternate wetting and drying, although the straw is affected badly and cracks are occurred at straw surface, even then the dense ITZ can be seen in Figure 4.14(d). Whereas, in some cases, the equivalent developmental straw length at both surfaces of the concrete composite may be the cause of straw fracture which ultimately resulted in comparatively declined residual properties. Some minor cracks can also be seen in the straw in matrix that has undergone natural weathering for 4 years (Figure 4.14 (c)), still this condition is much better than that under alternate wetting and drying. The slippage of fibre contributes towards higher toughness and energy absorption. Furthermore, the transference of load application is based on fiber-cement matrix [264]. Therefore, the dominancy of straw-slippage against straw

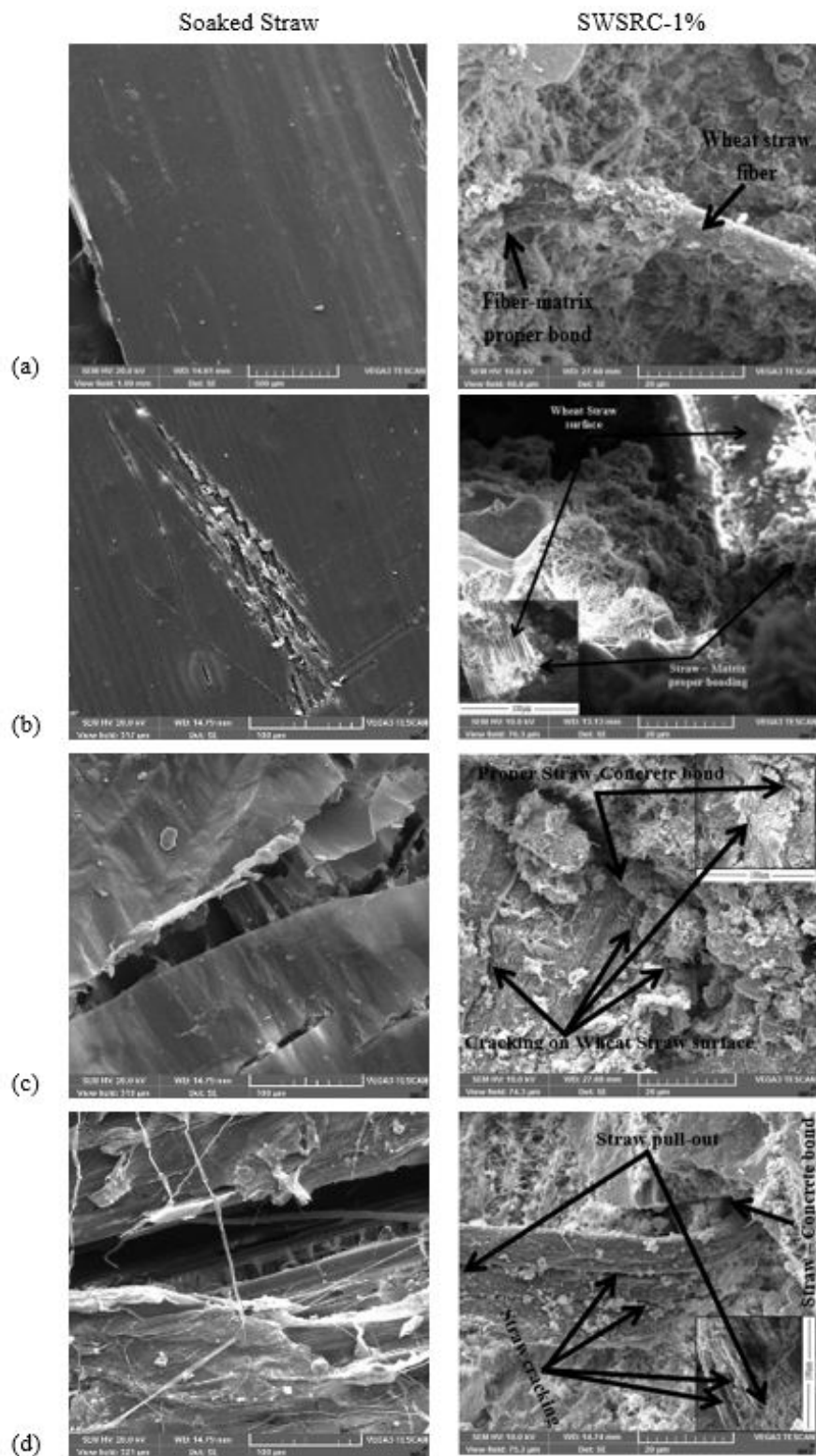


FIGURE 4.14: Micro-structural analysis of Soaked Straw and SWSRC-1% at (a) 0-day age (taken from Farooqi and Ali [267]), (b) 4-years aged under room conditions, (c) 4-years aged under climatic conditions and (d). 4-years aged under alternate wetting and drying.

fracture in case of optimized matrix i.e. SWSRC-1% seems highly favourable to be used in structural applications like concrete pavements. As the high crack propagation rate is one of the major concerns in pavements due to moving loads.

4.4 Empirical Modelling

4.4.1 Background of WSRC Properties at 4 Years

The mechanical static properties (i.e. compressive, splitting-tensile and flexural properties) of controlled conventional concrete (PC) and concrete reinforced with straw (soaked, boiled, and chemically treated) having contents of 1%, 2%, and 3%, by mass of wet concrete (SWSRC 1-3%, BWSRC 1-3%, and CWSRC 1-3%) are determined experimentally at 0-day age (i.e. after 28 days of curing) and at 4-years age after exposure to idealized room conditions, climatic conditions, and alternate wetting and drying conditions. It is intended for potential use of agricultural waste, i.e. wheat straw as an alternative material for structural applications. Based on the current study, the optimization of straw content and the treatment technique for its long-term durability is applied at all the three stages, i.e. room, climatic, and alternate wetting and drying conditions, and is given in Table 4.6. The residual properties i.e. σ_r , CTI_r , SS_r , STI_r , MoR_r , and FTI_r at all the three ageing conditions are considered for optimization. The σ_r , SS_r , and MoR_r of recommended SWSRC-1% are significantly increased at all the three ageing conditions in comparison to that of all other considered WSRC matrices. But, with respect to reference values, i.e. PC, the σ_r , SS_r , and MoR_r of recommended WSRC matrix are slightly decreased by 14%, 4%, and 7%, respectively, at room conditions, 14%, 2%, and 2%, respectively, at climatic conditions and 13%, 3%, and 24%, respectively, at alternate wetting and drying.

However, as also reported by Karihaloo and Wang [272], the main contribution of dispersed natural fibres in cement composites is towards toughness improvement, not the strength. So, accordingly, the CTI_r , STI_r and FTI_r of recommended

SWSRC-1% is remarkably increased by 2%, 89%, and 116%, respectively, at room conditions, 5%, 27%, and 108%, respectively, at climatic conditions and 62%, 41%, and 99%, respectively, at alternate wetting and drying in comparison to that of referenced PC values. As far as CTI_r , STI_r and FTI_r of WSRC specimens are concerned, decrements are observed in recommended values as compared to the WSRC with high (i.e. $\geq 2\%$) straw contents. This might be due to excess of low-density straw in concrete which accommodate more strain/deformation/displacement, ultimately results in higher toughness but lower strengths. Hence, conclusively, SWSRC-1% performed much better in terms of strengths and toughness indices among all considered WSRC matrices and the referenced PC as well, however, slight decrement in strengths w.r.t PC can be countered with significantly enhanced toughness. Same matrix with soaked straw of 1% content is optimized in the reference study made at 0-day age [267]. So, this prevailing long-term better performance of SWSRC-1% is recommended for structural applications.

4.4.2 Empirical Relation Between Flexural Properties and Structural Long-term Performance

Figure 4.15 shows the relations between the Modulus of Rupture (MoR) and Flexural Toughness Index (FTI) of PC and optimized WSRC matrix (i.e. SWSRC-1%) with the time period in years and the empirical relations between them. The empirical relations are derived from the averaged experimental values of MoR and FTI for considered specimens determined at 0-day age and after 4 years of ageing under room conditions, climatic conditions and alternate wetting and drying conditions. For the numerical prediction of PC and SWSRC-1% performance in terms of time (i.e. years), the value of R^2 for devising equations is 1, in the way as also done by [273]. Furthermore, the climatic variations, in terms of temperature, humidity and precipitation, of Islamabad, Pakistan as observed during ageing period, i.e. January 2016 - December 2019 (Figure 4.2), are considered similar for the numerical prediction of WSRC structures up to 20 years. Accordingly, predicted MoR, by using equations $y = 7.69e - 0.1x$ and $y = 7.64e - 0.06x$ of PC

TABLE 4.6: Optimization of straw content and treatment for wheat straw reinforced concrete after 4-years age.

WSRC matrix	4-years Aged under Room Conditions				4-years Aged under Climatic Conditions				4-years Aged under AWD condition									
	σ (MPa)	CTI	SS	FTI	σ (MPa)	CTI	SS	FTI	σ (MPa)	CTI	SS	FTI	σ (MPa)	CTI	SS	FTI		
(1)	(2)	(3)	(4)	(5)	(6)	(7)	(8)	(9)	(10)	(11)	(12)	(13)	(14)	(15)	(16)	(17)	(18)	(19)
Ref.	19.9	1.32	1.79	1.00	8.14	1.00	17.5	1.49	1.34	1.00	6.16	1.00	13.8	1.38	1.22	1.00	5.15	1.00
val.	± 4	± 0.2	± 0.6	± 0.0	± 6	± 0.0	± 3	± 0.4	± 0.5	± 0.0	± 2	± 0.0	± 6	± 0.6	± 0.8	± 0.0	± 1	± 0.0
Max.	17.1	1.35	1.71	1.93	7.59	2.16	15.0	1.57	1.32	1.31	6.02	2.08	12.0	2.45	1.18	1.55	3.91	1.99
SWS.	± 6	± 0.1	± 1.3	± 0.4	± 9	± 1.0	± 9	± 0.5	± 1.2	± 0.7	± 3	± 0.9	± 7	± 1.1	± 2.2	± 0.6	± 2	± 1.3
Val.	(1%)	(1%)	(1%)	(2%)	(1%)	(1%)	(1%)	(1%)	(1%)	(2%)	(1%)	(1%)	(1%)	(2%)	(1%)	(2%)	(1%)	(1%)
Max.	16.1	2.0	1.44	1.85	6.31	1.74	13.1	1.49	1.20	1.48	5.73	1.73	8.0	1.51	1.07	1.42	3.66	2.34
BWS.	± 2	± 0.3	± 0.6	± 0.8	± 0.5	± 0.6	± 3	± 0.8	± 0.1	± 0.4	± 0.4	± 0.5	± 6	± 0.4	± 0.5	± 0.8	± 0.6	± 1.0
Val.	(1%)	(2%)	(1%)	(2%)	(1%)	(1%)	(1%)	(2%)	(1%)	(1%)	(1%)	(2%)	(1%)	(2%)	(1%)	(2%)	(1%)	(2%)
Max.	14.1	1.55	1.16	1.71	5.25	1.67	10.6	1.41	1.02	1.39	4.78	1.80	7.2	1.50	0.91	1.43	2.83	1.77
CWS.	± 4	± 0.4	± 0.8	± 1.0	± 0.4	± 0.3	± 5	± 0.8	± 0.6	± 0.5	± 0.7	± 0.6	± 7	± 1.1	± 0.9	± 0.6	± 0.3	± 0.2
Val.	(1%)	(2%)	(1%)	(1%)	(1%)	(1%)	(1%)	(2%)	(1%)	(1%)	(1%)	(1%)	(1%)	(1%)	(1%)	(2%)	(1%)	(1%)
Reco.	17.1	1.35	1.71	1.89	7.59	2.16	15.0	1.57	1.32	1.27	6.02	2.08	12.0	2.24	1.18	1.41	3.91	1.99
SS%	± 6	± 0.1	± 1.3	± 0.3	± 9	± 1.0	± 9	± 0.5	± 1.2	± 0.3	± 3	± 0.9	± 7	± 0.8	± 2.2	± 0.9	± 2	± 1.3

1. Residual strengths and toughness indices are taken into account for optimization

2. Values in () shows percentage (%) content of straw

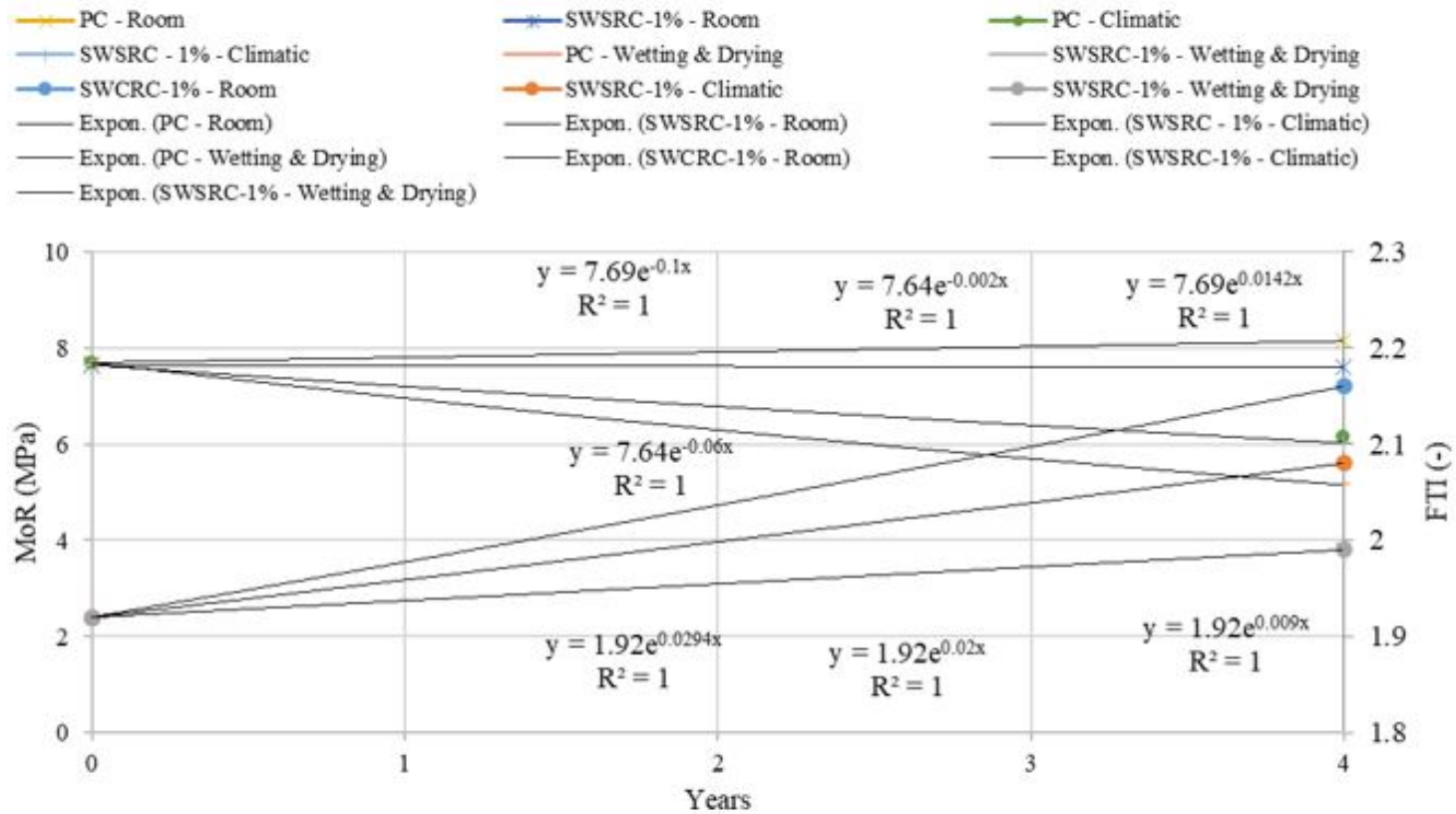
and SWSRC-1%, respectively, at 5, 10, 15, and 20 years is 5.8 MPa, 4.4 MPa, 3.4 MPa, and 2.6 MPa, respectively and 5.7 MPa, 4.2 MPa, 3.1 MPa, and 2.3 MPa, respectively under real climatic conditions. Similarly, the predicted *FTI* of SWSRC-1% at 5, 10, 15, and 20 years is 2.12, 2.35, 2.59 and 2.86, respectively under real climatic conditions. However, *FTI* of PC will remain 1 as PC specimens collapsed suddenly after bearing the maximum loading. Likewise, *MoR* and *FTI* for PC and SWSRC-1% under other considered conditions at 5, 10, 15, and 20 years can also be anticipated by using respective empirical equations. The predicted properties of SWSRC-1% under real climatic conditions are comparable in terms of *MoR* and appreciable in terms of toughness.

4.4.3 Design Life Anticipation of WSRC Structure

As for as the structural performance is concerned, the strength is not the only parameter to depict performance of a structure. The toughness (in addition to strength) also contributes towards structural performance [249, 256, 257]. Furthermore, the primary function of incorporating dispersed fibres in cement concrete is to have improved toughness, not the strength [272].

The micro cracks, which usually occur before even maximum loading, are arrested by dispersed fibres through sewing or bridging mechanism which ultimately will enhance the energy absorption capacity and load carrying capability of the respective structure. The rigid pavements are more likely to have development of early-age cracks and their excessive propagation due to the moving vehicular loading.

In addition to that, pavements are directly and continuously exposed to natural weathering/climatic conditions throughout the design life. Therefore, keeping in mind the pavement applications, current study is conducted. Finding of this long-term durability study on wheat straw reinforced concrete seems more favorable for such type of structural applications.



Note: The values at 0-year is taken from reference study i.e. Farooqi and Ali, 2019

FIGURE 4.15: Empirical relationship between flexural properties (i.e. *MoR* and *FTI*) of PC and SWSRC-1% with time.

TABLE 4.7: Performance index of PC and WSRC at 5, 10, 15 and 20 years.

	Room Conditions	Climatic Conditions	Accelerated Conditions
(1)	(2)	(3)	(4)
PI_{PC}	1.00 _(4-years)	1.00 _(4-years)	1.00 _(4-years)
	1.01 _(5-years)	0.97 _(5-years)	0.95 _(5-years)
	1.04 _(10-years)	0.86 _(10-years)	0.77 _(10-years)
	1.09 _(15-years)	0.77 _(15-years)	0.67 _(15-years)
	1.13 _(20-years)	0.71 _(20-years)	0.60 _(20-years)
PI_{WSRC}	1.00 _(4-years)	1.00 _(4-years)	1.00 _(4-years)
	1.01 _(5-years)	0.98 _(5-years)	0.93 _(5-years)
	1.09 _(10-years)	0.91 _(10-years)	0.71 _(10-years)
	1.18 _(15-years)	0.88 _(15-years)	0.63 _(15-years)
	1.28 _(20-years)	0.87 _(20-years)	0.61 _(20-years)

Hence, to consider the effect of toughness along with the strength of a fibre reinforced concrete structure for anticipating its long-term durable performance, a performance index is devised in current study. This performance index is devised in light of the prevailing flexural behavior of optimized WSRC from 0 age up to the 4 years. The reason for using flexural behavior is to start with the structures like concrete pavements, in which flexural properties are governing parameter. The devised performance index is as follows:

$$PI = \frac{PI_{MoR} + PI_{FTI}}{2} \quad (4.1)$$

Where

$$PI_{MoR} = \frac{MOR_{5, 10, 15, 20years}}{MOR_{4 \text{ years}}}$$

$$PI_{FTI} = \frac{FTI_{5, 10, 15, 20years}}{FTI_{4 \text{ years}}}$$

The net performance index is taken as the average of performance index against the strength, i.e. Modulus of Rupture (MoR), and performance index against toughness, i.e. flexural toughness index (FTI). Accordingly, the net performance

index for PC and optimized WSRC is calculated by using the devised equation for 5, 10, 15, and 20 years under room, climatic and accelerated (i.e. alternate wetting and drying) conditions (Table 4.7). The performance index for both PC and WSRC at 4 years is a unit value. All the other PI are evaluated with respect to unit value as the performance of structure will improve in case PI value is greater than 1. The declination of PI from one represents the deterioration of structure. So, conclusively, it can be said that the values nearest to 1 or ≥ 1 represents the comparable performance of structure. As far as the PI of PC and WSRC up to 20 years under exposure to room conditions are concerned, the performance of both structures is increasing with passage of time. This behavior is expected for conventional concrete as to attain ultimate properties with time. Whereas, the noticeable thing here is that, from 10 years onwards, the PI of WSRC is more than that of PC due to the contribution of toughness. Similarly, under natural weathering i.e. climatic conditions (which are most likely to occur in routine), the performance of WSRC structure would be more than that of PC up to 20 years as PI is more than that of PC. But, under accelerated/severe conditions, WSRC structure would likely to have low, yet comparable, performance as compared to that of PC due to degradation of straw in result of induced extravagant humid and temperature variations. However, at 20 years of accelerated conditions, the PI of WSRC becomes more than that of PC, which depicts that the performance of WSRC structure will become stable as soon as straw is exhausted completely against the accelerated conditions. In light of above discussion, it can be summarized that, for the pavements which usually have a design life of 20 years and are exposed to natural weathering/climatic conditions, the performance of WSRC seems highly favorable.

4.5 Summary

The durability of concrete reinforced with agricultural waste, i.e. wheat straw is evaluated after exposure to room, climatic, and alternate wetting and drying conditions for 4 years. The residual static properties of Plain Concrete (PC)

and Wheat Straw (soaked, boiled and chemically treated) Reinforced Concrete (WSRC) with 1%, 2%, and 3% contents are determined experimentally. In-depth mechanism of straw and straw-concrete bond is studied along with the prediction of WSRC structure performance. The conclusions are as follow:

- Soaked Wheat Straw Reinforced Concrete with 1% content (SWSRC-1%) is optimized among all the WSRC matrices in terms of residual strengths, residual energies absorbed and residual toughness indices.
- At room conditions, the residual strengths of SWSRC-1% under compressive, splitting-tensile and flexural loadings are decreased slightly by 14%, 4% and 7%, respectively. Whereas, its residual energy absorption and toughness index is significantly enhanced by 133% and 116%, respectively in case of flexural loading.
- The residual compressive, splitting-tensile and flexural toughness indices are increased by 5%, 27% and 108%, respectively under the exposure of climatic conditions. Unlikely, the residual strengths are slightly declined. Similarly, a sharp fall in residual properties of both PC and SWSRC-1% is observed due to degradation of straw under accelerated (i.e. alternate wetting and drying) circumstances.
- When the residual properties of PC and SWSRC-1% are compared with the 0-day aged respective specimens as reported in reference study, the effect of straw degradation under different conditions is observed. However, the declination rate of 4years aged PC and SWSRC-1% specimens in comparison to respective 0-day aged specimens is more or less same (i.e. ranges from 2 – 49%).
- The comparable residual properties of SWSRC-1%, at all the three ageing conditions, are due to dense interfacial transition zone of straw concrete matrix as revealed by SEM analysis. The climatic conditions slightly effect the chemical composition of soaked straw as observed from TGA and XRD patterns. Whereas, induced excessive humid and temperature variations in case

of accelerated ageing have adverse effects on straw surface and composition which ultimately resulted in straw fracture instead of pulling out.

- The net performance index for SWSRC-1% came out to more than that of PC at room and climatic conditions. Hence, structural performance of SWSRC-1% up to 20 years is comparable with that of PC.

In order to achieve structural performance, the toughness also contributes towards structural strength [249, 256, 257]. As, dispersed fibres are incorporated with the intention to enhance toughness, not the strength [272]. So, the minute decrement in the residual strength would be effectively compensated with remarkably improved toughness. In addition to that, the bridging mechanism, due to presence of dispersed straw, would also resist the cracks progression, ultimately enhancing the load carrying capability of the pavements. Therefore, based on conducted study, wheat straw reinforced concrete (WSRC) with 1% soaked straw content can be used as a construction material for structural applications (i.e. rigid pavements) with design life up to 20 years. However, the structural capacity of WSRC, in terms of flexural strength, i.e. governing parameter for rigid pavement design, is recommended to be investigated in detail.

Chapter 5

Structural Capacity of Wheat Straw Reinforced Concrete for Pavements

Related Articles:

M. U. Farooqi and M. Ali, “Contribution of plant fibers in improving the behavior and capacity of reinforced concrete for structural applications,” *Construction and Building Materials*, vol. 182, pp. 94-107, 2018. (ISI I.F. 4.064, HEC W-Platinum Category)

M. U. Farooqi and M. Ali, “Flexural behavior of wheat straw reinforced concrete for pavement applications,” *In Proceedings of 36th Cement And Concrete Science Conference*, Cardiff, UK, 2016.

5.1 Background

Based on the studies conducted for optimization of wheat straw reinforced concrete (WSRC) and its long-term durable performance, the probable use of WSRC for rigid pavement applications is recommended in summary of Chapter 4. This is perceived that the enhancement in energy absorption capability of wheat straw

reinforced cement composites, in comparison with controlled composites, is might be due to the rough surface of straw after simple pre-treatment, which forms relatively better bonding between straw and cement matrix as in an interlocking phenomenon. This better bonding between straw and matrix provides the sewing effect which enhances the energy absorption of composite by resisting the crack formation and propagation. Furthermore, due to organic nature of straw, durability is also a considerable factor. So, the performance of straw reinforced optimized matrix is also evaluated for the residual properties against 4-years ageing under room, climatic and accelerated ageing conditions. The residual behavior of WSRC is also favorable in terms of enhanced toughness even after 4-years. The anticipated performance of WSRC structure up to 20 years is also considerable especially under climatic conditions.

Therefore, on the basis of indication of improved properties reported in Chapter 3 and 4, there is a need to study plant fibre (i.e. wheat straw) reinforced concrete in detail for its various properties along with its behavior especially for civil engineering structural applications. However, to the best of author's knowledge, no study has been conducted on in-depth behavior and capacities of wheat straw reinforced concrete with steel rebars. Hence, in this chapter, the contribution of plant fibre (i.e. wheat straw) is studied for enhancing the capacities and improving the behavior of concrete reinforced with flexural and shear steel rebars for its use in civil engineering structural applications especially in concrete pavements. Beam-lets of Plain Concrete (PC) and optimized Wheat Straw Reinforced Concrete (WSRC) with the flexural and shear reinforcement are studied under flexural loading. The flexural strength and behavior (i.e. primary parameter for design of concrete pavements) are investigated for the possible application of WSRC in rigid pavements. The monotonic testing is performed only in this Chapter 5 in accordance with the scope of this PhD research. In addition to this, the moment capacity design equation and concrete pavement thickness design equation are also devised. Theoretical and experimental results are compared and discussed. Accordingly, the rest of the chapter is presented in a manner like: Section 5.2 portrays the materials used and casting, specimen details and testing methodology whereas, all the

results and analyses are presented in Section 5.3. Section 5.4 shows the discussion regarding development of empirical relations for moment capacity design equation and concrete pavement thickness design equation. All the findings of this study are summarized in Section 5.5.

5.2 Materials and Experimental Procedures

5.2.1 Raw Ingredients

The ingredients that are used for preparing PC, and WSRC are the Ordinary Portland Cement from the brand which is available locally, lawrence-pur sand, Margalah crush/aggregates, tap/potable water and the wheat straw that are available commercially. The size of aggregates used is restricted up to 20 mm. Wheat straw, extracted from agricultural residues, are obtained from a near-by source. A random selection is made to get the commercially available wheat straw. The average dimensions of wheat straw are approximately $25mm \times 5mm \times 1.2mm$. The average is being obtained from randomly selected wheat straw. The physical properties of wheat straw were determined experimentally by [18, 183, 225, 266, 274]. The density of straw ranged from 55 to 119 kg/m^3 . Whereas, the water absorption capacity of wheat straw was up to three times of its own weight at 20. The tensile and shear strength of wheat straw ranged from 21.2 to 40.0 MPa and 4.91 to 7.26 MPa, respectively. The chemical analysis of wheat straw was done by [226] as reported by [227]. The primary chemical composition of wheat straw after chemical analysis showed that it was rich in carbohydrates (i.e. hemicellulose, cellulose, and lignin). Minerals (i.e. calcium and phosphorus), proteins, silica, acid detergent fibres and ash were also present in straw along with 84 – 91 % dry matter. The presence of wax, dry, and dust particles on the surface of straw can result in poor bond between straw and concrete matrix. Hence, for removal of wax, dry, and dust particles from the surface of straw, some preparation/treatment is required. Therefore, for this purpose, a simple pre-treatment technique is adopted in order to ensure the straw as a low-cost construction material. In this pre-treatment



FIGURE 5.1: Prepared wheat straw.

technique, the wheat straw are remained soaked in water for 15 minutes. After that, straw are air surface dried. This process is adopted for having a better bond between straw and cement concrete composite. These prepared straw are used as dispersed reinforcement for making WSRC and are shown in Figure 5.1. The longitudinal and transverse reinforcement in PC and WSRC beam-lets are the $\varnothing 6$ steel rebars of Grade – 280 (i.e. $f_y=280$ MPa). The diameter of steel rebars is same (i.e. $\varnothing 6$) for both longitudinal and transverse reinforcement.

5.2.2 Mix Design and Procedure for Casting

The cement, sand, and aggregate proportions for preparing the plain concrete are 1, 2, and 4, respectively, i.e. 331 kg cement, 704 kg sand, 1550 kg aggregates are taken for preparing 1 m³ of plain concrete. The water-cement ratio used in preparation of PC is 0.55, i.e. 182 kg/ (m³ of PC). All the materials (i.e. cement, sand and aggregates) are put simultaneously in the drum mixer for preparing the PC mix. Water is added at the end. The mixer is rotated for five minutes to have a homogenous PC mix. However, for the preparation of wheat straw reinforced concrete, straw are put in the mixer having fresh plain concrete. The percentage content and approximate length of straw are 1%, by mass of plain concrete, and 25 mm, respectively. The water-cement ratio for WSRC is 0.60. In this way, 254 kg, 542 kg, 1194 kg, 152 kg and 27 kg of cement, sand, aggregate, water and straw, respectively, are used to prepare 1 m³ of WSRC. The mixer is then rotated for

two minutes to get WSRC mix. The WSRC mix did not seem to be workable and homogenous at that stage. The mixer is again rotated for two minutes for having the homogenous and better WSRC mix. Because at this stage, bleeding from WSRC mix can be occurred in result of adding more water. Therefore, the mixing time is increased which resulted in a successful approach for having a homogenous and workable WSRC mix. The slump test for PC, and WSRC is performed. The value of slump for PC and WSRC is 40 mm and 20 mm, respectively. It may be noted that a decrease in slump of WSRC as compared to that of PC is observed in spite of the fact that that the water-cement ratio in case of WSRC is more than that for PC. This is might be due to the fact that a considerable amount of water is absorbed by the air-surface dried straw in WSRC mix.

The prepared PC and WSRC is then poured in the beam-let moulds having steel bars tied with stirrups in three successive layers for the preparation of PC and WSRC specimens followed by 25 blows of tamping rod after each layer. Whereas, in case of WSRC, the lifting (i.e. 100 – 150 mm) and free falling of the beam-let moulds after each layer is done for self-compaction by removing air voids. The de-moulding of specimens is done after 24 hours and are kept in water tank for the curing of 28 days before testing. The designated 28 days compressive strength of 1 : 2 : 4 PC mix is 20 MPa. However, for this scenario, 100 mm diameter and 200 mm high cylinder specimens of PC and WSRC are cast and tested under compressive loading. The calculated compressive strengths of PC and WSRC range from 22.3 to 22.8 MPa and 21.5 to 22.0 MPa, respectively. And, for calculating Modulus of Rupture (MoR), $102 \times 102 \times 457$ mm beam-let specimens are cast and tested under flexural loading. The calculated MoR of PC and WSRC range from 9.0 to 9.2 MPa, and 9.8 to 10.2 MPa, respectively.

5.2.3 Specimens

Beam-lets of 102 mm width, 102 mm depth and 457 mm length are cast for PC and WSRC with flexural and shear steel rebars to perform the flexural strength test. A total of ten beam-lets (i.e. five for PC and five for WSRC) are cast. The reason for

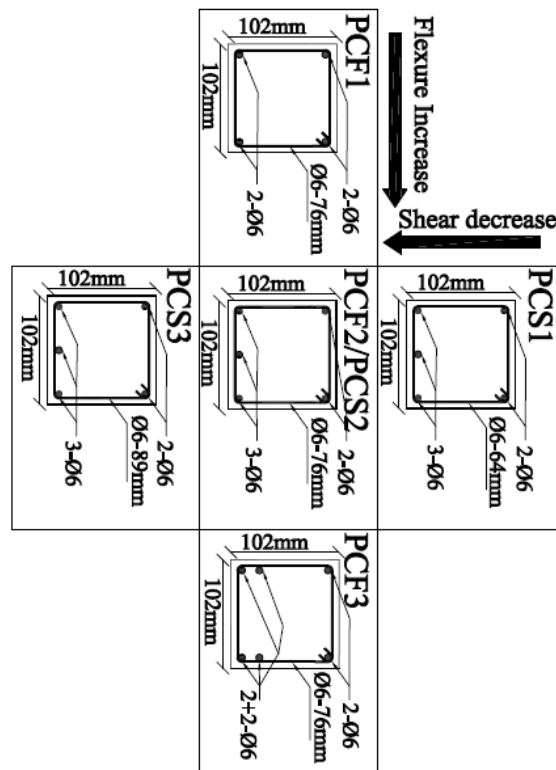
TABLE 5.1: Labelling scheme of PC and WSRC beam-lets with steel rebars.

Sr No.	Flexural	Shear	Steel ratio	Labels	
				PC	WSRC
(1)	(2)	(3)	(4)	(5)	(6)
1	2-Ø6	Ø6 – 76 mm	0.016	PCF1	WSF1
2	3-Ø6	Ø6 – 76 mm	0.020	PCF2/PCS2	WSF2/WSS2
3	2+2-Ø6	Ø6 – 76 mm	0.025	PCF3	WSF3
4	3-Ø6	Ø6 – 64 mm	0.020	PCS1	WSS1
5	3-Ø6	Ø6 – 89 mm	0.020	PCS3	WSS3

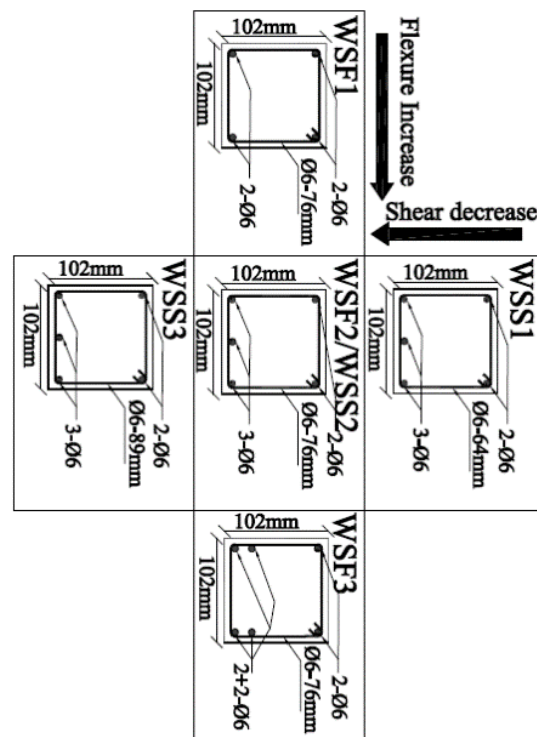
casting beam-lets is to get an indication of flexural strength of WSRC with steel rebars keeping in mind the primary parameter (i.e. flexural strength) in design of rigid pavements for resisting vehicular loading. These beam-lets are considered as prototypes. One specimen for each combination of PC and WSRC is cast. Other researchers also considered one prototype for one combination [275–277]. It may also be noted that averaged material properties are being taken.

For varying flexural reinforcement, the number of Ø6 bars are varied by 2, 3, and 4 bottom bars by having steel ratios of 0.016, 0.020, and 0.025, respectively. Keeping in mind the placement of rebars in the beam-let moulds, having width of 102 mm only, the smaller diameter rebars (i.e. Ø6 steel rebars) are used in all the specimens. However, the stirrups spacing is kept constant, i.e. 76 mm. Whereas, in case of varied shear reinforcement, the stirrups spacings are varied by 64, 76, and 89 mm, but the number of longitudinal bars is kept constant, i.e. 3 bottom bars.

It may be noted that the relative comparison between reinforced concrete (RC) and WSRC with steel rebars is made. So, longitudinal and transverse rebars diameter in a particular combination of RC and WSRC with steel rebars kept same. Labelling scheme for PC and WSRC specimens with flexural and shear steel rebars is given in Table 5.1. However, the flexural and shear reinforcement detailing for PC and WSRC is shown in Figure 5.2.



(a)



(b)

FIGURE 5.2: Beam-lets cross-sections of PC and WSRC with flexural and shear reinforcement detailing (a) PC, and (b) WSRC.

5.2.4 Testing Methodology

5.2.4.1 Flexural Strength Test

For studying the flexural behavior of PC and WSRC with flexural and shear reinforcement and for the determination of flexural strength (FS), flexural energies absorbed (i.e. FE_1 , FEM , FEP , and FE), and flexural toughness index (FTI), beam-lets are tested in the flexural testing machine as per ASTM C78 / C78M – 18 (Standard Test Method for Flexural Strength of Concrete - Using Simple Beam with Third-Point Loading). The servo-hydraulic machine is used to apply the flexural load. A dial gauge is attached at the mid of beam-lets to record the mid-span deflection.

The testing setup, i.e. schematic diagram and experimental setup, is shown in Figure 5.3. The crack propagation in the beam-lets under the flexural loading and the load – deflection curves are recorded. Crack propagation is observed with visual inspection. The first crack is noted and/or observed with the naked eye and the corresponding load is recorded. The load at which first crack is occurred (L_1), the maximum load (L_m), the ultimate load (L_u), the maximum deflection (Δ), the no. of cracks at ultimate load, and failure mode are extracted from this information.

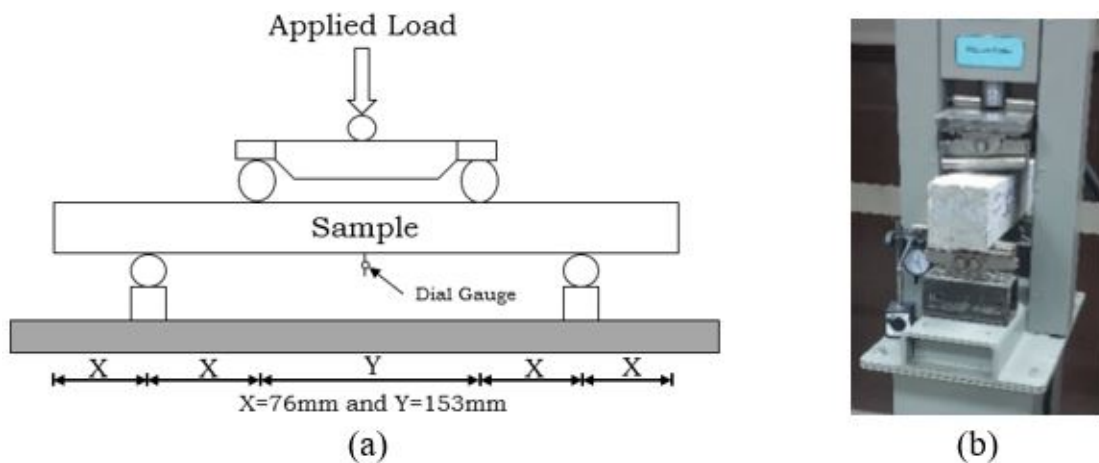


FIGURE 5.3: Testing setup (a) Schematic diagram, and (b) Experimental setup.

5.3 Test Results and Analyses

5.3.1 Properties under Flexural Loading

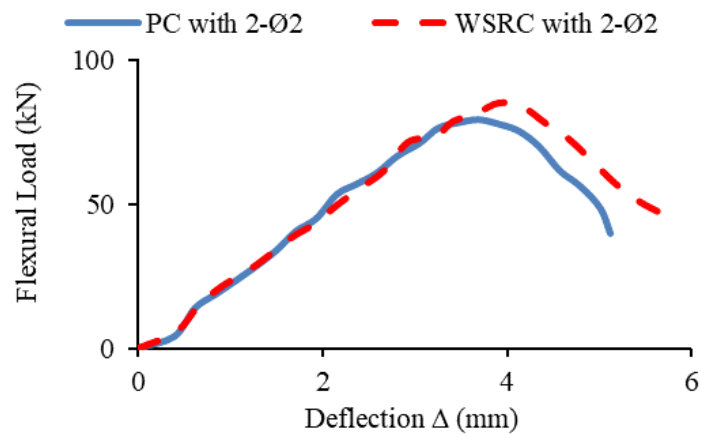
5.3.1.1 Specimens with Varying Flexural and Constant Shear Reinforcement (i.e. $\varnothing 6$ -76 mm)

Flexural Behavior of Specimens with Varying Flexural Steel Rebars:

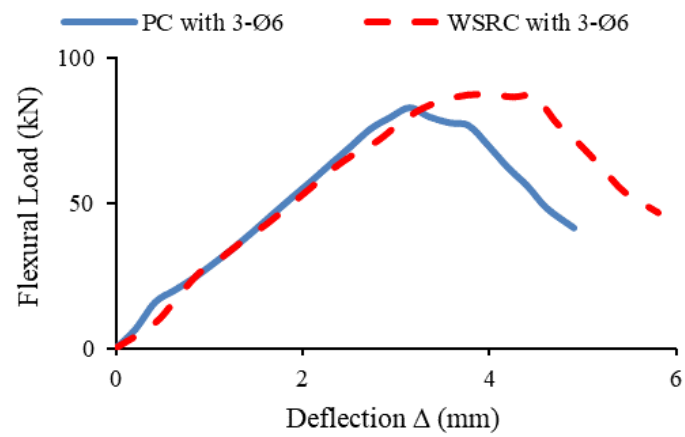
The load-deflection curves of PC and WSRC beam-lets with varying flexural reinforcement and constant shear reinforcement (i.e. $\varnothing 6 - 76mm$) are shown in Figure 5.4. For PC and WSRC with varying flexural reinforcement and constant shear reinforcement (i.e. $\varnothing 6 - 76mm$), the first crack, cracks at the maximum loading, cracks at the ultimate loading, and the tested beam-let specimens are shown in Figure 5.5. In case of both PC and WSRC, the flexural reinforcement is increased by $\varnothing 6$, $3 - \varnothing 6$, and $2 + 2 - \varnothing 6$. The linear behavior is observed in all the load-deflection curves until the appearance of first crack. However, post the first crack, an improved behavior of WSRC specimens can be observed as less steepness in the curve and more deflection before the ultimate load can be noted compared to that of PC, indicating towards the tough behavior of WSRC. As far as WSRC with flexural reinforcement is observed, the specimen with the steel rebars of $3 - \varnothing 6$ shows the more tough behavior compared to the other WSRC specimens. The behaviors of PC and WSRC specimens, with flexural steel reinforcement, under the flexural loading are also observed. Certain information i.e. first crack length and number of cracks at the maximum load and at the ultimate load are revealed. The first cracks in case of PCF1, WSF1, PCF2, WSF2, PCF3, and WSF3 are appeared at 84.1%, 83.7%, 91.2%, 89.2%, 92.9%, and 90.5%, respectively, of their respective peak loads. However, the severity of cracks, that is observed with naked eye, in case of WSRC specimens is less than in case of PC specimens. The observed length of the first crack in WSRC beam-lets is also less than that of the respective PC beam-lets. It is also noted that the first crack length is decreased with increase in flexural reinforcement. The length of the first

crack in PCF1, PCF2, and PCF3 beam-lets is approximately 89mm, 70mm, and 63mm, respectively, and it is approximately 63mm, 54mm, and 51mm in WSF1, WSF2, and WSF3 beam-lets, respectively. At the maximum loading, the cracks width and length, and the number of cracks, are more in PC specimens when compared to that in respective WSRC specimens. Again, at the ultimate load, the number of cracks, cracks width and length are slightly more than that of observed at the ultimate load. It is observed that although the no. of cracks in WSRC specimens are slightly more or equal in some cases in comparison with PC. But the crack width or severity in PC specimens is much more as compared to WSRC specimens, when noted with the naked eye. It has been found that WSRC beam-lets perform better than that of PC beam-lets. The utilization of wheat straw in concrete enhanced the post cracking performance of tested beams-lets.

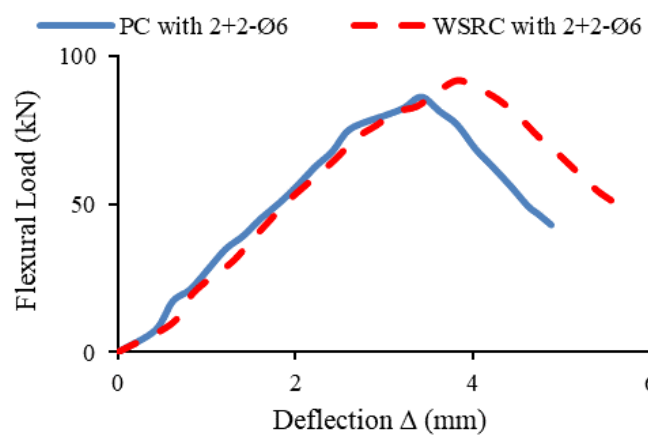
Effect of Flexural Steel Rebars on Load, Deflection and Cracks: The load details, maximum deflections, number of cracks occurred at ultimate failure, and failure modes for PC and WSRC with varying flexural reinforcement and constant shear reinforcement (i.e. $\varnothing 6 - 76 \text{ mm}$) are given in Table 5.2. The load at which the first crack occurred is taken from the load-deflection curves of respective tested beam-lets. The load at which first crack occurs for PCF1, WSF1, PCF2, WSF2, PCF3, and WSF3 are 66.7 kN, 71.4 kN, 75.4 kN, 77.6 kN, 80.3 kN, and 83.0 kN, respectively. The load at which first crack occurs of WSF1, WSF2, and WSF3 are increased by 4.7 kN, 2.2 kN, and 2.7 kN, respectively, when compared with that of PCF1, PCF2, and PCF3, respectively. Here, it can be noted that the crack resistance of WSRC is more than that of PC as the first cracks are occurred at comparatively high loads in case of WSRC beam-lets in comparison with PC beam-lets. This crack resistance is due to the incorporation of straw in the concrete composite. A linear increase is observed in load at which first crack occurs for both PC and WSRC beam-lets with increasing flexural rebars and constant shear rebars. Similarly, the maximum load is also taken from the load-deflection curve of the tested specimens. The maximum load for PCF1, WSF1, PCF2, WSF2, PCF3, and WSF3 are 79.3 kN, 85.3 kN, 82.7 kN, 87.0 kN, 86.4 kN, and 91.8 kN, respectively. The maximum load of WSF1, WSF2, and WSF3



(a)

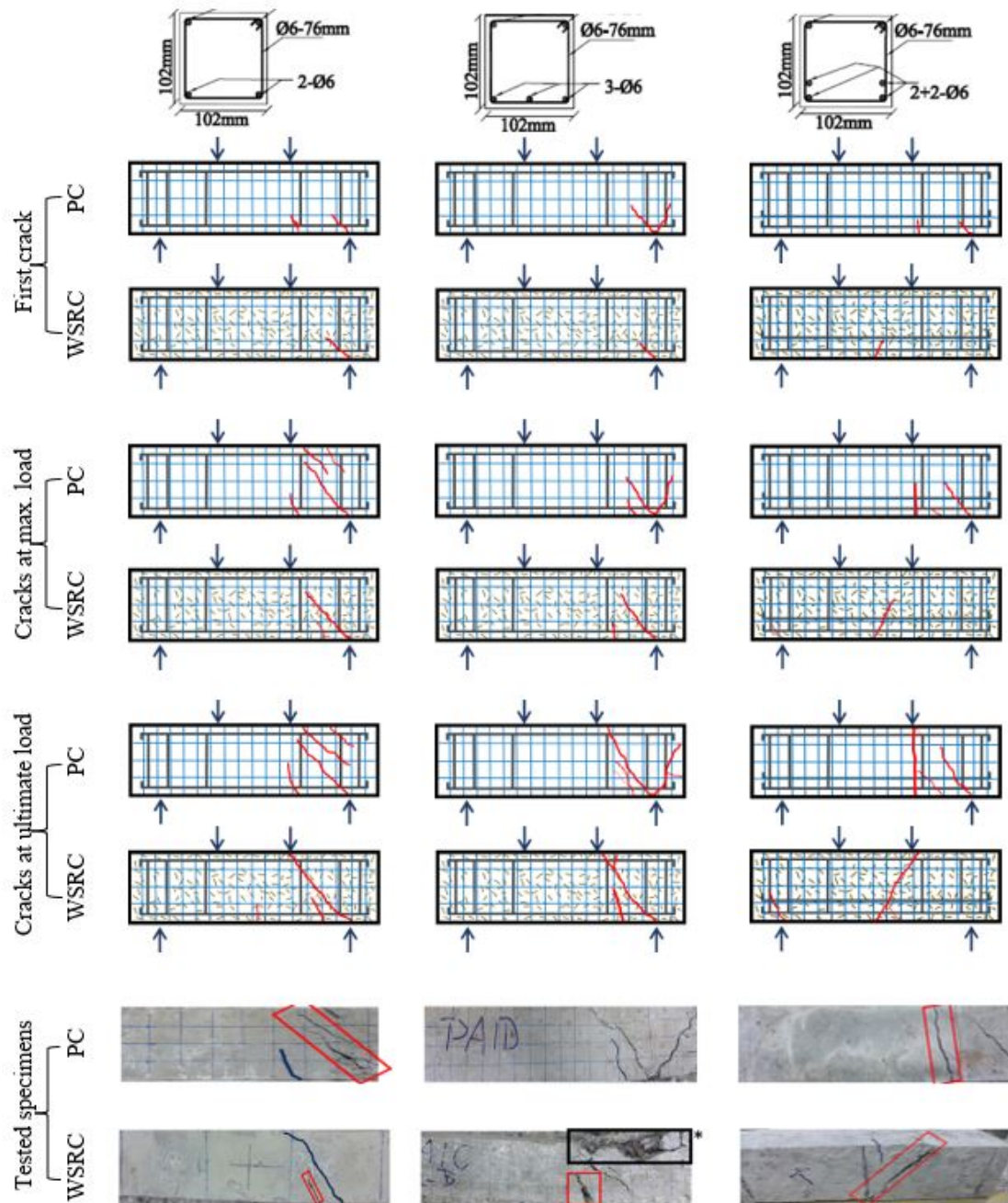


(b)



(c)

FIGURE 5.4: Load – deflection curves of PC and WSRC with flexural reinforcement (a) 2 – Ø6, (b) 3 – Ø6, and (c) 2 + 2 – Ø6 and constant shear reinforcement (i.e. Ø6 – 76mm).



*Tested WSRC specimen is broken intentionally to observe straw-concrete interaction.

FIGURE 5.5: Crack behavior of PC and WSRC specimens during flexural loading with varying flexural reinforcement and constant shear reinforcement (i.e. $\text{Ø}6 - 76\text{mm}$).

are increased by 7.5%, 5%, and 6%, respectively, when compared with that of PCF1, PCF2, and PCF3, respectively. The observed trend in case of maximum load is similar to that as observed in case of load at first crack. Similarly, the ultimate load of WSF1, WSF2, and WSF3 are increased by 13.8%, 12.6%, and

10%, respectively, when compared to the ultimate load of PCF1, PCF2, and PCF3, respectively. Overall, the addition of wheat straw in concrete increases the load carrying capacities of the WSRC beam-lets. The maximum deflection (Δ) of PC and WSRC beam-lets is recorded with the help of dial gauge. The values of maximum deflection are also given in Table 5.2. The maximum deflections which are occurred in case of WSRC specimens are more than that in case PC specimens. The Δ for PCF1, WSF1, PCF2, WSF2, PCF3, and WSF3 are 5.12mm, 5.76mm, 4.91mm, 5.81mm, 4.88mm, and 5.76mm. However, the decrement in the mid-span deflection is observed in the specimens with increased flexural reinforcement. This decrease in deflections at mid-spans might be due to the increase in stiffness of the respective beam-lets with increased flexural reinforcement. The stiffness of the beam-lets is proportional with the steel ratio [109]. The number of cracks at the ultimate failure in tested beam-lets is also noted and is also given in Table 5.2. The number of cracks in PCF1, WSF1, PCF2, WSF2, PCF3, and WSF3 beam-lets are 4, 3, 4, 3, 3, and 2, respectively. The crack lengths and crack widths in PC beam-lets are more than that in WSRC beam-lets. The reason behind the relatively less crack width and smaller crack length in WSRC beam-lets than that in PC beam-lets is the presence of wheat straw. Due to the presence of wheat straw, the bridging phenomenon and crack arresting is observed in WSRC specimens. The straw resists the development of first cracks firstly, then the crack propagation is also resisted due to the arresting of cracks with straw. The failure modes of the tested beam-lets are identified as shear, diagonal, balanced and flexural failures etc. based on the location/type of cracks. The observed failure modes on the respective specimens are given in Table 5.2. The observed failure mode for PCF1 and WSF1 is flexural, for PCF2 and WSF2 is balanced, and that for PCF3 and WSF3 is shear. Flexural failure mode indicates that the failure is caused by flexural cracks, shear failure mode indicates that the failure is caused by shear cracks (i.e. propagated at 45°), and balanced failure mode indicates that the number of flexural and shear cracks are almost the same at the time of ultimate failure.

A close-up view of fibre/straw and concrete interaction in the composite at the

TABLE 5.2: Loads and Deflections for tested PC and WSRC beam-lets with varying flexural reinforcement and constant shear reinforcement (i.e. $\varnothing 6 - 76 \text{ mm}$).

Loads and Deflections	Specimens					
	PC			WSRC		
	2- $\varnothing 6$	3- $\varnothing 6$	2+2- $\varnothing 6$	2- $\varnothing 6$	3- $\varnothing 6$	2+2- $\varnothing 6$
(1)	(2)	(3)	(4)	(5)	(6)	(7)
Load at First Crack (kN)	66.7	75.4	80.3	71.4	77.6	83.0
Maximum Load (kN)	79.3	82.7	86.4	85.3	87.0	91.8
Ultimate Load (kN)	39.8	41.3	43.1	45.3	46.5	47.4
Maximum Deflection (mm)	5.12	4.91	4.88	5.76	5.81	5.76
Cracks at Ultimate Load (-)	4	4	3	3	3	2
Failure Mode (-)	Flexure	Balanced	Shear	Flexure	Balanced	Shear

broken surface of WSRC beam-let with steel rebars is shown in Figure 5.6. The broken surface of the specimen is examined with the naked eye for observing the straw failure mechanism in the concrete composite. It is noted that, as an approximation, there is a ratio of 70 : 30 in the straw failure between fracture and pulling-out of straw. The fracture mechanism of straw is observed in the case where there is an almost equal development length of straw at both sides of fracture surfaces. It shows that the bond strength between straw and matrix is more than tensile strength of straw. However, the straw pull-out phenomenon occurs in case of less embedded length of straw at any one side of fractured surfaces. It shows that the bond strength at one side between straw and matrix is less than the tensile strength of wheat straw.

Effect of Flexural Rebars on Flexural Strength, Flexural Energies Absorbed, and Flexural Toughness Index: The flexural strength (FS), flexural energies absorption, and flexural toughness index (FTI) of beam-lets with varying flexural reinforcement and constant shear reinforcement (i.e. $\varnothing 6 - 76 \text{ mm}$) are given in Table 5.3. The flexural strength of PCF1, WSF1, PCF2, WSF2, PCF3, and WSF3 are calculated by using the maximum load from the load-deflection curves of the respective specimens. The flexural strength of PCF1, WSF1, PCF2, WSF2, PCF3, and WSF3 are 34.6 MPa, 37.2 MPa, 36.0 MPa, 38.2 MPa, 37.7



FIGURE 5.6: Straw – concrete interaction with naked eye.

MPa, and 40.1 MPa, respectively. An increase of 7.5%, 5.8%, and 6.2% in flexural strength of WSF1, WSF2, and WSF3, respectively, is observed when compared to that of PCF1, PCF2, and PCF3, respectively. The area under the load-deflection curve up to load, at which first crack occurred, is taken as energy absorption up to first crack (FE1). The FE1 of WSF1, WSF2, and WSF3 are increased by 5.9 kN.mm, 17.7 kN.mm, and 18.4 kN.mm, respectively, when compared with that of PCF1, PCF2, and PCF3, respectively. The increase in FE1 for PC and WSRC specimens is observed with increased flexural reinforcement. The area under load-deflection curve from first crack load to maximum load is taken as energy absorbed from first crack to maximum load (FEM). The FEM of WSF1, WSF2, and WSF3 are increased by 19%, 82%, and 34%, respectively, as compared to that of PCF1, PCF2, and PCF3, respectively. The convex decrease is observed here in FEM for both PC and WSRC beam-lets with increase in flexural reinforcement. Flexural energy absorbed from maximum load to ultimate load (FEP) is taken as the area under load-deflection curve from maximum load to ultimate load. The FEP of PCF1, WSF1, PCF2, WSF2, PCF3, and WSF3 are 93.9 kN.mm, 118.4 kN.mm, 115.1 kN.mm, 147.4 kN.mm, 95.0 kN.mm, and 137.5 kN.mm, respectively. Again, the FEP of WSRC specimens are more than that of PC specimens. The total area under load – deflection curve or the summation of FE1, FEM, and FEP is taken

as total flexural energy absorbed (FE). The similar increasing trend in energies absorbed by WSRC specimens as compared to energies absorbed by PC specimens is observed here. An overall increase of 17%, 30%, and 27% in the FE of WSF1, WSF2, and WSF3, respectively, is observed when compared to that of PCF1, PCF2, and PCF3, respectively. The ratio of total flexural energy absorbed to the flexural energy absorbed up to load at which occurrence of first crack takes place (i.e. FE/FE1) is taken as flexural toughness index. The flexural toughness index of PCF1, WSF1, PCF2, WSF2, PCF3, and WSF3 are 2.75, 3.02, 2.43, 2.70, 2.02, and 2.32, respectively. The flexural toughness index of WSF1, WSF2, and WSF3, are increased by 10%, 11%, and 10%, respectively, when compared with that of respective PC specimens. A slight increase in toughness index of the specimens with flexural reinforcement of 3 – $\varnothing 6$ is observed, when compared to other WSRC matrix.

It may be noted that over all the FS, FE1, and FE are increased with an increase in flexural reinforcement, but a decrement is observed in FEM, FEP and FTI. The reason for the decrease in FEM might be the reduction of gap between first crack load and maximum load due to which area under the curve from first crack load to maximum load reduces.

A comprehensive comparison of FS, FEP, FE, FTI, and deflection (Δ) of PC and WSRC with varying flexural reinforcement (i.e. 2- $\varnothing 6$, 3- $\varnothing 6$, and 2+2- $\varnothing 6$) and with constant shear reinforcement (i.e. $\varnothing 6 - 76 \text{ mm}$) is shown in Figure 5.7. Overall, all the WSRC specimens with flexural steel rebars are performed better than respective PC specimens. The improved properties of WSRC in terms of flexural strength, the post cracking behavior, and toughness are observed in comparison to PC; resulting in more displacement for WSRC specimens with flexural steel rebars. As far as WSRC specimens are concerned, only the FEP in case of specimen with 3 – $\varnothing 6$ flexural reinforcement and $\varnothing 6 - 76 \text{ mm}$ shear reinforcement is significantly higher than other considered WSRC specimens. Otherwise all the other properties are more or less same with slight variation, i.e. increase in properties with an increase in flexural reinforcement.

TABLE 5.3: Flexural strengths, Flexural energies absorbed (FE1, FEM, FEP, FE), and Flexural Toughness Index (FTI) for PC and WSRC beam-lets with varying flexural reinforcement and constant shear reinforcement (i.e. $\varnothing 6 - 76 \text{ mm}$).

Properties	Specimens					
	PC			WSRC		
	2- $\varnothing 6$	3- $\varnothing 6$	2+2- $\varnothing 6$	2- $\varnothing 6$	3- $\varnothing 6$	2+2- $\varnothing 6$
(1)	(2)	(3)	(4)	(5)	(6)	(7)
FS (MPa)	34.6	36.0	37.7	37.2	38.2	40.1
FE1 (kN.mm)	91.0	104.1	125.9	96.9	121.8	144.3
FEM (kN.mm)	65.6	33.3	33.2	77.9	60.0	40.4
FEP (kN.mm)	93.9	115.1	95.0	118.4	147.4	137.5
FE (kN.mm)	250.5	252.5	254.1	293.3	329.2	322.1
FTI (-)	2.75	2.43	2.02	3.02	2.70	2.23

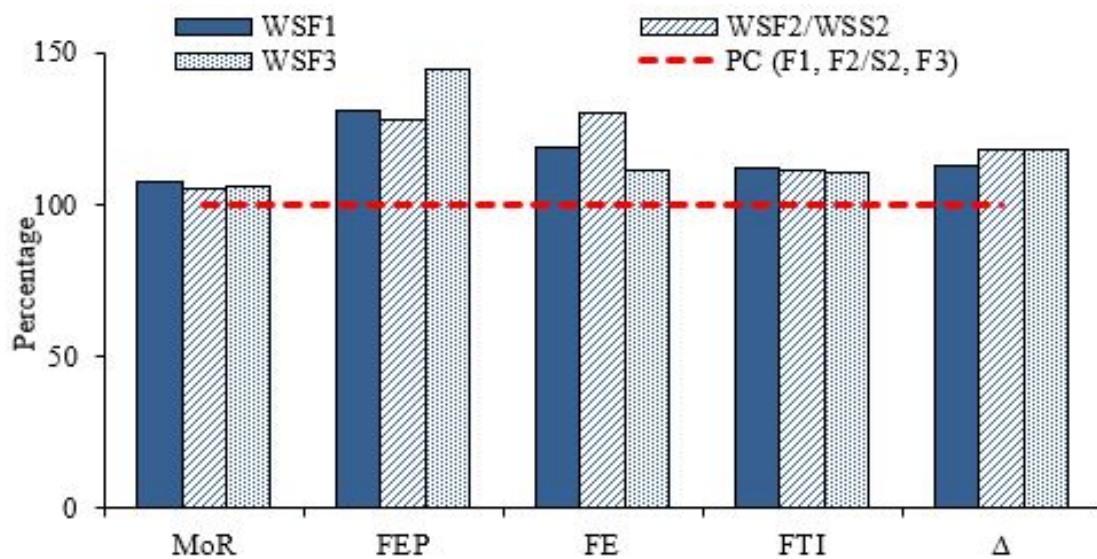


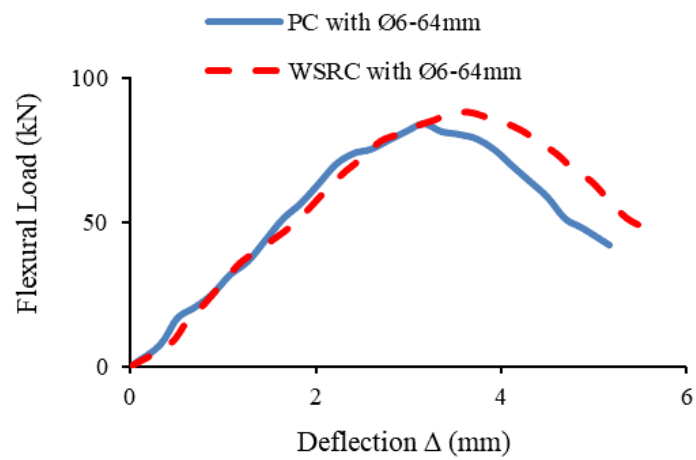
FIGURE 5.7: Comparison of FS, FEP, FE, FTI, and Δ of PC and WSRC with varying flexural reinforcement (i.e. 2- $\varnothing 6$, 3- $\varnothing 6$, and 2+2- $\varnothing 6$) with constant shear reinforcement (i.e. $\varnothing 6 - 76 \text{ mm}$).

5.3.1.2 Specimens with Varying Shear and Constant Flexural Rebars (i.e. 3 – $\emptyset 6$)

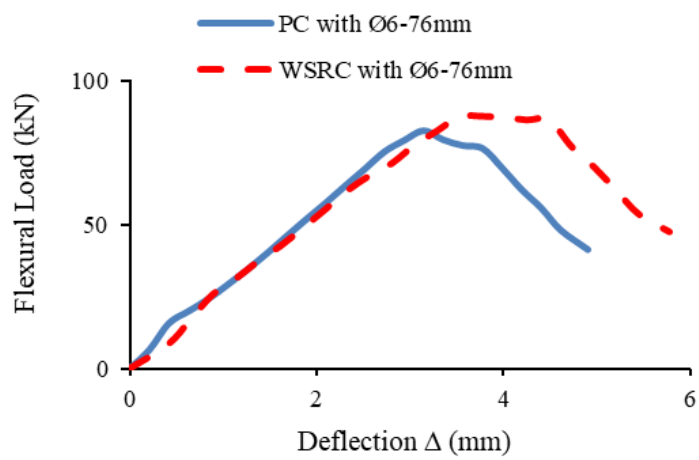
Flexural Behavior of Specimens with Varying Shear Steel Rebars: The load – deflection curves of PC and WSRC with shear reinforcement (i.e. $\emptyset 6 – 64\text{ mm}$, $\emptyset 6 – 76\text{ mm}$, and $\emptyset 6 – 89\text{ mm}$) and with constant flexural reinforcement (i.e. 3 – $\emptyset 6$) are shown in Figure 5.8. For PC and WSRC with constant flexural reinforcement (i.e. 3 – $\emptyset 6$) and varying shear reinforcement, the first crack, cracks at the maximum loading, cracks at the ultimate loading, and the tested beam-let specimens are shown in Figure 5.9. In case of both PC and WSRC, the shear reinforcement is decreased by $\emptyset 6 – 64\text{ mm}$, $\emptyset 6 – 76\text{ mm}$, and $\emptyset 6 – 89\text{ mm}$. Here again, the flexible behavior and toughness of WSRC specimens with shear steel rebars can be observed from load-deflection curves in comparison to respective PC specimens. The more displacement in case of WSRC specimens with shear reinforcement is observed. This is due to the presence of wheat straw. The resistance to cracking and the crack arresting behavior is occurred due to which the WSRC specimens show more displacement and bear load for more time as compared to that in case of respective PC specimens. In case of WSRC specimens, the beam-let with shear reinforcement of $\emptyset 6 – 76\text{ mm}$ shows the relatively better behavior in comparison to other considered WSRC specimens. As in that case, an improved behavior after the maximum load is noted. The cracking mechanism in the PC and WSRC specimens with shear reinforcement (i.e. shear steel rebars) is also observed while testing. The formation of cracks at the different levels (i.e. first crack, at maximum loading, and at the ultimate loading) is revealed. The first cracks in case of PCS1, WSS1, PCS2, WSS2, PCS3, and WSS3 are appeared at 89.5%, 91.3%, 91.2%, 88.6%, 93.8%, and 91.3%, respectively, of their respective maximum loads. The width and severity of first cracks is relatively much lesser than that cracks which are occurred at maximum and ultimate loading in case of PC. The crack resistance in WSRC specimens with more shear reinforcement (i.e. $\emptyset 6 – 64\text{ mm}$) is more than that of all other considered specimens. The lengths of the first crack in WSRC beam-lets, that are observed with naked eye, are also less than that of the respective PC beam-lets. It can be noted with the naked

eye that the cracks length and width, and the number of cracks, are more in PC beam-lets when compared to that in respective WSRC specimens. It is found that the crack resistance in WSRC beam-lets with shear reinforcement is much better than that in PC beam-lets. However, among all WSRC specimens with shear reinforcement, the one with the minimum shear reinforcement of $\varnothing 6 - 64 \text{ mm}$ and flexural reinforcement of $3 - \varnothing 6$ shows better crack arresting as compared to other considered WSRC specimens. An enhancement in the post-cracking behavior, due to the incorporation of wheat straw, is observed.

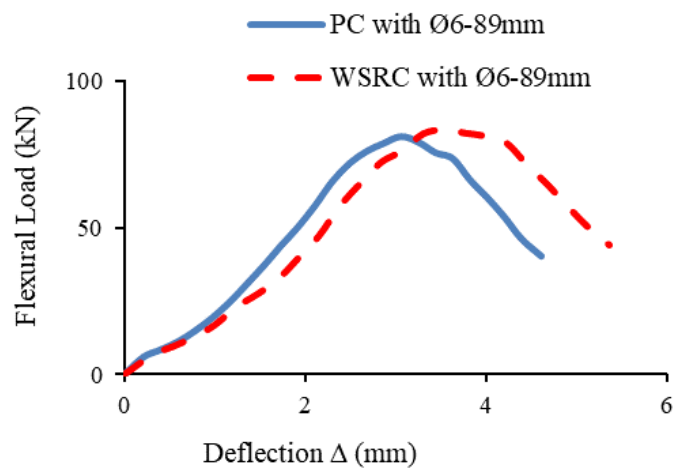
Effect of Shear Steel Rebars on Load, Deflection and Cracks: Loads, deflections, number of cracks occurred at ultimate failure, and failure modes for tested PC and WSRC beam-lets with varying shear reinforcement (i.e. $\varnothing 6 - 64 \text{ mm}$, $\varnothing 6 - 76 \text{ mm}$, and $\varnothing 6 - 89 \text{ mm}$) and with constant flexural reinforcement (i.e. $3 - \varnothing 6$) are given in Table 5.4. The first crack load for PCS1, WSS1, PCS2, WSS2, PCS3, and WSS3 are 75.2 kN, 80.4 kN, 75.4 kN, 77.6 kN, 75.9 kN, and 76.1 kN, respectively. The load at first crack of WSS1, WSS2, and WSS3 are increased by 6.9%, 2.9%, and 0.3%, respectively, when compared with that of PCS1, PCS2, and PCS3, respectively. It can be found that the improved crack resistance is due to the incorporation of wheat straw in the concrete. The crack resistance is decreased with the decrease in shear reinforcement. The maximum load is also taken from the load-deflection curve of the tested specimens. The maximum load for PCS1, WSS1, PCS2, WSS2, PCS3, and WSS3 are 83.9 kN, 88.1 kN, 82.7 kN, 87.6 kN, 80.9 kN, and 83.4 kN, respectively. The maximum load of WSS1, WSS2, and WSS3 are increased by 4.2 kN, 4.9 kN, and 2.5 kN, respectively, when compared with that of PCS1, PCS2, and PCS3, respectively. Similarly, the ultimate load of WSS1, WSS2, and WSS3 are increased by 7.2%, 14.8%, and 9.7%, respectively, when compared to the ultimate load of PCS1, PCS2, and PCS3, respectively. In general, an increase in the load carrying capacities of WSRC specimens with shear reinforcement are enhanced. The values of maximum deflection are also given in Table 5.4. The maximum deflections which occur in case of WSRC specimens are more than that in case PC specimens. An increase of 10.5%, 17.7%, and 16.3% in the deflections of WSS1, WSS2, and WSS3 specimens



(a)

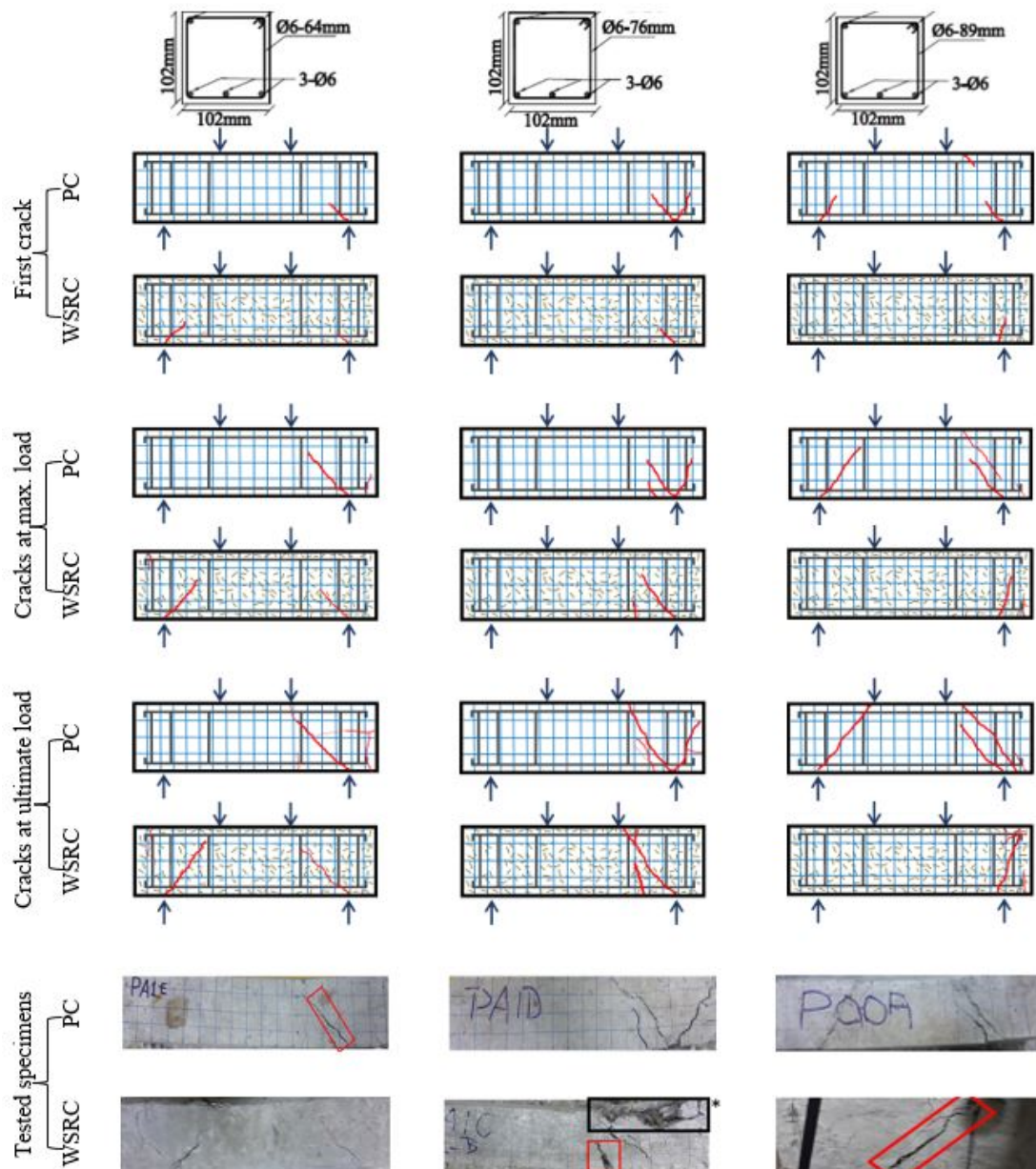


(b)



(c)

FIGURE 5.8: Load – deflection curves of PC and WSRC with shear reinforcement (a) $\varnothing 6 - 64 \text{ mm}$, (b) $\varnothing 6 - 76 \text{ mm}$, and (c) $\varnothing 6 - 89 \text{ mm}$ and constant flexural reinforcement (i.e. $3 - \varnothing 6$).



*Tested WSRC specimen is broken intentionally to observe straw-concrete interaction.

FIGURE 5.9: Crack behavior of PC and WSRC specimens during flexural loading with varying shear reinforcement and constant flexural reinforcement (i.e. 3 – Ø6).

is observed when compared to that of PCS1, PCS2, and PCS3 specimens. The number of cracks at the ultimate failure in tested beam-lets are also noted by the naked eye and is also given in Table 5.4. The number of cracks in PCS1, WSS1, PCS2, WSS2, PCS3, and WSS3 beam-lets are 4, 3, 4, 3, 4, and 4, respectively. The crack lengths and crack widths in PC beam-lets are more severe than that in respective WSRC beam-lets. Here again as in case of WSRC with flexural

TABLE 5.4: Loads and deflections for tested PC and WSRC beam-lets with varying shear reinforcement and constant flexural reinforcement (i.e. 3 – Ø6).

Loads and Deflections	Specimens					
	PC			WSRC		
	Ø6– 64 mm	Ø6– 76 mm	Ø6– 89 mm	Ø6– 64 mm	Ø6– 76 mm	Ø6– 89 mm
(1)	(2)	(3)	(4)	(5)	(6)	(7)
Load at First Crack (kN)	75.2	75.4	75.9	80.4	77.6	76.1
Maximum Load (kN)	83.9	82.7	80.9	88.1	87.6	83.4
Ultimate Load (kN)	41.9	41.3	40.2	44.9	47.4	44.1
Maximum Deflection (mm)	5.16	4.91	4.61	5.70	5.78	5.36
Cracks at Ultimate Load (-)	4	4	4	3	3	4
Failure Mode (-)	Diagonal tension	Balanced	Shear	Diagonal tension	Balanced	Shear

reinforcement, due to the presence of wheat straw, the bridging phenomenon and crack arresting is observed. The straw resists the development of first cracks firstly, then the crack propagation is also resisted due to the arresting of cracks with the help of straw as in case of all WSRC specimens with flexural and shear reinforcement. Based on the location/type of cracks, the failure modes of tested PC and WSRC beam-lets are also identified as flexural, balanced and shear failures etc. The observed failure modes are given in Table 5.4. The observed failure mode for PCS1 and WSS1 is diagonal tension, for PCS2 and WSS2 is balanced, and that for PCS3 and WSS3 is shear. Here the diagonal tension failure mode indicates the combination of shear and longitudinal stress.

Effect of Shear Rebars on Flexural Strength, Flexural Energies Absorbed, and Flexural Toughness Index: The flexural strength (FS), flexural energies absorbed, and flexural toughness index (FTI) for PC and WSRC beam-lets with varying shear reinforcement (i.e. Ø6 – 64 mm, Ø6 – 76 mm, and Ø6 – 89 mm) and constant flexural reinforcement (i.e. 3 – Ø6) are given in Table 5.5. The flexural strength of PCS1, WSS1, PCS2, WSS2, PCS3, and WSS3 are calculated by using the maximum load from the load-deflection curves of the respective specimens. The flexural strength of PCS1, WSS1, PCS2, WSS2, PCS3,

and WSS3 are 36.6 MPa, 38.4 MPa, 36.0 MPa, 38.2 MPa, 35.3 MPa, and 36.4 MPa, respectively. Flexural strength of WSS1, WSS2, and WSS3 is increased by 4.9%, 5.8%, and 3.1%, respectively, when compared to that of PCS1, PCS2, and PCS3, respectively. Here a decrease in flexural strength of WSRC specimens is observed with the decrease in shear reinforcement. The FEM and FE of WSS1, WSS2, and WSS3 are increased by 42.5%, 81.9%, and 82.2% and 16.8%, 30%, and 21.1%, respectively, as compared to that of PCS1, PCS2, and PCS3, respectively. As for as the FEP of WSRC specimens with shear reinforcement is concerned, there is an increase of 8.1%, 26.9%, and 30% is observed in comparison to that of respective PC specimens. However, an over-all decrease in the energies absorbed is observed with the decrease in shear reinforcement from $\varnothing 6 - 64 \text{ mm}$ to $\varnothing 6 - 89 \text{ mm}$. The same is in the case of flexural toughness index of WSRC specimens with shear steel rebars. The flexural toughness index of WSS1, WSS2, and WSS3 are increased by 0.3%, 11%, and 6.6%, respectively when compared to that of PCS1, PCS2, and PCS3, respectively. An increased toughness index of the specimens with shear reinforcement of $\varnothing 6 - 76 \text{ mm}$ is observed, when compared to other considered WSRC matrices.

It may be noted that, in general, the flexural properties of WSRC are increased with an increase in shear reinforcement. Overall, WSRC with shear reinforcement (i.e. $\varnothing 6 - 64 \text{ mm}$, $\varnothing 6 - 76 \text{ mm}$, and $\varnothing 6 - 89 \text{ mm}$) and with constant flexural reinforcement of $3 - \varnothing 6$ again perform very well under the flexural loading.

A clear comparison of FS, FEP, FE, FTI, and Δ of PC and WSRC with varying shear reinforcement (i.e. $\varnothing 6 - 64 \text{ mm}$, $\varnothing 6 - 76 \text{ mm}$, and $\varnothing 6 - 89 \text{ mm}$) and with constant flexural reinforcement (i.e. $3 - \varnothing 6$) is shown in Figure 5.10. Overall, all the WSRC specimens along with shear steel rebars behaved much better than respective PC beam-let specimens. The enhanced flexural strength, the post cracking behavior, and toughness indices of WSRC with shear steel rebars are observed in comparison to PC. As far as the effect of shear reinforcement in WSRC specimens is concerned, decrease in flexural properties with the decrease in shear reinforcement is observed.

TABLE 5.5: Flexural strengths, Flexural energies absorbed (FE1, FEM, FEP, FE), and Flexural Toughness Index (FTI) for PC and WSRC beam-lets with varying shear reinforcement and constant flexural reinforcement (i.e. 3- ϕ 6).

Properties	Specimens					
	PC			WSRC		
	$\emptyset 6 - 64 \text{ mm}$	$\emptyset 6 - 76 \text{ mm}$	$\emptyset 6 - 89 \text{ mm}$	$\emptyset 6 - 64 \text{ mm}$	$\emptyset 6 - 76 \text{ mm}$	$\emptyset 6 - 89 \text{ mm}$
(1)	(2)	(3)	(4)	(5)	(6)	(7)
FS (MPa)	36.6	36.0	35.3	38.4	38.2	36.4
FE1 (kN.mm)	101.5	104.1	90.8	118.4	121.8	103.2
FEM (kN.mm)	45.4	33.3	29.8	64.7	60.0	54.3
FEP (kN.mm)	131.6	115.1	99.0	142.3	147.4	125.7
FE (kN.mm)	278.6	252.5	219.7	325.4	329.2	266.1
FTI (-)	2.74	2.43	2.42	2.75	2.70	2.58

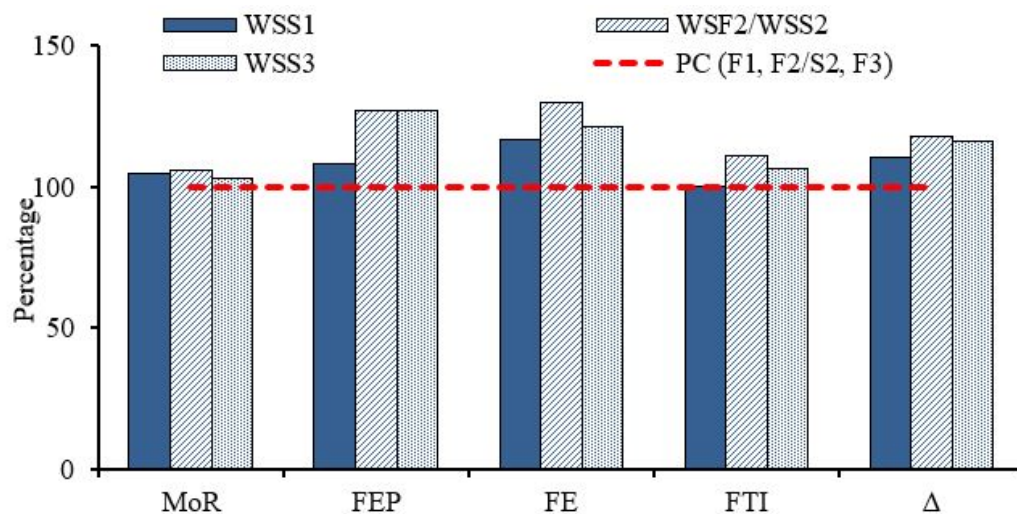


FIGURE 5.10: Comparison of FS, FEP, FE, FTI, and Δ of PC and WSRC with varying shear reinforcement (i.e. $\emptyset 6 - 64 \text{ mm}$, $\emptyset 6 - 76 \text{ mm}$, and $\emptyset 6 - 89 \text{ mm}$) and with constant flexural reinforcement (i.e. 3 - $\emptyset 6$).

5.4 Discussion

Nilson *et al.* [119] reported the equation (i.e. $M_r = T_s(d - a/2)$, where $T_s = A_s \times f_y$, and $a = (A_s \times f_y) / (0.85 \times f_c' \times b)$ for the calculation of moment capacity of plain concrete. However, in modified equation by Beshara *et al.* [118], tensile strength can be considered below N.A. by using fibre reinforced concrete due to its tough nature. There is no major change in block depth 'a' above N.A. The modified equation is: $M_{F1} = T_s(d - a/2) + T_f \{(t - t_f/2) - a/2\}$. Here, in this modified equation, the fibre's tensile strength in the effective height of equivalent stress in tensile region is added in Nilson's equation. The tensile strength of fibres in Beshara's equation can be calculated by using $T_f = [1.64V_f(l_f/\phi_f)] b t_f$ where, V_f is volume of fibres in concrete, l_f is length of fibres, and ϕ_f is diameter of fibres. However, the equation proposed by Beshara *et al.* [118] is modified by the authors of this study in terms of T_f to calculate the effective height of equivalent stress of wheat straw reinforced concrete in tension region. Beshara *et al.* used combination of volume, length, and diameter of fibres for calculating the tensile strength of FRC. Whereas, in current study, a simplified approach is adopted for tensile strength of WSRC (TWSRC), where $T_{WSRC} = [(MoR_{WSRC} - MoR_{PC})/2] \times b \times t_f$ instead of fibre volume and dimensions as in case of Beshara's equation. The modified equation of moment capacity of WSRC comes out to be $M_{WSRC} = T_s(d - a/2) + T_{WSRC} \{(t - t_f/2) - a/2\}$ with usual notations. The logic behind the addition of factored MoR difference of WSRC w.r.t PC is that, when the applied load exceeds the moment capacity of concrete, the cracks start to appear. The crack resistance comes into existence when the crack is propagated up to the steel rebars. However, in case of FRC, the dispersed fibres resist first crack formation. In addition to formation of first crack, the crack propagation is also delayed due to crack arresting by fibres. So, in this way, the load carrying capacity of FRC is increased. Furthermore, once cracks reach up to the steel reinforcement, the tensile strength of fibres is also added with the steel rebars for resisting cracks. The similar type of behavior is observed, for WSRC with steel rebars, in current study.

TABLE 5.6: Comparison of theoretical and experimental moment capacities for PC and WSRC with flexural and shear rebars.

Parameter	Unit	Specimens					
		Flexural Rebars			Shear Rebars		
		2-Ø6	3-Ø6	2+2-Ø6	Ø6 – 64 mm	Ø6 – 76 mm	Ø6 – 89 mm
(1)	(2)	(3)	(4)	(5)	(6)	(7)	(8)
Area of steel (A_s)	in^2	0.20	0.25	0.29	0.25	0.25	0.25
M_r for PC (1)	$kN.mm$	2436	2836	3286	2836	2836	2836
M_{PCEXP} for PC (4)	$kN.mm$	3021	3149	3293	3198	3149	3081
M_{WSRC} for WSRC (2)	$kN.mm$	2670	2970	3407	2970	2970	2970
$M_{WSRCEXP}$ for WSRC (4)	$kN.mm$	3249	3337	3497	3356	3337	3176

1. $M_r = Ts(d - a/2)$, where $Ts = A_s \times f_y$, and $a = (A_s \times f_y) / (0.85 \times f_c' \times b)$
2. $M_{WSRC} = Ts(d - a/2) + T_{WSRC}(t - t_f/2) - a/2$, where $T_{WSRC} = [MoR_{WSRC} - MoR_{PC}/2] \times b \times t_f$
3. $f_y = 280 \text{ MPa}$, $d = 76 \text{ mm}$, $f_c'_{PC} = 22.5 \text{ MPa}$, $f_c'_{WSRC} = 21.8 \text{ MPa}$, $b = 102 \text{ mm}$, $t = 102 \text{ mm}$, $t_f = h/2 = 51 \text{ mm}$, $[MoR]_{WSRC} = 3.42 \text{ MPa}$, $[MoR]_{PC} = 3.30 \text{ MPa}$
4. $M_{PCEXP} = v_{PCEXP} \times X$ and $M_{WSRCEXP} = v_{WSRCEXP} \times X$ Where $v_{PCEXP} = L_{mPC}/2$ and $v_{WSRCEXP} = L_{mWSRC}/2$, where L_{mPC} and L_{mWSRC} are taken from Table 5.2 and 5.4, and $X = 76 \text{ mm}$ (Refer to Figure 5.3 (a))

The comparison of PC and WSRC with flexural and shear rebars by the equations devised by Nilson et al. and modified equation, respectively, along with the experimental moment capacities is also made. The theoretical and experimental moment capacities of reinforced concrete and WSRC with steel rebars is given in Table 5.6. The experimental moment capacity (i.e. M_{Exp}) is calculated by using the area of shear capacities for the respective specimens (i.e. $V_{Exp} \times X$).

However, theoretical moment capacity (i.e. M_r) of RC is calculated by using Nilson's equation [119]. Whereas, in case of WSRC with steel rebars, the equation proposed by Beshara *et al.* [118] and modified by authors of current study, is used. For a beam with $f_y = 280 \text{ MPa}$, $d = 76 \text{ mm}$, $f'_{cPC} = 22.5 \text{ MPa}$, $b = 102 \text{ mm}$, and $A_s = 0.25$, the M_r comes out to be 2836 kN-mm by using the Nilson's equation. The increased M_r by WSRC are observed when put in the equation developed for WSRC. For a WSRC beam with $f_y = 280 \text{ MPa}$, $d = 76 \text{ mm}$, $f'_{cWSRC} = 21.8 \text{ MPa}$, $b = 102 \text{ mm}$, $t = 102 \text{ mm}$, $t_f = h/2 = 51 \text{ mm}$, $[MoR]_{WSRC} = 3.42 \text{ MPa}$, $[MoR]_{PC} = 3.30 \text{ MPa}$ and $A_s = 0.25$, the M_{WSRC} comes out to be 2970 kN-mm by using modified Beshara's equation. A maximum increase of 9.8% in moment capacity of WSRC (i.e. M_{WSRC}) with flexural reinforcement (i.e. 2 – Ø6) and shear reinforcement (i.e. Ø6 – 64 mm) is observed when compared to the moment capacity (M_r) by the respective specimen of reinforced concrete. However, as far as the difference between theoretical and experimental moment capacities is concerned, an overall difference of $\pm 20\%$ is observed.

The experimental shear capacities (V) of PC and WSRC with flexural and shear steel rebars are taken as half of the maximum load as the beam-lets are tested in three-point load test. Whereas, the theoretical shear capacities are determined from the theoretical moment capacities of the respective specimens. The theoretical and experimental shear capacities for PC and WSRC are given in Table 5.7. Likewise, in moment capacities, the shear capacities for WSRC are also increased when compared to that of RC. A maximum increase of 7.5% is observed in experimental shear capacity of WSRC specimens with shear rebars ($V_{WSRCExp}$) as compared to the respective reinforced specimens.

TABLE 5.7: Comparison of theoretical and experimental shear capacities for PC and WSRC with flexural and shear rebars.

Shear Capacities		Specimens						
		Unit	Flexural Rebars			Shear Rebars		
Symbol	Formula*		2-Ø6	3-Ø6	2+2-Ø6	Ø6 – 64 mm	Ø6 – 76 mm	Ø6 – 89 mm
(1)	(2)	(3)	(4)	(5)	(6)	(7)	(8)	(9)
V_{PCTheo}	$V_{PCTheo} = M_{PCTheo}/X$	kN	32.0	37.2	43.1	37.2	37.2	37.2
V_{PCExp}	$V_{PCExp} = L_{mpc}/2$	kN	39.7	41.3	43.2	42.0	41.3	40.4
$V_{WSRCTheo}$	$V_{WSRCTheo} = M_{WSRCTheo}/X$	kN	35.0	39.0	44.8	39.0	39.0	39.0
$V_{WSRCExp}$	$V_{WSRCExp} = L_{mWSRC}/2$	kN	42.6	43.9	45.9	44.1	43.9	41.7

1) $*M_{PCTheo}$ and $M_{WSRCTheo}$ is taken from Table 5.6 and $X = 76mm$ (Refer to 5.3 (a))

2) L_{mpc} and L_{mWSRC} is taken from Table 5.2 and 5.4

However, in theoretical shear capacities, the maximum of 9.6% increase in the theoretical shear capacity of WSRC with rebars is observed when compared to the respective specimen of reinforced concrete. Here again, a difference of approximately $\pm 20\%$ is observed in theoretical and experimental shear capacities.

In the rigid pavements, the vehicular load is resisted by the flexural strength of concrete. The steel reinforcement in rigid pavements is not used for carrying load but for controlling the formation of cracks or resisting the propagation of cracks [210]. Conventional concrete pavements are generally classified as jointed plain concrete pavement (JPCP), jointed reinforced concrete pavement (JRCP), and continuous reinforced concrete pavement (CRCP). The addition of straw in the jointed plain concrete pavement can lead to more crack resistance in the pavements. The propagation of cracks in wheat straw reinforced concrete can also be delayed by the help of dispersed straw. Whereas, in case of jointed and continuous reinforced concrete pavement, the incorporation of wheat straw in the concrete along with steel rebars can result in the enhanced flexural strength of concrete which is reported in the current study. This enhanced flexural strength will then result in improved load carrying capacity of jointed/continuous reinforced concrete pavement along with the crack resistance. The incorporation of fibres can also be helpful for steel rebars in resisting the cracks. Hence, the wheat straw reinforced concrete can be concluded in reduction of steel reinforcement. Huang [211] reported that the basic rigid pavement design equation as per American Association of State Highway and Transportation Officials (AASHTO) 1993: II-45 is used for the design of rigid pavements. The equation is as follows:

$$\log_{10}W_{10} = Z_R S_o + 7.35 \log_{10} (D + 1) - 0.06 + \frac{\log_{10} \left[\frac{\Delta PSI}{4.5-1.5} \right]}{1 + \frac{1.624 \times 10^7}{(D+1)^{8.46}}} + (4.22 - 0.32Pt) \left[\frac{S'_c C_d [D^{0.75} - 1.132]}{215.63j \left[D^{0.75} - \frac{18.42}{\left(\frac{E_c}{k}\right)^{0.25}} \right]} \right] \tag{5.1}$$

Where:

W_{18} = Traffic load in equivalent standard axle loads

Z_R = Standard normal deviation for desired reliability

S_O = Overall standard deviation

D = Slab thickness (in)

ΔPSI = Serviceability index

S'_c = Flexural strength of concrete (psi)

Cd = Drainage coefficient

J = Load transfer coefficient

E_c = Elastic modulus of concrete (psi)

k = subgrade reaction modulus (psi/in)

However, in case of wheat straw reinforced concrete specimens with the steel re-bars, the flexural strengths are increased as compared to that of plain concrete. The flexural strengths of PC and WSRC with flexural and shear re-bars along with the increment factor of WSRC w.r.t PC are given in Table 5.8. The flexural strengths of WSRC specimens, with steel reinforcement 2 – Ø6, 3 – Ø6, 2 + 2 – Ø6, Ø6 – 64 mm, Ø6 – 76 mm, and Ø6 – 89 mm, are increased by a factor of 1.08, 1.05, 1.06, 1.05, 1.05, and 1.03, respectively, when compared to that of respective PC specimens. The average increment in WSRC with respect to PC comes out to be 1.05.

Therefore, to cater the effect of tensile stresses induced at bottom of pavement surface due to the applied traffic loading, the added strength of straw in case of WSRC pavements can be accounted by simply modifying the above mentioned AASHTO rigid pavement design equation by using the increment factor of flexural strength. Hence, the S'_c in the equation is modified for the flexural strength of WSRC for incorporating the effect of tensile strength due to addition of wheat straw and is as follows:

$$s'_{WSRC} = MoR_{WSRC} \times 1.05$$

Where 1.05 is the averaged increment factor in flexural strength of WSRC. The modified pavement slab thickness design equation with the incorporation of s'_{WSRC} will become as follows:

$$\begin{aligned} \log_{10}W_{10} = & Z_R S_o + 7.35 \log_{10} (D + 1) - 0.06 + \frac{\log_{10} \left[\frac{\Delta PSI}{4.5-1.5} \right]}{1 + \frac{1.624 \times 10^7}{(D+1)^{8.46}}} \\ & + (4.22 - 0.32Pt) \left[\frac{s'_{WSRC} C_d [D^{0.75} - 1.132]}{215.63j \left[D^{0.75} - \frac{18.42}{\left(\frac{E_c}{k}\right)^{0.25}} \right]} \right] \end{aligned} \tag{5.2}$$

As per Portland Cement Association and AASHTO design methods for rigid pavements, the same method is used for continuous reinforced concrete pavement as used for jointed plain and reinforced concrete pavement. The only difference that can occur in the thickness design of continuous reinforced concrete pavement and conventional concrete pavement is in the load transfer coefficient. As in case of continuous reinforced concrete pavement, the value of load transfer coefficient can be reduced from 8 cm to 7.4 cm, which will cause the reduction in slab thickness of 2 cm. However, the deflections and critical stresses in continuous reinforced concrete pavement are more or less same as in case of jointed plain/reinforced concrete pavement. Therefore, it is recommended that same thickness should be used. So, the above-mentioned equations are solved for PC and WSRC specimens to calculate the thickness of PC and WSRC pavement, respectively. The solved thickness is compared with solved design example of AASHTO 1993: II-45.

For PC and WSRC specimens, all the design parameters (i.e. given in Table 5.9) are kept constant as taken in the example which is done in AASHTO 1993: II-45 except the concrete material properties i.e. flexural strength (S'_c) and modulus of elasticity (E_c). The variation in the concrete pavement slab thickness of PC and WSRC specimens in comparison with the solved AASHTO 1993: II-45 equation is given in Table 5.10. Considering the modified equation to account the effect of straw, the WSRC pavement thickness is reduced by 7% as compared to that of PC. In addition to that, due to the addition of straw in concrete, the bridging

mechanism occurs, which enhances the energy absorption of WSRC by resisting the crack formation. This bridging/sewing effect is due to the relatively better bond of straw with surrounded concrete matrix because of the rough surface of straw after pre-treatment. Furthermore, once the cracks are formed, the crack width and crack propagation under the traffic loading is also restricted and delayed, respectively, due to the crack arresting mechanism which occurs with incorporation of straw. In short, the improved post-cracking behavior can be achieved in WSRC pavements with 7% less thickness as for PC. Accordingly, the cost analysis for the construction of PC and WSRC pavements is also made. The construction cost of WSRC pavement, designed as per proposed modified Eq. 5.2, can be reduced up to 14% when compared to that of conventionally designed PC pavement (Table 5.10).

As far as CRCP is concerned, the straw incorporation along with steel reinforcement, can lead towards enhanced flexural strengths in addition to better post cracking behavior. Because, in this scenario, the added flexural strength, due to the incorporation of fibres, in the flexural strength of concrete will provide more crack resistance. The increased flexural strengths of WSRC with steel rebars are also reported in current study. In case of cracks occurrence, the time period for cracks to propagate up to steel rebars will be enhanced due to crack arresting by straw in the concrete cover. And, in the worst condition, when the cracks reach up to the steel rebars, the straw will also be enriching the crack resisting capability of steel rebars, as can be observed in Figure 5.5 and 5.9. The whole phenomenon is contributed towards punch-out resistance in WSRC pavements. The percentage area of steel can also be reduced by some percentage. This will reduce the quantity of steel reinforcement to be used in continuous reinforced concrete pavement. Thus, ultimately will result in reducing the overall cost of pavement by 14%. In addition to that, embodied carbon emissions (CO_{2e}) are also calculated, in the same way as also done by [278], by using the materials (cement, sand, aggregates) coefficients from ICE Inventory V3.0, for both PC and WSRC pavements. It is observed that CO_{2e} emissions against WSRC pavements can be reduced up to 28%, as compared to that of PC pavements.

TABLE 5.8: Increased flexural strengths of WSRC specimens w.r.t PC specimens.

Flexural Strengths	Specimens					
	Flexural Rebars			Shear Rebars		
	2- $\emptyset 6$	3- $\emptyset 6$	2+2- $\emptyset 6$	$\emptyset 6$ - 64 mm	$\emptyset 6$ - 76 mm	$\emptyset 6$ - 89 mm
(1)	(2)	(3)	(4)	(5)	(6)	(7)
FS_{PC} (MPa)	34.6	36.0	37.7	36.6	36.0	35.3
FS_{WSRC} (MPa)	37.2	38.2	40.1	38.4	38.2	36.4
Increment Factor (FS_{WSRC}/FS_{PC})	1.08	1.06	1.05	1.05	1.06	1.03

TABLE 5.9: Design parameters for 1998 AASHTO rigid pavement design model.

Parameter	Value
(1)	(2)
Equivalent Standard Axle Loads (W18)	5100000
Reliability (R)	95%
Standard Deviation (S_o)	0.30
Elastic Modulus of Concrete (E_c)	Variable (psi)
Elastic strength of Concrete (S_c)	Variable (psi)
Poisson's ratio of Concrete (μ)	0.15
Seasonal k-value (k)	72 psi/n
Initial serviceability (p_i)	4.2
Terminal serviceability (p_t)	2.5

TABLE 5.10: Comparison of PC and WSRC pavement in terms of thicknesses, cost and CO_{2e} emissions.

Specimens	Flexural Strength (S'c)	Modulus of Elasticity (EC)	Pavement Slab Thickness (cm)	Thickness Reduction w.r.t PC	Construction Cost (per m ³) (PKR)	Construction Cost* (per lane per km) (Million PKR)	Cost Reduction w.r.t PC	Embodied Carbon** (per lane per km) ($\times 10^5$ kg-CO _{2e})	(CO _{2e}) Reduction w.r.t PC	Remarks
	(MPa)	(MPa)	(cm)	-	(PKR)	(Million PKR)	-	($\times 10^5$ kg-CO _{2e})	-	
(1)	(2)	(3)	(4)	(5)	(6)	(7)	(8)	(9)	(10)	(11)
JPCP	4.50	34,474	25	-	-	-	-	-	-	AASHTO-93 II-45 [279] Reference Design
PC	3.30	19,445	29	-	13,500/-	23.5/-	-	5.4	-	Thickness as per AASHTO 93 II-45 [279] Current Study
WSRC	3.59	18,742	27	-7%	12,527/-	20.3/-	-14%	3.9	-28%	Reduced thickness as per proposed Eq. (5.2) Current Study

*The considered lane width is 6m.

**The CO_{2e} coefficients are taken from ICE Inventory V3.0, for calculation of emissions.

5.5 Summary

The plant fibre (i.e. wheat straw) in concrete with flexural and shear reinforcement are investigated in this experimental study. Straw of 1% content, by mass of wet concrete, and length of 25mm are added in the same mix (i.e. 1 : 2 : 4) as for PC. The contribution of plant fibre (i.e. wheat straw) is studied for improving the capacities and behavior of concrete reinforced with flexural and shear steel rebars for its use in concrete pavements. Plain Concrete (PC), and Wheat Straw Reinforced Concrete (WSRC) with the flexural and shear reinforcement are studied. In addition to this, the moment capacity design equation and concrete pavement thickness design equation are also proposed. The conclusions are as follows:

- A maximum load increase of 7% in the first crack initiation is observed for WSRC with flexural rebars as compared to that of PC. And the maximum load is increased by 7.6% in comparison to PC. In WSRC, the number of cracks, crack widths, and crack lengths are decreased up to 25%, 140% and 66%, respectively, when compared to the respective PC specimens.
- WSRC with flexural reinforcement show enhancement up to 7.5%, 44.8%, 30.44%, and 11.7% in FS, FEP, FE, and FTI, respectively, as compared to the respective PC beam-lets. The moment capacities of WSRC with flexural and shear rebars are increased up to 2.8% and 2%, respectively, in comparison to that of PC.
- As far as the WSRC specimens with shear rebars are considered, the maximum increases of 6.9% and 7% in first crack and ultimate loads, respectively, are observed when compared to the respective loads of PC specimens with shear rebars. Here again, the severity of cracks in terms of quantity, width, and length are decreased up to 20%, 75% and 50%, respectively, in WSRC specimens as compared to respective PC specimens.
- Increase in FS, FEP, FE, and FTI of WSRC with shear steel rebars are up to 6%, 27%, 30.1%, and 11.2% w.r.t that of respective PC specimens. Shear

capacities of WSRC specimens with flexural and shear rebars are increased up to 7.3% and 6.3%, respectively, in comparison to that of respective PC specimen.

- The pavement slab thickness, construction cost and CO_{2e} emissions are decreased by 7%, 14% and 28%, respectively, for WSRC as compared to PC for same load parameters. In addition to that, the improved behavior, delay in first crack initiation, more resistance in crack propagation and better post-cracking behavior of WSRC is observed which is favorable under traffic loading.

So, based on the conducted research, it can be postulated that the WSRC with steel rebars is likely to have the potential to be used for concrete pavement applications. Also, the proposed equations for moment capacity and concrete pavement thickness design can be applicable for wheat straw reinforced concrete. However, the performance of WSRC road panels/test section is recommended to be explored in detail.

Chapter 6

Structural Performance of Wheat Straw Reinforced Concrete Pavement

Related Articles:

M. U. Farooqi and M. Ali, “Construction practices for first ever wheat straw reinforced concrete pavement for light traffic,” *In proceedings of 5th International Conference on Sustainable Construction Materials and Technologies (SCMT5)*, London, UK, 2019.

6.1 Background

The favorable outcomes of wheat straw in cement concrete composites, in terms of comparable and durable behavior against static loading even after the exposure to multiple natural and accelerated ageing conditions for a long period of 48-months, has developed good enough rationale to use it for civil engineering structural applications. In pursuance, the in-depth behavior and capacities of wheat straw reinforced concrete, with flexural and shear steel rebars, are explored for its possible use in rigid pavements. The enhanced moment capacities of WSRC

lead towards the formulation of empirical design equation for WSRC pavements in accordance with AASHTO 1993 pavement design guide for rigid pavements. Upon integration of obtained results in the devised modified design equation, a reduction of 7% in thickness is recommended for WSRC pavements when replacing the PC pavements. However, the validation of this reduction in pavement thickness, obtained in result of laboratory testing, is recommended under the application of vehicular movement and real environmental conditions.

Therefore, in pursuance of the recommendations made in Chapter 3 and Chapter 5, the field study is performed to evaluate the optimized Wheat Straw Reinforced Concrete (Chapter 3) with reduced thickness design in terms of structural capacity (Chapter 5) under real circumstances, i.e. vehicular loading and varied environmental/climatic conditions. Accordingly, the structural capacities of Plain Concrete (PC) and optimized (i.e. 1% soaked wheat straw, by mass of wet concrete) Wheat Straw Reinforced Concrete (WSRC) pavement test sections are investigated in detail. For this purpose, the Jointed Plain Concrete Pavement (JPCP) and Jointed Wheat Straw Reinforced Concrete Pavement (JWSRCP) test sections are constructed in the campus premises of Capital University of Science and Technology, Islamabad, Pakistan. The construction practice for the first ever constructed natural fibre (i.e. wheat straw) reinforced concrete pavement is reported in this Chapter 6. The experimental investigation of cores extracted from PC and WSRC pavement test sections along with their structural capacity is made after exposure to traffic movement for the 18-months period. To account the effect of cyclic loading for fatigue cracking analysis, the test sections are exposed to the real traffic movement for a period of 18-months. The occurrence of cracks and their progression under loading are also recorded. The validation of reduced thickness of pavement in case of WSRC, as reported in Chapter 5, is also made. In addition to that, the micro-structural analysis is also performed to verdict the uniform dispersion of straw in the surrounded matrix. The rest of the chapter is compiled in a way like: Section 6.2 portrays the materials used, laying technique for WSRC pavement section, test sections detailing and testing mechanism whereas; all the experimental findings along with analysis are provided in Section 6.3. Section 6.4

is comprising of modelling for the formulation of WSRC performance index and co-relation between laboratory and field testing, followed by the summary of all the findings in Section 6.5.

6.2 Materials and Testing Mechanism

6.2.1 Raw Materials

Cement, sand and aggregates obtained from BESTWAY cement (a local brand), Lawrence-purr quarries and Margallah quarries, respectively are used to prepare plain concrete (PC). As provided by manufacturer, the percentage contents of CaO , SiO_2 , Al_2O_3 , FE_2O_3 , MgO and SO_3 in cement (having 52 ± 3 28-days strength) are 61.7%, 21%, 5.04%, 3.24%, 2.56% and 1.51%, respectively. The maximum aggregate size used is 19.5 mm. Tap/potable water is used. However, for wheat straw reinforced concrete (WSRC), commercially available wheat straw having approximate length, width and depth of 25 mm, 5 mm and 1.2 mm, respectively, are also used in addition to above-mentioned conventional PC ingredients. The approximate ranges for density, tensile strength and shear strength, in physical characterization of wheat straw are, 55 to 119 kg/m^3 , 21.2 to 40.0 MPa and 4.91 to 7.26 MPa, respectively [18, 156, 159, 225, 266].

6.2.1.1 Wheat Straw Processing

A simple pre-treatment to remove dry matter (i.e. dust particles/impurities) from the surface of straw, by keeping the natural state of raw wheat straw ingredients intact, proved to be an effective technique for obtaining better results after incorporation in concrete matrix [267]. Accordingly, wheat straw, which are obtained from a locally available commercial source, are soaked in potable/tap water for a period of approximately 20 minutes with the intention of removing dry matter (i.e. dust/impurities/wax etc.) from the surface of straw. Wheat straw are air-dried after removing from water. The prepared/treated wheat straw are shown in

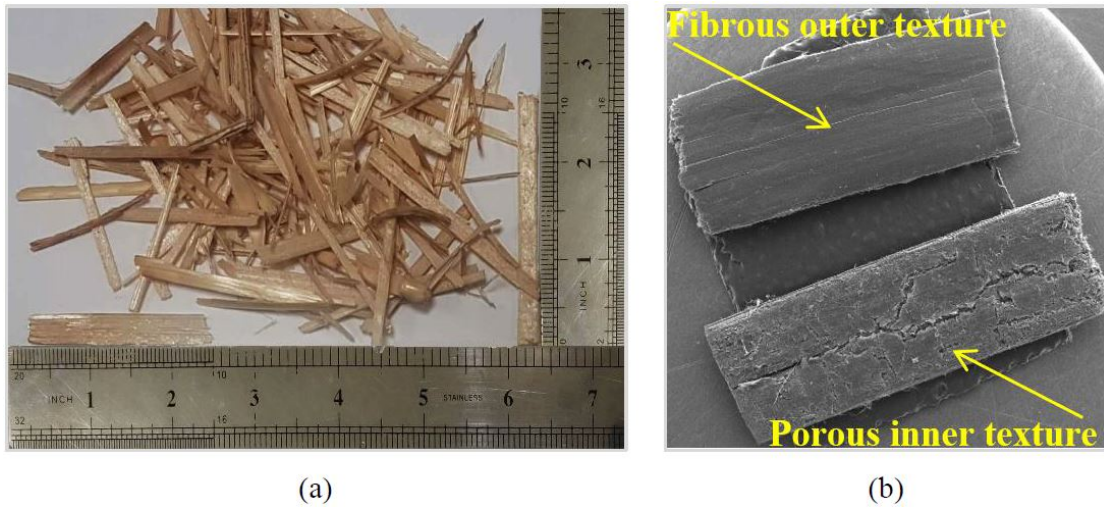


FIGURE 6.1: Wheat straw (a) with naked eye and (b) SEM image from 2mm.

Figure 6.1(a). The cleanliness in the natural/raw straw texture can be observed by naked eye.

6.2.1.2 Micro-structural Testing of Wheat Straw

Moreover, the micro-structural analysis of processed wheat straw is also performed through Scanning Electron Microscope (SEM), Energy Dispersive X-ray (EDX), X-Ray Diffraction (XRD), and Thermogravimetric analysis (TGA). The SEM image of wheat straw from both sides is shown in Figure 6.1(b) showing the plain fibrous texture at one side and porous texture at the other end. This porous texture may be helpful to provide interlocking mechanism between straw and cement matrix, for having proper straw – matrix bonding. The graphical presentation of EDX, XRD and TGA for wheat straw is shown in Figure 6.2. The chemical analysis of wheat straw, in terms of percentage contents of elements, performed by EDX analysis is given in Table 6.1. Similar findings are also reported by [226, 227]. 3KW having radiation of $\text{CuK}\alpha$ ($\lambda = 1.54$) is used for determination of wheat straw crystallinity. Crystallographic analysis, as shown in Figure 6.2(b), shows that, at around 2θ , the variation in maximum crystalline peak is ranged in 26.10° to 29.89° , however, the peak in amorphous case ranges from 23.71° to 25.58° . Thermal stability of wheat straw is obtained through TGA analysis by using Perkin Elmeris instrument (Figure 6.2(c)). The straw degradation, in terms of weight loss is determined by

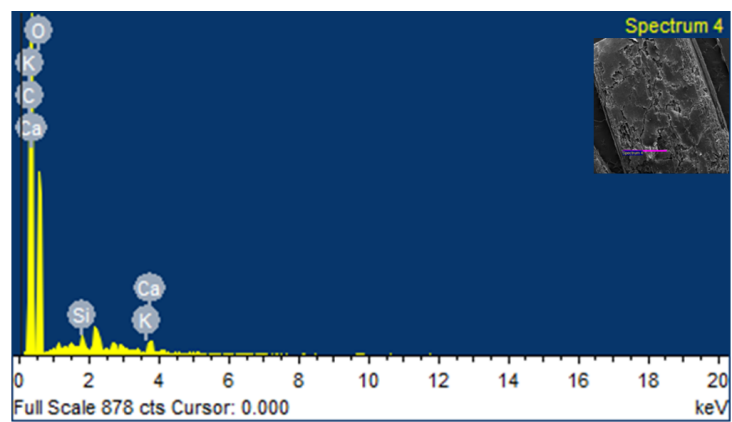
TABLE 6.1: Percentage (%) contents of elements in Wheat Straw.

Element	Intensity Conc.	Weight %	Weight % Sigma	Atomic %
(1)	(2)	(3)	(4)	(5)
Carbon (C)	0.5519	58.19	1.50	65.17
Oxygen (O)	0.2723	41.12	1.49	34.57
Silicon (Si)	0.8414	0.20	0.05	0.10
Potassium (K)	0.9526	0.10	0.05	0.04
Calcium (Ca)	0.9041	0.38	0.06	0.13
Total:		100.00		100.00

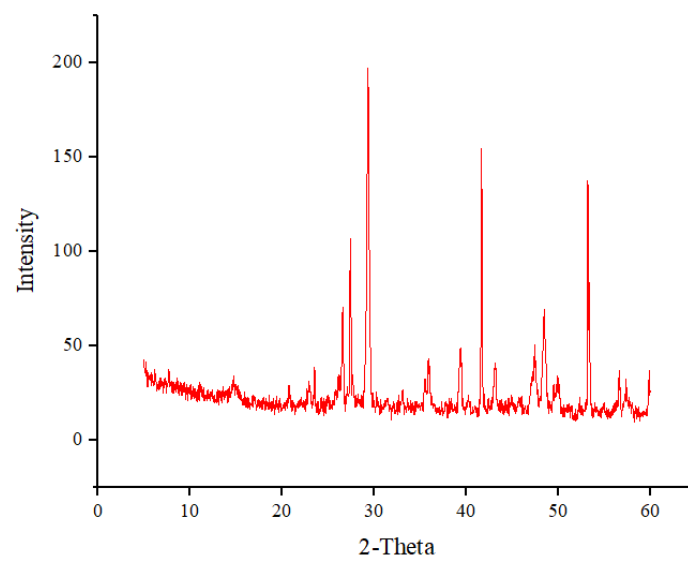
heating 25 mg straw up to 500 °C @10°/min. The weight loss of approximately 3.99 to 7.01% is observed up to the 100 °C temperature, which could be due to moisture content elimination from straw, indicating the thermal stability of straw.

6.2.2 Mix Design, Mixing Procedure, Laying Technique and Material Testing

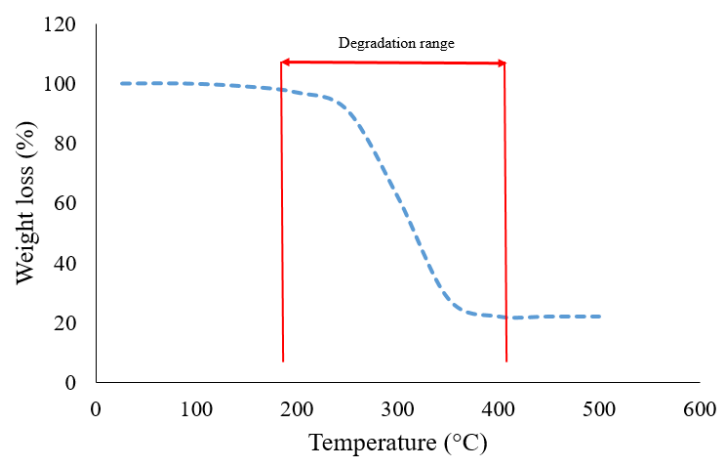
Mix design ratio of 1 : 2 : 4 : 0.60 (C: S: A: W), i.e. 331 kg cement, 704 kg sand, 1550 kg aggregates and 182 kg water per m³ of concrete, is used for the preparation of Plain Concrete (PC) mix. However, for wheat straw reinforced concrete (WSRC) mix, wheat straw, having an averaged approximate length of 25 mm, are also used in addition to the ingredients as mentioned for PC. Accordingly, 254 kg cement, 542 kg sand, 1194 kg aggregates, 152 kg water and 27 kg wheat straw are taken to prepare 1 m³ of WSRC. The conventional rotary tilting mixer is used for mixing purpose. For mixing one batch of PC, all the raw materials are added in the mixer in the following order; cement, sand, aggregates and then water, followed by a mixing of 3 minutes at the rate of 10–12 rpm. But, for mixing WSRC, a different technique is opted as recommended by Farooqi and Ali [267] to get a homogeneous mix and to avoid balling effect, which is usually observed in mixing of natural fibre reinforced concrete. All the materials (i.e. cement, sand,



(a)



(b)



(c)

FIGURE 6.2: Wheat Straw analysis (a) EDX, (b) XRD and (c) TGA.



FIGURE 6.3: Workability tests (a) Slump value and (b) Compaction factor test of PC and WSRC mix

aggregates and straw) are distributed in three equal portions, which are deployed in mixer one after another, layer wise. The major portion of water (i.e. 60%) is added before start of mixing. Initial mixing time is 180 seconds, then the remaining water is added and the mixing is done again for 60 more seconds. The slump and compaction factor tests are also performed for PC and WSRC (Figure 6.3). The slump values for PC and WSRC are come out to be 25 and 0 mm, respectively. Whereas, the compaction factors for PC and WSRC are come out to be 0.99 and 0.95, respectively.

The different stages in preparation/construction of PC and WSRC pavement test sections, i.e. earthwork preparation, levelling, lean layer with marked levels, batching, mixing, pouring, laying, finishing, finally prepared test sections, curing, and vehicular movement on constructed test sections, are shown in Figure 6.4. For laying of PC and WSRC, the material is transported from mixer to the respective final positions with the help of wheel barrows. The concrete is continuously

deposited to its final position, without any undue delay, with proper advance planning and good workmanship for avoiding stiffening/drying-out/segregation. The compaction of concrete, for eliminating entrapped air from the mix, is done with the help of internal vibrator. The Darby and strike-off boards are used for levelling the concrete mix. The WSRC mix finished surface is achieved by putting extra efforts on the surface levelling and by manually removing the straw where chipped-off length is more than 50% of its embedded length during finishing. The water curing of PC and WSRC test sections is done afterwards. The curing is done by ponding technique for 28 days (Figure 6.4(g)). In addition, to gauge the early-age shrinkage cracking, linear shrinkage, i.e. taken as % increase or % decrease in specimen length is also calculated during the curing period. The longitudinal length of PC and WSRC test sections is reduced by 1.8% and 1.0%, respectively. However, in transverse dimensions, the reduction of 1.6% and 0.9% is observed for PC and WSRC, respectively. Hence, the linear longitudinal and transverse shrinkage of WSRC test section is reduced by 45% and 43%, respectively, as compared to that in PC test section. This reduction is might be due to the presence and uniform distribution of dispersed straw in concrete that ultimately contribute towards less initiation of cracks in WSRC pavement test section.

6.2.2.1 Compressive Strength Test of Cylinder Specimens

In parallel, the cylindrical moulds, having dimensions of 150 mm × 300 mm (Diameter × Height) as per ASTM C31 standard, are also filled with PC and WSRC for laboratory testing. The cylinder is filled in five layers with 25 uniform blows of tamping rod after each layer as per ASTM C192. However, for WSRC, a slight lifting and free falling of cylinder is also done after each layer for proper consolidation. The cylinders are de-moulded after 24 hours and placed in curing tank for the period of 28 days. Afterwards, the specimens are removed from curing tank and are air-dried for 24 hours. Later on, the specimens are capped with Sulphur with the intention of uniform distribution of load. These specimens for PC and WSRC are then tested under compressive loading, as per ASTM C39 test



(a)



(b)



(c)



(d)



(e)



(f)



(g)



(h)

FIGURE 6.4: Stages in construction (a) Earthwork Preparation, (b) Levelling, (c) Lean layer & Levels, (d) Batching & Mixing, (e) Pouring, Laying & Finishing, (f) PC & WSRC Test Sections, (g) Curing and (h) Vehicular Movement.

standards, for the determination of compressive strengths, corresponding strains, compressive energies absorption and compressive toughness indices.

The stress-strain curves and tested cylinder specimens for PC and WSRC are shown in Figure 6.5. Comparatively a tough behavior with less stiffness and more strain capacity is observed for WSRC as compared to that of PC (Figure 6.5(a)). This may be due to more energy absorption capability of WSRC, due to crack arresting and bridging mechanism as shown in Figure 6.5(b). However, the fragments of conventionally brittle natured PC are broken and can be seen on the base plate of test assembly. The arresting of micro-cracks (which generally occurs before the ultimate maximum loading) by the dispersed fibre in a cement composite through sewing effect causes the enhanced toughness in case of fibre reinforced concrete [272].

Accordingly, the compressive strengths (σ_c), corresponding strains (ϵ_c), energies absorbed under compressive loading (Cem_c , Cep_c , Ce_c) and toughness indices (CTI_c) of PC and WSRC cylinder specimens are given in Table 6.2. The σ_c of WSRC is slightly declined by 7% when compared to that of PC, as expected in case of natural fibres addition in concrete which is also reported by [40, 66, 238, 280]. This slight decrement in σ_c in case of WSRC is catered by significant enhancement of its energy absorption capability. The area under σ_c - ϵ_c curves are calculated for compressive energy absorption (Ce_c) for both PC and WSRC, as also done by [66, 71, 250]. This energy absorption per unit concrete volume is calculated in MJ/m^3 [254, 255]. This total energy is further bifurcated in energy absorption up to maximum σ_c (Cem_c) and energy absorption from maximum σ_c to maximum ϵ_c (Cep_c). However, the ratio of Ce_c to Cem_c is calculated for the toughness index (CTI_c). The noticeable point here is that, Cem_c in case of WSRC is almost equivalent to Ce_c in case of PC showing the remarkable enhancement of energy absorption capacity of WSRC. Whereas, almost 97% more post peak-stress energy is absorbed by WSRC cylinder specimen as compared to that of PC. As far as energies absorption in case of WSRC is concerned, almost 33% of the total energy is absorbed after the maximum stress level indicating the improved post stress behavior of WSRC. This behavior leads towards improved performance, as the

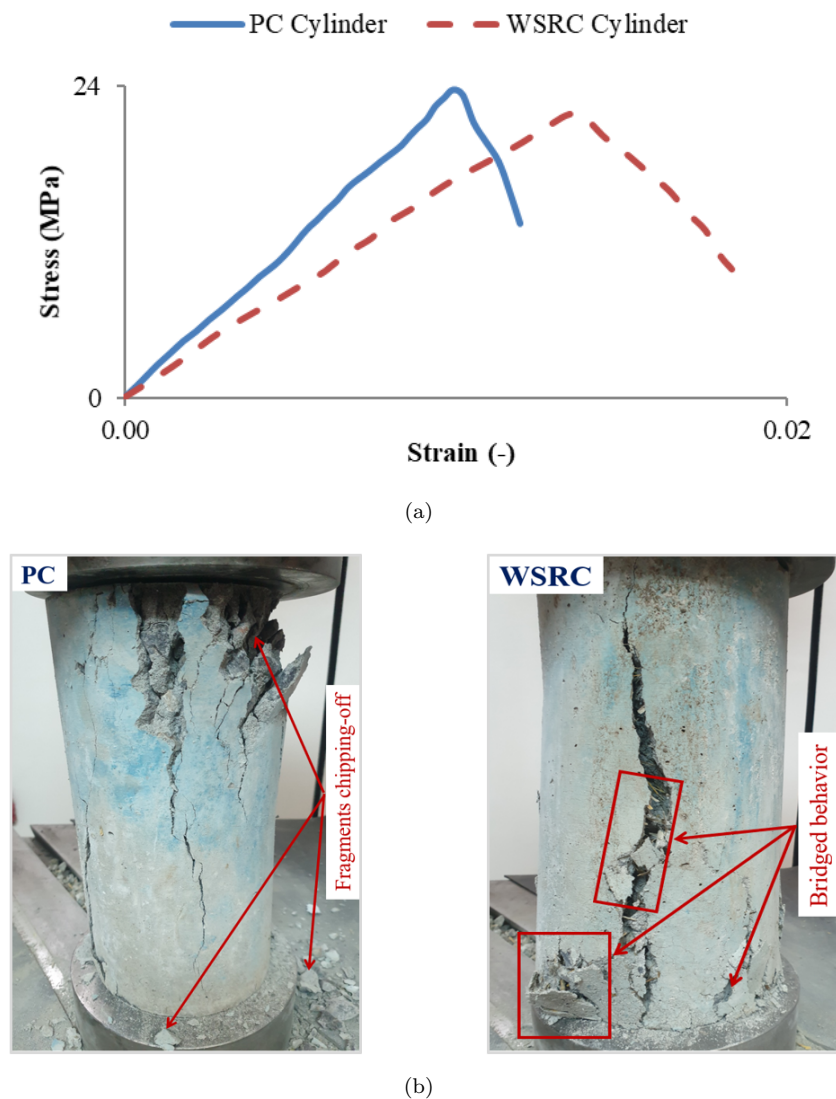


FIGURE 6.5: Compressive behavior (a) Stress – strain curves and (b) tested specimens of PC and WSRC cylinders

contribution of toughness in addition to compressive strength results in enhanced structural strength [256, 257].

6.2.3 Test Sections

Jointed Plain Concrete Pavement (JPCP) and Jointed Wheat Straw Reinforced Concrete Pavement (JWSRCP) test sections are constructed for structural evaluation. The plan of JPCP and JWSRCP along with respective longitudinal and cross sections are shown in Figure 6.6. The dimensions for each pavement test

TABLE 6.2: Compressive properties of PC and WSRC cylinders.

Cylinder Specimens	σ_c (MPa)	ϵ_c $\times 10^{-2}$	Compressive Energies Absorbed			CTI_c
			Cem_c (kJ/m ³)	Cep_c (kJ/m ³)	Ce_c (kJ/m ³)	
(1)	(2)	(3)	(4)	(5)	(6)	(7)
PC	23.7 ± 0.6	0.99 ± 0.16	115.4 ± 4.1	39.3 ± 1.4	154.6 ± 5.5	1.34 ± 0.05
WSRC	21.9 ± 0.4	1.36 ± 0.13	154.5 ± 3.9	77.4 ± 1.9	231.9 ± 5.8	1.50 ± 0.06

section are 35 sq. meter, i.e. 7 m × 5 m (Length × Width). Shoulders of width 0.5 m are provided on both sides of pavement test sections (Figure 6.6a). The layer thicknesses in case of plain concrete pavement test section is designed by using AASHTO 1993: II-45 design guide equation which is stated below:

$$\log_{10}W_{10} = Z_R S_o + 7.35 \log_{10}(D + 1) - 0.06 + \frac{\log_{10} \left[\frac{\Delta PSI}{4.5-1.5} \right]}{1 + \frac{1.624 \times 10^7}{(D+1)^{8.46}}} + (4.22 - 0.32Pt) \left[\frac{S_c C_d [D^{0.75} - 1.132]}{215.63 J \left[D^{0.75} - \frac{18.42}{Ec k^{0.25}} \right]} \right] \quad (6.1)$$

The design consideration parameters, which are used in this equation, to solve it for concrete layer thickness are listed in Table 6.3. By analyzing the equation 6.1, by using the design consideration parameters, the thickness of concrete layer came out to be 25.4 cm. The wearing concrete layer is based on compacted earthwork of 15 cm. However, to provide construction table and to avoid the direct interaction of concrete layer with soil particles, a 5 cm thick layer of lean plain concrete (1 : 4 : 8) layer is also laid above the compacted earthwork layer (Figure 6.6(c)).

As far as JWSRCP test section is concerned, the same sequence, i.e. compacted earthwork with lean plain concrete (1 : 4 : 8) on it followed by the WSRC layer, is followed. However, in this scenario, the WSRC layer thickness is 23.6 cm, i.e. 7% less than that of PC layer, is laid as recommended by Farooqi and Ali [262], for the comparative performance analysis. The recommended 7% less thickness in case of WSRC, as compared to PC, is analyzed by the following proposed modified

TABLE 6.3: Design considerations for concrete layer thickness in plain concrete pavement test section.

Parameter(s)	Value(s)
(1)	(2)
Equivalent Standard Axle Loads (W18)	12.67×10^6 ESALs
Reliability(R) – [$Z_r = -1.645$]	95%
Standard Deviation (S_o)	0.35
Elastic Modulus of Concrete (E_c)	2.8×10^3 MPa
Flexural Strength of Concrete (S'_c)	4.5 MPa
Poisson’s ratio of Concrete (μ)	0.15
Seasonal k-value (k)	550 psi/in
Drainage Coefficient (C_d)	1
Initial serviceability (pi)	4.5
Terminal serviceability (pt)	2.5
Δ PSI (pi – pt)	2

WSRC pavement design equation:

$$\log_{10}W_{10} = Z_R S_o + 7.35 \log_{10} (D + 1) - 0.06 + \frac{\log_{10} \left[\frac{\Delta PSI}{4.5-1.5} \right]}{1 + \frac{1.624 \times 10^7}{(D+1)^{8.46}}} + (4.22 - 0.32Pt) \left[\frac{s'_{WSRC} C_d [D^{0.75} - 1.132]}{215.63j \left[D^{0.75} - \frac{18.42}{\left(\frac{E_c}{k}\right)^{0.25}} \right]} \right] \tag{6.2}$$

Where; $s'_{WSRC} = MoR_{WSRC} \times 1.05$. However, all the other design considerations are kept same as for PC design (Table 6.4). Accordingly, the subsequent layers are adjusted to maintain the top surface level by raising the thickness of compacted earthwork to 16.8 cm (Figure 6.6(c)). However, the lean plain concrete (1 : 4 : 8) is same, i.e. 5 cm for both the test sections. The longitudinal section for both the test sections is shown in Figure 6.6(b) to have an overall idea. Furthermore, as already discussed in Chapter 4, that the noted temperature during the studied

period is as low as 2 °C and as high as 48 °C (Figure 4.2). Therefore, there is a need to cater the effect of hot and cold climate on expansion and contraction, respectively, of cement concrete. Accordingly, a 25 mm transverse expansion joint is also provided in between both the JPCP and JWSRCP test sections. The dowel bars with reinforcement details; $\phi 6@30$ cm c/c with plastic sheets capped at both ends, are also provided at the expansion joint (Figure 6.6(a) and 6.6(c)). These plastic sheets and caps around the dowel bars provide space for movement of bars with slab during expansion and contraction. Furthermore, the joint width is filled with a compressible elastic filler, followed by approximately 25 mm depth of sealer to restrict moisture infiltration. In addition, the bonding of aggregates as well as straw with the composite is due to the cement mortar. The rough surfaced aggregates provide better bonding with matrix as compared to straw due to relatively smooth surface. However, prompt runoff of surface water due to provided slope and surface vaporization after rainfall would repeal the moisture infiltration in WSRC pavements. In addition, the 45% and 43% reduction in longitudinal and transverse shrinkage, respectively, of WSRC pavement in comparison to that of PC, also contribute towards resistance against ingress of moisture in WSRC pavements.

6.2.4 Test Sections Evaluation

6.2.4.1 Compressive Strength Test of Cores

The cores from PC and WSRC pavement test sections are drilled and tested initially for water absorption. The water absorption of PC and WSRC cores came out to be 3.23% and 5.14%, respectively. Afterwards, the compressive strength test, as per AASHTO T24M / T24 and ASTM C42M (Standard Test Method for Obtaining and Testing Drilled Cores) and ASTM C39/C39M-20 (Standard Test Method for Compressive Strength of Cylindrical Concrete Specimens), is performed.

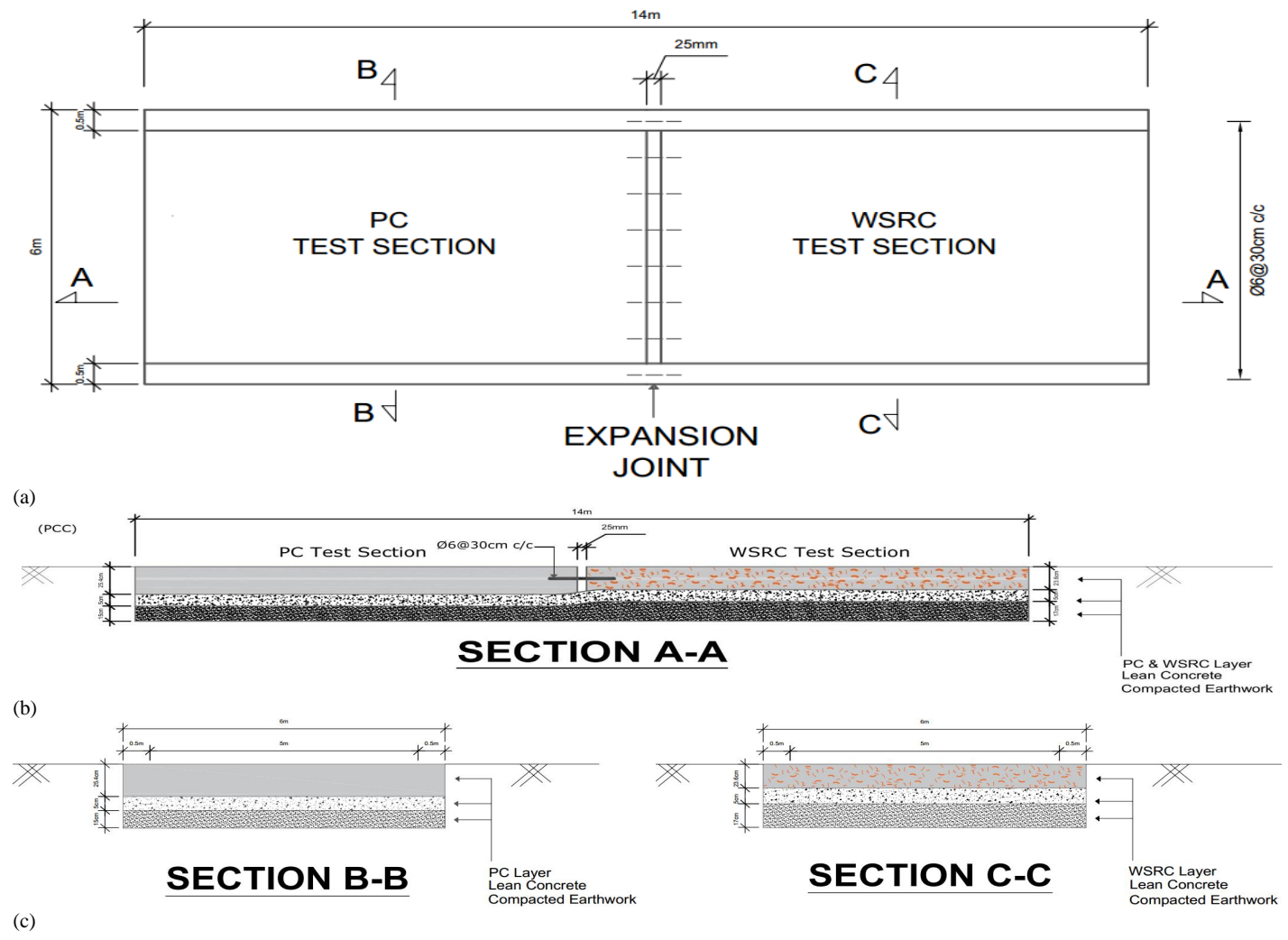


FIGURE 6.6: PC and WSRC pavement test sections drawings (a) Plan, (b) Longitudinal section, and (c) Cross sections.

The dimensions of drilled cores are 100 mm × 200 mm (Diameter × Height). In this way, the diameter to length ratio is 2, which is in specified range i.e. 1.9 to 2.1. Therefore, there is no need to apply standard factor as per AASHTO T24M/T24. Furthermore, as per mentioned standard, there is also no need of applying core-strength correction factors (ACI 214 2010) in case of 100 mm dia cores. The drilled cores are tested in compressive testing machine along with attached strain gauge assembly, after Sulphur capping, for experimental determination of field compressive strength (σ_f), corresponding strain (ϵ_f), energies absorption (Cem_f , Cep_f , Cef), and toughness indices (CTI_f). The real test assembly for extracting the cores from test sections is shown in Figure 6.7.

6.2.4.2 Micro-structural (i.e. SEM) Analysis of WSRC

The Scanning Electron Microscopic (SEM) analysis is performed on the specimen extracted from drilled cores of WSRC pavement test section. The validation of uniform dispersion of straw in bulk quantity concrete, in case of WSRC test section, is intended from SEM analysis. The condition and failure mechanism of straw in concrete matrix and the straw – concrete bonding is also revealed from this analysis. The sample is coated with Plasma prior to take SEM images from 10 kV VEGA3 TESCAN.

6.2.4.3 Pavement Deflection Measurement

Deflection basins of Jointed Plain Concrete Pavement (JPCP) test section and Jointed Wheat Straw Reinforced Concrete Pavement (JWSRCP) test section is determined experimentally for structural performance evaluation. AASHTO T256 / ASTM D4695 (Standard Test Methods for General Pavement Deflection Measurements) is adopted for this testing to evaluate the bearing capacity or load carrying capacity of PC and WSRC pavement test sections. As per this standard, among four, the non-continuous static device i.e. Benkelman beam apparatus is used for deflection measurements in JPCP and JWSRCP test sections. The schematic



FIGURE 6.7: Core drilling test assembly.

diagram and in placed test assembly of Benkelman beam apparatus are shown in Figure 6.8.

6.2.4.4 Visual Inspection to Observe Crack Initiation and Propagation

The vigilant visual monitoring is done for observing the phenomenon of cracks initiation, development and their propagation, under the application of load and exposure to climatic conditions for 18-months period, in PC and WSRC pavement test sections. The performance of concrete pavement also depends upon crack widths and cracks spacings as per AASHTO guide [279]. Accordingly, the cracking details (i.e. lengths, widths and spacings etc.) are determined by visual monitoring and inspection as also done by [215, 216]. The PC and WSRC pavement test

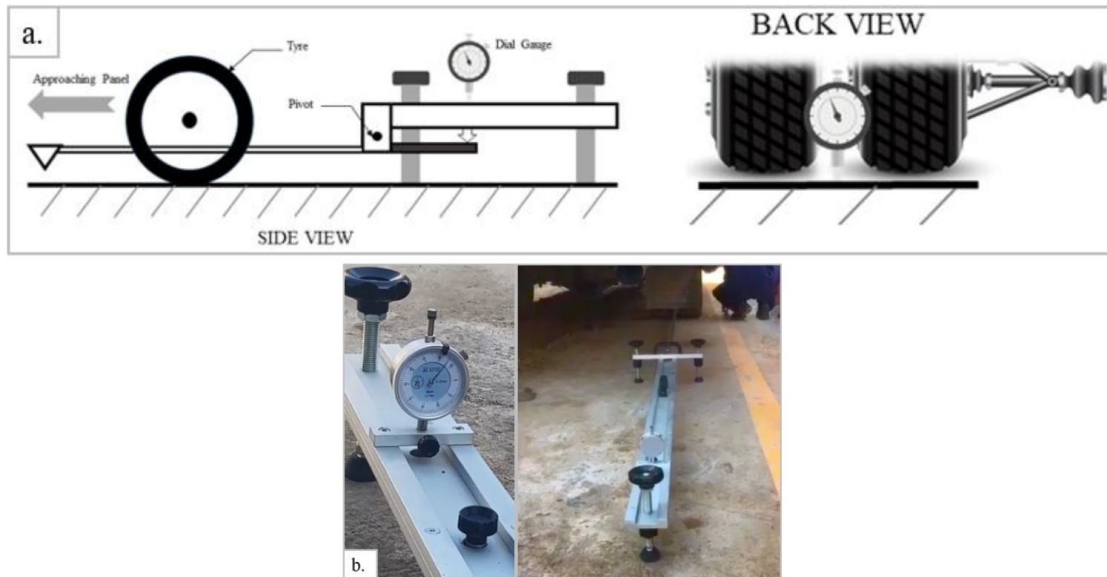


FIGURE 6.8: Benkelman beam apparatus (a) Schematic diagram and (b) In-placed test assembly.

sections are distributed in small patches by marking grids on them. The measuring scale/tape and Vernier caliper is used, where required.

6.3 Result Findings

6.3.1 Compressive Properties of Test Sections Cores

6.3.1.1 Compressive Behavior

The compressive stress-strain curves of PC and WSRC drilled cores along with the tested core specimens are shown in Figure 6.9. Approximately, symmetrical behavior of WSRC core is observed in line with PC core. However, WSRC depicts more strain capacity in comparison to that of PC as predicted through the behavior of cylinder specimens in laboratory testing. The dispersed straw in concrete, here again, play their role in absorbing more energy, compared to PC, for enhancing strain capability. Also, an overall shift of curves towards right i.e. increment in strain is observed for both PC and WSRC cores when compared to the respective curves in case of cylinder specimens. This behavior of WSRC

showed comparatively tough property which might be achieved through proper mixing and dispersion of straw, when prepared in bulk quantity. Furthermore, the tested core specimens of PC and WSRC are shown in Figure 6.9(b). From here, the reason behind tough behavior of WSRC can be validated as, it is observed that the tested cores of WSRC shows only cracking once again due to sewing effect in matrix when straw keep on arresting the cracks even upon application of maximum stress. This seems to be highly favorable behavior in terms of pavements where micro-cracks occur and propagate rapidly due to the application of moving loads ultimately results in punch-outs. Similar type of behavior is observed in tested cylinder specimen of WSRC. A relatively more deteriorated side of tested WSRC core i.e. (top-left corner) is intentionally broken to observe the straw failure mechanism and its condition, which is shown in superscript of Figure 6.9(b). There is dominance of straw pull-out behavior as compared to straw fracture which results in more strain and energy absorption capability of WSRC. The pull-out/slippage of straw, instead of fracture, is due to its higher tensile strength and this phenomenon contributes in enhancing energy absorption capacity of natural fibre reinforced concrete [19, 267]. On the other hand, as expected, the PC core is crushed and its fragments are broken, however don't fall due to test/strain gauge assembly binding, showing the typical brittle behavior of PC.

6.3.1.2 Compressive Strengths, Corresponding Strains, Compressive Energies Absorption and Compressive Toughness Indices of Drilled Cores

The compressive properties of cores, drilled during field investigation of PC and WSRC pavement test sections, are determined experimentally. The definitions and calculations along with standards for all the studied compressive properties of cores are same as taken in case of PC and WSRC cylinder specimens. Accordingly, the σ_f , ϵ_f , Cem_f , Cep_f , Ce_f , and CTI_f of PC and WSRC cores are given in Table 6.4. The compressive strengths of cores are usually less than that of respective cylinder specimens with the same material. Therefore, in line with this, although, the σ_f of WSRC core is also decreased here by 5%, as compared to that of PC, however,

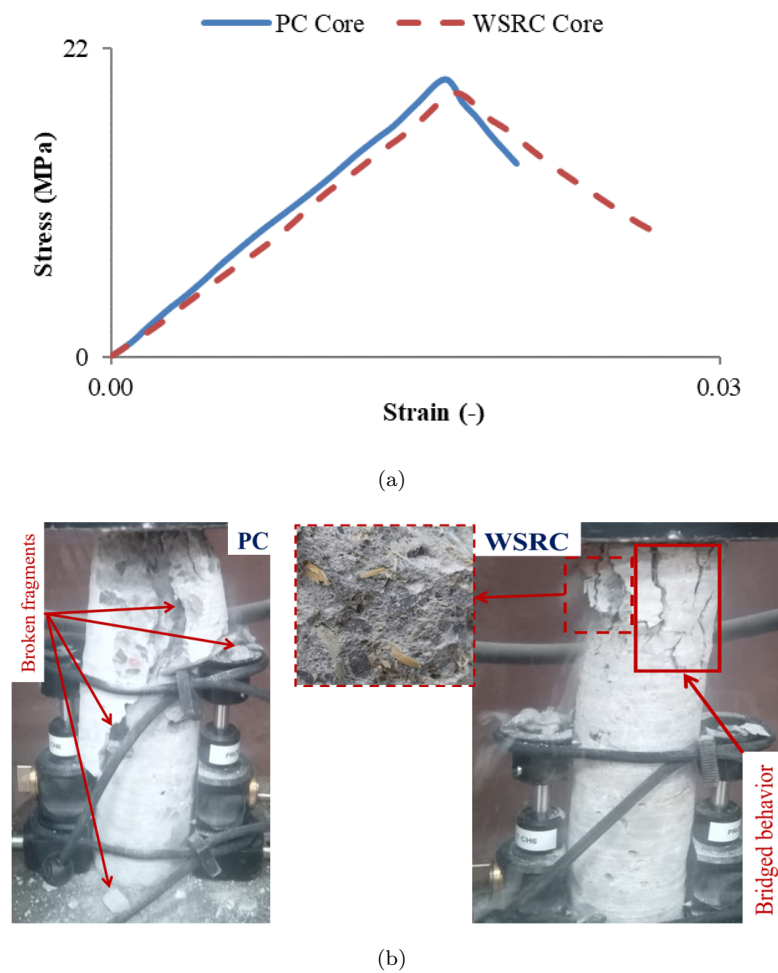


FIGURE 6.9: Compressive behavior (a) Stress – strain curves and (b) tested specimens of PC and WSRC cores.

this decrement is reduced when compared to that in case of cylinder specimens. This might be due to better mixing, compaction and proper dispersion of straw in concrete when mix at a larger scale and consolidated in a proper way. This improved behavior in case of cores can also be observed in energies absorbed. The Cem_f of WSRC is almost equal to that of PC showing the symmetrical behavior up to the maximum stress. But later on, as expected, the conventional PC collapsed immediately after the maximum stress and a sudden fall is observed. Whereas, in case of WSRC core, 136% more energy is absorbed after maximum stress as compared to that of PC core. This is even better as compared to that as observed in cylinder specimens. This results in 34% enhanced energy absorption capacity of concrete reinforced with dispersed wheat straw as compared to plain concrete. Ultimately, the CTI_f of WSRC core is 38% higher than that of PC

TABLE 6.4: Compressive properties of PC and WSRC cores.

Core Specimens	σ_f (MPa)	ϵ_f $\times 10^{-2}$	Compressive Energies Absorbed			CTI_f
			Cem_c (kJ/m ³)	Cep_c (kJ/m ³)	Ce_c (kJ/m ³)	
(1)	(2)	(3)	(4)	(5)	(6)	(7)
PC	19.8 ± 0.4	1.5 ± 0.20	161.8 ± 6.2	59.1 ± 1.2	220.8 ± 7.4	1.37 ± 0.04
WSRC	18.8 ± 0.2	1.7 ± 0.14	156.6 ± 4.4	139.5 ± 1.6	296.1 ± 6.0	1.89 ± 0.03

core. This toughness factor, when added in slightly declined strength, contributes a lot in overall performance of structures particularly the pavements. As the rigid pavements are in dire need of the crack arresting techniques in any case to resist the initiation and then propagation of cracks.

6.3.2 Micro-structural Analysis

6.3.2.1 SEM Analysis of Straw-concrete Matrix

As shown in Figure 6.9(b), the uniform dispersion of straw in concrete is observed with the naked eye. In addition, the phenomenon of pulled-out straw (with dominance) and fractured straw are also observed on the intentionally broken exposed surface of concrete. To validate these observations and to reveal in-depth failure mechanism of straw in concrete along-with the straw – matrix bonding, the samples are taken from tested WSRC drilled cores for the SEM analysis. The SEM images of straw-concrete matrix are presented in Figure 6.10. Both the straw pulling-out and fracture mechanisms are explored. In Figure 6.10(a), the resistance of straw against fracture due to its tensile strength is turning into slippage or pulling-out of straw from matrix. This phenomenon is observed with dominance in tested core specimen. The straw pulling-out mechanism is more favorable in terms of enhancement in energy absorption and toughness. Furthermore, this resistance of straw against fracture contributes its major role in arresting the cracks in rigid pavements before initiation and their propagation under moving loads, once initiated, as well. On the other hand, equivalent development length of straw or in

case of more applied stress than straw’s tensile strength, the straw are ruptured. Relatively less (only a few in number) pulled out cum ruptured straw are also observed on the exposed surface of tested core. The condition of that straw is shown in Figure 6.10(b). Although, the straw is ruptured at the end, but its condition shows the resistance which is provided by straw before fracture. This resistance results in straw fracture in layers, as can be seen in figure, when stress is applied in the direction of its longitudinal axis. The less occurrence of fractured straw might also be due to the application of compressive stress, not tensile and flexural one. However, the validation of uniform dispersion of straw in concrete, when prepared and laid at such a larger scale, is revealed from both the images. The dense Interfacial Transition Zone (ITZ) in terms of properly indulged bonding of straw with the surrounding concrete matrix, can easily be observed (Figure 6.10).

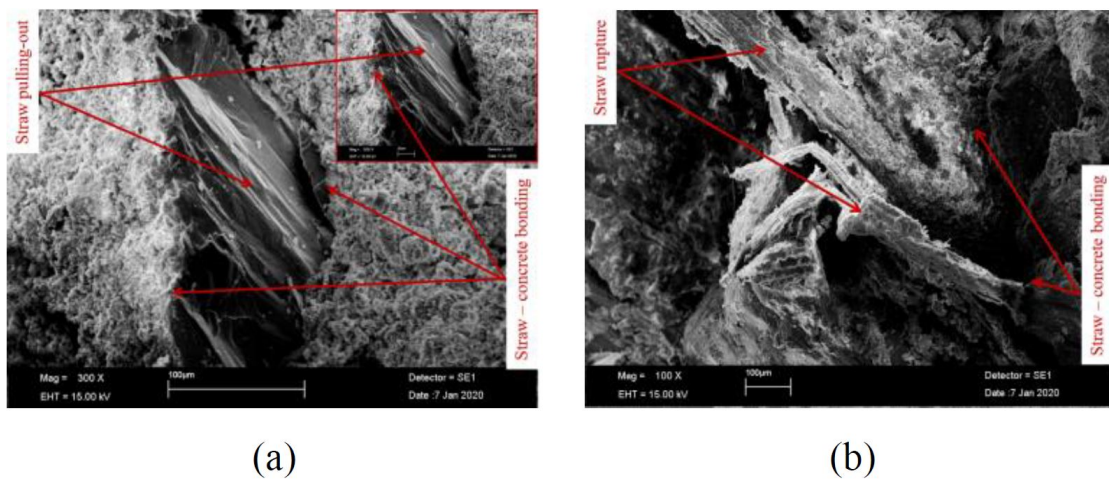


FIGURE 6.10: SEM images of (a) Pulling-out and (b) Rupture of straw in concrete.

6.3.3 Deflection Measurements of Test Sections

6.3.3.1 Vehicular Movement on Test Sections in terms of ESAL’s

The pavement test sections are exposed to the repeated movement of heavy traffic to get an idea regarding fatigue cracking that usually occurs as a result of combination of material, traffic and environmental factors. As, PC and WSRC pavement

test sections are constructed in a developing sector with on-going 2 – 3 construction projects of multi-storey buildings. So, these test sections provide a way to all the incoming and outgoing traffic/vehicles comprises of various types of civil engineering construction materials i.e. cement, sand, aggregates, steel, concrete, bricks etc. All this material is transported on construction site through under study pavement test sections via wide range of vehicles like dumpers, 10 and 18 – wheelers, transit mixers etc. The outgoing vehicles are the same as incoming but without material, as material is dumped on the construction site. Conclusively, each vehicle provides two passes on both PC and WSRC pavement test sections (as constructed in series), one loaded and the other is unloaded (Figure C1 in Annexure C).

The vehicular movement on PC and WSRC pavement test sections, over 18 – months period, is observed through manual survey with the help of designated staff at the entry point towards test sections. The details of vehicle types along with the materials details and their loaded and unloaded passes with respective weights are given in Table 6.5. However, as per AASHTO design guide for pavements (1993), to standardize the effect of mix traffic i.e. single, double and tandem axle vehicles on pavements, the weights of vehicles are converted in to Equivalent Standard Axle Loads (ESAL's). Load Equivalency Factors (LEF), as provided by AASHTO 1993 design guide, are used for weight to ESAL conversion.

Accordingly, the considered vehicular loads on Jointed Plain Concrete Pavement (JPCP) and Jointed Wheat Straw Reinforced Concrete Pavement (JWSRCP) test sections are converted in Equivalent Standard Axle Loads (ESAL's) by using Load Equivalency Factors (LEF) for rigid pavements against the constructed PC and WSRC layer thicknesses for respective vehicles, as provided in Table D10, Table D11 and Table D12 of AASHTO 1993 Design Guide for Pavement Structures. The ESAL's in case of each loaded and unloaded vehicle and the total ESAL's, passed through PC and WSRC test sections over 18 – months period, are also given in Table 6.5. A total of 2.7×10^6 ESAL's are passed over the under studied pavement test sections in the specified period of 18 – months.

TABLE 6.5: Quantification of ESAL's on PC and WSRC test sections over 18-months period.

Vehicle	Material	No. of Passes	Actual Weight		ESAL's	
			Loaded Tonne	Unloaded Tonne	Loded + Unloaded $\times 10^6$	Total
(1)	(2)	(3)	(4)	(5)	(6)	(7)
Transit Mixer	Wet Concrete	79	2544	1147	0.66 + 0.03	0.69
Dumper	Sand	37	1510	503	0.61 + 0.01	0.61
	Aggregates	14	800	191	0.64 + 0.00	0.64
	Soil	3	113	41	0.03 + 0.00	0.04
Bedford Truck	Bricks	49	1200	667	0.17 + 0.01	0.18
18-Wheeler	Steel	16	2380	290	0.52 + 0.00	0.52
10-Wheeler	Cement	33	674	450	0.04 + 0.01	0.05
Pickup	Scaf./wood	15	38	10	0.00 + 0.00	0.00
Trolley	Sand	7	127	48	0.01 + 0.00	0.01
	Aggregates	3	75	20	0.01 + 0.00	0.01
Total:						2.7×10^6

The LEF for calculations of ESAL's are taken from Table D10, D11, D12 of AASHTO 1993 pavement design guide.

6.3.3.2 Load Carrying Capacities of PC and WSRC Pavement Test Sections

As mentioned in previous section, the mixed traffic loading (including multi-axle loadings) effect on pavements is encountered in terms of Equivalent Standard Axle Load (ESAL) to be taken as design consideration for pavement. The Load Equivalency Factor (LEF) is used for calculation of ESAL's for respective weight-axle loading combinations. The background of ESALs is encompassed with the live nature of pavements. As with every pass of each vehicle, the pavement is deflected up to some extent to bear the load of that particular vehicle in the form of deflection basin/bowl. After the vehicle is passed, the pavement structure regains its position but with a little permanent deformation. In this way, every pass of a vehicle causes a damage to the underlying pavement layer as per its loading condition. Therefore, the design life of pavements is based on the quantum of

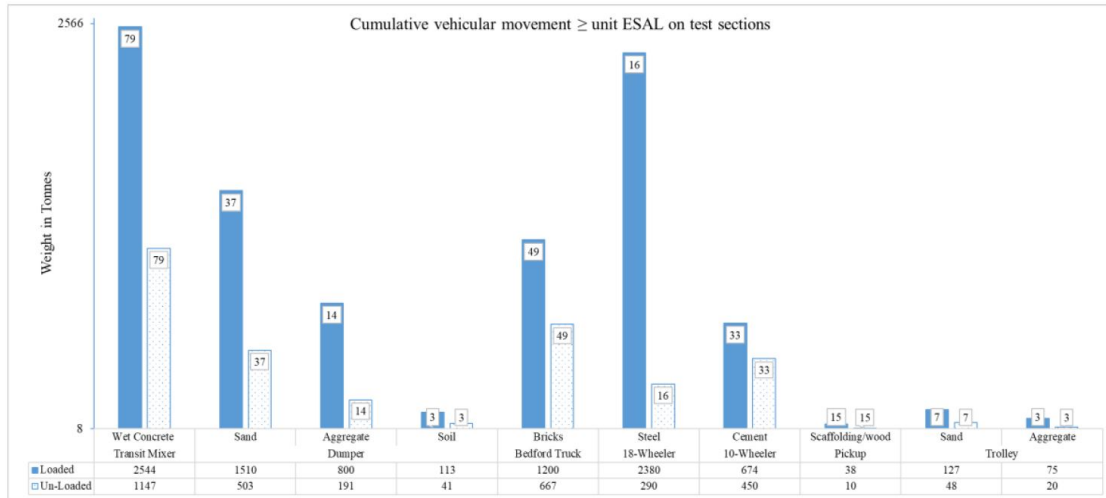


FIGURE 6.11: Per pass damaging vehicles with \geq ESAL on PC and WSRC pavement test sections.

vehicles pass over it. The higher the number of vehicles passes; the sooner will be the design life of pavement will come to end. Therefore, the primary design consideration in case of pavements is associated with ESAL's. As per standard definition, the vehicle having one ESAL (i.e. 8.2 tonnes) will cause unit damage to the pavement per pass. This definition doesn't mean that one pass of vehicle having the weight equivalent to double ESAL's (i.e. 16.4 tonnes) will cause double damage. Instead, it will cause 16 times more damage than in case of one ESAL; which basically is calculated from 4-power formula. In this way, each added tonne of loading greater than the standard axle load will damage the pavement with 4-times more extent than in standard case. Accordingly, among all the vehicles passed from PC and WSRC test sections, the cumulative vehicles of all types which are resulting in damaging of test sections, i.e. with at least 8.2 tonne (unit ESAL) or more, along with their no. of passes are shown in Figure 6.11. It is observed that concrete transit mixer, dumpers of sand, Bedford (design failure) trucks with loaded bricks and 18 – wheeler long haul trucks with steel loaded on them are major damage contributors. However, the damage provided by lighter weighed vehicles along with un-loaded passes for each vehicle is also accumulated.

In pursuance of structural performance of PC and WSRC pavement test sections, the deflection measurements are made on both the test sections. The key measure

for evaluation of pavement's structural capacity is the deflection [132]. Accordingly, the Benkelman beam (BB) test is performed for the determination of deflections at several pre-determined points of PC and WSRC pavement test sections. The deflection measurements are taken at two different stages i.e. one under the loaded wheel path of specified vehicle/dumper on test section and the other is on a parallel unloaded portion of same test section. Deflection measurements at five different points on each test section are calculated with an interval of 1m between each point. Lever mechanism is followed while measuring deflections through Benkelman beam upon application of static or creep loading [281]. The BB test requires a standard temperature of $35^{\circ}C$ for its conduct which is not achievable all the time. So, to meet this requirement, a temperature correction factor is to be applied for deflection when measured at other than standard temperature. The 10 – wheeler dumper (loaded with 800 cft aggregates) is used for deflection measurements. The rear axle weight is 40 tonnes having 5.62 kg/cm^2 tyre pressure. The deflection gauge readings and deflections (i.e. D_o , D_i and D_f), mean deflection (D) at each point, the corrected deflection after temperature correction (X_i), and mean deflection (μ) of all the 5 points for both PC and WSRC pavement test sections are given in Table 6.6. All the above-mentioned parameters are also taken for un-loaded parallel points on both test sections as well for later on calculations of Load Transfer Efficiency (LTE). It is observed that the WSRC pavement test section shows slightly more (i.e. 5%) deflection when compared to PC pavement test section. The more deflection can be attributed towards a number of factors, including combined effect of reduced thickness and improved toughness, in JWS-RCP test section. However, the dominant factor, against enhanced toughness, seems to be the incorporation of uniformly dispersed straw as also reported by Farooqi and Ali [262]. Whereas, the PC slab/test-section, as expected, shows less deflection depicting the conventional brittle nature of plain concrete. The deflection basins/bowls, calculated by BB, of PC and WSRC pavement test sections are also shown in Figure 6.12 for having a clearer picture of pavement test sections performance after undergoing 2.7×10^6 ESAL's in 18 – months period. At the start and end points, this difference in deflection is less. As at joints, the load

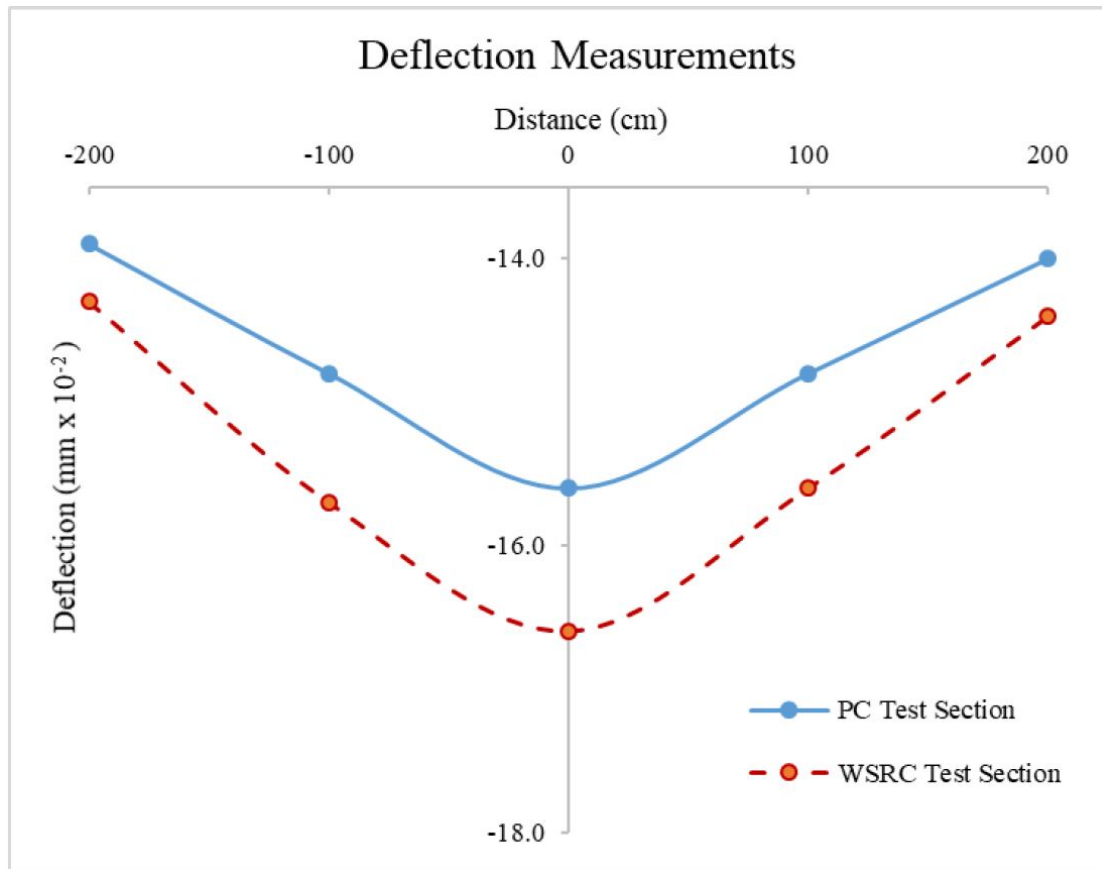


FIGURE 6.12: Benkelman beam deflection measurements for PC and WSRC pavement test sections

might be transferred to other slabs/test sections. However, the mid-span deflection of both PC and WSRC test sections are showing the true picture of their behavior with comparatively less brittle behavior in case of WSRC. This tough cum ductile behavior will ultimately result in enhanced load carrying capacity of WSRC pavement test section as more energy will be absorbed due to presence of dispersed straw in concrete and pavement will bear more load without initiation of any distress/cracking.

6.3.3.3 Load Transfer Efficiency (LTE) of PC and WSRC Pavement Test Sections

The potential location/point of distress in a jointed plain concrete pavement is the joint and each and every crack in it. Distresses like punchouts, faulting, corner breaks etc. are the commonly occurred distresses in this situation.

TABLE 6.6: Benkelman beam deflection measurements for PC and WSRC pavement test sections for both loaded and unloaded cases.

Test Sections	Location No	Dial Gauge Reading (DGR)			Deflection (mm) =DGR*Least Count			D	Temperature correction	Corrected Deflection Xi	Mean Deflection (mm) μ	$Xi = \mu$	$(Xi = \mu)^2$	Standard Deviation
		Do	Di	Df	Do	Di	Df							
		(3)	(4)	(5)	(6)	(7)	(8)							
(1)	(2)	(3)	(4)	(5)	(6)	(7)	(8)	(9)	(10)	(11)	(12)	(13)	(14)	(15)
PC Loaded	1	10.96	10.91	10.84	0.110	0.109	0.108	0.109	0.03	0.139	0.146	-0.014	0.0002	0.010
	2	11.30	12.00	11.99	0.113	0.120	0.120	0.118	0.03	0.148		-0.005	0.0000	
	3	12.49	12.66	12.62	0.125	0.127	0.126	0.126	0.03	0.156		0.003	0.0000	
	4	11.30	12.00	11.99	0.113	0.120	0.120	0.118	0.03	0.148		-0.005	0.0000	
	5	11.06	11.01	10.94	0.111	0.110	0.109	0.110	0.03	0.140		-0.013	0.0002	
Un-Loaded	1	2.63	2.58	2.51	0.026	0.026	0.025	0.026	0.03	0.056	0.062	-0.097	0.009	0.101
	2	2.54	3.24	3.23	0.025	0.032	0.032	0.030	0.03	0.060		-0.093	0.009	
	3	4.10	4.04	4.04	0.041	0.040	0.040	0.041	0.03	0.071		-0.082	0.007	
	4	3.81	3.83	3.81	0.038	0.038	0.038	0.038	0.03	0.068		-0.085	0.007	
	5	2.78	2.76	2.73	0.028	0.028	0.027	0.028	0.03	0.058		-0.095	0.009	
WSRC Loaded	1	11.31	11.26	11.19	0.113	0.113	0.112	0.113	0.03	0.143	0.153	-0.010	0.00011	0.010
	2	12.22	12.92	12.91	0.122	0.129	0.129	0.127	0.03	0.157		0.004	0.00002	
	3	13.51	13.68	13.64	0.135	0.137	0.136	0.136	0.03	0.166		0.013	0.00018	
	4	12.51	12.63	12.39	0.125	0.126	0.124	0.125	0.03	0.155		0.002	0.00001	
	5	11.36	11.34	11.31	0.114	0.113	0.113	0.113	0.03	0.143		-0.009	0.00009	
Un-Loaded	1	3.98	3.93	3.86	0.040	0.039	0.039	0.039	0.03	0.069	0.076	-0.084	0.007	0.086
	2	3.89	4.59	4.58	0.039	0.046	0.046	0.044	0.03	0.074		-0.079	0.006	
	3	5.18	5.35	5.31	0.052	0.054	0.053	0.053	0.03	0.083		-0.070	0.005	
	4	5.16	5.18	5.16	0.052	0.052	0.052	0.052	0.03	0.082		-0.071	0.005	
	5	4.13	4.11	4.08	0.041	0.041	0.041	0.041	0.03	0.071		-0.082	0.007	

The excessive loads or poor load design combinations cause the loss of load transferring at cracks and joints results in further deterioration of these distresses and/or initiation of additional new cracks/distresses. Therefore, the joints and cracks are main consideration while designing the rigid pavements [282]. The interlocking of aggregates in plain concrete provides the load transfer mechanism by resisting the vertical movement at joints and/or crack openings.

Moreover, this mechanism depends on the quantum of load and its repetitions and slab thickness. But, the effectiveness of this interlocking is limited to the small cracks and joints openings. As, greater the distance between opening of joint and/or cracks, the less will be the contact of surfaces and hence, load efficiency will be decreased based on the transference of load through shear. Afterwards, to enhance load transfer ability across joints and cracks in rigid pavements, the usage of steel dowels, key joints, tie bars and steel plates etc. are also used.

Accordingly, the Load Transfer Efficiency (LTE) for Jointed Plain Concrete Pavement (JPCP) and Jointed Wheat Straw Reinforced Concrete Pavement (JWSRCP) test sections, with dowels in both the cases, are also evaluated and are given in Table 6.7. The loaded and un-loaded corrected deflection measurements, as provided in Table 6.6, are used for the determination of LTE at each considered point. The averaged LTE for JPCP and JWSRCP test sections come out to 42.7% and 49.5%, respectively. The significant increase of 16% in LTE of JWSRCP test section, in comparison to JPCP test section, is due to the presence of wheat straw in addition to interlocking aggregates in concrete. The more energy absorption capability and strain capacity, as reported in previous sections, of WSRC pavement test section is the reason behind more LTE.

Furthermore, as already discussed, the effectiveness of LTE is reduced rapidly with every crack occurrence and the severity of cracks, in terms of crack mouth opening, in each crack. Therefore, the delay in crack initiation and resistance of crack propagation, due to the crack arresting mechanism provided by the presence of dispersed straw in concrete, results in comparatively less cracks and with smaller mouth openings, respectively. As, the load transfer efficiency (LTE) is gained

TABLE 6.7: Load Transfer Efficiency (LTE) of PC and WSRC pavement test sections.

Test Section	Corrected Deflections		Load Transfer Efficiency (LTE)	Averaged Load Transfer Efficiency (LTE)
	Loaded	Unloaded		
	mm	mm	%	%
(1)	(2)	(3)	(4)	(5)
PC	0.139	0.056	40.1	42.7
	0.148	0.060	40.7	
	0.156	0.071	45.3	
	0.148	0.068	46.2	
	0.140	0.058	41.1	
WSRC	0.143	0.069	48.6	49.5
	0.157	0.074	46.9	
	0.166	0.083	49.8	
	0.155	0.082	52.6	
	0.143	0.071	49.6	

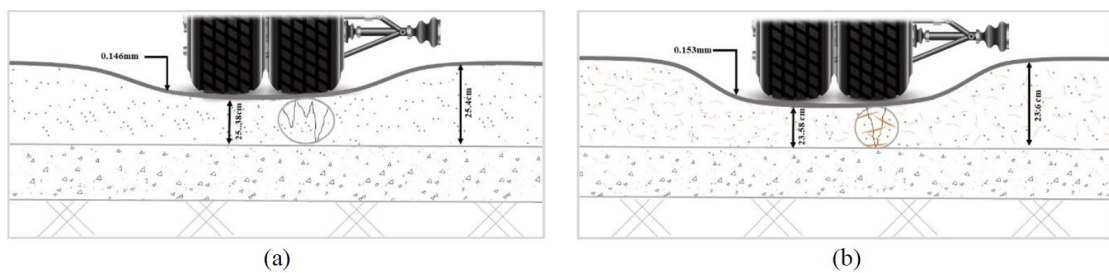


FIGURE 6.13: Behavior of (a) JPCP and (b) JWSRCP test sections in terms of LTE.

through shear, hence, the accomplishment of closer contact between two edges of surfaces at crack mouth opening is resulted in enhanced load transfer efficiency in jointed wheat straw reinforced concrete pavement test section. This mechanism of enhanced Load Transfer Efficiency in Jointed Wheat Straw Reinforced Concrete Pavement test section in comparison to Jointed Plain Concrete Pavement test section is shown in Figure 6.13 for having a clearer idea.

6.3.4 Crack Progression in PC and WSRC Pavement Test Sections

6.3.4.1 Crack Formation, Propagation and Patterns

The crack width, which leads towards development of punchouts is performance criterion of rigid pavements as per NCHRP 1-37A. Punchouts are one of the severe pavement distresses and usually occur as the result of clustered cracks based on their spacings [216]. The occurrence of cracks, their patterns, their propagation and finally punch-outs are surveyed, by bifurcation of the PC and WSRC pavement test sections into grids of $1 \times 1.1 \text{ m}^2$, at 28 days and 6, 12, and 18 months for observing early-age cracking and long-term cracks progression under the effect of vehicular movement, respectively. Accordingly, the JPCP and JWSRCP test sections with grids and their surface conditions at 6-months are shown in Figure 6.14. The approximate quantification of cracks with minimum and maximum widths are surveyed at all the considered stages. The clusters of cracks i.e. multiple cracks with $\leq 0.5 \text{ m}$ spacing, are also observed. Table 6.8 illustrates the cracks progression data for JPCP and JWSRCP test sections. The dimensions of cracks particularly crack widths, at 28-days in JPCP and JWSRCP test sections and at 6-months in JWSRCP section only, are too small to be measured. However, the no. of cracks along with their lengths and widths are progressed upon application of vehicular loading with passage of time. But this progression, in case of JWSRCP test section, is much less as compared to that in JPCP test section. The spacing in cracks is reduced with passage of time leading towards the formation of clusters of cracks. These cracks clusters are further progressed towards the development of punch-outs. The noticeable point here is that the crack openings and lengths are considerably less in case of JWSRCP test section due to crack arresting by straw. This phenomenon also results in less no. of cracks and more spacing between them to have restricted no. of crack clusters. Ultimately, it is found that no punch-out is developed in JWSRCP test section even after 18-months as compared to JPCP test section, where 2 punchouts are observed at 6-months (Figure 6.14)

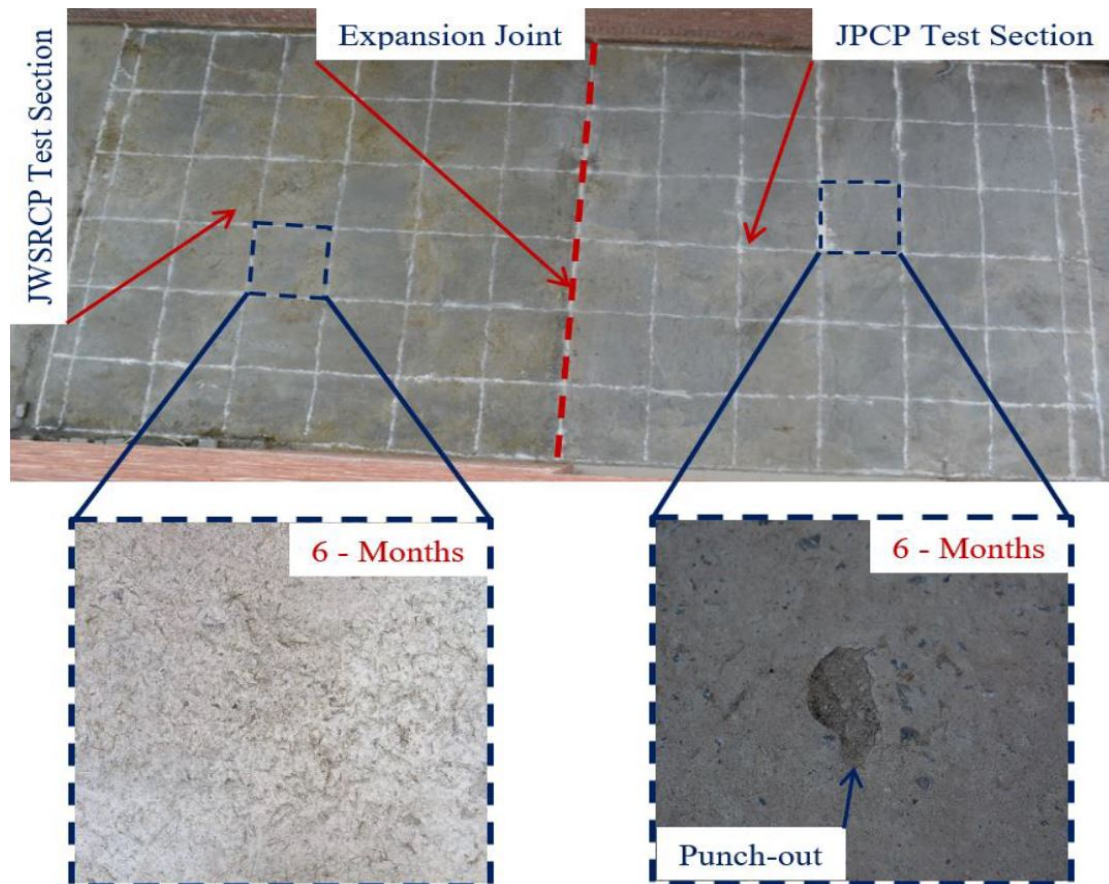


FIGURE 6.14: Cracks progression on JPCP and JWSRCP test sections.

which is raised up to 9 no. of punch-outs over 18-months. As also mentioned in earlier section, this crack arresting by straw in cement concrete proves to be highly favorable for the rigid pavements as ultimately resulted in enhanced Load Transfer Efficiency (LTE) of Jointed Wheat Straw Reinforced Concrete Pavement (JWSRCP) test section.

6.4 Modelling

6.4.1 Reduced Thickness Validation of WSRC Pavement

The compressive strength isn't the only parameter to gauge the structural performance of any structure, but the contribution of toughness is also there [249, 256, 257]. And, the dispersed straw are added with the intention to enhance

TABLE 6.8: Cracks progression and punch-out(s) in JPCP and JWSRCP test sections over 18-months period.

Test	Cracks	28-days	6	12	18
Section	Progression		Months	Months	Months
(1)	(2)	(3)	(4)	(5)	(6)
JPCP	Avg. Width (mm)	-	0.11	0.14	0.16
	Max. Length (m)	0.08	0.18	0.27	0.33
	Avg. Spacing (m)	3.6	2.9	2.1	1.1
	Cluster (no.)	1	5	12	19
	Punch-out (no.)	-	2	4	9
JWSRCP	Avg. Width (mm)	-	-	0.09	0.12
	Avg. Length (m)	0.03	0.08	0.12	0.19
	Avg. Spacing (m)	4.6	4.1	3.3	2.1
	Cluster (no.)	-	-	3	6
	Punch-out (no.)	-	-	-	-

the toughness of brittle natured conventional concrete pavement, not the strength [272]. The early-ager development/initiation of micro-cracking in rigid pavement, which are used to propagate rapidly under the application of loaded vehicular movement can be reduced with the help of dispersed straw. The straw, with the crack arresting mechanism, enhances the capacity of matrix to absorb higher energy. The reduced cracks and less cracks mouth openings will not let loose contact between the surfaces at edges of the cracks, which ultimately provides more contact area for effective load transfer efficiency of respective slab/panel/pavement, as load transfers through shear. As already mentioned, that Jointed Plain Concrete Pavement (JPCP) test section is designed with 25.4 cm thickness as per AASHTO design equation for rigid pavements (equation 6.1). Whereas, Jointed Wheat Straw Reinforced Concrete Pavement (JWSRCP) test section has 7% less thickness, as compared to JPCP test section, as recommended in an earlier study by Farooqi and Ali [262] via modified design equation for WSRC (equation 6.2). Therefore, the comparative performance indication of both the test sections is desired for the validation of modified empirical design equation for WSRC pavements proposed

by [262] .

Accordingly, for incorporating the toughness consideration in addition to the strength in the structural integrity of rigid pavements, the formulation of a performance index is done in current study. This performance index is based on the obtained results of Jointed Wheat Straw Reinforced Concrete Pavement (JWS-RCP) test section with respect to the controlled results in the case of conventional Jointed Plain Concrete Pavement (JPCP). The formulated performance index is as follows:

$$PI_{WSRC} = \frac{PI_{\sigma_f} + PI_{CTI_f} + PI_{\mu} + PI_{\mu'}}{4} \tag{6.3}$$

Where:

$$PI_{\sigma_f} = \frac{\sigma_{fWSRC}}{\sigma_{fPC}}$$

$$PI_{CTI_f} = \frac{CTI_{fWSRC}}{CTI_{fPC}}$$

$$PI_{\mu} = \frac{\mu_{WSRC}}{\mu_{PC}}$$

$$PI_{\mu'} = \frac{\mu'_{WSRC}}{\mu'_{PC}}$$

It may be noted here, that all the parameters used in equation (6.3) are those which are obtained during field investigation of JPCP and JWSRCP test sections. Furthermore, all the considered parameters are indexed with the base i.e. reference values obtained as the findings of JPCP test section. The WSRC net performance index is the averaged value of performance indices in terms of field investigated properties i.e. compressive strength (σ_f), compressive toughness index (CTI_f), mean Benkelman beam deflection in loaded case (μ) and mean Benkelman beam un-loaded deflection (μ'). The controlled value, as for JPCP test section, is the unit value. So, the Performance Index (PI) of WSRC is evaluated with respect to that unit value means the value greater than 1 will be depicting the better performance of WSRC pavement with the extent based on the positive incremental difference from 1. However, the PI with unit value 1 depicts the same performance

TABLE 6.9: Performance index of JPCP and JWSRCP test sections.

Test Section	Considered Properties	Obtained Results	Respective PI	Mean PI
(1)	(2)	(3)	(4)	(5)
$JPCP_{ref}$	σ_f (MPa)	19.8	1.00	1.00
(Design thickness of 25.4cm as per eq. 6.1)	CTI_f (-)	1.37	1.00	
	μ	0.146	1	
	μ'	0.062	1.00	
JWSRCP	σ_f (MPa)	18.8	0.95	1.15
(Design thickness of 23.6cm as as per eq. 6.2 by [262])	CTI_f (-)	1.89	1.38	
	μ	0.153	1.05	
	μ'	0.076	1.23	

level of WSRC as of PC. And the values ≤ 1 indicate low performance of WSRC, as the closer the value to 1 the more will be the comparable performance of WSRC with PC. The net mean Performance Indices (PI) of JWSRCP test section in comparison with JPCP test section are given in Table 6.9. Overall, 15% enhanced performance of JWSRCP test section having 7% less design thickness, with respect to reference JPCP test section, is indicated as per obtained findings. This enhanced performance of JWSRCP section leads towards validation of modified design equation (6.2) for WSRC pavements [262].

6.4.2 Empirical Relationship Between Laboratory and Field Testing for WSRC Pavements

WSRC pavement test section with the optimized straw content (i.e. 1%, as reported by [267]) is constructed along with PC test section to evaluate the comparative performances of both the sections. However, the construction of multiple test sections to study variable parameters and/or properties of WSRC is not feasible all the time due to various constraints. So, there is a need to develop a co-relation between laboratory and field investigation of WSRC with the intention to anticipate

the performance of WSRC pavements through laboratory testing and findings. Accordingly, the cylinder specimens are cast at the time of laying of JWSRCP test section to be examined in laboratory for compressive properties (i.e. σ_c , ϵ_c , Cem_c , Cep_c , Ce_c , and CTI_c). Afterwards, the cores are drilled from test sections and are tested in laboratory in the same manner as for cylinder specimens. The same compressive properties (i.e. σ_f , ϵ_f , Cem_f , Cep_f , Ce_f , and CTI_f) are determined experimentally. The symmetry in the behaviors of cylinders and cores are observed but with varied result values. Accordingly, an empirical relationship, based on the obtained results, in the form of equation is developed, in the way as also reported by [273]. The empirical relation is devised in the current work by using the experimental data of laboratory and onsite tests by having best fit curve. By using this curve along with the simplified input coefficient variable, the numerical prediction of field results, i.e. core compressive strengths (σ_f) can be made from data of laboratory results. The formulated empirical equation is as follows:

$$\sigma_f = 13 \ln \sigma_c - 20 \quad (6.4)$$

Where; σ_c is the compressive strength values obtained through laboratory testing and σ_f is the numerically predicted onsite compressive strength.

By using this equation (6.4), the field values can be extracted through testing of standard specimens of WSRC with desired variables. These field values then can be used for the prediction of WSRC pavement performance as per devised performance index in earlier section.

6.5 Summary

The structural performance of concrete reinforced with plant fibres is evaluated for rigid pavement applications. The experimental laboratory and field investigations of Jointed Plain Concrete Pavement (JPCP) and Jointed Wheat Straw Reinforced Concrete Pavement (JWSRCP), with 1% straw content, test sections are made in

detail. In-depth crack progression mechanism and straw-concrete bonding in JWSRCP test section along with its structural integrity are explored. The conclusions are as follows:

- The compressive energies absorbed by WSRC cylinder specimens and drilled cores are significantly enhanced by 50% and 34%, respectively, with 97% and 136%, respectively, higher energies absorption post the maximum stress in comparison with PC. However, compressive strengths in case of WSRC cylinders and cores are slightly declined by 7% and 5%, respectively, when compared to that of PC.
- The uniform dispersion of straw in concrete, when mixed in bulk quantity and laid with proper compaction, is observed with dominance of straw slippage/pull-out mechanism that results in enhanced energy absorption capacity of WSRC, as revealed by SEM analysis.
- The Benkelman beam deflection measurements show 5% more deflection in WSRC pavement test section as compared to PC pavement test section after the application of 2.7×10^6 ESAL's over 18-months period. The more deflection indicates the tough nature of WSRC which is then resulted in 16% more Load Transfer Efficiency (LTE) of JWSRCP test section, when compared to that of conventionally brittle JPCP test section.
- The cracks progression mechanism in JWSRCP test section is far less i.e. the crack widths, lengths and clusters are reduced by 25%, 42%, and 32%, respectively, with not a single punch-out even after 18-months, than that in JPCP test section.
- The mean performance index of JWSRCP, having 7% less design thickness than JPCP, is enhanced up to 15% which shows the comparable structural performance of WSRC with respect to PC for rigid pavement applications.

WSRC having 1% soaked straw, by mass of wet concrete, is optimized due to better material properties and admissible durability. The enhanced structural capacity of

optimized WSRC, in terms of flexural strength, is come out with modified design equation resulting in 7% less thickness. Consequently, the JWSRCP, constructed as per modified design, is performed better than that of conventionally designed PC pavement. Thus, based on the laboratory and field investigation findings in this doctoral study, Jointed Wheat Straw Reinforced Concrete Pavement (JWSRCP) is likely to be executed as commercial lane in 12,131 km length of highways, i.e. 4.6% of Pakistan road network system to accommodate heavy traffic, i.e. 65% of total commercial freight. In this way, the economical and sustainable development can be achieved in terms of 14% construction cost and 28% CO_{2e} emissions reduction, respectively. However, the Life Cycle Cost Analysis (LCCA) and Life Cycle Assessment (LCA), in terms of sustainability (from cradle to grave) for WSRC pavements are recommended to be explored in detail.

Chapter 7

Conclusions and Recommendations

7.1 Conclusions

The overall objective of the research program is to provide the economical and durable design, and construction techniques for new rigid pavements to have improved and better road network. However, this doctoral study has aimed to explore five correlated tasks. The identification of pavement distresses and quest for possible remedial measures led towards the exploration of alternative economical construction material, i.e. natural fibres. Wheat straw are selected to start with. The optimization, in terms of straw content and treatment technique, is made for having Wheat Straw Reinforced Concrete (WSRC) with favorable material properties. Experimental investigations, under compressive, splitting-tensile and flexural loadings, are made to evaluate mechanical properties of WSRC with 1%, 2%, and 3% content of soaked, boiled and NaOH treated straw. The residual behaviors of WSRC matrices are also determined experimentally after exposure to room, climatic and accelerated ageing conditions for 4 years. The structural capacity of optimized WSRC with flexural and shear reinforcement is also evaluated and a modified design equation is proposed for WSRC pavements. The first ever

Jointed WSRC Pavement (JWSRCP) test section is also constructed on the basis of proposed design for field investigations. The structural performance of JWSRCP is evaluated in terms of deflection and in-depth crack progression mechanism after application of vehicular loading and real climatic conditions. The properties of Plain Concrete (PC) are taken as reference in all the tasks. Micro-structural analysis is also performed at all the stages. The findings of conducted research contribute towards attainment of specific goals of this PhD study.

The summarized conclusions of this doctoral study are as follows:

- The most commonly occurred distresses in rigid pavements of developing countries are early-age micro cracking and punch-outs. The cracking rate in concrete pavements are related to multiple factors like differential settlement, shrinkage, poor resistance against tension and bending. Reinforcement of concrete with dispersed fibres can enhance the tensile bending performance of rigid pavements [22, 27, 29].
- Soaked Wheat Straw Reinforced Concrete, having 1% straw content, (SWSRC-1%) is optimized in terms of enhanced CTI, STI and FTI by 91%, 105% and 92%, respectively, when compared to that of PC.
 - The changed surface conditions of straw in case of boiling and chemical treatment are resulted in comparatively less performance of BWSRC and CWSRC. And, 1% straw, by mass of wet concrete, show better mechanical properties in comparison with 2% and 3% straw content.
 - As revealed from SEM, the better bonding of uncracked surfaced soaked straw with the surrounding matrix is resulted in enhanced properties of SWSRC. Contrary to this, the boiling and chemical treatment results in straw damage as revealed by XRD and TGA.
- Likewise, after 4 years, SWSRC-1% is performed better, in terms of enhanced residual strengths, residual energies absorbed and residual toughness indices, among all the WSRC matrices.

- At 4-years age under natural weathering conditions, the CTI_r , STI_r , and FTI_r of SWSRC-1% are increased by 5%, 27% and 108%, respectively.
- Dense interfacial transition zone is observed between straw – matrix bond at all the three ageing conditions, as revealed by SEM. Soaked straw is slightly affected by the natural weathering, as extracted from XRD and TGA patterns.
- Performance index for a WSRC structure, under the exposure to open-air weathering for 20-years, is comparable with that of PC.
- The improved post-cracking behavior, delay in first crack initiation, and more resistance against crack propagation in case of WSRC is observed, which is highly favorable for concrete pavements. Based on enhanced flexural strength, a modification in AASHTO design is proposed for WSRC pavements.
 - Considerable enhancement of 7.5%, 44.8%, 30.4%, and 11.7% in FS, FEP, FE, and FTI, respectively, of WSRC with flexural rebars are observed when compared to PC. Accordingly, the moment capacities of WSRC with flexural and shear rebars also increased up to 2.8% and 2%, respectively, in comparison to PC.
 - Increase in FS, FEP, FE, and FTI of WSRC with shear steel rebars are up to 6%, 27%, 30.1%, and 11.2% w.r.t that of respective PC specimens. Shear capacities of WSRC specimens with flexural and shear rebars are increased up to 7.3% and 6.3%, respectively.
 - As per proposed design for WSRC pavements, the slab thickness is decreased up to 7% for WSRC as compared to PC for same design considerations. Accordingly, the construction cost and CO_{2e} emissions are also reduced by 14% and 28%, respectively, as compared to PC.
- The mean performance index of JWSRCP, having 7% less design thickness than JPCP, is enhanced up to 15%, which shows the comparable structural performance of WSRC with respect to PC for rigid pavement applications.

- The Ce_c and Ce_f of WSRC are significantly increased by 50% and 34%, respectively, with 97% and 136% higher Cep_c and Cep_f , respectively, in comparison with PC.
- As per Benkelman beam apparatus testing, μ in JWSRCP is 5% more than that in JPCP after the application of 2.7×10^6 ESAL's over 18-months period. The higher μ is further resulted in 16% more LTE of JWSRCP.
- As far as the crack progression mechanism in JWSRCP test section is concerned, the crack widths, lengths and clusters are shrunk by 25%, 42%, and 32%, respectively, with not a single punch-out even after 18-months, w.r.t JPCP test section.

Hence, based on the laboratory and field investigation findings in this doctoral study, Jointed Wheat Straw Reinforced Concrete Pavement (JWSRCP) is likely to have the potential as dedicated additional lane in 12,131 km length of highways, i.e. 4.6% of Pakistan road network system, to accommodate heavy traffic, i.e. 65% of total commercial freight. In this way, the economical and sustainable development of rigid pavements can be achieved in terms of 14% less construction cost and 28% less CO_{2e} emissions, respectively.

7.2 Recommendations for Future Research

There is always an open way to explore multiple horizons in never ending research process. The same is at the end of this particular research step, i.e. this doctoral study. There are various gaps to be explored for the sustainable development of rigid pavements by using the locally and abundantly available natural fibres. Accordingly, the future recommendations are summarized as follows:

- The behavior of continuous wheat straw reinforced concrete pavement should also be evaluated under real traffic and climatic conditions (keeping in mind moisture infiltration factor).

-
- The Life Cycle Cost Analysis (LCCA) of wheat straw reinforced concrete pavement, by including the processing and transportation of wheat straw as well, should also be done to explore the economic aspect of its utilization as a product.
 - For the sustainable development, the Life Cycle Assessment (LCA), from cradle to grave, of wheat straw reinforced concrete pavement should also be performed in detail.
 - In addition, straw pre-treatment techniques, in terms of enhancing durability, should also be explored to have more optimized matrix.
 - In parallel, the potential of other locally available natural/agricultural/plant fibres (i.e. rice straw and sugar-cane bagasse) for the possible use as an alternative civil engineering construction material should also be explored with intention to have sustainable development.
 - The combination of all the three available natural fibres to be incorporated in cementitious composites would also be an interesting study.

Bibliography

- [1] J. E. Hiller and J. R. Roesler, “Determination of critical concrete pavement fatigue damage locations using influence lines,” *Journal of Transportation Engineering*, vol. 131, no. 8, pp. 599–607, 2005.
- [2] J. P. Romualdi and G. B. Batson, “Mechanics of crack arrest in concrete,” *Journal of Engineering Mechanics*, vol. 89, 1963.
- [3] J. P. Romualdi and J. A. Mandel, “Tensile strength of concrete affected by uniformly distributed and closely spaced short lengths of wire reinforcement,” *Journal Proceedings*, vol. 61, no. 6, pp. 657–672, 1964.
- [4] H. W. Reinhardt and A. E. Naaman, “High performance fibre reinforced cement composites,” *Mains Germany: Third International RILEM Workshop*, 1999.
- [5] A. Bentur and S. Mindess, “Fiber reinforced cementitious composites,” *Modern concrete technology series: Taylor and Francis, Second Edition.*, 2007.
- [6] E. Erdogmus, “Use of fiber-reinforced cements in masonry construction and structural rehabilitation,” *Fibers*, vol. 3, no. 1, pp. 41–63, 2015.
- [7] J. Perez-Garcia, B. Lippke, D. Briggs, J. B. Wilson, J. Bowyer, and J. Meil, “The environmental performance of renewable building materials in the context of residential construction,” *Wood and Fiber Science*, vol. 37, pp. 3–17, 2007.

- [8] A. Hassan, M. Arif, and M. Shariq, “A review of properties and behaviour of reinforced geopolymer concrete structural elements—a clean technology option for sustainable development,” *Journal of Cleaner Production*, pp. 118–762, 2019.
- [9] D. Qian, R. Yu, Z. Shui, Y. Sun, C. Jiang, F. Zhou, and Y. He, “A novel development of green ultra-high-performance concrete (UHPC) based on appropriate application of recycled cementitious material,” *Journal of Cleaner Production*, pp. 121–231, 2020.
- [10] V. Jittin, A. Bahurudeen, and S. D. Ajinkya, “Utilisation of rice husk ash for cleaner production of different construction products,” *Journal of Cleaner Production*, pp. 121–578, 2020.
- [11] G. Ramakrishna and T. Sundararajan, “Studies on the durability of natural fibres and the effect of corroded fibres on the strength of mortar,” *Cement and Concrete Composites*, vol. 27, no. 5, pp. 575–582, 2005.
- [12] P. Paramasivam, G. K. Nathan, and N. D. Gupta, “Coconut fibre reinforced corrugated slabs,” *International Journal of Cement Composites and Lightweight Concrete*, vol. 6, no. 1, pp. 19–27, 1984.
- [13] K. G. Satyanarayana, K. Sukumaran, P. S. Mukherjee, C. Pavithran, and S. G. K. Pillai, “Natural fibre-polymer composites,” *Cement and Concrete composites*, vol. 12, no. 2, pp. 117–136, 1990.
- [14] V. Agopyan, H. Savastano, V. M. John, and M. A. Cincotto, “Developments on vegetable fibre–cement based materials in são paulo, brazil: an overview,” *Cement and Concrete Composites*, vol. 27, no. 5, pp. 527–536, 2005.
- [15] R. D. T. Filho, L. Ghavami, G. L. England, and K. Scrivener, “Development of vegetable fibre–mortar composites of improved durability,” *Cement and Concrete Composites*, vol. 25, no. 2, pp. 185–196, 2003.

- [16] Z. Li, L. L. Wang, and X. A. Wang, "Cement composites reinforced with surface modified coir fibers," *Journal of composite materials*, vol. 41, no. 12, pp. 1445–1457, 2007.
- [17] S. S. Munawar, K. Umemura, and S. Kawai, "Characterization of the morphological, physical, and mechanical properties of seven nonwood plant fiber bundles," *Journal of Wood Science*, vol. 53, no. 2, pp. 108–113, 2007.
- [18] I. Merta and E. K. Tschegg, "Fracture energy of natural fibre reinforced concrete," *Construction and Building Materials*, vol. 40, pp. 991–997, 2013.
- [19] M. Ali, "Use of coconut fibre reinforced concrete and coconut-fibre ropes for seismic-resistant construction," *Materiales de Construcción*, vol. 73, 2016.
- [20] V. Ramakrishnan, G. Y. Wu, and G. Hosalli, "Flexural fatigue strength, endurance limit, and impact strength of fiber reinforced concretes," *Transportation Research Record*, pp. 12–26, 1989.
- [21] C. Achilleos, D. Hadjimitsis, K. Neocleous, K. Pilakoutas, P. O. Neophytou, and S. S. Kallis, "Proportioning of steel fibre reinforced concrete mixes for pavement construction and their impact on environment and cost," *Sustainability*, vol. 3, no. 7, pp. 965–983, 2011.
- [22] S. Gupta, V. K. Rao, and J. Sengupta, "Evaluation of polyester fiber reinforced concrete for use in cement concrete pavement works," *Road Materials and Pavement Design*, vol. 9, no. 3, pp. 441–461, 2011.
- [23] A. G. Graeff, K. Pilakoutas, K. Neocleous, and M. V. N. Peres, "Fatigue resistance and cracking mechanism of concrete pavements reinforced with recycled steel fibres recovered from post-consumer tyres," *Engineering Structures*, vol. 45, pp. 385–395, 2012.
- [24] N. Salemi and K. Behfarnia, "Effect of nano-particles on durability of fiber-reinforced concrete pavement," *Construction and Building Materials*, vol. 48, pp. 934–941, 2013.

- [25] A. Rai and D. Y. Joshi, “Applications and properties of fibre reinforced concrete,” *International Journal of Engineering Research and Applications*, vol. 4, no. 5, pp. 123–131, 2014.
- [26] D. Sinha, C. B. Mishra, and R. V. Solanki, “Comparison of normal concrete pavement with steel fiber reinforced concrete pavement,” *Indian Journal of Applied Research*, vol. 4, no. 8, pp. 233–235, 2014.
- [27] S. A. Kanalli, R. Palankar, B. Kumar, P. Kumar, and P. SK, “Comparative study of polymer fibre reinforced concrete with conventional concrete pavement. IJRET:,” *International Journal of Research in Engineering and Technology-ISSN*, pp. 1163–2319, 2014.
- [28] K. K. Paramod, A. K. Desai, Shivamant, and R. B. Shrikant, “Steel fiber reinforced concrete pavement: A review.,” *International Journal for Innovative Research in Science and Technology*, vol. 10, no. 1, pp. 275–276, 2015.
- [29] P. R. Kumar, S. Vijaybaskaran, R. PrasannaVenkatesh, S. V. Saravannamoorth, and M. Srinath, “Effect of steel and polypropylene fibres on the strength characteristics of a cement concrete overlay,” *International Journal of ChemTech Research*, vol. 6, no. 8, pp. 621–627, 2015.
- [30] M. Shamsaei, I. Aghayan, and K. A. Kazemi, “Experimental investigation of using cross-linked polyethylene waste as aggregate in roller compacted concrete pavement,” *Journal of Cleaner Production*, vol. 165, pp. 290–297, 2017.
- [31] A. Sassani, A. Arabzadeh, H. Ceylan, S. Kim, S. S. Sadati, K. Gopalakrishnan, and H. Abdulllah, “Carbon fiber-based electrically conductive concrete for salt-free deicing of pavements,” *Journal of Cleaner Production*, vol. 203, pp. 799–809, 2018.
- [32] E. Khankhaje, M. Rafeizonooz, M. R. Salim, R. Khan, J. Mirza, and H. C. Siong, “Sustainable clean pervious concrete pavement production incorporating palm oil fuel ash as cement replacement,” *Journal of Cleaner Production*, vol. 172, pp. 1476–1485, 2018.

- [33] A. Alsaif, R. Garcia, F. P. Figueiredo, K. Neocleous, A. Christofe, M. Guadagnini, and K. Pilakoutas, “Fatigue performance of flexible steel fibre reinforced rubberised concrete pavements,” *Engineering Structures*, vol. 193, pp. 170–183, 2019.
- [34] J. Chen, R. Chuu, H. Wang, L. Zhang, X. Chen, and Y. Du, “Alleviating urban heat island effect using high-conductivity permeable concrete pavement,” *Journal of Cleaner Production*, vol. 237, pp. 117–722, 2019.
- [35] R. Chan, M. A. Santana, A. M. Oda, R. C. Paniguel, L. B. Vieira, A. D. Figueiredo, and I. Galobardes, “Analysis of potential use of fibre reinforced recycled aggregate concrete for sustainable pavements,” *Journal of Cleaner Production*, vol. 218, pp. 183–191, 2019.
- [36] E. J. Elizondo-Martínez, V. C. Andrés-Valeri, J. Rodríguez-Hernández, and C. Sangiorgi, “Selection of additives and fibers for improving the mechanical and safety properties of porous concrete pavements through multi-criteria decision-making analysis,” *Sustainability*, vol. 12, no. 6, pp. 23–92, 2020.
- [37] S. Chen, “Strength of steel fibre reinforced concrete ground slabs,” *Proceedings of the Institute of Civil Engineers, Structures, and Buildings*, pp. 157–163, 2004.
- [38] Y. Mohammadi, H. M. Ghasemzadeh, T. Talari, and M. A. Ghorbani, “Replacing fibre reinforced concrete with bitumen asphalt in airports,” *Proceeding World Academy of Science Engineering and Technology*, vol. 58, pp. 30–34, 2009.
- [39] M. F. Canovas, N. H. Selva, and G. M. Kawiche, “New economical solutions for improvement of durability of portland cement mortars reinforced with sisal fibres,” *Materials and Structures*, vol. 25, no. 7, pp. 417–422, 1992.
- [40] M. A. Aziz, P. Paramasivam, and S. L. Lee, “Prospects for natural fibre reinforced concretes in construction,” *International Journal of Cement Composites and Lightweight Concrete*, vol. 3, no. 2, pp. 123–132, 1981.

- [41] J. Wei and B. Gencturk, “Degradation of natural fiber in cement composites containing diatomaceous earth,” *Journal of Materials in Civil Engineering*, vol. 30, no. 11, p. 04018282, 2018.
- [42] M. G. G.V.S. Deniel James I, “544.1r-96 state-of the-art report on fiber reinforced concrete,” *ACI Manual of Concrete Practice—Part 6*, 2003.
- [43] B. Mobasher, G. J. Haupt, and A. Pivacek, “Cement based cross-ply laminates,” *Advanced Cement Based Materials*, vol. 6, no. 3-4, pp. 144–152, 1997.
- [44] F. A. Silva, J. A. M. Filho, R. D. T. Filho, and E. R. M. Fairbairn, “Effect of reinforcement ratio on the mechanical response of compression molded sisal fibre textile reinforced concrete,” *High Fibre Reinforced Cement Composites*, pp. 175–182, 2007.
- [45] G. Ramakrishnan and T. Sundararajan, “Long-term strength and durability evaluation of sisal fiber composites,” *In Durability and Life Prediction in Biocomposites, Fibre-Reinforced Composites and Hybrid Composites*, pp. 211–255, 2019.
- [46] R. D. T. Filho, K. Scrivener, G. L. England, and K. Ghavami, “Durability of alkali-sensitive sisal and coconut fibres in cement mortar composites,” *Cement and Concrete composites*, vol. 22, no. 2, pp. 127–143, 2000.
- [47] Z. Li, L. Wang, and X. Wang, “Flexural characteristics of coir fiber reinforced cementitious composites,” *Fibers and Polymers*, vol. 7, no. 3, pp. 286–294, 2006.
- [48] M. Sivaraja, N. Velmani, and M. S. Pillai, “Study on durability of natural fibre concrete composites using mechanical strength and microstructural properties,” *Bulletin of Materials Science*, vol. 33, no. 6, pp. 719–729, 2010.

- [49] B. Poletanović, I. Merta, A. Šajna, A. M. Pranjić, and A. Mladenović, “Comparison of physical and mechanical properties of cementitious mortars reinforced with natural and synthetic fibres prior and after wet/dry cycles,” *Academic Journal of Civil Engineering*, vol. 37, no. 2, pp. 433–437, 2019.
- [50] J. Wei and B. Gencturk, “Degradation of natural fiber in cement composites containing diatomaceous earth,” *Journal of Materials in Civil Engineering*, vol. 30, no. 11, pp. 401–8282, 2019.
- [51] V. Mahalakshmi and P. S. Devi, “Prediction of mechanical and durability properties of treated natural fibres concrete,” *International Journal of Engineering Science*, pp. 217–288, 2019.
- [52] B. A. Akinyemi, A. Bamidele, and E. Joel, “Response of coir fibre reinforced cement composites to water repellent chemical additive and microwave accelerated curing,” *Cellulose*, vol. 26, no. 8, pp. 4987–4999, 2019.
- [53] M. Pigeon, J. Marchand, and R. Pleau, “Frost resistant concrete,” *Construction and Building Materials*, vol. 10, no. 5, pp. 339–348, 1996.
- [54] S. H. Kim and J. M. Gregory, “Straw to grain ratio equation for combine simulation,” *Journal of Biosystems Engineering*, vol. 40, no. 4, pp. 314–319, 2015.
- [55] S. Searle and C. Malins, “Availability of cellulosic residues and wastes in the eu,” *International Council on Clean Transportation*, 2013.
- [56] R. R. C. Bakker, H. W. Elbersen, R. P. Poppens, and J. P. Lesschen, “Rice straw and wheat straw-potential feedstocks for the biobased economy,” *NL Agency*, 2015.
- [57] S. Ammara, A. Fakhra, and A. Amber, “Processing of rice and wheat husk for the potential utilization of material for pottery products,” *International Research Journal of Environmental Sciences*, vol. 3, no. 7, pp. 7–14, 2014.
- [58] A. Neville, “Properties of concrete (vol. 4): Longman london,” 1995.

- [59] H. G. Van Oss and A. C. Padovani, “Cement manufacture and the environment part ii: environmental challenges and opportunities,” *Journal of Industrial ecology*, vol. 7, no. 1, pp. 93–126, 2003.
- [60] B. Cai, J. Wang, J. He, and Y. Geng, “Evaluating co2 emission performance in china’s cement industry: an enterprise perspective,” *Applied energy*, vol. 166, pp. 191–200, 2016.
- [61] S. Supino, O. Malandrino, M. Testa, and D. Sica, “Sustainability in the eu cement industry: the italian and german experiences,” *Journal of Cleaner Production*, vol. 112, pp. 430–442, 2016.
- [62] S. A. Memon, I. Wahid, M. K. Khan, M. A. Tanoli, and M. Bimaganbetova, “Environmentally friendly utilization of wheat straw ash in cement-based composites,” *Sustainability*, vol. 10, no. 5, p. 1322, 2018.
- [63] M. Sellers and N. O. Nawari, “Bamboo fibre-reinforced composites for tall buildings,” *Journal of Construction and Building Materials*, vol. 1, no. 1, 2016.
- [64] Y. Florentin, D. Pearlmutter, B. Givoni, and E. Gal, “A life-cycle energy and carbon analysis of hemp-lime bio-composite building materials,” *Energy and Buildings*, vol. 156, pp. 293–305, 2017.
- [65] M. Patel, C. Bastioli, L. Marini, and E. Würdinger, “Environmental assessment of bio-based polymers and natural fibres,” *Netherlands: Utrecht University*, 2002.
- [66] M. Ali, A. Liu, H. Sou, and N. Chouw, “Mechanical and dynamic properties of coconut fibre reinforced concrete,” *Construction and Building Materials*, vol. 30, pp. 814–825, 2012.
- [67] M. Rahim, O. Douzane, T. A. Le, G. Promis, and T. Langlet, “Characterization and comparison of hygric properties of rape straw concrete and hemp concrete,” *Construction and Building Materials*, vol. 102, pp. 679–687, 2016.

- [68] J. E. Fernandez, “Flax fibre reinforced concrete – a natural fibre bio composite for sustainable building materials.,” *High Performance Structures and Materials*, C.A Brebbia and W.P. Wilde, Editors Seville, pp. 193–207, 2002.
- [69] E. Booya, K. Gorospe, H. Ghaednia, and S. Das, “Durability properties of engineered pulp fibre reinforced concretes made with and without supplementary cementitious materials,” *Composites Part B: Engineering*, vol. 172, pp. 376–386, 2019.
- [70] S. Mehdipour, I. M. Nikbin, S. Dezhampanah, R. Mohebbi, H. Moghadam, S. Charkhtab, and A. Moradi, “Mechanical properties, durability and environmental evaluation of rubberized concrete incorporating steel fiber and metakaolin at elevated temperatures,” *Journal of Cleaner Production*, pp. 120–126, 2020.
- [71] S. Mindess and L. Zhang, “Impact resistance of fibre reinforced concrete,” *In proceedings of the institution of civil engineers structures and buildings*, SBI: 69–76 (Paper no. 700063), 2009.
- [72] C. Asasutjarita, J. Hirunlabh, J. Khedari, S. Charoenvai, B. Zeghmami, and U. C. Shin, “Development of coconut coir-based lightweight cement board,” *Construction and Building Materials*, vol. 21, no. 2, pp. 277–288, 2007.
- [73] M. Ali and N. Chouw, “Dynamic testing of coir fibre reinforced concrete beam,” *8th International conference on Shock and Impact Loads On Structures*, University of Adelaide, Australia, pp. 137–144, 2009.
- [74] D. S. Mahler and Z. B. Kharoufa, “Image processing for a pavement crack monitor,” tech. rep., 1990.
- [75] J. Bisschop and J. van Mier, “How to study drying shrinkage microcracking in cement-based materials using optical and scanning electron microscopy,” *Cement and concrete research*, vol. 32, no. 2, pp. 279–287, 2002.
- [76] J. Feiteira, E. Tsangouri, E. Gruyaert, C. Loris, G. Louis, and N. D. Belie, “Monitoring crack movement in polymer-based self-healing concrete through

- digital image correlation, acoustic emission analysis and sem in-situ loading,” *Materials and Design*, vol. 115, pp. 238–246, 2017.
- [77] W. Choi, S. Jang, and H. Yun, “Interface bond characterization between fibre and cementitious matrix,” *International Journal of Polymer Science*, 2015.
- [78] M. D. D’Ambrosia, S. Altoubat, C. Park, and D. A. Lange, “Early age tensile creep and shrinkage of concrete with shrinkage reducing admixtures,” *In Proc., of the 6th International Conference on Creep, Shrinkage, and Durability Mechanics of Concrete and Other QuasiBrittle Materials*, 2001.
- [79] A. C. A. Suja and M. M. Marliyas, “Identification of problems in rigid pavements in ampara district and proposed solutions.,” 2016.
- [80] H. J. Treybig, P. Smith, and H. VonQuintus, “Overlay design and reflection cracking analysis for rigid pavements—vol. 1. development of new design criteria.,” 1977.
- [81] F. Hernández-Olivares, G. Barluenga, B. Parga-Landa, M. Bollati, and B. Witoszek, “Fatigue behaviour of recycled tyre rubber-filled concrete and its implications in the design of rigid pavements,” *Construction and building materials*, vol. 21, no. 10, pp. 1918–1927, 2007.
- [82] M. Mubarak, A. Elhady, and H. Sallam, “Mixed mode fracture toughness of recycled tire rubber-filled concrete for airfield rigid pavements,” *International Journal of Pavement Research and Technology.*, 2013.
- [83] L. Sheng, L. Xingwu, and L. Zhaohui, “Interlaminar shear fatigue and damage characteristics of asphalt layer for asphalt overlay on rigid pavement,” *Construction and Building Materials*, vol. 68, pp. 341–347, 2014.
- [84] R. S. McDaniel, J. Olek, B. J. Magee, A. Behnood, and R. Pollock, “National cooperative highway research program, nchrp synthesis 463,” *Pavement Patching Practices-A Synthesis of Highway Practice*, 2014.

- [85] T. Subramani and A. Kumaravel, "Analysis of polymer fibre reinforced concrete pavements by using ansys," *International Journal of Application or Innovation in Engineering and Management (IJAIEM)*, pp. 132–139, 2016.
- [86] Y. Guan, Y. Gao, R. Sun, M. C. Won, and Z. Ge, "Experimental study and field application calcium sulfoaluminate cement for rapid repair of concrete pavements," *Frontiers of Civil and Structural Engineering*, vol. 11, no. 3, pp. 338–345, 2017.
- [87] K. Kim, S. Han, M. Tia, and J. Green, "Optimization of parameters to minimize horizontal cracking in continuously reinforced concrete pavement (CRCP) using finite element analysis," *97th Annual Meeting of Transportation Research Board. (No. 18-00263)*, 2018.
- [88] G. D. Zollinger, "Investigation of punchout distress of continuously reinforced concrete pavement," 1990.
- [89] X. Shi, A. Mukhopadhyay, D. Zollinger, and Z. Grasley, "Economic input-output life cycle assessment of concrete pavement containing recycled concrete aggregate," *Journal of cleaner production*, vol. 225, pp. 414–425, 2019.
- [90] M. B. Khurshid, M. Irfan, S. Labi, and K. C. Sinha, "Cost effectiveness of rigid pavement rehabilitation treatments," in *Proceedings of 7th International Conference on Managing Pavement Assets (ICMPA)*, Citeseer, 2008.
- [91] M. J. Minhoto, J. C. Pais, P. A. Pereira, and L. G. Picado-Santos, "The influence of temperature variation in the prediction of the pavement overlay life," *Road materials and pavement design*, vol. 6, no. 3, pp. 365–384, 2005.
- [92] M. A. Rasol, V. Pérez-Gracia, M. Solla, J. C. Pais, F. M. Fernandes, and C. Santos, "An experimental and numerical approach to combine ground penetrating radar and computational modelling for the identification of early cracking in cement concrete pavements," *NDT & E International*, p. 102293, 2020.

- [93] R. Chaudry and A. B. Memon, "Effects of variation in truck factor on pavement performance in pakistan," *Mehran University Research Journal of Engineering and Technology*, vol. 32, no. 1, pp. 19–30, 2013.
- [94] S. Singh, G. D. Ransinchung, and K. Monu, "Sustainable lean concrete mixes containing wastes originating from roads and industries," *Construction and Building Materials*, vol. 209, pp. 619–630, 2019.
- [95] Y. Mehta, D. Cleary, and A. W. Ali, "Field cracking performance of air-field rigid pavements," *Journal of Traffic and Transportation Engineering (English Edition)*, vol. 4, no. 4, pp. 380–387, 2017.
- [96] S. I. Sarsam, "Comparative assessment of using visual and close range photogrammetry techniques to evaluate rigid pavement surface distresses," *Trends in Transport Engineering and Applications*, vol. 2, no. 2, pp. 28–36, 2019.
- [97] R. Silva, J. de Brito, and R. Dhir, "Use of recycled aggregates arising from construction and demolition waste in new construction applications," *Journal of Cleaner Production*, vol. 236, p. 117629, 2019.
- [98] R. H. Al-Rubae, A. A. Shubber, and H. Saad Khaleefah, "Evaluation of rigid pavement using the pavement condition index: A case study," *MSE&E*, vol. 737, no. 1, p. 012128, 2020.
- [99] C. Niken, M. Karami, P. Sasana, *et al.*, "Deep-hair-cracks mechanism of rigid pavement in humid tropical weather," in *IOP Conference Series: Materials Science and Engineering*, vol. 857, p. 012028, IOP Publishing, 2020.
- [100] M. Saberian, J. Li, and S. Setunge, "Evaluation of permanent deformation of a new pavement base and subbase containing unbound granular materials, crumb rubber and crushed glass," *Journal of Cleaner Production*, vol. 230, pp. 38–45, 2019.
- [101] P. N. Balagur and S. P. Shah, "Fibre reinforced cement composites," *Civil Engineering Series McGraw-Hill*, 1992.

- [102] M. Imam, L. Vandewalle, F. Mortelmans, and G. D. Van, "Shear domain of fibre reinforced high-strength concrete beams," *Engineering structures*, vol. 19, no. 9, pp. 738–747, 1997.
- [103] S. Furlan and J. B. de Hanai, "Shear behavior of fibre reinforced concrete beams," *Cement and Concrete Composites*, vol. 19, no. 4, pp. 359–366, 1997.
- [104] I. D. James, V. Gopalaratnam, and M. A. Galinat, "State of the art report on fibre reinforced concrete," *Manual Concrete Practice*, vol. 21, pp. 2–66, 2002.
- [105] A. F. Ashour, "Flexural and shear capacities of concrete beams reinforced with GFRP bars," *Construction and building materials*, vol. 20, no. 10, pp. 1005–1015, 2006.
- [106] K. S. Kene, V. S. Vairagade, and S. Sathawane, "Experimental study on behavior of steel and glass-fibre-reinforced-concrete composites," *Bonfring International Journal of Industrial Engineering and Management Science*, vol. 2, no. 4, p. 125, 2012.
- [107] V. R. Rathi, A. V. George, and S. R. Nawale, "Experimental study on glass-fibre-reinforced-concrete moderate deep beam," *International Journal of Innovative Research in Science Engineering and Technology*, vol. 3, no. 3, pp. 10639–10645, 2014.
- [108] A. Committee, "State of the art report on fibre reinforced concrete.," *Michigan, Farmington Hills*, 1996.
- [109] M. M. Kamal, M. A. Safan, Z. A. Etman, and R. A. salma, "Behavior and strength of beams cast with ultra high strength concrete containing different type of fibres," *HBRC journal*, vol. 10, no. 1, pp. 55–63, 2014.
- [110] J. Liu, H. Chen, B. Guan, K. Liu, J. Wen, and Z. Sun, "Influence of mineral nano-fibers on the physical properties of road cement concrete material," *Construction and Building Materials*, vol. 190, pp. 287–293, 2018.

- [111] A. M. Brandt, “Fibre reinforced cement-based (FRC) composites after over 40 years of development of building and civil engineering,” *Composite Structures*, vol. 86, pp. 3–8, 2008.
- [112] A. J. Majumdar, “Glass fibres and compositions containing glass fibres.” US Patent 3,887,386.
- [113] R. F. Zollo, “Fiber-reinforced concrete: an overview after 30 years of development,” *Cement and concrete composites*, vol. 19, no. 2, pp. 107–122, 1997.
- [114] V. Corinaldesi and G. Moriconi, “Durable fiber reinforced self-compacting concrete,” *Cement and concrete research*, vol. 34, no. 2, pp. 249–254, 2004.
- [115] L. C. Hollaway, “A review of the present and future utilisation of FRP composites in the civil infrastructure with reference to their important in-service properties,” *Construction and building materials*, vol. 24, no. 12, pp. 2419–2445, 2010.
- [116] R. Bagherzadeh, A. H. Sadeghi, and M. Latifi, “Utilizing polypropylene fibers to improve physical and mechanical properties of concrete,” *Textile Research Journal*, vol. 82, no. 1, pp. 88–96, 2011.
- [117] A. L. Ardeshana and A. K. Desai, “Durability of fiber reinforced concrete of marine structures,” *International Journal of Engineering Research and Applications*, vol. 2, no. 4, pp. 215–219, 2012.
- [118] F. B. A. Beshara, G. I. Shaaban, and T. S. Mustafa, “Nominal flexural strength of high strength fibre reinforced concrete beams,” *Arabian Journal for Science and Engineering*, vol. 37, no. 2, pp. 291–301, 2012.
- [119] A. Nilson, D. Darwin, and C. Dolan, “Design of concrete structures, 14th edition,” 2010.
- [120] D. Yoo and Y. S. Yoon, “Structural performance of ultra-high-performance concrete beams with different steel fibers,” *Engineering Structures*, vol. 102, pp. 409–423, 2015.

- [121] J. A. Purkiss, "Steel fibre reinforced concrete at elevated temperatures," *International Journal of Cement Composites and Lightweight Concrete*, vol. 6, no. 3, pp. 179–184, 1984.
- [122] B. Boulekbache, M. Hamrat, M. Chemrouk, and S. Amziane, "Flexural behaviour of steel fibre-reinforced concrete under cyclic loading," *Construction and Building Materials*, vol. 126, pp. 253–262, 2016.
- [123] A. Gholamhoseini, A. Khanlou, G. MacRae, A. Scott, S. Hicks, and R. Leon, "An experimental study on strength and serviceability of reinforced and steel fibre reinforced concrete (sfrc) continuous composite slabs," *Engineering Structures*, vol. 114, pp. 171–180, 2016.
- [124] S. P. Patil and K. K. Sangle, "Tests of steel fibre reinforced concrete beams under predominant torsion," *Journal of Building Engineering*, vol. 6, pp. 157–162, 2016.
- [125] A. T. Noaman, B. A. Bakar, H. M. Akil, and A. Alani, "Fracture characteristics of plain and steel fibre reinforced rubberized concrete," *Construction and Building Materials*, vol. 152, pp. 414–423, 2017.
- [126] M. Khan and M. Ali, "Use of glass and nylon fibers in concrete for controlling early age micro cracking in bridge decks," *Construction and Building Materials*, vol. 125, pp. 800–808, 2016.
- [127] Y. Wang, S. Backer, and V. C. Li, "An experimental study of synthetic fibre reinforced cementitious composites," *Journal of Materials Science*, vol. 16, no. 2, pp. 391–396, 1987.
- [128] A. F. Mufti, G. L. Jaeger, B. Bakht, and L. D. Wegner, "Experimental investigation of fibre-reinforced concrete deck slabs without internal steel reinforcement," *Canadian Journal of Civil Engineering*, vol. 20, no. 3, pp. 398–406, 1993.

- [129] J. Aidoo, K. A. Harries, and M. F. Petrou, “Fatigue behavior of carbon fiber reinforced polymer-strengthened reinforced concrete bridge girders,” *Journal of Composites for Construction*, vol. 8, no. 6, pp. 501–509, 2004.
- [130] M. Khan and M. Ali, “Effectiveness of hair and wave polypropylene fibers for concrete roads,” *Construction and Building Materials*, vol. 166, pp. 581–591, 2018.
- [131] C. Maalouf, C. Ingrao, F. Scrucca, T. Moussa, A. B. nd C. Tricase, and F. Asdrubali, “An energy and carbon footprint assessment upon the usage of hemp-lime concrete and recycled-pet façades for office facilities in france and italy,” *Journal of Cleaner Production*, vol. 170, pp. 1640–1653, 2018.
- [132] L. Zhou, Q. Wuand, and J. Ling, “Comparison of fwd and benkelman beam in evaluation of pavement structure capacity,” *In Paving Materials and Pavement Analysis*, pp. 405–411, 2010.
- [133] A. Korjenic, V. Petránek, J. Zach, and J. Hroudová, “Development and performance evaluation of natural thermal-insulation materials composed of renewable resources,” *Energy and Buildings*, vol. 43, no. 9, pp. 2518–2523, 2011.
- [134] J. Pinto, B. Vieira, H. Pereira, C. Jacinto, P. Vilela, A. Paiva, S. Pereira, V. M. C. F. Cunha, and H. Varum, “Corn cob lightweight concrete for non-structural applications,” *Construction and Building Materials*, vol. 34, pp. 346–351, 2012.
- [135] Y. Wu, C. Xia, L. Cai, A. C. Garcia, and S. Q. Shi, “Development of natural fiber-reinforced composite with comparable mechanical properties and reduced energy consumption and environmental impacts for replacing automotive glass-fiber sheet molding compound,” *Journal of Cleaner Production*, vol. 184, pp. 92–100, 2018.
- [136] A. O, D, O. M. Osuolale, and E. M. Ibitogbe, “Strength evaluation of co-cos nucifera fibre reinforced concrete,” *Journal of Engineering and Applied Sciences*, vol. 14, no. 21, pp. 8061–8066, 2019.

- [137] M. R. Ahmad, B. Chen, M. A. Haque, and S. F. A. Shah, "Utilization of industrial and hazardous waste materials to formulate energy-efficient hydrothermal bio-composites," *Journal of Cleaner Production*, vol. 250, p. 119469, 2020.
- [138] H. E. Gram, "Durability of natural fibres in concrete," *Research Institute, Stockholm, ISSN (0346-6906)*, vol. 183, no. 1, 1983.
- [139] T. R. D. Filho, J. Kuruvilla, G. Khusrow, and L. E. George, "The use of sisal fibre reinforcement in cement based composites.," *Revista Brasileira de Engenharia Agrícola e Ambiental*, vol. 3, no. 2, pp. 245–256, 1990.
- [140] F. R. D. Toledo, K. Ghavami, M. A. Sanjuán, and G. L. England, "Free, restrained and drying shrinkage of cement mortar composites reinforced with vegetable fibres," *Cement and Concrete Composites*, vol. 27, no. 5, pp. 537–546, 2005.
- [141] M. Terai and K. Minami, "Fracture behavior and mechanical properties of bamboo reinforced concrete members," *Procedia Engineering*, vol. 10, pp. 537–546, 2011.
- [142] T. sen and H. N. J. Reddy, "Strengthening of RC beams in flexure using natural jute fibre textile reinforced composite system and its comparative study with CFRP and GFRP strengthening systems," *International Journal of Sustainable Built Environment*, vol. 2, no. 1, pp. 41–55, 2013.
- [143] T. sen and H. N. J. Reddy, "Flexural strengthening of rc beams using natural sisal and artificial carbon and glass fabric reinforced composite system," *Sustainable Cities and Society*, vol. 10, pp. 195–206, 2014.
- [144] A. Agarwal, B. Nanda, and D. Maity, "Experimental investigation on chemically treated bamboo reinforced concrete beams and columns," *Construction and Building Materials*, vol. 71, pp. 610–617, 2014.

- [145] O. Onuaguluchi and N. Banthia, “Plant-based natural fibre reinforced cement composites: A review,” *Cement and Concrete Composites*, vol. 68, pp. 96–108, 2016.
- [146] W. Wang and N. Chouw, “The behaviour of coconut fibre reinforced concrete (CFRC) under impact loading,” *Construction and Building Materials*, vol. 134, pp. 452–461, 2017.
- [147] J. Chen and N. Chouw, “Flexural behaviour of flax FRP double tube confined coconut fibre reinforced concrete beams with interlocking interface,” *Composite Structures*, vol. 192, pp. 217–224, 2018.
- [148] T. Jami, S. R. Karade, and L. P. Singh, “A review of the properties of hemp concrete for green building applications,” *Journal of Cleaner Production*, pp. 117–852, 2019.
- [149] G. N. C. Das, P. Paramshivam, and S. L. Lee, “Coir reinforced cement pastes composites,” *In: Conference proceedings of our world in concrete and structures*, pp. 111–116, 1979.
- [150] D. J. Cook and P. Chindaprasirt, “Influence of loading history upon the compressive properties of concrete.,” *Magazine of Concrete Research*, vol. 32, no. 111, pp. 89–100, 1980.
- [151] S. Yang, D. J. Kim, and H. J. Kim, “Rice straw–wood particle composite for sound absorbing wooden construction materials.,” *Bioresource Technology*, vol. 86, no. 2, pp. 117–121, 2003.
- [152] M. Bouhicha, F. Aouissi, and S. Kenai, “Performance of composite soil reinforced with barley straw,” *Cement and Concrete Composites*, vol. 27, no. 5, pp. 617–621, 2005.
- [153] T. Ashour, H. Wieland, H. Georg, F. J. Bockisch, and W. Wu, “The influence of natural reinforcement fibres on insulation values of earth plaster for straw bale buildings,” *Materials and Design*, vol. 31, no. 10, pp. 4676–4685, 2010.

- [154] T. Ashour, H. Georg, and W. Wu, “Performance of straw bale wall: A case of study,” *Energy and Buildings*, vol. 43, no. 8, pp. 1960–1967, 2011.
- [155] M. T. Albahtiti, A. R. Hayder, D. Peri, and L. Davis, “Assessment of wheat fibre reinforced cementitious matrix,” *The IES Journal Part A: Civil and Structural Engineering*, vol. 6, no. 3, pp. 211–221, 2013.
- [156] B. Belhadj, M. Bederina, N. Montrelay, J. Houessou, and M. Quéneudec, “Effect of substitution of wood shavings by barley straws on the physico-mechanical properties of lightweight sand concrete,” *Construction and Building Materials*, vol. 66, pp. 247–258, 2014.
- [157] B. Belhadj, M. Bederina, Z. Makhloufi, A. Goullieux, and M. Quéneudec, “Study of the thermal performances of an exterior wall of barley straw sand concrete in an arid environment,” *Energy and Buildings*, vol. 87, pp. 166–175, 2015.
- [158] F. Parisi, D. Asprone, L. Fenu, and A. A. Prota, “Experimental characterization of italian composite adobe bricks reinforced with straw fibers,” *Composite Structures*, vol. 122, pp. 300–307, 2015.
- [159] O. Aksoğan, H. Binici, and E. Ortlek, “Durability of concrete made by partial replacement of fine aggregate by colemanite and barite and cement by ashes of corn stalk, wheat straw and sunflower stalk ashes,” *Construction and Building Materials*, vol. 106, pp. 253–263, 2016.
- [160] M. Bederina, B. Belhadj, M. S. Ammari, A. Gouilleux, Z. Makhloufi, N. Montrelay, and M. Quéneudéc, “Improvement of the properties of a sand concrete containing barley straws—treatment of the barley straws,” *Construction and Building Materials*, vol. 115, pp. 464–477, 2016.
- [161] C. S. Chin and B. Nepal, “Material properties of agriculture straw fibre-reinforced concrete,” *Ecological Wisdom Inspired Restoration Engineering. EcoWISE (Innovative Approaches to Socio-Ecological Sustainability)*, Springer, Singapore., 2019.

- [162] D. Jiang, P. An, S. Cui, S. Sun, J. Zhang, and T. Tuo, "Effect of modification methods of wheat straw fibers on water absorbency and mechanical properties of wheat straw fiber cement-based composites," *Advances in Materials Science and Engineering*, 2020.
- [163] C. Yuzhong *et al.*, "Plant straw cement lath and group standing mould technology [j]," *Wall Materials Innovation & Energy Saving in Buildings*, vol. 8, 2006.
- [164] H. Meng, *Research on Performance of Ecological Lightweight Cement-Based Wall Materials & Elasto-Plastic Analysis Model of Multi-Ribbed Wall*. PhD thesis, PhD thesis, School of Civil Engineering, Xi'an University of Architecture . . . , 2007.
- [165] F. Liu, Y. Zhang, and Z. Lu, "Hollow fiber concrete sandwich of compressed straw brick block," *China, 200910020713.3*, 2009.
- [166] D. A. Bainbridge, "Houses of straw: Building solid and environmentally conscious foundations," *Engineering and Technology for Sustainable World*, vol. 12, no. 4, pp. 7–8, 2005.
- [167] K. Joseph, R. D. Tolêdo Filho, B. James, S. Thomas, and L. H. De Carvalho, "A review on sisal fiber reinforced polymer composites," *Revista Brasileira de Engenharia Agrícola e Ambiental*, vol. 3, no. 3, pp. 367–379, 1999.
- [168] M. Gupta and R. Srivastava, "Tensile and flexural properties of sisal fibre reinforced epoxy composite: A comparison between unidirectional and mat form of fibres," *Procedia materials science*, vol. 5, pp. 2434–2439, 2014.
- [169] K. R. Sumithra and A. Dadapheer, "Experimental investigation on the properties of sisal fibre reinforced concrete," *Int. Res. J. Eng. Technol.*, vol. 4, pp. 2774–2777, 2017.
- [170] F. Oriola, J. Afolayan, J. Sani, and Y. Adamu, "Estimating the shear strength of sisal fibre reinforced concrete," *Nigerian Journal of Technology*, vol. 38, no. 3, pp. 557–65, 2019.

- [171] F. de Andrade Silva, N. Chawla, and R. D. de Toledo Filho, "An experimental investigation of the fatigue behavior of sisal fibers," *Materials Science and Engineering: A*, vol. 516, no. 1-2, pp. 90–95, 2009.
- [172] K. M. M. Rao and K. M. Rao, "Extraction and tensile properties of natural fibers: Vakka, date and bamboo," *Composite structures*, vol. 77, no. 3, pp. 288–295, 2007.
- [173] H. Danso, "Properties of coconut, oil palm and bagasse fibres: as potential building materials," *Procedia Engineering*, vol. 200, pp. 1–9, 2017.
- [174] N. Sathiparan, M. N. Rupasinghe, and B. H. Pavithra, "Performance of coconut coir reinforced hydraulic cement mortar for surface plastering application," *Construction and Building Materials*, vol. 142, pp. 23–30, 2017.
- [175] R. H. Lumingkewas, A. Husen, and R. Andrianus, "Effect of fibers length and fibers content on the splitting tensile strength of coconut fibers reinforced concrete composites," in *Key Engineering Materials*, vol. 748, pp. 311–315, Trans Tech Publ, 2017.
- [176] E. Jayamani, S. Hamdan, M. R. Rahman, and M. B. Bakri, "Comparative study of dielectric properties of hybrid natural fiber composites," *Procedia Engineering*, vol. 97, no. 0, pp. 536–544, 2014.
- [177] A. Gopinath, M. S. Kumar, and A. Elayaperumal, "Experimental investigations on mechanical properties of jute fiber reinforced composites with polyester and epoxy resin matrices," *Procedia Engineering*, vol. 97, pp. 2052–2063, 2014.
- [178] S. P. Kundu, S. Chakraborty, and S. Chakraborty, "Effectiveness of the surface modified jute fibre as fibre reinforcement in controlling the physical and mechanical properties of concrete paver blocks," *Construction and Building Materials*, vol. 191, pp. 554–563, 2018.

- [179] M. Mansur and M. Aziz, “A study of jute fibre reinforced cement composites,” *International Journal of Cement Composites and Lightweight Concrete*, vol. 4, no. 2, pp. 75–82, 1982.
- [180] P. Wambua, J. Ivens, and I. Verpoest, “Natural fibres: can they replace glass in fibre reinforced plastics?,” *Composites science and technology*, vol. 63, no. 9, pp. 1259–1264, 2003.
- [181] B. Poletanovic, J. Dragas, I. Ignjatovic, M. Komljenovic, and I. Merta, “Physical and mechanical properties of hemp fibre reinforced alkali-activated fly ash and fly ash/slag mortars,” *Construction and Building Materials*, vol. 259, p. 119677, 2020.
- [182] P. S. Lam, S. Sokhansanj, X. Bi, S. Mani, J. Lim, *et al.*, “Physical characterization of wet and dry wheat straw and switchgrass—bulk and specific density,” in *2007 ASAE Annual Meeting*, p. 1, American Society of Agricultural and Biological Engineers, 2007.
- [183] M. J. O’Dogherty, A. J. Huber, J. Dyson, and C. J. Marshall, “A study of physical and mechanical properties of wheat straw,” *Journal of Agricultural Engineering Research*, vol. 62, no. 2, pp. 133–142, 1995.
- [184] B. Nepal, *Agricultural straw fibre reinforced concrete for potential industrial ground-floor slab application*. PhD thesis, University of Liverpool, 2019.
- [185] W. Jianqiang and M. M. Christian, “Degradation mechanisms of natural fibre in the matrix of cement composites,” *Cement and Concrete Research*, vol. 73, pp. 1–16, 2015.
- [186] Y. Libo, S. Shen, and N. Chouw, “Microstructure, flexural properties and durability of coir fibre reinforced concrete beams externally strengthened with flax FRP composites,” *Composites Part B: Engineering*, vol. 80, pp. 343–354, 2015.

- [187] S. Karthiga and M. Mariappan, “Study of mechanical and durability properties of concrete with natural hybrid fiber,” *International Journal of Engineering Science*, pp. 216–276, 2019.
- [188] P. Peter, N. N. Soh, Z. A. Akasah, and M. A. Mannan, “Durability evaluation of cement board produced from untreated and pre-treated empty fruit bunch fibre through accelerating ageing,” *In IOP Conference Series: Materials Science and Engineering*, vol. 713, no. 1, pp. 12–19, 2020.
- [189] M. D. D. Klerk, M. Kayondo, G. M. Moelich, W. I. de Villiers, R. Combrinck, and W. P. Boshoff, “Durability of chemically modified sisal fibre in cement-based composites,” *Construction and Building Materials*, vol. 241, pp. 117–835, 2020.
- [190] V. Agopyan, H. Savastano, J. V. M, and M. A. Cincotto, “Developments on vegetable fibre–cement based materials in são paulo, brazil: an overview,” *Cement and Concrete Composites*, vol. 27, no. 5, pp. 527–536, 2005.
- [191] C. Juarez, A. Duran, P. Valdez, and G. G. Fajardo, “Performance of “agave lecheguilla” natural fiber in portland cement composites exposed to severe environment conditions,” *Building and environment*, vol. 42, no. 3, pp. 120–126, 2007.
- [192] M. F. Silva, F. R. D. Toledo, and F. EMR, “Mechanical behavior and durability of compression molded sisal fibre cement mortar laminates,” *1st International RILEM Conference on Textile Reinforced Concrete (ICTRC)*, *Rilem Publications*, pp. 171–180, 2006.
- [193] A. D’Almeida, M. F. J. Mello, and F. R. D. Toledo, “Use of curaua fibres as reinforcement in cement composites,” *Chemical Engineering Transactions*, vol. 17, pp. 1717–1722, 2009.
- [194] J. P. Won, K. S. Hwang, C. G. Park, and H. G. Park, “Evaluation of crack control and permeability of hydrophilic pva fibre reinforced concrete composites,” *Journal of Korea Concrete Institute*, vol. 16, no. 2, pp. 391–396, 2004.

- [195] M. H. Kim, J. H. Kim, Y. R. Kim, and Y. P. Kim, "An experimental study on the mechanical properties of hpfrcs reinforced with the micro and macro fibres," *Journal of Korea Concrete Institute*, vol. 17, no. 2, pp. 263–271, 2005.
- [196] D. R. Lankard and J. K. Newell, "Preparation of highly reinforced steel fiber reinforced concrete composites," *Special Publication*, vol. 81, pp. 287–306, 1984.
- [197] S. P. Singh and S. K. Kaushik, "Fatigue strength of steel fibre reinforced concrete in flexure," *Cement and Concrete Composites*, vol. 25, no. 7, pp. 779–786, 2003.
- [198] T. Kamada and C. V. Li, "The effects of surface preparation on the fracture behavior of ecc/concrete repair system," *Cement and Concrete Composites*, vol. 22, no. 6, pp. 423–431, 2003.
- [199] W. Elsaigh, E. Kearsley, and J. Robberts, "Steel fibre reinforced concrete for road pavement applications," *24th Annual Southern African Transport Conference, SATC 2005: Transport Challenges for 2010*, pp. 191–201, 2005.
- [200] H. Hu, P. Papastergiou, H. Angelakopoulos, M. Guadagnini, and K. Pilakoutas, "Flexural performance of steel fibre reinforced concrete with manufactured and recycled tyre steel fibres," *In Construction Materials for Sustainable Future*, pp. 904–911, 2017.
- [201] S. Y. Choi, J. S. Park, and W. T. Jung, "A study on shrinkage control of fibre reinforced concrete pavement," *Procedia Engineering*, vol. 14, pp. 2815–2822, 2011.
- [202] M. E. Glavind, "Fiber concrete: State of the art report. framework program cement-based composite materials under the material technological program," *Concrete Centre, Danish Technological Institute*, 1993.

- [203] J. M. Yang, H. O. Shin, and D. Y. Yoo, "Benefits of using amorphous metallic fibers in concrete pavement for long-term performance," *Archives of Civil and Mechanical Engineering*, vol. 17, no. 4, pp. 750–760, 2017.
- [204] A. Priyadarshree, A. K. Chhotu, and V. Kumar, "Use of bamboo in low volume rigid pavement as reinforced material: A review," *Journal of Civil Engineering and Environmental Technology*, vol. 1, no. 3, pp. 14–16, 2014.
- [205] R. Patel and V. Patel, "Using jute fiber in cement concrete pavement with irc mix design and ambuja mix design," IRC, 2018.
- [206] Z. Ullah, B. S. J. Hammad, F. A. Waris, and F. A. Soomro, "Behaviour of tensile strength energy to control concrete spalling in rigid pavements by using rice straw concrete," 2019.
- [207] T. Ahmed, M. U. Farooqi, and M. Ali, "Compressive behavior of rice straw-reinforced concrete for rigid pavements," *MS&E*, vol. 770, no. 1, p. 012004, 2020.
- [208] D. Patel and V. M. Patel, "Application of sugarcane bagasse fibres as concrete composites for rigid pavement," *Indian Journal of Research*, vol. 4, no. 4, pp. 4–5, 2015.
- [209] M. Khan and M. Ali, "Effect of super plasticizer on the properties of medium strength concrete prepared with coconut fiber," *Construction and Building Materials*, vol. 182, pp. 703–715, 2018.
- [210] N. Delatte, "Concrete pavement design, construction, and performance," *Taylor and Francis*, 2008.
- [211] Y. H. Huang, "Pavement analysis and design," 2004.
- [212] A. Rahim and M. Abd, *In-situ tests for subgrade resilient modulus characterization*. PhD thesis, University of Mississippi, 2001.
- [213] B. S. Mohammed, M. Adamu, and M. S. Liew, "Evaluating the effect of crumb rubber and nano silica on the properties of high volume fly ash roller

- compacted concrete pavement using non-destructive techniques,” *Case studies in construction materials*, vol. 8, pp. 380–391, 2018.
- [214] A. Joshaghani, “Identifying the problematic areas with structural deficiencies of pavements using non-destructive tests (NDT),” *International Journal of Pavement Engineering*, vol. 20, no. 11, pp. 1359–1369, 2019.
- [215] E. Kohler and J. Roesler, “Active crack control for continuously reinforced concrete pavements,” *Transportation research record*, vol. 1900, no. 1, pp. 19–29, 2004.
- [216] R. Fang and J. Chen, “Effects of design and construction factors on continuously reinforced concrete pavement performance,” *In Applied Mechanics and Materials*, vol. 97, pp. 138–145, 2011.
- [217] D. Ren, L. Houben, L. Rens, and A. Beeldens, “Active crack control for continuously reinforced concrete pavements in belgium through partial surface notches,” *Transportation Research Record*, vol. 2456, no. 1, pp. 33–41, 2014.
- [218] W. De, Pieter, H. D. Backer, and S. Depuydt, “Active crack control in continuously reinforced concrete pavements (CRCP),” in *High Tech Concrete: Where Technology and Engineering Meet*, pp. 1389–1397, 2018.
- [219] S. M. Kim, Y. K. Cho, and J. H. Lee, “Advanced reinforced concrete pavement: Concept and design,” *Construction and Building Materials*, vol. 231, p. 117130, 2020.
- [220] F. O. Slate and K. C. Hover, “Micro-cracking in concrete. fracture mechanics of concrete,” *International Journal of Application or Innovation in Engineering and Management*, pp. 132–139, 1984.
- [221] P. Giri and S. Kharkovsky, “Detection of surface crack in concrete using measurement technique with laser displacement sensor,” *IEEE Transactions on Instrumentation and Measurement*, vol. 65, no. 8, pp. 1951–1953, 2016.

- [222] S. Mezhoud, P. Clastres, H. Houari, and M. Belachia, “Field investigations on injection method for sealing longitudinal reflective cracks,” *Journal of Performance of Constructed Facilities*, vol. 32, no. 4, p. 04018041, 2018.
- [223] X. Kong and J. Li, “Non-contact fatigue crack detection in civil infrastructure through image overlapping and crack breathing sensing,” *Automation in Construction*, vol. 99, pp. 125–139, 2019.
- [224] X. Li, X. Lv, W. Wang, J. Liu, M. Yu, and Z. You, “Crack resistance of waste cooking oil modified cement stabilized macadam,” *Journal of Cleaner Production*, vol. 243, p. 118525, 2020.
- [225] R. Ahmadi, B. Souri, and M. Ebrahimi, “Evaluation of wheat straw to insulate fired clay hollow bricks as a construction material,” *Journal of Cleaner Production*, vol. 254, p. 120043, 2020.
- [226] M. Yasin, A. W. Bhutto, A. A. Bazmi, and S. Karim, “Efficient utilization of rice-wheat straw to produce value added composite products,” *International Journal of Chemical and Environmental Engineering*, vol. 1, no. 2, pp. 136–143, 2010.
- [227] S. K. Tehmina and M. Umarah, “Wheat straw: A pragmatic overview,” *Research Journal of Biological Sciences*, vol. 4, no. 6, pp. 673–675, 2012.
- [228] H. Nielsen, L. Baxter, G. Sclippab, C. Morey, F. Frandsen, and K. Dam-Johansen, “Deposition of potassium salts on heat transfer surfaces in straw-fired boilers: a pilot-scale study,” *Fuel*, vol. 79, no. 2, pp. 131–139, 2000.
- [229] B. Caslin and J. Finnan, “Straw for energy fact sheet,” *Teagasc*, 2010.
- [230] S. T. Mac an Bhaired, E. Walsh, P. Hemmingway, A. L. Maglinao, S. C. Capareda, and K. P. McDonnell, “Analysis of bed agglomeration during gasification of wheat straw in a bubbling fluidised bed gasifier using mullite as bed material,” *Powder technology*, vol. 254, pp. 448–459, 2014.

- [231] L. Wanga, T. Løvåsb, and E. Houshfarb, “Effect of sewage sludge addition on potassium release and ash transformation during wheat straw combustion,” *Chemical Engineering*, vol. 37, pp. 7–12, 2014.
- [232] A. Petrella, D. Spasiano, S. Liuzzi, U. Ayr, P. Cosma, V. Rizzi, M. Petrella, and R. Di Mundo, “Use of cellulose fibers from wheat straw for sustainable cement mortars,” *Journal of sustainable cement-based materials*, vol. 8, no. 3, pp. 161–179, 2019.
- [233] W. Cai, J. Liu, P. Liu, Z. Liu, H. Xu, B. Chen, Y. Li, Q. Zhou, M. Liu, and M. Ni, “A direct carbon solid oxide fuel cell fueled with char from wheat straw,” *International Journal of Energy Research*, vol. 43, no. 7, pp. 2468–2477, 2019.
- [234] A. Medyńska-Juraszek, I. Ówielkag-Piasecka, M. Jerzykiewicz, and J. Trynda, “Wheat straw biochar as a specific sorbent of cobalt in soil,” *Materials*, vol. 13, no. 11, p. 2462, 2020.
- [235] S. Deng, H. Tan, X. Wang, X. Lu, and X. Xiong, “Ash fusion characteristics and mineral matter transformations during sewage sludge/petrochemical sludge co-firing with wheat straw,” *Journal of Cleaner Production*, p. 121103, 2020.
- [236] L. Yan, Y. W. Mai, and L. Ye, “Effects of fibre surface treatment on fracture-mechanical properties of sisal-fibre composites,” *Composite Interfaces*, vol. 12, no. 1–2, pp. 141–163, 2005.
- [237] L. Jianxin, “Analysis of the pull-out of single fibres from low-density polyethylene,” 1992.
- [238] H. S. Ramaswamy, B. M. Ahuja, and S. Krishnamoorthy, “Behavior of concrete reinforced with jute, coir and bamboo fibres,” *International Journal of Cement Composites and Lightweight Concrete*, vol. 5, no. 1, pp. 3–13, 1983.

- [239] D. Ray, B. K. Sarkar, A. K. Rana, and N. R. Bose, "Effect of alkali treated jute fibres on composite properties," *Bulletin of materials science*, vol. 24, no. 2, pp. 129–136, 2001.
- [240] L. K. Aggarwal, "Studies on cement-bonded coir fibre boards," *Cement and Concrete Composites*, vol. 14, no. 1, pp. 63–69, 1992.
- [241] P. Mani and K. G. Satyanarayana, "Effects of the surface treatments of lignocellulosic fibers on their debonding stress," vol. 4, pp. 17–24, 1990.
- [242] M. Brahmakumar, C. Pavithran, and R. M. Pillai, "Coconut fibre reinforced polyethylene composites: effect of natural waxy surface layer of the fibre on fibre/matrix interfacial bonding and strength of composites," *Composites Science and technology*, vol. 65, no. 3, pp. 563–569, 2005.
- [243] H. Gu, "Tensile behaviors of the coir fibre and related composites after naoh treatment," *Materials and Design*, vol. 30, no. 9, pp. 3931–3934, 2009.
- [244] C. Sawsen, K. Fouzia, B. Mohamed, and G. Moussa, "Effect of flax fibers treatments on the rheological and the mechanical behavior of a cement composite," *Construction and Building Materials*, vol. 79, pp. 229–235, 2015.
- [245] M. Ali and N. Chouw, "Experimental investigations on coconut-fibre rope tensile strength and pullout from coconut fibre reinforced concrete," *Construction and Building Materials*, vol. 41, pp. 681–690, 2013.
- [246] C. Lim, N. Gowripalan, and V. Sirivivatnanon, "Microcracking and chloride permeability of concrete under uniaxial compression," *Cement and Concrete Composites*, vol. 22, no. 5, pp. 353–360, 2000.
- [247] A. Zia and M. Ali, "Behavior of fiber reinforced concrete for controlling the rate of cracking in canal-lining," *Construction and Building Materials*, vol. 155, pp. 726–739, 2017.
- [248] M. A. Mannan and C. Ganapathy, "Concrete from an agricultural waste-oil palm shell (ops)," *Building and Environment*, vol. 39, no. 4, pp. 441–448, 2004.

- [249] A. M. Ismail, “Compressive and tensile strength of natural fibre-reinforced cement base composites,” *Al-Rafidain Engineering*, vol. 15, no. 2, pp. 42–51, 2007.
- [250] A. K. Salain, I. N. Saturja, M. A. Wirayasa, and I. M. Jaya, “Mechanical properties of coconut fibre-reinforced concrete.,” 2014.
- [251] U. Nirmal, N. Singh, J. Hashim, S. T. W. Lau, and N. Jamil, “On the effect of different polymer matrix and fibre treatment on single fibre pullout test using betelnut fibres,” *Materials & Design*, vol. 32, no. 5, pp. 2717–2726, 2011.
- [252] A. Committee and I. O. for Standardization, “Building code requirements for structural concrete (aci 318-08) and commentary,” American Concrete Institute, 2008.
- [253] N. Suksawang, S. Wtaife, and A. Alsabbagh, “Evaluation of elastic modulus of fiber-reinforced concrete,” 2018.
- [254] S. Wang, C. Zhang, R. Wang, C. Song, and C. K. Shang, “Fragmentation-based dynamic size effect of layered roller compacted concrete (RCC) under impact loadings,” vol. 192, pp. 58–69, 2018.
- [255] L. Zhang, S. Feih, S. Daynes, M. Y. Chang, and J. Wang, “Energy absorption characteristics of metallic triply periodic minimal surface sheet structures under compressive loading,” *Additive Manufacturing*, vol. 23, pp. 505–515, 2018.
- [256] C. I. A. Xiangrong and X. U. Shilang, “Uniaxial compressive properties of ultra-high toughness cementitious composite,” *Journal of Wuhan University of Technology – Mat. Sci. Ed.*, vol. 26, no. 4, pp. 762–769, 2011.
- [257] K. Kesner and S. L. Billington, “Experimental response of precast infill panels made with dfrcc.,” *DFRCC International Workshop, Takayama, Japan.*, 2002.

- [258] A. Alsabbagh, S. Wtaife, A. Shaban, N. Suksawang, and E. Alshammari, "Enhancement of rigid pavement capacity using synthetic discrete fibers," in *IOP Conference Series: Materials Science and Engineering*, vol. 584, p. 012033, IOP Publishing, 2019.
- [259] C. Deacon, "Welded steel fabric in industrial ground floor construction," *Concrete (London)*, vol. 25, no. 7, pp. 41–44, 1991.
- [260] M. O. Kim and A. C. Bordelon, "Age-dependent properties of fiber-reinforced concrete for thin concrete overlays," *Construction and Building Materials*, vol. 137, pp. 288–299, 2017.
- [261] M. O. A. Mtallib and A. I. Marke, "Comparative evaluation of the flexural strength of concrete and colcrete," *Nigerian Journal of Technology*, vol. 29, no. 1, pp. 13–22, 2010.
- [262] M. U. Farooqi and M. Ali, "Contribution of plant fibers in improving the behavior and capacity of reinforced concrete for structural applications," *Construction and Building Materials*, vol. 182, pp. 94–107, 2018.
- [263] M. Khan, M. Cao, and M. Ali, "Effect of basalt fibers on mechanical properties of calcium carbonate whisker-steel fiber reinforced concrete," *Construction and Building Materials*, vol. 192, pp. 742–753, 2018.
- [264] S. R. Ferreira, M. Pepe, E. Martinelli, F. A. Silva, and T. R. D. Filho, "Influence of natural fibers characteristics on the interface mechanics with cement-based matrices," *Composites Part B: Engineering*, vol. 140, pp. 183–196, 2018.
- [265] M. Khan and M. Ali, "Improvement in concrete behavior with fly ash, silica-fume and coconut fibres," *Construction and Building Materials*, vol. 203, pp. 174–187, 2019.
- [266] A. Kumar, S. K. Antil, V. Rani, P. Antil, D. Jangra, R. Kumar, and C. I. Pruncu, "Characterization on physical, mechanical, and morphological properties of indian wheat crop," *Sustainability*, vol. 12, no. 5, p. 2067, 2020.

- [267] M. U. Farooqi and M. Ali, “Effect of pre-treatment and content of wheat straw on energy absorption capability of concrete,” *Construction and Building Materials*, vol. 524, pp. 572–583, 2019.
- [268] Y. Park, Y. H. Kim, and S.-H. Lee, “Long-term flexural behaviors of gfrp reinforced concrete beams exposed to accelerated aging exposure conditions,” *Polymers*, vol. 6, no. 6, pp. 1773–1793, 2014.
- [269] A. V. Oskouei, M. Bazli, H. Ashrafi, and M. Imani, “Flexural and web crippling properties of gfrp pultruded profiles subjected to wetting and drying cycles in different sea water conditions,” *Polymer Testing*, vol. 69, pp. 417–430, 2018.
- [270] R. S. Olivito, O. A. Cevallos, and A. Carrozzini, “Development of durable cementitious composites using sisal and flax fabrics for reinforcement of masonry structures,” *Materials and Design*, vol. 57, pp. 258–268, 2014.
- [271] J. Wei and C. Meyer, “Degradation rate of natural fiber in cement composites exposed to various accelerated aging environment conditions,” *Corrosion science*, vol. 88, pp. 118–132, 2014.
- [272] B. L. Karihaloo and J. Wang, “Degradation rate of natural fiber in cement composites exposed to various accelerated aging environment conditions,” *Advanced Engineering Materials*, vol. 2, no. 11, pp. 726–732, 2000.
- [273] A. Sarkar and M. Hajihosseini, “The effect of basalt fibre on the mechanical performance of concrete pavement,” *Road Materials and Pavement Design*, pp. 1–12, 2018.
- [274] M. Bouasker, B. Naima, H. Dashnor, and A. M. Muzahim, “Physical characterization of natural straw fibres as aggregates for construction materials applications,” *Materials*, vol. 7, pp. 3034–3048, 2014.
- [275] A. K. Sachan and C. V. S. K. Rao, “Behaviour of fibre reinforced concrete deep beams,” *Cement and Concrete Composites*, vol. 12, pp. 211–218, 1990.

- [276] M. Ali, B. Nolot, and N. Chow, "Behaviour of coir fibre and rope reinforced concrete members with debonding length," *Proceedings of 9th PCEE, Uni of Auckland, New Zealand*, vol. 131, 2011.
- [277] M. Ali, "Seismic performance of coconut-fibre-reinforced-concrete columns with different reinforcement configurations of coconut-fibre ropes," *Construction and Building Materials*, vol. 70, pp. 226–230, 2014.
- [278] G. P. Hammond and C. I. Jones, "Embodied energy and carbon in construction materials," *Proceedings of the Institution of Civil Engineers-Energy*, vol. 161, no. 2, pp. 87–98, 2008.
- [279] G. AASHTO, "Guide for design of pavement structures," *American Association of State Highway and Transportation Officials, Washington, DC*, 1993.
- [280] U. Nirmal, N. Singh, J. Hashim, S. T. Lau, and N. Jamil, "On the effect of different polymer matrix and fibre treatment on single fibre pullout test using betelnut fibres," *Materials and Design*, vol. 32, no. 5, pp. 2717–2726, 2011.
- [281] W. K. Mampearachchi and A. Senadeera, "Determination of the most effective cement concrete block laying pattern and shape for road pavement based on field performance," *Journal of materials in civil engineering*, vol. 26, no. 2, pp. 226–232, 2014.
- [282] L. W. Teller and E. C. Sutherland, "The structural design of concrete pavements-part 4-a study of the structural action of several types of transverse and longitudinal joint designs," *Public Roads*, 1936.

Annexure A

Supplementary Data for Chapter 3

**Optimization of Wheat Straw Reinforced
Concrete Mix**

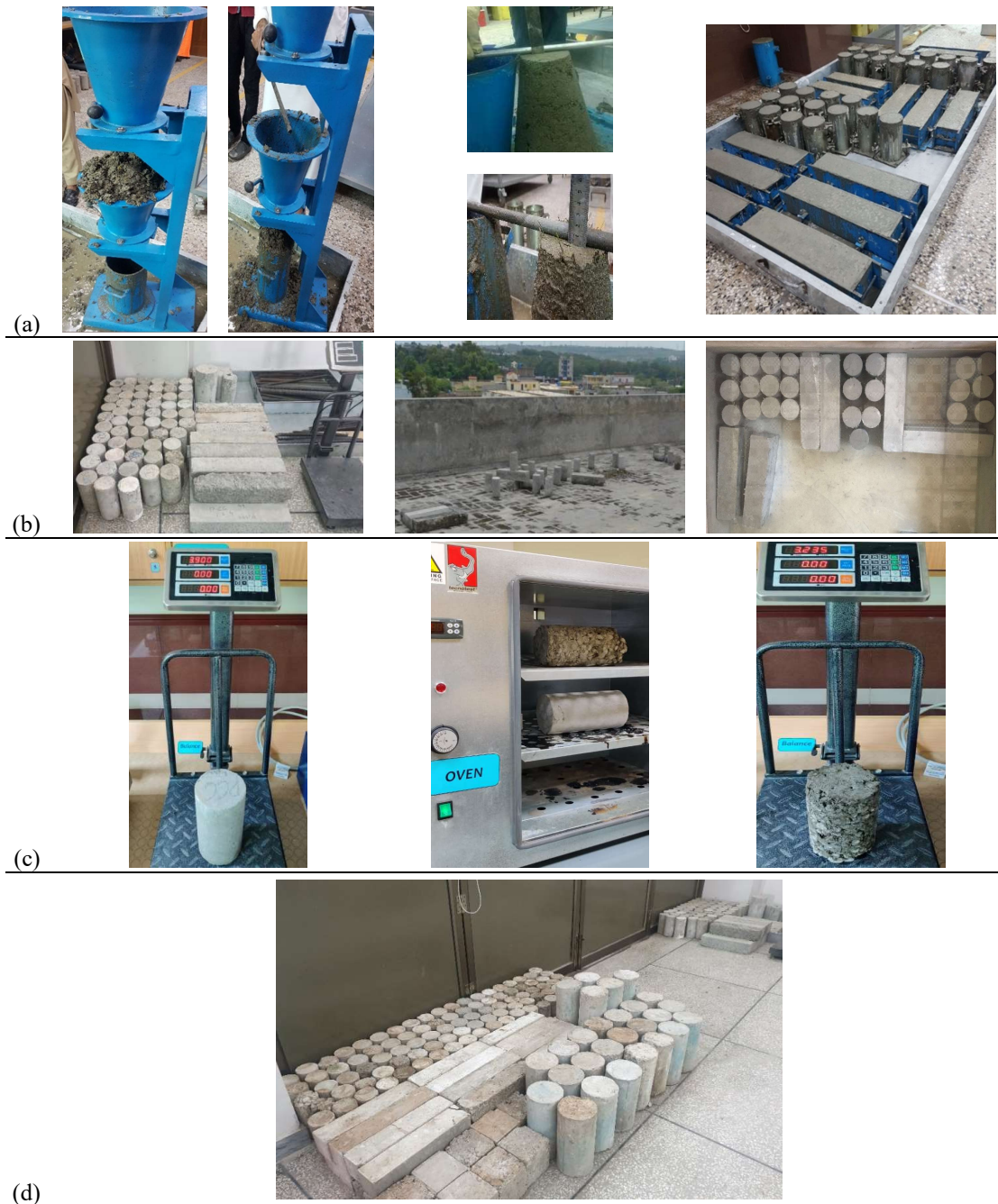


FIGURE A1: Specimens at different stages; (a) fresh state tests and moulding, (b) ageing conditions, (c) hardened state tests and (d) just before testing.

Annexure B

Supplementary Data for Chapter [4](#) Durability of Wheat Straw Reinforced Concrete

TABLE B1: Monthly-average climatic data of Islamabad, Pakistan (January 2016 - December 2019).

Month (s)	Year - 2016					Year - 2017					Year - 2018					Year- 2019				
	Temperature			Humidity	Rainfall	Temperature			Humidity	Rainfall	Temperature			Humidity	Rainfall	Temperature			Humidity	Rainfall
	(°C)			(%)	(mm)	(°C)			(%)	(mm)	(°C)			(%)	(mm)	(°C)			(%)	(mm)
	Low	High	Mean	Mean	Mean	Low	High	Mean	Mean	Mean	Low	High	Mean	Mean	Mean	Low	High	Mean	Mean	Mean
	(2)	(3)	(4)	(5)	(6)	(7)	(8)	(9)	(10)	(11)	(12)	(13)	(14)	(15)	(16)	(17)	(18)	(19)	(20)	(21)
January	8	19	12	33	7.26	8	16	11	47	52.35	8	19	12	27	0.65	9	17	13	42	77.8
February	10	22	15	31	10.95	10	21	15	40	18.67	11	21	15	38	24.36	10	18	15	54	156.2
March	14	24	19	46	87.93	13	25	18	36	22.51	15	26	20	38	11.45	13	23	20	48	110.5
April	18	31	24.5	33	23.15	19	33	26	29	40.04	18	30	24	36	39.66	21	32	30	36	57.9
May	24	37	30.5	24	15.1	25	37	31	25	9.8	23	35	30	25	11.56	25	36	34	26	35.7
June	29	40	34.5	26	10.19	27	38	32.5	31	26.71	29	38	34	29	26.88	29	41	38	24	28.9
July	18	37	33	45	72.03	28	37	32.5	45	39.55	28	36	32	48	107.13	30	38	36	45	257.1
August	27	36	31.5	43	27.82	27	36	31.5	46	44.42	27	35	31	55	62.1	17	36	33	59	323.7
September	25	36	30.5	37	10	24	34	28	39	11.03	24	33	28.5	47	27.77	25	32	34	52	157
October	20	32	26	21	0.83	19	31	24	24	0.12	23	31	28	28	4.1	21	28	30	41	52.3
November	14	27	19	18	0.52	14	24	18	26	2.12	17	25	22	28	17.6	15	21	24	46	55.2
December	11	24	15	18	0.35	10	20	14	29	16.75	12	21	16	24	2.9	10	20	16	37	33.4
Yearly Average	18.2	30.4	24.2	31.3	22.2	18.7	29.3	23.5	34.8	23.7	19.6	29.2	24.4	35.3	28.0	18.8	28.5	26.9	42.5	112.1
Std. Dev.	7.0	7.0	10.2	10.1	28.5	7.5	7.7	7.9	8.5	17.1	7.1	6.6	7.3	10.2	30.4	7.5	8.4	8.9	10.6	95.2

TABLE B2: Residual compressive properties (i.e. σ_r , Ce_r and CTI_r) of SWSRC at 4-years age.

Properties	Room conditions			Climatic conditions			Alternate wetting and drying		
	SWSRC-1%	SWSRC-2%	SWSRC-3%	SWSRC-1%	SWSRC-2%	SWSRC-3%	SWSRC-1%	SWSRC-2%	SWSRC-3%
(1)	(2)	(3)	(4)	(5)	(6)	(7)	(8)	(9)	(10)
σ_r (MPa)	-	16.3±0.4	15.6±0.6	-	12.9±0.2	10.9±0.5	-	8.4±0.2	6.2±0.7
Ce_r (kJ/m ³)	-	4602±17	2925±20	-	1879±16	3099±23	-	2528±26	1803±33
CTI_r (-)	-	1.14±0.05	1.90±0.08	-	1.37±0.07	1.18±0.13	-	2.45±0.11	1.99±0.09

TABLE B3: Residual compressive properties (i.e. σ_r , Ce_r and CTI_r) of BWSRC at 4-years age.

Properties	Room conditions			Climatic conditions			Alternate wetting and drying		
	BWSRC-1%	BWSRC-2%	BWSRC-3%	BWSRC-1%	BWSRC-2%	BWSRC-3%	BWSRC-1%	BWSRC-2%	BWSRC-3%
(1)	(2)	(3)	(4)	(5)	(6)	(7)	(8)	(9)	(10)
σ_r (MPa)	16.1±0.2	16.0±0.1	13.8±0.5	13.1±0.3	12.8±0.2	10.2±0.8	8.0±0.6	5.2±0.4	4.8±0.4
Ce_r (kJ/m ³)	3053±34	3933±37	3584±41	2738±19	3424±26	1409±13	1370±28	717±11	762±15
CTI_r (-)	1.28±0.06	2.00±0.03	1.52±0.04	1.14±0.05	1.49±0.08	1.45±0.06	1.51±0.04	1.51±0.07	1.18±0.09

TABLE B4: Residual compressive properties (i.e. σ_r , Ce_r and CTI_r) of CWSRC at 4-years age.

Properties	Room conditions			Climatic conditions			Alternate wetting and drying		
	CWSRC-1%	CWSRC-2%	CWSRC-3%	CWSRC-1%	CWSRC-2%	CWSRC-3%	CWSRC-1%	CWSRC-2%	CWSRC-3%
(1)	(2)	(3)	(4)	(5)	(6)	(7)	(8)	(9)	(10)
σ_r (MPa)	14.1±0.4	13.0±0.3	10.7±0.6	10.6±0.5	10.0±0.2	9.0±0.8	7.2±0.7	4.9±0.5	3.8±0.6
Ce_r (kJ/m ³)	2978±29	3565±22	2129±31	1193±17	1656±20	1267±33	1691±19	1076±13	535±16
CTI_r (-)	1.22±0.01	1.55±0.04	1.18±0.06	1.13±0.03	1.41±0.08	1.04±0.06	1.50±0.11	1.42±0.09	1.02±0.16

TABLE B5: Residual splitting-tensile properties (i.e. SS_r , Se_r and STI_r) of SWSRC - at 4-years age.

Properties	Room conditions			Climatic conditions			Alternate wetting and drying		
	SWSRC-1%	SWSRC-2%	SWSRC-3%	SWSRC-1%	SWSRC-2%	SWSRC-3%	SWSRC-1%	SWSRC-2%	SWSRC-3%
(1)	(2)	(3)	(4)	(5)	(6)	(7)	(8)	(9)	(10)
SS_r (MPa)	-	1.30±0.08	1.18±0.05	-	1.25±0.03	1.18±0.02	-	1.08±0.11	0.83±0.08
Se_r (J)	-	87.9±2.6	81.0±3.9	-	85.2±4.3	71.5±3.3	-	61.8±3.5	45.6±4.2
STI_r (-)	-	1.93±0.04	1.30±0.05	-	1.26±0.07	1.16±0.02	-	1.35±0.06	1.30±0.07

TABLE B6: Residual splitting-tensile properties (i.e. SS_r , Se_r and STI_r) of BWSRC at 4-years age.

Properties	Room conditions			Climatic conditions			Alternate wetting and drying		
	BWSRC-1%	BWSRC-2%	BWSRC-3%	BWSRC-1%	BWSRC-2%	BWSRC-3%	BWSRC-1%	BWSRC-2%	BWSRC-3%
(1)	(2)	(3)	(4)	(5)	(6)	(7)	(8)	(9)	(10)
SS_r (MPa)	1.44±0.06	1.21±0.09	1.02±0.05	1.20±0.01	1.20±0.02	0.91±0.06	1.07±0.05	0.95±0.06	0.62±0.09
Se_r (J)	73.1±2.2	77.6±3.0	60.5±1.8	91.6±0.8	81.1±1.0	60.4±2.5	81.5±2.3	73.0±2.6	51.7±3.3
STI_r (-)	1.85±0.08	1.78±0.10	1.50±0.09	1.48±0.04	1.21±0.06	1.20±0.08	1.34±0.07	1.42±0.08	1.20±0.10

TABLE B7: Residual splitting-tensile properties (i.e. SS_r , Se_r and STI_r) of CWSRC at 4-years age.

Properties	Room conditions			Climatic conditions			Alternate wetting and drying		
	CWSRC-1%	CWSRC-2%	CWSRC-3%	CWSRC-1%	CWSRC-2%	CWSRC-3%	CWSRC-1%	CWSRC-2%	CWSRC-3%
(1)	(2)	(3)	(4)	(5)	(6)	(7)	(8)	(9)	(10)
SS_r (MPa)	1.16±0.08	1.01±0.10	0.90±0.05	1.02±0.06	0.83±0.03	0.72±0.08	0.91±0.09	0.76±0.04	0.47±0.05
Se_r (J)	58.5±3.0	62.3±3.8	45.3±2.5	66.9±2.7	52.4±1.2	42.6±3.1	79.6±3.6	49.5±1.9	27.9±2.2
STI_r (-)	1.71±0.10	1.69±0.01	1.52±0.03	1.39±0.05	1.37±0.7	1.33±0.06	1.30±0.05	1.43±0.06	1.25±0.09

TABLE B8: Residual flexural properties (i.e. MoR_r , Fe_r and FTI_r) of SWSRC at 4-years age.

Properties	Room conditions			Climatic conditions			Alternate wetting and drying		
	SWSRC-1%	SWSRC-2%	SWSRC-3%	SWSRC-1%	SWSRC-2%	SWSRC-3%	SWSRC-1%	SWSRC-2%	SWSRC-3%
(1)	(2)	(3)	(4)	(5)	(6)	(7)	(8)	(9)	(10)
MoR_r (MPa)	-	6.65±0.06	4.58±0.03	-	5.10±0.04	4.04±0.08	-	3.26±0.13	2.65±0.10
Fe_r (J)	-	21.2±1.2	15.8±0.6	-	15.5±0.8	12.2±1.6	-	10.6±2.6	9.4±2.0
FTI_r (-)	-	1.74±0.02	1.99±0.04	-	1.64±0.05	1.58±0.06	-	1.47±0.09	1.08±0.10

TABLE B9: Residual flexural properties (i.e. MoR_r , Fe_r and FTI_r) of BWSRC at 4-years age.

Properties	Room conditions			Climatic conditions			Alternate wetting and drying		
	BWSRC-1%	BWSRC-2%	BWSRC-3%	BWSRC-1%	BWSRC-2%	BWSRC-3%	BWSRC-1%	BWSRC-2%	BWSRC-3%
(1)	(2)	(3)	(4)	(5)	(6)	(7)	(8)	(9)	(10)
MoR_r (MPa)	6.31±0.05	5.67±0.03	4.60±0.08	5.73±0.04	4.85±0.07	4.36±0.09	3.66±0.06	3.00±0.09	2.48±0.10
Fe_r (J)	26.9±1.2	21.8±0.6	17.2±1.6	17.4±1.0	14.9±1.4	12.1±2.0	12.3±1.3	9.4±2.1	6.1±3.0
FTI_r (-)	1.74±0.06	1.71±0.02	1.50±0.07	1.43±0.05	1.73±0.05	1.37±0.07	1.22±0.05	1.34±0.10	1.01±0.12

TABLE B10: Residual flexural properties (i.e. MoR_r , Fe_r and FTI_r) of CWSRC at 4-years age.

Properties	Room conditions			Climatic conditions			Alternate wetting and drying		
	CWSRC-1%	CWSRC-2%	CWSRC-3%	CWSRC-1%	CWSRC-2%	CWSRC-3%	CWSRC-1%	CWSRC-2%	CWSRC-3%
(1)	(2)	(3)	(4)	(5)	(6)	(7)	(8)	(9)	(10)
MoR_r (MPa)	5.25±0.04	4.72±0.08	3.18±0.06	4.78±0.07	4.20±0.09	2.91±0.11	2.83±0.03	2.45±0.06	2.10±0.08
Fe_r (J)	21.8±0.8	18.5±1.6	9.2±1.1	14.6±1.4	14.0±1.9	9.7±3.5	7.3±0.6	6.9±1.5	5.9±2.0
FTI_r (-)	1.67±0.03	1.54±0.06	1.34±0.04	1.80±0.06	1.55±0.08	1.47±0.08	1.77±0.02	1.56±0.06	1.43±0.07

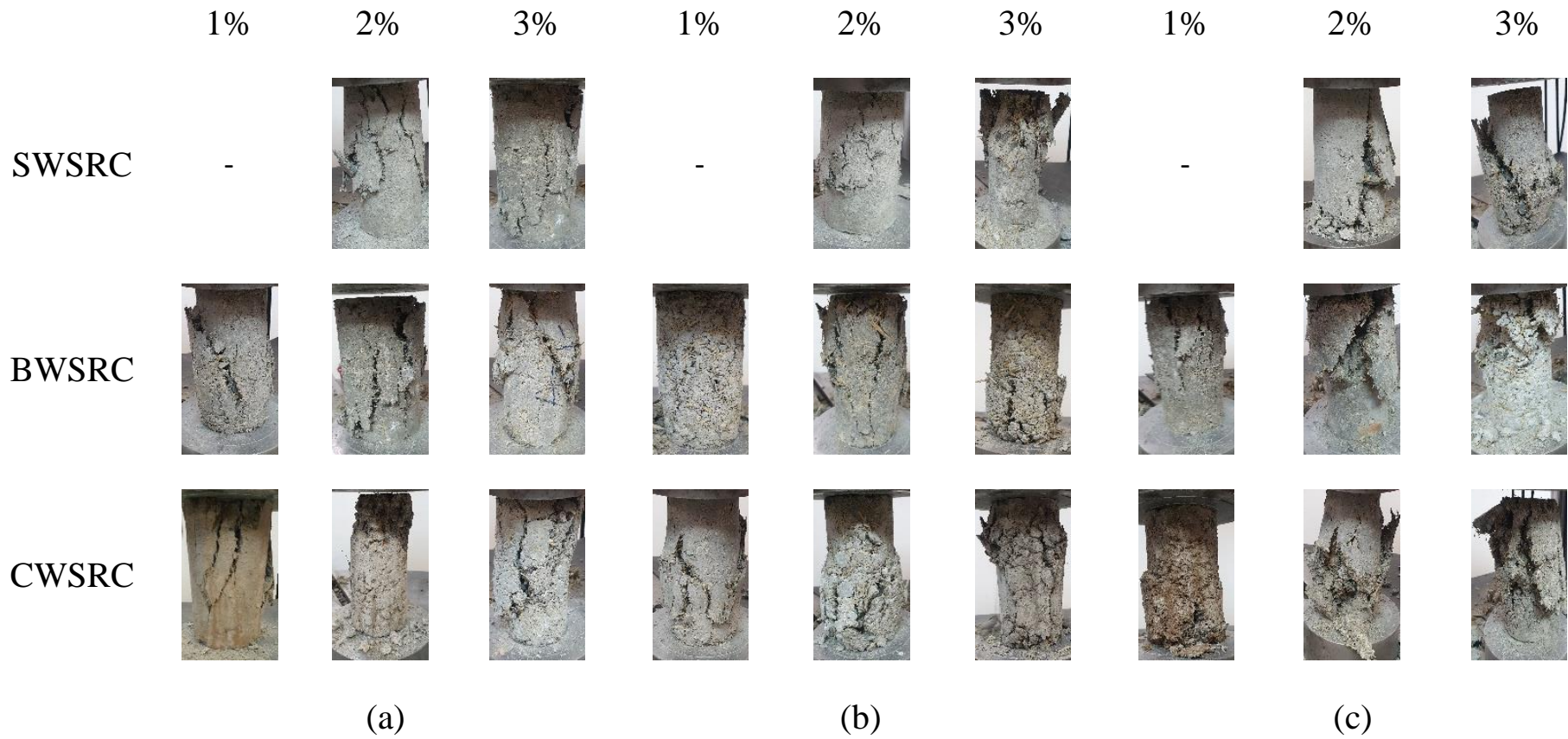


FIGURE B1: Tested cylinder specimens of SWSRC-2-3%, BWSRC-1-3% and CWSRC-1-3% under compressive loading after 4-years ageing under (a) room conditions, (b) climatic conditions, and (c) alternate wetting and drying conditions.

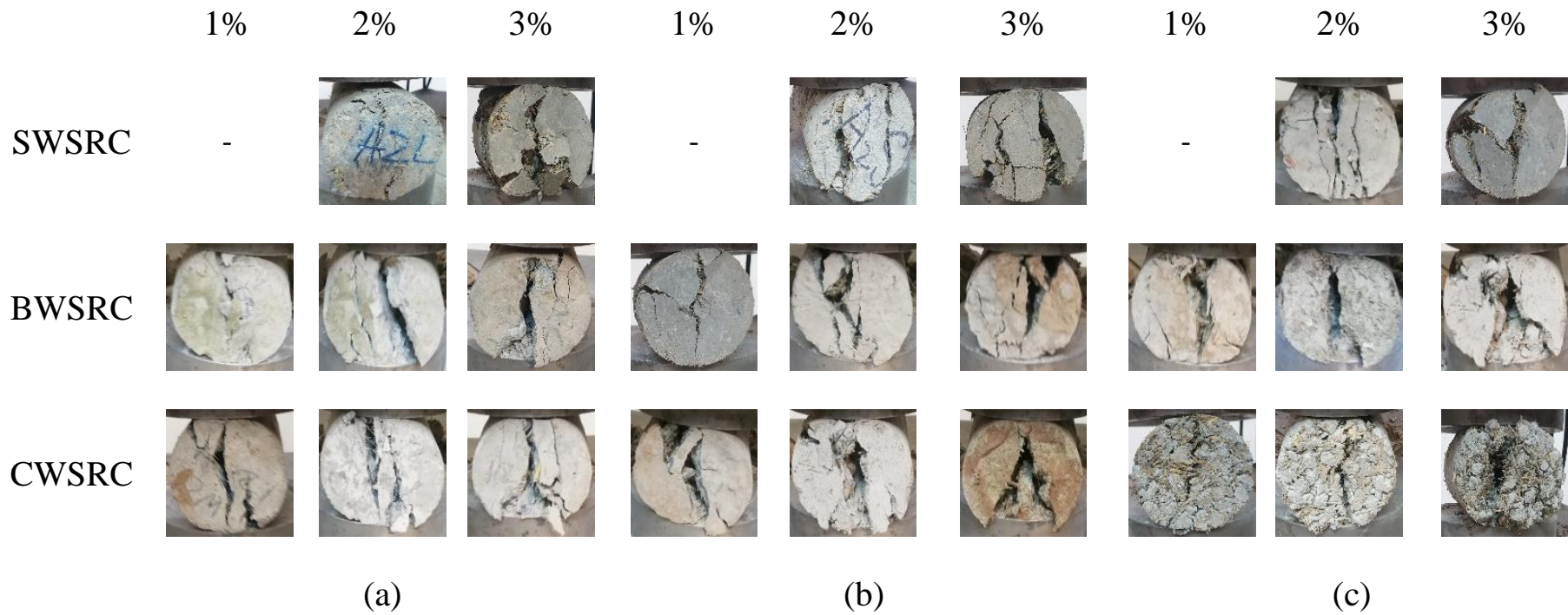


FIGURE B2: Tested cylinder specimens of SWSRC-2-3%, BWSRC-1-3% and CWSRC-1-3% under splitting-tensile loading after 4-years ageing under (a) room conditions, (b) climatic conditions, and (c) alternate wetting and drying conditions.

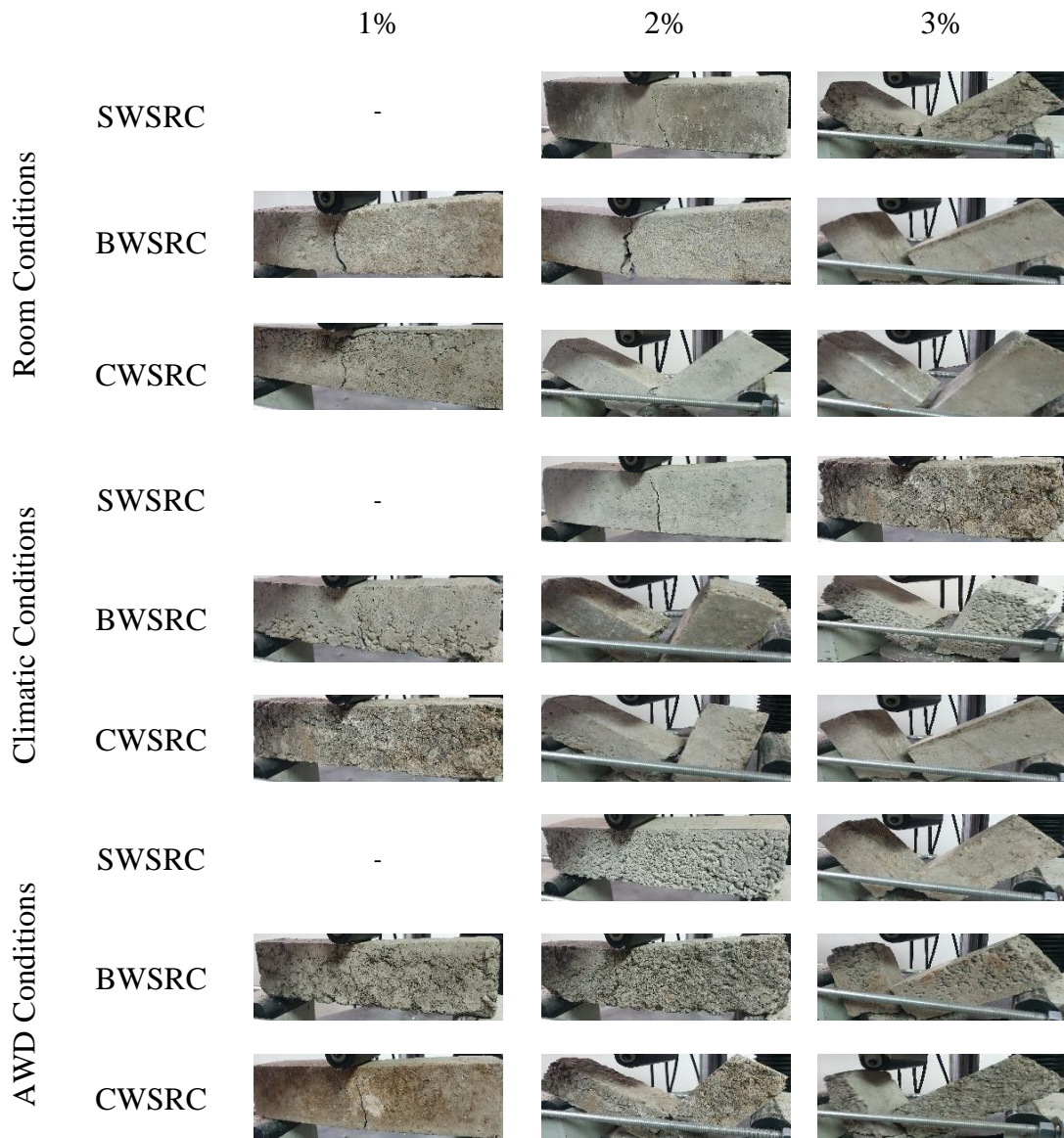


FIGURE B3: Tested specimens of SWSRC-1-3%, BWSRC-1-3% and CWSRC-1-3% under flexural loading after 4-years ageing under (a) room conditions, (b) climatic conditions, and (c) alternate wetting and drying conditions.

Annexure C

Supplementary Data for Chapter 6

Structural Performance of Wheat Straw
Reinforced Concrete Pavement



FIGURE C1: Trip cycles of heavy commercial vehicles to and from construction site through PC and JWSRCP test sections.